A mechanistic investigation into candidate markers of telomere-induced senescence in normal human epidermal keratinocytes

dos Santos Soares Martins de Castro, Alicia Maria

A mechanistic investigation into candidate markers of telomere-induced senescence in normal human epidermal keratinocytes

Alice Maria dos Santos Soares Martins de Castro

A thesis submitted in partial fulfilment of the requirements of the University of London for the degree of Doctor of Philosophy

The program of research was carried out in the Centre for Clinical and Diagnostic Oral Sciences, Institute of Dentistry, Barts and The London School of Medicine and Dentistry, University of London

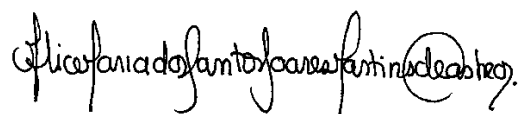February 2014

Statement of Originality

I, Alice Maria dos Santos Soares Martins de Castro, confirm that the research included within this thesis is my own work or that where it has been carried out in collaboration with, or supported by others, that this is duly acknowledged below and my contribution indicated. Previously published material is also acknowledged below.

I attest that I have exercised reasonable care to ensure that the work is original, and does not to the best of my knowledge break any UK law, infringe any third party's copyright or other Intellectual Property Right, or contain any confidential material.

I accept that the College has the right to use plagiarism detection software to check the electronic version of the thesis.

I confirm that this thesis has not been previously submitted for the award of a degree by this or any other university.

The copyright of this thesis rests with the author and no quotation from it or information derived from it may be published without the prior written consent of the author.

February 2014

Details of collaboration and publications:

I have established a collaboration with Dr Utz Herbig's lab for the detection of HOPX *in situ*.

Abstract

Telomere dysfunction is one mechanism of cellular and tissue ageing. Dysfunctional telomeres in fibroblasts are recognised as DNA double-strand breaks (DSBs) and trigger the DNA damage pathway of senescence. However, telomere uncapping in normal human epidermal keratinocytes, via expression of the dominant negative mutant of the telomere repeat-binding factor 2 (TRF2$^{\Delta B \Delta M}$), resulted in a senescent-like arrest without a significant DNA damage response (DDR). This suggests that either keratinocytes are unusually sensitive to telomere uncapping and the low DDR is sufficient to induce senescence or that dysfunctional telomeres may also be signalled through an alternative pathway. Subsequent analysis revealed genes HIST2H2BE, ICEBERG, S100A7 and HOPX as potential markers for telomere dysfunction-induced senescence (TDIS) since they were induced by telomere uncapping and seemed to be regulated by telomerase. The aim of this project was to assess the specificity of these candidate markers for TDIS and to select the most promising for use as a biomarker. To this end, keratinocytes were exposed to doses of ionising radiation, capable of generating transient or permanent damage to the DNA, or transduced with retroviral constructs expressing p14^{ARF}, p16^{INK4a}, p53 or TRF2$^{\Delta B \Delta M}$ and the gene expression levels of the candidates assessed after a recovery period or at the early stages of senescence. Whilst S100A7, HOPX or ICEBERG were not induced by a transient or persistent DDR or by p16^{INK4a}, ICEBERG and HOPX were induced by p53 and p14^{ARF} when these were ectopically expressed at higher levels. Thus, S100A7 seems to be the most specific early marker for telomere dysfunction in keratinocytes since it was selectively induced by telomere uncapping via expression of TRF2$^{\Delta B \Delta M}$ and not by DSBs or by over expression of p14^{ARF}, p53 or p16^{INK4a}. S100A7 may have the potential to identify cells with telomere dysfunction in human epithelia and body fluids.

Contents

Acknowledgements

Abbreviations

53BP1	p53 binding protein 1
AAV	adeno-associated virus
ARF	alternate reading frame
AT	ataxia telangiectasia
ATM	ataxia telangiectasia mutated
BER	base-excision repair
BICMS	Blizard Institute of Cell and Molecular Sciences
BICR	Beatson Institute for Cancer Research
BLAST	basic local alignment search tool
BPE	bovine pituitary extract
Cdk	cyclin-dependent kinase
Chk	checkpoint kinase
CMV	cytomegalovirus
CR	caloric restriction
DAPI	4',6-diamidino-2-phenylindole
DC	dyskeratosis congenita
DDR	DNA damage response
DMEM	Dulbecco's modified Eagle's medium
DMSO	dimethyl sulfoxide
DNA	deoxyribonucleic acid
DNA-SCARS	DNA segments with chromatin alterations reinforcing senescence
DSB	double-strand break
dsRNA	double-stranded RNA
EDTA	ethylenediaminetetraacetic acid
EGF	epidermal growth factor
FAD	flavin adenine dinucleotide
FCS	fetal calf serum

FOXO	forkhead box O
GFP	green fluorescent protein
HDACI	histone deacetylase inhibitor
HEPES	N-2-hydroxyethylpiperazine-N'-2-ethanesulfonic acid
HIRA	histone repressor A
HKG	housekeeping gene
HPV	human papillomavirus
HR	homologous recombination
HSC	hematopoietic stem cell
IL	interleukine
IR	ionising radiation
KGM	keratinocyte growth medium
LB	Luria-Bertani
LTR	long terminal repeat
M-MuLV	Moloney murine leukemia virus
Mcm	mini chromosome maintenance protein
MCS	multiple cloning site
miRNA	micro RNA
MPD	mean population doubling
mtDNA	mitochondrial DNA
mTR	murine telomerase RNA
NCBI	National Centre for Biotechnology Information
NER	nucleotide-excision repair
NHEJ	non-homologous end joining
NHEK	normal human epidermal keratinocyte
NIH	National Institutes of Health
NMR	naked mole rat
OIS	oncogene-induced senescence
PAGE	polyacrylamide gel electrophoresis
PBS	phosphate-buffered saline
PCNA	proliferating cell nuclear antigen

PCR	polymerase chain reaction
PFA	para-formaldehyde
PGC	Peroxisome proliferator-activated receptor gamma co-activator
PML	promyelocytic leukaemia
POT1	protection of telomeres 1
pRb	retinoblastoma protein
PTEN	phosphatase and tensin homolog
PVDF	polyvinylidene fluoride
qPCR	quantitative or real-time PCR
RDR	recombination-dependent replication
RISC	RNA-induced silencing complex
RNA	ribonucleic acid
RNAi	RNA interference
ROS	radical oxygen species
RT	reverse transcriptase
RT PCR	reverse transcriptase PCR
SA-β-gal	senescence-associated β-galactosidase
SAHF	senescence-associated heterochromatic foci
SASP	senescence-associated secretory phenotype
SD	seeding density
SDS	sodium dodecyl sulfate
shRNA	short hairpin RNA
siRNA	short interfering RNA
SRF	serum response factor
SSB	single-strand break
STELA	single telomere elongation length analysis
SV40	simian virus 40
T_a	annealing temperature
TBS	Tris-buffered saline
TDIS	telomere dysfunction-induced senescence

TE	Tris-EDTA
TERC	telomerase RNA component
TERT	telomerase reverse transcriptase
TIF	telomere-dysfunction induced foci
T_m	melting temperature
TRF	telomeric repeat-binding factor
TRF2$^{\Delta B \Delta M}$	dominant-negative TRF2
VEGF	vascular endothelial growth factor
WRN	Werner syndrome helicase
WS	Werner's syndrome
β-ME	beta-mercaptoethanol or 2-mercaptoethanol

List of Figures

List of Tables

Chapter 1. General Introduction.

1.1. Introduction to Ageing

Definition of Ageing

Ageing has been defined as,

The collection of changes that render human beings progressively more likely to die (Medawar, 1952).

A universal, progressive, intrinsic and degenerative process, as it happens in all organisms within a species and is characterised by a continuous set of changes, which would occur even in a stress-free environment, and ultimately results in physiological failure and death (Strehler, 1962; Aspinall, 2003).

The intrinsic, inevitable, and irreversible age-related process of loss of viability and increase in vulnerability (Comfort, 1979).

Although ageing does not occur in all species it is an event shared by most, which suggests that the ageing process provides some selective evolutionary advantage to those which experience it. Several explanations have been proposed for why organismal ageing occurs (Aspinall, 2003).

Evolutionary theories of ageing

Evolutionary theories of ageing arose from the need of a unifying explanation for the incredible variation in ageing rates and longevity across species. They are all based on the observation that the force of natural selection declines with age and, until the first half of the twentieth century, were merely conjectured in a theoretical, non-experimental way (reviewed in (Gavrilov & Gavrilova, 2002)).

The first theory of ageing was proposed by August Weismann in 1891 and it is known as the 'theory of programmed death'. Weismann believed cells possessed a programmed death mechanism that would operate like a clock to count generations from the first stage of embryonic development. This would determine the lifespan of each generation of cells and, consequently, of the individual. He believed this mechanism was developed by natural selection to benefit the young in detriment of the old. His idea that somatic cells possess a cell division limit was challenged by the experimental work of Alexis Carrell in 1912 which wrongly suggested that cells proliferated indefinitely in culture and were, therefore, intrinsically 'immortal'. The concept of a cell division limit, known today as the 'Hayflick Limit', was experimentally confirmed just 50 years later by Hayflick and Moorhead (Hayflick & Moorhead, 1961). Weismann was also the author of the 'germ-plasm theory' which acknowledged the two main types of cells in the body, germ cells and somatic cells, and believed in the "perishable and vulnerable nature of the soma" in favour of the germ line. This idea relates to one of the modern theories of ageing, 'the disposable soma theory'.

Modern theories of ageing which are currently accepted were developed on the second half of the twentieth century. The 'mutation accumulation theory' postulated by Peter Medawar in 1952 (Medawar, 1952) argues against Weismann's 'programmed death theory' and states that detrimental mutations acting in early life will be strongly selected against (not passed on to the next generation), whilst mutations deleterious for later life will prevail as the individual has already passed them on to the next generation. As a consequence, mutations detrimental for later life will passively accumulate and generate the panoply of changes characteristic of old age (ageing phenotype).

The 'antagonistic pleiotropy theory' (Kirkwood & Austad, 2000), advanced by George Williams in 1957, proposes that the reason late-acting detrimental genes might not be selected against is because they provided a selective advantage in early life. Therefore, pleiotropic genes (genes with more than one effect) might be actively conserved in the gene pool because of their beneficial effect but, as a consequence, the organism would have to endure the antagonistic effect; this is also known as the 'pay later theory'.

More recently, Thomas Kirkwood and Robin Holliday proposed an update on the antagonistic pleiotropy theory, called the 'disposable soma theory' (Kirkwood, 1977; Kirkwood & Austad, 2000). The authors refer to a special class of gene mutations with the purpose of saving energy for reproduction (positive early effect) by partially disabling molecular proofreading (repair mechanisms) in somatic cells (negative later effect). The idea is that higher organisms adopt an energy saving strategy for the maintenance of somatic cells with the purpose of accelerating development and reproduction which will, however, result in deterioration and death.

The genetic basis of ageing and lifespan

Following groundbreaking discoveries in cell biology and molecular pathways in the 1990's the original concept of ageing might be in need of revision. Research shows that ageing, like other biological processes, is regulated by classical signalling pathways and transcription factors (reviewed in (Kenyon, 2010)). Thus, although the process of ageing is in fact intrinsic, the question of whether it is 'inevitable and irreversible' (Comfort, 1979) might be debatable.

The first evidence that organismal lifespan can be manipulated came from a seminal study in *C. elegans* where a mutation (in the *daf-2* hormone receptor) in the insulin/IGF-1 pathway more than doubled the lifespan of the worms (Kenyon *et al*, 1993). This was followed by evidence that mutations in other metabolic pathways could also affect lifespan, which was interestingly accompanied by considerable improvements in healthspan, in various model systems. These include pathways signalled by the kinase target of rapamycin (TOR), AMP kinase (AMPK), sirtuins (SIRTs) and by insulin/IGF-1 receptors, through forkhead box O (FOXO) and other transcription factors. These nutrient and stress sensors mediate lifespan extension in response to environmental and physiological cues and caloric restriction (Fig. 1.1), for instance, has been shown to extend lifespan in species ranging from yeast to primates (Kenyon, 2010). They do so by regulating processes such as autophagy (Kenyon, 2010), mitochondrial function and even the activity of the central tumour suppressor p53 (Sahin & DePinho, 2012).
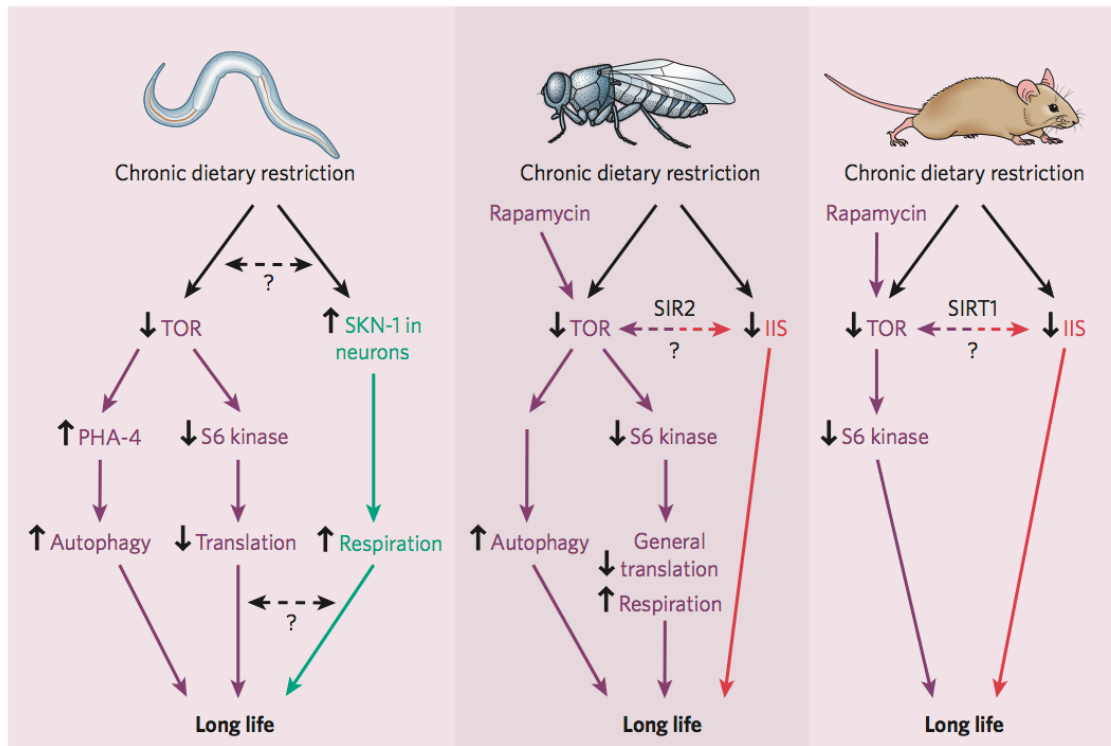
Figure 1.1. Pathways that influence lifespan extension in response to caloric restriction in worms, flies and mice. Chronic dietary restriction extends lifespan by down-regulating TOR activity. In order for caloric restriction to extend lifespan in worms and flies via TOR inhibition it requires autophagy. whilst in flies and mice sirtuins are required instead. Legend: TOR = target of rapamycin; IIS = insulin/IGF-1 signalling (*in* (Kenyon, 2010)).

In addition to metabolic pathways, telomere maintenance in particular and DNA integrity in general have a crucial role in ageing. Several studies underscore the importance of telomere dysfunction and of the main molecular effectors of cellular senescence as driving forces of the ageing process at the organismal level (Campisi & d'Adda di Fagagna, 2007; Sahin & DePinho, 2010; 2012).

1.2. Cellular senescence

Replicative senescence and the end-replication problem

The concept of replicative senescence emerged in the 1960s from the work of Leonard Hayflick and Paul Moorhead (Hayflick & Moorhead, 1961). They meticulously documented the development and characterisation of 25 strains of human fibroblasts, derived from organs such as skin, lung and kidney, all of foetal origin. Diploid cell strains shared a similar growth history which could be divided into three phases: Phase I, or early growth phase, from when cells were obtained from the original tissue until the primary cultures were established; Phase II, or rapid growth phase, when cells were serially sub-cultivated and cultures exhibited high rates of cell division and metabolism; and Phase III, or terminal phase, characterised by accumulation of debris, altered cellular morphology and cell division arrest. Cells could remain in this phase for several months until they eventually died. These findings contradicted earlier work (Carrel, 1912), later shown to be experimentally flawed, which suggested that diploid cells were able to proliferate indefinitely. Thus, possible explanations for the 'Phase III phenomenon', such as the presence of virus, composition of the growth medium or metabolite depletion with subculture, were tested. However, experimental evidence strongly supported the occurrence of senescence at the cellular level (Hayflick & Moorhead, 1961). Firstly, the authors showed that the same pool of medium allowed for both growth and cellular degeneration; then, unless virus can distinguish between female and male cells they were also not a plausible cause for the Phase III phenomenon. This is because when two populations of cells with distinct doubling potential, an actively dividing female strain and a senescent male strain, were mixed and cultured for 17 doublings, the resulting population was composed solely of female cells. The results from this experiment and others showing that cells retain 'memory' of their passage number when frozen suggested that senescence is a process intracellularly determined and that its engagement is a function of cumulative cell doublings, not of calendar time (Hayflick & Moorhead, 1961; Hayflick, 1965). All cell strains exhibited a consistent maximum number of doublings, their 'passage potential'. This cell division limit, known as the 'Hayflick Limit', is the total number of population doublings (PDs)

a normal cell population can undergo in culture before reaching replicative exhaustion. Hayflick and Moorhead's work was pioneer in conclusively establishing that normal human diploid cells exhibit a finite lifespan in culture and challenged the incorrect notion of cellular 'immortality' which had prevailed for the previous 50 years. The authors argued that replicative senescence was the result of the gradual depletion, over generations in culture, of an intrinsic factor to a critical level that when surpassed became inconsistent with further cell division.

The shortening of chromosome ends, or telomeres, consequence of the 'end-replication problem', was first suggested as the intrinsic factor responsible for the limited doubling potential of clones of normal somatic cells by Alexey Olovnikov in 1971 (Olovnikov, 1971). Olovnikov theoretically predicted that the replication of linear genomes (as opposed to circular genomes) came with inherent loss of genetic material. James Watson reached a similar conclusion, independently, one year later (Watson, 1972) and this phenomenon became known as the end-replication problem. Basically, during each cell division, DNA replication is incomplete at the 5' end of the lagging strand, due to the directional limitation of the DNA polymerase, resulting in loss of terminal DNA after each round. In his 'Theory of Marginotomy' (Olovnikov, 1973) Olovnikov suggested that either the existence of a catalytically inactive zone in the DNA-polymerase or the need for an initiating RNA-primer would result in incomplete replication at the DNA ends. Therefore, a mechanism to maintain chromosome ends would be required or loss of terminal sequences would ensue. More importantly, Olovnikov predicted the biological significance of this phenomenon. Gradual erosion of telomeric DNA could explain how cells were able to 'count' doublings. Also, since critical loss of the 'buffer' terminal regions would risk permanent loss of adjacent genes this could trigger senescence and, thus, explain the 'Hayflick limit'. He also suggested that germ line cells and tumour cells were able to avert telomere erosion by expression of a special form of polymerase, non-existent in normal somatic cells. This would ensure protection of important genetic information in germ cells and confer immortality to tumour cells. Olovnikov's theory was not adopted as an explanation for the 'Hayflick limit' due to lack of experimental validation. This became possible over the following decade with the discovery of both the telomeric DNA sequence and the enzyme telomerase, as well as the development of experimental methods to measure telomere length such as

telomere restriction fragment (TRF) analysis (Allshire *et al*, 1988) and single telomere length analysis, or STELA (Baird *et al*, 2003).

The structure of telomeric DNA was first characterised in the ciliated protozoan *Tetrahymena thermophila* (Blackburn & Gall, 1978). Restriction endonuclease digestion of *Tetrahymena*'s extrachromosomal DNA revealed a terminal rDNA linear fragment composed of characteristic hexa-nucleotide TTGGGG repeats organised in tandem. A few years later Allshire *et al* made the surprising discovery that the telomeric repeats of Tetrahymena cross hybridised with human telomeres, as well as with telomeres of several other eukaryotes including the mouse (Allshire *et al*, 1988). The authors used restriction endonucleases which can digest total genomic DNA, with the exception of the telomeric repeat tracts whose distinctive feature is their lack of restriction sites, fragments were separated by gel electrophoresis, blotted into a nylon membrane and finally incubated with a radio-labelled telomeric probe (containing *Tetrahymena*'s TTGGGG repeats). Following exposure to autoradiographic film the long undigested telomeric fragments appeared as a DNA smear. This seem to be variable in size which was very interesting since it could be indicative of the heterogeneity in telomere length observed in different organisms. The ultimate confirmation that hybridisation was occurring at the telomeres was demonstrated by using a restriction enzyme, in addition to the other endonucleases, which can digest telomeric DNA. The smear completely disappeared after this treatment conclusively showing that it consisted of telomeric DNA. This was also supported by the observation that the smear was more homogeneous and of higher molecular weight in germline DNA than in somatic DNA (Allshire *et al*, 1988). Later it was shown to directly reflect the amount of TTAGGG repeats, and not other repeat types present in sub-telomeric regions, suggesting that TTAGGG was the telomeric DNA sequence in humans (Allshire *et al*, 1989). In addition, since TTAGGG probes were found to hybridise very strongly with telomeric smear in human and mouse DNA the two species apparently share the same telomeric sequence. These findings were very important as this technique could be used to assess telomere length and total amount of telomeric DNA by assessing the amount of probe that hybridises with the fragments and the size of the smear itself. Southern blot analysis using telomeric probes was the first technique used to measure average telomere length and became known as Telomere Restriction Fragment analysis.

Using TRF analysis Harley & Greider (Harley *et al*, 1990) were able to show for the first time that loss of telomeric DNA did in fact occur with serial passage in culture. They cultured human fibroblasts strains until terminal passage, an established method to assess *in vitro* ageing, and analysed both the size distribution and total amount of terminal restriction fragments (telomeres) by Southern blot analysis (TRF analysis). They observed a consistent 2Kb decrease in average telomere length with cumulative population doublings (PDs). This was accompanied by a decrease in the total amount of telomeric DNA as observed by the reduced intensity of the smear measured by densitometry and which is direct function of the amount of TTAGGG probe hybridising with telomeric DNA. This indicates true loss of DNA and not just rearrangement of telomeres in relation to restriction sites. Telomeric loss was also not a result of general DNA degradation or loss during preparation since other internal repetitive sequences remained unaltered in size and quantity. Authors also discarded loss as a function of growth stage. Making use of TRF analysis, Harley and Greider were able to establish that telomere loss was in fact a function of doublings *in vitro* whose rate was more consistent with incomplete copying of the template at the DNA ends rather than due to degradation of terminal regions, for example. These findings support Olovnikov's theory (Olovnikov, 1971; 1973) that incomplete end replication and consequent telomere loss with each doubling is responsible for the Hayflick Limit. Similar findings were obtained in human skin, regarding decrease in mean telomere length as well as total telomeric DNA with donor age, and also based on TRF analysis, demonstrating that loss of telomeric repeats not only occurs with ageing *in vitro* but also *in vivo* (Lindsey *et al*, 1991).

During the 1980s, the DNA polymerase capable of specifically elongating terminal DNA (telomerase) was finally discovered based on the ongoing work of Carol Greider and Elizabeth Blackburn in *Tetrahymena*. This was based on observations that telomeres in this model organism were dynamic structures which could actually increase in length. Given the known limitation of conventional DNA polymerases to fully replicate the ends of chromosomal DNA it was unlikely that these enzymes were responsible for telomere elongation in *Tetrahymena*. Greider and Blackburn (Greider & Blackburn, 1985) observed that *Tetrahymena* extracts contained telomere elongation activity with specific incorporation of dGTP and dTTP in a characteristic 6-base pattern, TTGGGG. They determined this by sequentially adding different combinations of radio-labelled and unlabelled nucleotides to

the extracts in presence of a synthetic single stranded DNA template composed of *Tetrahymena*'s TTGGGG repeats. The DNA products obtained from each reaction were resolved in a sequencing gel and detected by autoradiography. A repeating pattern of two labelled dGTPs and four unlabelled dTTPs bands was obtained only for combinations of these two nucleotides and absent for all other combinations as well as in conditions where the telomeric template was absent or when DNA polymerase I was used instead of *Tetrahymena* extract. In all, this suggested that tandemly repeated TTGGGG sequences were being synthesised. This work presented the first evidence of a terminal transferase-like activity that specifically adds telomeric repeats onto a synthetic telomere template. This synthesis demonstrated characteristics of an enzyme-catalysed reaction such as high reaction efficiency and substrate affinity as well as susceptibility to heat and proteinase K treatment. Greider and Blackburn went on to show that telomerase from *Tetrahymena* can correctly add *Tetrahymena* telomeric repeats (TTGGGG) to template oligomers from yeast and other organisms so long as they contained G-rich telomeric sequences (Greider & Blackburn, 1985; 1987). Telomerase turned out to be a ribonucleoprotein enzyme whose protein component seemed necessary for template recognition whilst the RNA component seemed responsible for its specificity (Greider & Blackburn, 1987; 1989).

Following the cloning of the human reverse transcriptase subunit of telomerase, hTERT (Nakamura *et al*, 1997), the opportunity to manipulate telomere length became available and finally allowed for the hypothesis that telomere shortening triggers senescence to be tested. Bodnar *et al* (Bodnar *et al*, 1998) found that expression of telomerase in normal cells corrected telomere length and, as a consequence, allowed cells to evade senescence and to acquire an extended replicative potential. This was demonstrated by ectopically expressing the catalytic component of telomerase, hTERT in two human strains, of foreskin fibroblasts and retinal pigment epithelial cells, using plasmid vectors. As expected, transfected clones showed telomerase activity, as assessed by the TRAP assay, in opposition to non-transfected controls. This was accompanied by an increase in mean telomere length, as measured by TRF analysis, and lifespan extension in the cells expressing telomerase. In contrast, controls arrested proliferation and engaged senescence as demonstrated by selective staining for the senescence associated β-galactosidase marker to levels consistent with senescence. Therefore, correction of telomere loss by expression of the enzyme capable of elongating

telomeres seemed to allow these cells to evade or, at least, delay senescence. These findings strongly suggest that telomere loss, in the absence of telomerase, is the intrinsic property that controls the replicative potential of normal diploid cells and, thus, the number of cell divisions they can undergo until the onset of senescence. This work finally established a relationship of causality between telomere shortening and replicative senescence.

Further investigation using mouse models revealed that the shortest telomere, and not average telomere length, was the determining factor in the engagement of senescence (Hemann *et al*, 2001). Hemann *et al* made use of the recently engineered late generation telomerase-null mice (Blasco *et al*, 1997) possessing a phenotype indicative of telomere dysfunction which is characterised by infertility accompanied by germ cell apoptosis and a high incidence of chromosome end-to-end fusions. When these animals, telomerase-deficient with short telomeres (*mTR-/-* G6) were crossed with animals heterozygous for telomerase activity and thus with long telomeres (*mTR +/-*) they produced offspring with an equal amount of short and long telomeres and differing only in telomerase activity. This made it possible to distinguish between the cellular response elicited by the shortest telomere and the one triggered by decreased mean telomere length. The telomerase positive offspring (*mTR+/-* F1) displayed a wild-type phenotype, similar to the heterozygous parental mice. In contrast, the telomerase-null offspring (*mTR-/-* F1) showed increased germ cells apoptosis accompanied by a corresponding decrease in testis weight and a number of chromosome fusions similar to that found in the telomerase-null parental mice (*mTR-/-* G6). Since both offsprings have a similar number of short telomeres, the results indicate that the presence of telomerase (in *mTR+/-* F1) rescues the telomere dysfunction phenotype. The strong phenotype exhibited by telomerase-deficient *mTR-/-* F1 animals also suggests that the presence of critically short telomeres is sufficient to elicit a cellular response. To confirm this finding, the authors performed telomere length analysis in splenocytes of these animals using quantitative fluorescent *in situ* hybridisation (Q-FISH). They found that although average telomere length was very similar between the telomerase-proficient and telomerase-deficient offspring, the latter contained a significantly high number of telomeres completely lacking detectable telomeric repeats, which were specifically absent in the telomere length distribution of the heterozygous offspring. This suggested that in these animals telomerase was restoring telomere length by

adding repeats to the shortest telomeres, therefore preferentially rescuing them, rather than by increasing the mean telomere length of all telomeres.

A couple of years later, with the development of STELA, an innovative molecular technique for analysis of individual telomere length, it was confirmed that at senescence there is almost complete loss of telomeric repeats (Baird *et al*, 2003). Single Telomere Length Analysis, or STELA, consists in applying single molecule PCR to accurately measure telomere length of the same chromosome end (XpYp, for example) in all cells (both dividing and non-dividing) of a sample population. It exploits the fact that all telomeres end in a single stranded 3' G-rich overhang and makes use of an oligonucleotide linker which anneals and is ligated to the 5' end of the telomere using the overhang as a specific template. A linker-specific primer is then used in conjunction with a primer specific for a sub-telomeric region of a particular chromosome. This allows for amplification of an individual amplicon for each specific telomere which offers the distinct advantage of detecting subtle changes in telomere length and abruptly shortened telomeres. STELA analysis of XpYp telomeres in normal human diploid fibroblast strains (Baird *et al*, 2003) revealed that at senescence some telomeres showed almost no TTAGGG repeats (roughly 45bp) indicating that telomere loss occurs from a subset of chromosomes. It also showed that the distribution of telomere lengths was bimodal, resulting from inter-allelic differences of up to 6.5Kb which shows large heterogeneity in telomere length between alleles. Further analysis of individual alleles during clonal expansion from a single cell of a particular strain revealed that, as for different strains, all subclones entered replicative senescence at different XpYp lengths, again with some showing almost complete loss of telomeric repeats. Since starting telomere length is the same, the unexpected heterogeneity observed between alleles suggests these differences are inherited. Also, as telomeres shorten gradually with each doubling independently of initial allele size and since rate of erosion seems consistent with loss due to incomplete end-replication, other mechanisms possibly contribute to more substantial changes in telomere length. These data also point to a highly stochastic process rather than to a synchronised 'clock'-like event determining the engagement of senescence.

This is consistent with classical studies which showed that the replicative potential of individual clones within a population of normal cells is highly variable (Smith & Hayflick, 1974) and that it is even distinct between daughter

cells in mitotic pairs (Smith & Whitney, 1980). The doubling potential of human foetal diploid fibroblasts was assessed after isolation from mass culture at different stages of its lifespan (Smith & Hayflick, 1974). Contrarily to earlier findings, where the limited number of clones selected happened to reflect the replicative potential of the culture (Hayflick, 1965), the wide range of individual cells tested showed a high extent of heterogeneity in their doubling potential when compared to the mass culture they derived from (Smith & Hayflick, 1974). More detailed and meticulous analysis (Smith & Whitney, 1980) revealed that this variation was intrinsic to each clone, since recloning of a clone with a high doubling potential originated subclones exhibiting varied division potential. Moreover, Smith and Whitney analysed the behaviour of two cells originating from the same mitosis and observed that their maximum replicative capability can differ by as many as 8PDs. Both the rapid occurrence of intraclonal variation and the large heterogeneity in daughter cells arising from the same mitotic event suggest that the doubling potential of human diploid cells is determined stochastically.

These studies also pointed to a bimodal distribution of clones in a cell population which was consistent with findings obtained on bulk cultures. Clones obtained from human diploid fibroblast cultures seemed to originate from two distinct subpopulations, one capable of a maximum of 8 doublings and another with a much higher doubling potential. The group with limited doubling potential appeared to increase with incremental doublings of the mass culture at the time of cloning (Smith & Hayflick, 1974). The ability of cells to incorporate nucleotides or their analogues, such as ^{3}H-thymidine or 5-bromodeoxyuridine (BrdU), into their DNA indicates that they are undergoing active DNA replication and are, therefore, in cycle. Thymidine incorporation was used to determine the fraction of cells entering S phase at each passage of the lifespan of cultures of human diploid fibroblasts (Cristofalo & Sharf, 1973). This analysis revealed that the fraction of unlabelled cells (non-dividing) increased with serial passage. This gradual reduction in the thymidine labelling index was shown not to be due to an increase in length of the cell cycle towards the culture's maximum lifespan. In addition, it was found that non-dividing cells were present in the culture at early passages and some actively dividing cells could also still be found at late passages (Cristofalo & Sharf, 1973; Grove & Cristofalo, 1977). This suggests that cells in a population do not divide synchronously, that there is a stochastic factor determining their exit decision from the cell cycle and finally

that cultures are bimodal mixtures of dividing and senescent cells the proportion of which changes with time in culture.

Although telomere shortening provided the first molecular explanation for the replicative exhaustion of cells in culture or replicative senescence, other telomere-independent factors can also trigger senescence. Thus the general term cellular senescence being adopted instead.

Cellular senescence

Whilst the term replicative senescence is applied to cells that cease to divide as a consequence of replicative exhaustion through telomere shortening, the term cellular senescence is more general and applies to all the situations where the senescent program can be activated. Several stimuli can induce senescence; these can be generally divided into factors that generate a DNA damage response (DDR) and factors that do not. Eroded or dysfunctional telomeres, non-telomeric DNA damage in the form of DSBs, chemicals that interfere with chromatin structure (histone deacetylase inhibitors (HDACIs), for example) and strong mitogenic signals (from oncogenes or proliferation genes) which cause DNA damage, are signalled through ATM or ATR and activate the tumour suppressor p53 with a sustained DDR. Additionally, physiological stress arising from inappropriate support layer in culture, lack of nutrients or growth factors, oxidative stress and mitogenic signals are signalled through the tumour suppressor p16^{INK4a} and activate the retinoblastoma protein (pRb) or, alternatively, through ARF activating p53, without a DDR (reviewed in (Rodier & Campisi, 2011)). The senescence program is thus controlled by the p53 and p16^{INK4a}-pRb pathways (Fig. 1.2).

Senescence can be defined as a permanent block to further replication, however, cells that do not divide can also be quiescent, apoptotic or terminally differentiated. The distinction between senescence and quiescence, apoptosis or terminal differentiation has been demonstrated experimentally. For instance, keratinocytes prevented from terminally differentiating by being cultured in low levels of calcium engage senescence and are subsequently able enter the differentiation program once the calcium concentration is increased (Norsgaard *et al*, 1996). In addition, whilst the proliferative capacity of human keratinocyte cultures decreases over time (Rheinwald & Green, 1975a), the

apoptotic rate remains constant throughout their lifespan (Norsgaard *et al*, 1996). Finally, quiescence in culture can be induced by serum starvation or by cell confluence but, as opposed to senescence, it is a transient growth arrest reversible by re-addition of serum to the growth medium or by sub-cultivation. Although longer periods of confluence do lead to the accumulation of p16^{INK4a} and result in senescence (Munro *et al*, 2001).
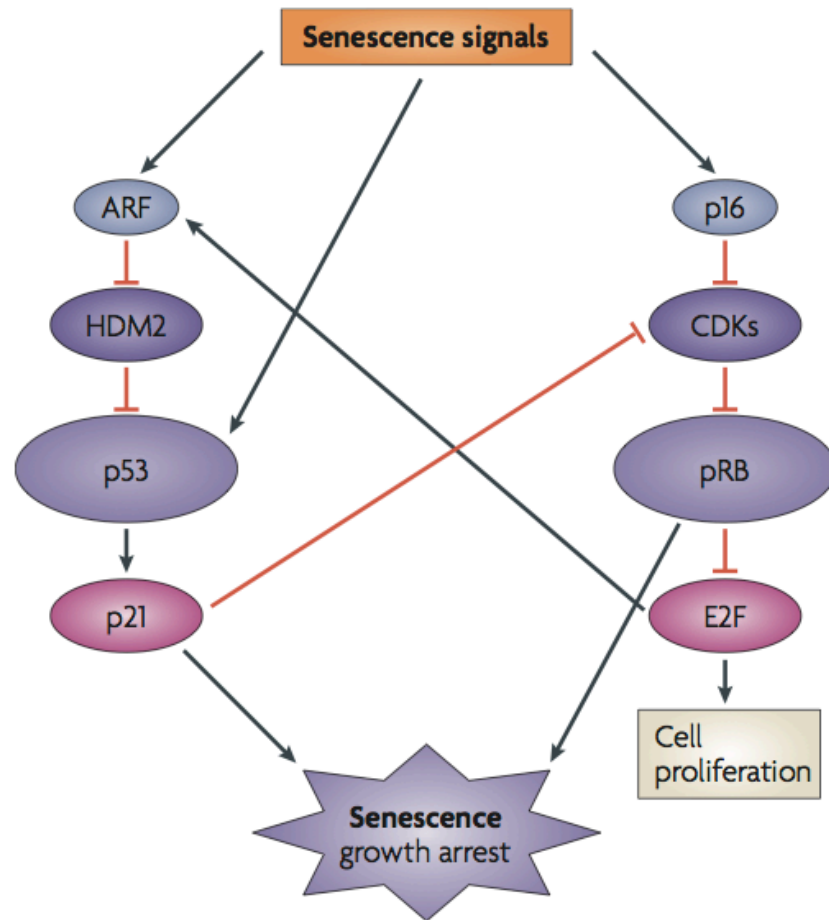
Figure 1.2. Molecular pathways of senescence. p53 and pRb are the central effectors of senescence and control the p53 and p16^{INK4a}/pRb pathways (*in* (Campisi & d'Adda di Fagagna, 2007)).

Only mitotic cells are able to undergo senescence since post-mitotic cells have already lost their ability to divide due to terminal differentiation. Nevertheless, although most terminally differentiated cells are post-mitotic

some characteristically retain mitotic potential, as is the case of lymphocytes whose function is to undergo clonal expansion upon stimulation by the appropriate antigen. Mitotic cells can, therefore, remain quiescent in proliferative tissues and be promptly induced to divide in the presence of the appropriate stimuli, including oncogenic or mitogenic signals leading to cancer. One of the first features senescent cells acquire is resistance to mitogenic and apoptotic signals. This is accompanied by morphological and biochemical changes in addition to a distinct gene expression profile. These features, which characterise senescence, are generally known as the senescent phenotype (reviewed in (Campisi & d'Adda di Fagagna, 2007)).

The senescent phenotype

Senescent cells are thought to arrest growth in phase G1 of the cell cycle (Grove & Cristofalo, 1977; Di Leonardo *et al*, 1994; Serrano *et al*, 1997; Herbig *et al*, 2004), and are henceforth unable to resume DNA replication. The senescence growth arrest is permanent and irreversible under normal culture conditions (Fig. 1.3). Cells increase greatly in size (Hayflick, 1965) with a characteristic morphology and remain metabolically active despite being reproductively sterile. Senescent cells express a senescence-associated beta galactosidase (SA-βgal) which indicates β-galactosidase activity detectable at pH 6.0 (Dimri *et al*, 1995) and is thought to reflect an increase in lysosomal mass (Lee *et al*, 2006). Increase in mitochondrial mass has also been reported in senescent cells (Passos *et al*, 2007b). Senescence is also accompanied by a series of drastic general changes in gene expression whose patterns tend to be cell-type specific (Shelton *et al*, 1999).

Most senescent cells express the two main cyclin-dependent kinase inhibitors (CDKIs) p21^{WAF1} (or CDKN1a) and p16^{INK4a} (or CDKN2a) (Fig. 1.3), which are components of tumour-suppressor pathways governed by the transcriptional regulators p53 and pRb which activate senescence (Campisi, 2001a). Expression of these cell cycle inhibitors results in pRb-directed inactivation of the transcription factor E2F and its target genes (cyclin A, PCNA, c-FOS, for example) involved in cell-cycle progression. These genes can also be silenced by pRb-mediated reorganisation of chromatin into senescence-associated heterochromatic foci or SAHFs (Narita *et al*, 2003).

Many senescent cells also over-express genes that encode for secreted proteins which have the potential of altering the tissue microenvironment (Campisi & d'Adda di Fagagna, 2007; Rodier & Campisi, 2011). The senescence secretome includes, amongst others, matrix metalloproteinases (MMPs) and inflammatory cytokines, such as interleukines 6 and 8 (IL-6 and IL-8), secreted by dermal fibroblasts and keratinocytes (Shelton *et al*, 1999; Kang *et al*, 2003; Coppé *et al*, 2008) and growth factors, such as vascular endothelial growth factor (VEGF), secreted by fibroblasts (Coppé *et al*, 2006). These factors which have been defined as the senescence-associated secretory phenotype or SASP (Coppé *et al*, 2008), are secreted as a consequence of persistent DDR signalling, possibly in an attempt from senescent cells to communicate their compromised state and request clearance by the immune system (Rodier *et al*, 2009). However, they have also been associated with cell migration and invasiveness, characteristics which define tumour progression (Coppé *et al*, 2010).

Finally, senescent cells harbour two main types of persistent nuclear foci, SAHFs and DNA-SCARS, which account for the irreversibility of the senescent state (Fig. 1.3). Senescence-associated heterochromatic foci, or SAHFs, are nuclear structures containing heterochromatin which have been associated with stable repression of E2F target genes through accumulation of pRb in their promoters. Activation of pRb is a requirement for SAHF formation and E2F target gene silencing and is thought to contribute to changes in gene expression associated with senescence (Narita *et al*, 2003). DNA segments with chromatin alterations reinforcing senescence, or DNA-SCARS, are persistent DNA foci, present in senescent cells with sustained DDR signalling, that associate with PML nuclear bodies and contain activated forms of DDR proteins such as p53 and CHK2. However, as opposed to transient foci, these lack the DNA repair proteins RPA and RAD51, single-stranded DNA and DNA synthesis. DNA-SCARS also associate with histone H2AX, which is responsible for their stabilisation and modulation of growth arrest and cytokine secretion associated with senescence. Although these dynamic structures require p53 and pRb to trigger the growth arrest, they can be formed independently of these cell cycle regulators (Rodier *et al*, 2011). A specialised type of DNA-SCARS are the persistent DNA damage foci that colocalise with telomeres, also known as telomere dysfunction–induced foci, or TIFs (d'Adda di Fagagna *et al*, 2003; Takai *et al*, 2003; Herbig *et al*, 2004).
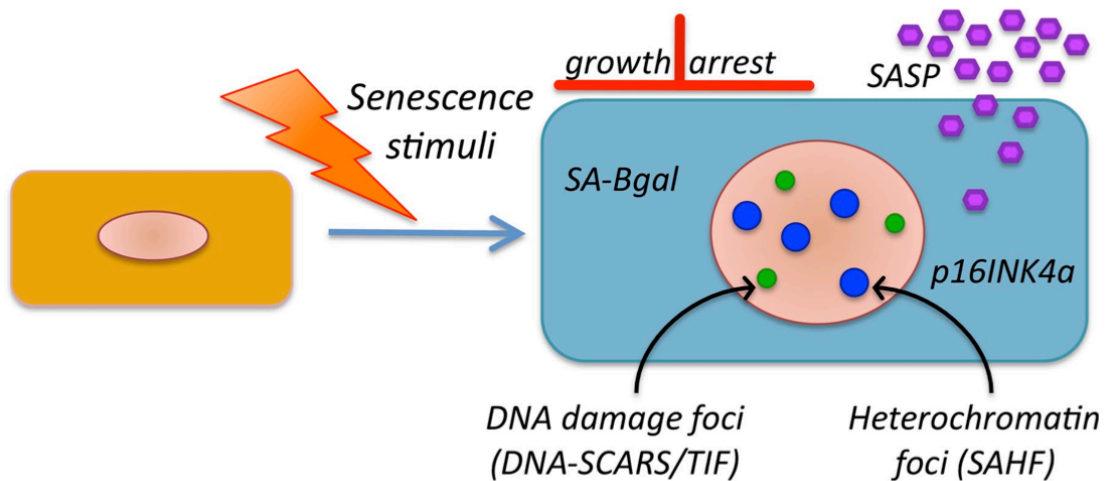
Figure 1.3. The senescent phenotype. Hallmarks of senescent cells include irreversible growth arrest, expression of SA-βgal and p16^{INK4a}, secretion of growth factors, cytokines, proteases, and other proteins (SASP), and nuclear foci containing DDR proteins (DNA-SCARS/TIF) or heterochromatin (SAHF) (*in* (Rodier & Campisi, 2011)).

None of the above features can be used in isolation as a specific indicator of cellular senescence. However, the combination of various of these features can be used to accurately identify senescent cells and distinguish them from their quiescent or terminally differentiated counterparts. Expression of p16^{INK4a} is an important hallmark of senescence since it is not associated with quiescence or terminal differentiation (Hara *et al*, 1996; Serrano *et al*, 1997). Also, p16^{INK4a}-related organisation of heterochromatin into SAHFs, also does not occur in quiescent cells (Narita *et al*, 2003). Finally, p16^{INK4a} expression has been shown to increase in mouse and human tissues with age (Krishnamurthy *et al*, 2004; Ressler *et al*, 2006) and to be an accurate indicator of physiological age (Waaijer *et al*, 2012).

Hayflick's early observations regarding senescence in culture (Hayflick & Moorhead, 1961) lead him to establish two important connections for which there is strong evidence today. First, the fact that tumour cells appear to undergo unlimited proliferation in culture might indicate that senescence, by permanently preventing it, evolved as a tumour-suppression mechanism. Second, the aged-like phenotype senescent cells presented in culture

prompted Hayflick to establish a connection between replicative senescence and organismal ageing. Senescence can contribute to ageing *in vivo* either by causing a decline in the regenerative capacity of the tissue by targeting the stem cell compartment (intrinsic ageing of stem cells) or by affecting the tissue microenvironment indirectly via the senescent secretome. Consequently, senescence is regarded as an example of antagonistic pleiotropy because it prevents tumourigenesis early in life but, due to accumulation of senescent cells in mitotic tissues, may promote cancer and ageing later in life (Campisi, 2005; Campisi & d'Adda di Fagagna, 2007).

1.3. Senescence, tumour suppression and ageing.

Senescence as a tumour suppressor mechanism

Several lines of evidence support the idea that senescence acts as a tumour-suppressor mechanism. The concept was first proposed by L. Hayflick in the 1960s (Hayflick, 1965) when he observed that normal diploid cells could only escape senescence by acquiring cancer-like properties. Thus, whilst one of the hallmarks of senescence is the establishment of permanent cell cycle arrest, the ability to divide indefinitely is characteristic of cancer (Hanahan & Weinberg, 2000). In addition, most cancer cells harbour mutations in the p53 or the p16^{INK4a}/pRb tumour suppressor pathways. This renders the main cell cycle regulators and effectors of senescence p53 and/or pRb dysfunctional, thus allowing cells to overcome the two main cell cycle checkpoints imposed by senescence (Campisi, 2001a; Finkel *et al*, 2007). Furthermore, neoplastic transformation by viral or cellular oncogenes requires the disruption of senescence checkpoints such as ATM and CHK2 (Gorgoulis *et al*, 2005; Bartkova *et al*, 2006).

Expression of oncogenic Ras in human or murine cells results in oncogenic-induced senescence (OIS) via accumulation of p53 and p16^{INK4a} (Serrano *et al*, 1997). It has been shown to promote DNA replication stress which contributes to stochastic telomere attrition and dysfunction (Suram *et al*, 2012). It also results in mitochondrial dysfunction, characterised by increased mitochondrial mass and production of ROS, which leads to oxidative stress. This contributes to OIS and depends on functional p53 and pRb (Lee *et al*, 1999; Moiseeva *et al*, 2009). The use of inhibitors of mitochondrial function in human cells expressing activated Ras induces senescent arrest (Moiseeva *et al*, 2009) which can be reversed by antioxidants (ROS scavengers) or by low oxygen treatment (Lee *et al*, 1999). Also, inactivation of p53 or p16^{INK4a} in mouse cells prevents Ras-induced G1 arrest allowing for transformation to occur (Serrano *et al*, 1997). Over-expression of other oncogenes (Mos and Cdc6) also results in induction of p16^{INK4a} and increased replicative stress consequently activating a DNA damage checkpoint. However, whilst inactivation of ATM suppressed senescence p16^{INK4a} depletion did not, suggesting variability in the response to different oncogenes (Bartkova *et al*, 2006).

Several *in vivo* studies corroborate these findings. Combined inactivation of tumour suppressors PTEN and p53 in mouse prostate results in invasive cancer and early death (Chen *et al*, 2005), whilst inactivation of ATM in a mouse tumour model also led to increased tumour size and invasiveness (Bartkova *et al*, 2006). Additionally, in a mouse model of Burkitt's lymphoma through *Myc* expression (Feldser & Greider, 2007) where animals were made *Terc*-deficient (*mTR$^{-/-}$*) the formation of tumours is suppressed by telomere dysfunction-induced senescence (TDIS). This response in animals with short telomeres was shown to be mediated by p53 since its deletion reversed the phenotype. Conversely, mouse models of p53 over-expression, either through a mutation that results in p53 activation (Tyner *et al*, 2002) or through introduction of extra transgenic copies of the p53 gene ('Super p53' mice) (García-Cao *et al*, 2002), exhibit significant cancer-resistance however accompanied by an onset of ageing phenotypes.

Additionally, the fact that senescence is more common in pre-malignancy than in malignancy also indicates that it may be a barrier to tumourigenesis. Senescent cells are abundant in pre-malignant lesions in mouse models of *Pten* deletion (Chen *et al*, 2005) and *Myc* expression (Feldser & Greider, 2007) but not in the cancers that arise from them. Evidence of senescence markers was also found in the early stages of human prostate (Chen *et al*, 2005), urinary bladder and breast (Bartkova *et al*, 2005), as well as in colon adenomas (Bartkova *et al*, 2006), lung hyperplasias (Bartkova *et al*, 2005; Gorgoulis *et al*, 2005) and dysplastic nevi (Michaloglou *et al*, 2005; Gorgoulis *et al*, 2005; Suram *et al*, 2012). In colon adenomas and lung hyperplasias, for instance, there was strong evidence of DNA damage-induced senescence, such as activated histone H2AX and CHK2, p53 accumulation, and apoptosis (Bartkova *et al*, 2005; Gorgoulis *et al*, 2005; Bartkova *et al*, 2006). In human nevi, colon and breast cancer precursor lesions, the majority of the DDR factors were found to associate with telomeres, indicating engagement of telomere dysfunction-induced senescence (Suram *et al*, 2012). Progression to cancer was associated with inactivation of p53 and 53BP1, and decreased apoptosis (Gorgoulis *et al*, 2005), whilst chemotherapy or reactivation of p53 in certain tumours caused tumour regression which was associated with senescence (Ventura *et al*, 2007; Xue *et al*, 2007; Coppé *et al*, 2008). All this body of work shows that oncogenic signalling contributes to replication stress and oxidative stress which leads to DNA DSBs, telomere dysfunction, genomic instability and selective pressure for p53 mutations, all factors that are

associated with the development of malignancy. Senescence (OIS, TDIS and DDR-induced) is activated at the early stages of transformation in an attempt to delay or prevent tumourigenesis and is, undoubtedly, a critical tumour suppressive response *in vivo*. This is underlined by the fact that several of the key molecules involved in senescence such as ATM (Savitsky *et al*, 1995), p53, CHK1 and CHK2 (Malkin *et al*, 1990) and p16^{INK4a} (Kamb *et al*, 1994) are all *bone fide* tumour suppressors.

Senescence, as it primarily entails permanent growth arrest, is thought to suppress tumourigenesis because cancer development requires cell proliferation (Hanahan & Weinberg, 2000). Surprisingly, senescence can also promote cancer (Rodier & Campisi, 2011). Senescent cells secrete various proteins, such growth factors, proteases, cytokines and other inflammatory factors, generally referred to as the SASP, which can contribute to development of malignancy (Coppé *et al*, 2008; 2010). Interleukines 6 and 8 (IL-6 and IL-8) induced pre-malignant epithelial cells to invade a basement membrane (Coppé *et al*, 2008) and VEGF, secreted by senescent fibroblasts, also stimulated endothelial cell migration and invasion which are changes associated with angiogenesis (Coppé *et al*, 2006). Also, matrix metaloproteinases which get secreted by senescent fibroblasts and keratinocytes were also associated with invasiveness (Kang *et al*, 2003; Coppé *et al*, 2010). Finally, this has also been observed *in vivo*, as senescent fibroblasts co-injected with pre-malignant or malignant epithelial cells induced tumours or accelerated tumour formation in mice (Krtolica *et al*, 2001). Another example comes from areas of micro-invasion in advanced SCCs where p16^{INK4a}-positive keratinocytes co-express the ɣ2 subunit of laminin 5, a basement membrane protein associated with increased directional mobility (Natarajan *et al*, 2003). The same phenotype is observed in senescent keratinocytes and in keratinocyte migration during wound healing (Natarajan *et al*, 2003; 2006). This suggests that although senescence prevents tumourigenesis it can also contribute to cancer later on, through changes it causes in the cellular microenvironment (Fig. 1.4). The paradoxical effect of senescence in cancer is one of the contexts in which it is an example of antagonistic pleiotropy; another is how senescence also contributes to ageing.
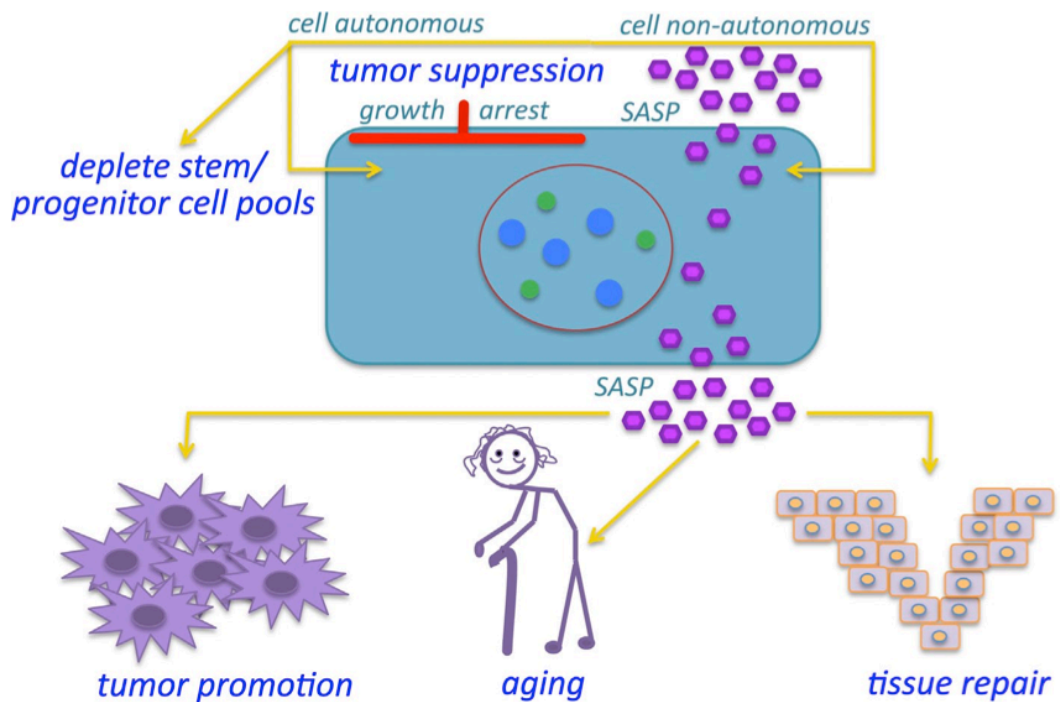
Figure 1.4. The paradoxical effects of senescence. Growth arrest is imposed by cell autonomous or intrinsic mechanisms (via p53 and p16^{INK4a}/ pRb tumour suppressor pathways) and cell non-autonomous or extrinsic mechanisms (via the SASP). The growth arrest suppresses malignant transformation but can also contribute to the depletion of proliferative (stem/progenitor) cell pools. Additionally, components of the SASP can also promote tumour progression, wound healing, and, possibly, contribute to ageing (*in* (Rodier & Campisi, 2011)).

The causal role of senescence in organismal ageing

Several observations from early studies suggested that senescence in culture might be implicated in ageing *in vivo*. Interestingly, species lifespan seemed to directly correlate with replicative lifespan in culture (reviewed in (Campisi, 2001b; Aspinall, 2003)). More importantly, an inverse correlation was found between donor age and the maximum number of population doublings cells undergo in culture before entering senescence, which suggested that replicative potential decreases continually with organismal ageing. In human fibroblasts (Hayflick & Moorhead, 1961) and keratinocytes (Rheinwald & Green, 1975a) the plating efficiency and lifetime in culture was found to be higher for cells obtained from young (fetal/newborn) donors than from older donors. In fact, cells originating from older donors give rise to a lower proportion of clones with high replicative potential (holoclones), which originate bigger colonies in culture. Conversely, clones displaying the lowest replicative potential (paraclones) and originating small colonies in culture are more abundant the older the donor (Barrandon & Green, 1987). However, this correlation has been questioned as it is not always observed and is also accompanied by some degree of variation (Cristofalo *et al*, 1998). Nevertheless, studies using cells derived from human with premature ageing conditions also support the idea that replicative potential in culture reflects ageing of the individual (Martin *et al*, 1970). Fibroblasts obtained from patients with Werner's syndrome, for instance, exhibit a reduced lifespan in culture when compared to age-matched controls (Kill *et al*, 1994). Despite these indications, the matter remained controversial because evidence for the presence of senescent cells *in vivo* and their accumulation with age was still lacking.

Until the 1990s, senescence in culture was identified on the basis of absence of DNA replication assessed through incorporation of synthetic nucleosides analogs of thymidine such as bromodeoxyuridine (5-BrdU) or tritiated thymidine (^{3}H-thymidine) (Cristofalo & Sharf, 1973) into newly synthesised DNA, or later by immunostaining for PCNA or proliferation marker Ki67. Ki67 is a general marker for proliferation as it is associated not only with the S phase of the cell cycle but also with G_1, G_2 and M, whilst it is absent in G_0 when cells are not cycling (Brown & Gatter, 2002). However, this characteristic is not exclusive to senescent cells as their quiescent or terminally differentiated counterparts are also arrested in the cell-cycle. In 1995, Dimri and colleagues (Dimri *et al*, 1995) found that senescent cells, identified based on their inability

to incorporate ^{3}H-thymidine, selectively exhibited β-galactosidase activity at pH6. This feature, designated senescence-associated β-galactosidase (SA-βgal), correlated with replicative age in fibroblasts, keratinocytes and other cell types in culture, and was absent in immortal cells. More importantly, SA-βgal positive cells were present in human skin samples (in both dermal fibroblasts and epidermal keratinocytes) and showed an increase in frequency and intensity with donor age. SA-βgal staining was the first senescence biomarker to be established as it provided groundbreaking evidence for the existence of senescent cells *in situ* and their accumulation with age *in vivo*. Despite being a distinctive and more specific feature of senescent cells, SA-βgal presented a few limitations regarding its use and specificity (Severino *et al*, 2000; Cristofalo, 2005). SA-βgal staining was found to increase not only as a function of replicative age in culture but also in response to environmental stressors such as exposure to H_2O_2 or cell density. Confluent cultures of immortal cells, for instance, showed increased frequency of SA-βgal staining as did confluent cultures of early passage diploid fibroblasts. Additionally, the utility of this marker in detecting senescent cells *in vivo* was also challenged as SA-βgal staining was reported in the lumen of hair follicles and glandular ducts regardless the age of the tissue donor (Severino *et al*, 2000). These limitations prompted the search for novel biomarkers of senescence.

The major cell cycle regulator and effector of the pRb pathway of senescence, p16^{INK4a} accumulates with senescence in various human cell types such as fibroblasts (Hara *et al*, 1996) and keratinocytes (Loughran *et al*, 1996; Munro *et al*, 1999), and in HSCs of old mice (Janzen *et al*, 2006). However, although most senescent cells express p16^{INK4a} not all do, as for the case of BJ foreskin fibroblasts which consistently express very low levels of p16^{INK4a} throughout their lifespan in culture (Beauséjour *et al*, 2003; Itahana *et al*, 2003). In keratinocytes p16^{INK4a} expression is exclusive to senescence and is not observed with terminal differentiation (Loughran *et al*, 1996). Several *in vivo* studies have established p16^{INK4a} as a robust senescence biomarker. p16^{INK4a} expression was found to directly correlate with chronological age in almost all tissues in the mouse (Krishnamurthy *et al*, 2004), in human peripheral blood T-lymphocytes (Liu *et al*, 2009) and in human skin, both epidermis and dermis, where it was accompanied by down-regulation of the *INK4a* locus repressor Bmi-1 (Ressler *et al*, 2006). A recent study (Waaijer *et al*, 2012) makes an interesting connection between p16^{INK4a} expression in the skin and how well a

person ages. Offspring from long-lived families, who display indicators of younger biological age, such as a lower mortality rate, lower prevalence of cardiovascular diseases, beneficial glucose and lipid metabolism, preservation of insulin sensitivity and better resistance to cellular stress *in vitro*, show a significantly lower frequency of p16^{INK4a}-positive cells in their skin, especially in the epidermis, than their age and environmentally matched partners. This suggests that p16^{INK4a} expression in human skin can also be a predictor of biological age, as persons displaying fewer p16^{INK4a} positive cells seem more likely to age better (Waaijer *et al*, 2012). This is in line with recent evidence obtained in a mouse model that clearance of p16^{INK4a} positive cells delays the onset of age-related diseases (Baker *et al*, 2011).

p16^{INK4a} signalling through the pRb tumour suppressor can establish self-maintaining senescence-associated heterochromatic foci (SAHFs), due pRb-induced changes in chromatin, that accumulate in senescent cells (Narita *et al*, 2003). SAHFs contain chromatin regulators (histone repressor A or HIRA and histone chaperone ASF1a) and heterochromatic proteins (histones H3 and macroH2A, HP1α, β and ɣ), which reflect the permanent changes in chromatin responsible for stably repressing the expression of genes involved in cell cycle progression associated with establishment of senescence. The formation of foci containing macroH2A seems to be driven by HIRA and ASF1a and to depend on flux of heterochromatic proteins through PML bodies (Zhang *et al*, 2005; 2007).

Whereas the previously described markers associate with ageing driven by p16^{INK4a}-dependent senescence, other changes occur which are associated with accumulation of DNA damage. Senescent cells accumulate molecular markers consistent with the presence of DNA DSBs; these include nuclear foci (DDR foci) containing activated H2AX (ɣ-H2AX) which colocalises with 53BP1 and other DDR proteins (d'Adda di Fagagna *et al*, 2003). These DNA damage foci are also found at dysfunctional telomeres with senescence, where they are designated telomere-dysfunction induced foci (TIFs) (Takai *et al*, 2003; d'Adda di Fagagna *et al*, 2003; Herbig *et al*, 2004). Persistent DDR foci mark unrepairable DNA lesions and have been recently characterised as DNA-SCARS or 'DNA segments with chromatin alterations reinforcing senescence' because they contain ɣ-H2AX and activated forms of other DDR mediators, associate with PML bodies and localise with sites of modified chromatin (Rodier *et al*, 2011). DDR foci have been used to show that DNA damage in the form of

DSBs accumulates not only in senescent cells but also in mouse tissues with ageing (Sedelnikova *et al*, 2004; Wang *et al*, 2009). An age-dependent increase in TIFs frequencies, indicating accumulation of DNA damage at the telomeres, has also been reported in gut and liver of mice (Hewitt *et al*, 2012) as well as in terminally differentiated tissues of old primates (Fumagalli *et al*, 2012).

Finally, the combined use of these novel biomarkers of senescence, namely p16^{INK4a} expression, telomere dysfunction (TIFs), activation of DDR (DDR foci) and heterochromatinisation of nuclear DNA (SAHFs), has been employed to demonstrate that senescent cells accumulate *in vivo* with age in primates. They can account for over 15% of the cell population in dermis of old animals therefore confirming that senescence is a physiological event (Herbig *et al*, 2006; Jeyapalan *et al*, 2007). Nevertheless, expression of senescence markers does not establish a causal relationship between senescence and ageing. Conclusive evidence for the causal role of senescence in organismal ageing was obtained from genetic mouse models with manipulations in the major cell cycle regulators and effectors of the cellular senescence pathways.

Mice with a mutation that results in activation of p53 show increased resistance to spontaneous tumours accompanied with a reduction in lifespan and early ageing-related phenotypes (Tyner *et al*, 2002). "Super p53" mice, however, exhibit similar tumour resistance but maintain a healthy lifespan and age normally. The authors argue that this may be because "super-p53" animals possess just an extra copy of the p53 which, like the additional normal p53 alleles, is under normal regulatory control, as opposed to the mice with activated p53 which have total levels of constitutively activated p53 increased (García-Cao *et al*, 2002). In fact, increased p53 activity, under normal regulatory control, has been shown not to contribute to accelerated ageing in certain mouse models (García-Cao *et al*, 2006; Matheu *et al*, 2007). A later study (Choudhury *et al*, 2007) showed that, at least in the context of telomere dysfunction, p21^{Waf1} is the effector responsible for the pro-ageing effects of p53 activation. Deletion of p21^{Waf1} in telomerase-deficient mice prolongs lifespan and improves stem cell function in the epithelial and haematopoietic systems without increasing the incidence of cancer.

Similarly, expression of the tumour suppressors p16^{ink4a} and Arf, products of the *Ink4a/Arf* locus, is attenuated in mouse kidney, ovary and heart by caloric restriction and correlates with decreased incidence of pathology in

these organs (Krishnamurthy *et al*, 2004). Expression of p16^{Ink4a} is also associated with decreased haematopoietic (Janzen *et al*, 2006) and pancreatic function (Krishnamurthy *et al*, 2006). However, deletion of p16^{Ink4a} partially rescues age-related defects in HSC proliferation and apoptotic rates and improves repopulating ability as well as the regenerative capacity of pancreatic β-cells (Janzen *et al*, 2006; Krishnamurthy *et al*, 2006). Consistently, mice with deletion of Bmi-1, a negative regulator of the *Ink4a/Arf* locus, exhibit compromised haematopoietic stem cell function, associated with impaired mitochondrial function and an increase in ROS level, and a shortened lifespan (Liu *et al*, 2009).

Whereas these studies (Janzen *et al*, 2006; Choudhury *et al*, 2007; Liu *et al*, 2009) attest to the contribution of intrinsic properties of senescent cells (cell-intrinsic ageing) to organismal ageing, additional work corroborates the idea that the senescence secretome also contributes to ageing (cell-extrinsic ageing) via changes in the microenvironment of both mitotic and post-mitotic tissue (Fig. 1.4). For instance, muscle satellite cells from aged mice show a decline in tissue regenerative capacity that can be restored when cells are exposed to blood supply from young animals via heterochronic parabiosis. Similarly, haematopoietic stem cell dysfunction resulting from age-associated changes in the supportive niche can also be reversed by exposure to circulation from young animals in an equivalent system (Mayack, 2010).

Stem cell numbers do not get depleted with age and actually increase in mouse intestine and skin (Martin *et al*, 1998a; Giangreco *et al*, 2008). However, the regenerative clone size upon injury is reduced with age (Martin *et al*, 1998a; 1998b). The stem cell hypothesis of ageing (Fig. 1.5) proposes that this is due to senescence probably because it promotes a decline in the replicative function of adult stem cells (Charruyer *et al*, 2009) in tissues with both high and low turnover rates. The activation of tumour suppressor mechanisms, such as senescence or apoptosis, is thought to be in place to prevent expansion of clones which have acquired malignant potential (damage to the genome or oncogenes) but can unintentionally contribute to ageing and late life cancer by impairing stem cell function and by altering their supporting niches (Sharpless & DePinho, 2007). This is also consistent with the antagonistic pleiotropy theory of ageing.
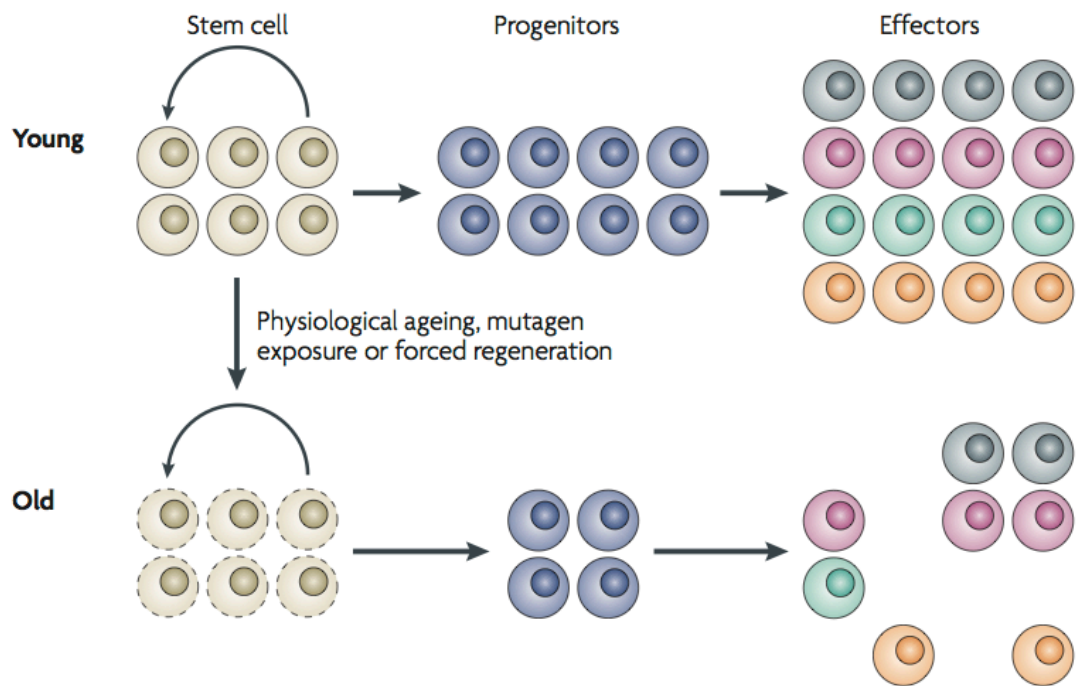
Figure 1.5. The stem cell theory of ageing. Stem cell numbers do not get depleted with age as the ability to self-renew (curved arrow) is maintained. Stem cell function however, measured as the ability to produce progenitors (blue) and differentiated effector cells (different colours), does decline (*in* (Sharpless & DePinho, 2007)).

1.4. Senescence, telomere dysfunction and ageing.

The telomere

Most eukaryotes use a complex telomerase-based system to stabilise their chromosome ends which has been proposed to have evolved from conserved t-loop structures (de Lange, 2004). The telomere system consists of telomeric-repeat DNA (Blackburn & Gall, 1978), telomerase, a telomere-specific reverse transcriptase (Greider & Blackburn, 1985; 1987) and telomere-specific proteins which bind the latter (de Lange, 2005). Therefore, modern telomeres solve both problems associated with the transition to linear genomes; the end-replication problem, where terminal DNA is lost after each round of replication, and the exposure of chromosome ends, where the open double-strand is at risk of being recognised and processed by the cell as a site of DNA damage (de Lange, 2004).

In mammals, telomeres are organised as a nucleoprotein complex (Fig. 1.6 a) that is know to exhibit a t-loop configuration. The characteristic t-loop structure was first unveiled by electron microscopy following psolaren/UV treatment of nuclei, deproteinisation and isolation of telomeric DNA obtained from four different mammalian sources (Griffith *et al*, 1999). The proposed structure of the human telomeric complex is represented in figure 1.6. It consists of a long sequence of TTAGGG repeats arranged as double-stranded DNA that ends in a short single-stranded 3' overhang. The telomeric DNA folds over itself forming a t-loop (telomeric loop) thus allowing the 3' overhang to invade the duplex and create a D-loop (displacement loop) of TTAGGG repeats associated with the single-stranded telomeric DNA-binding protein POT1 (protection of telomeres 1). The structure is further stabilised by two main protein complexes, TRF1 and TRF2 (Fig. 1.6 b), which bind the entire length of double-stranded telomeric DNA (de Lange, 2004; 2005).
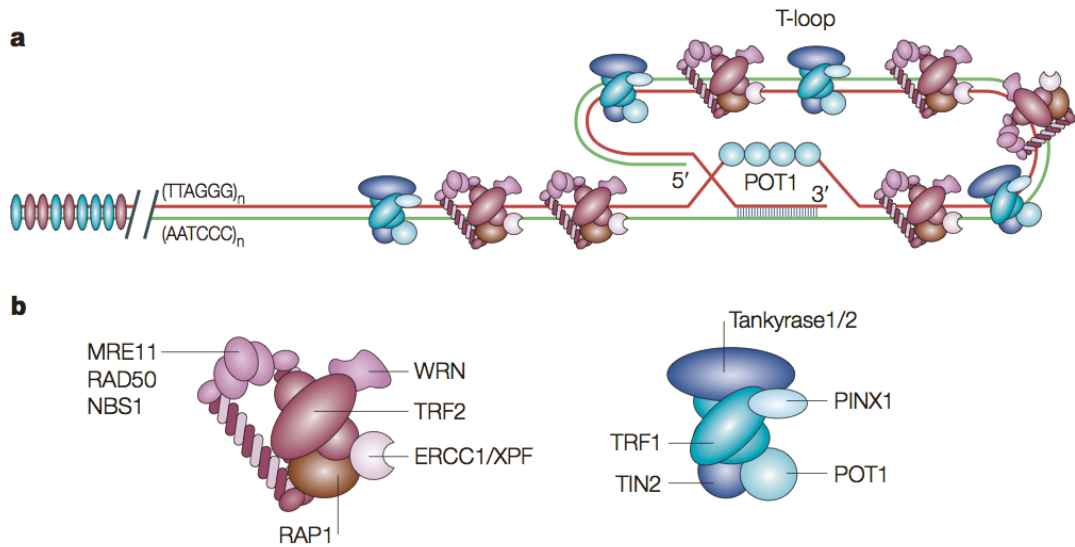
Figure 1.6. The human telomeric complex. a. Telomeres consist of telomeric DNA associated with a complex of protective and regulatory proteins (shelterin). Telomeric DNA is organised as an array of duplex TTAGGG repeats folded into a t-loop ending in a 100–200 nucleotide 3' single-stranded overhang which invades the telomeric duplex forming a displacement loop. TRF1 and TRF2 associate with the duplex TTAGGG repeats whilst POT1 binds the single-stranded 3'overhang. **b.** TRF2 (left) and TRF1 (right) complexes. Legend: TRF = telomeric repeat-binding factor; PINX1 = PIN2-interacting factor-1; POT1 = protection of telomeres-1; TIN2 = TRF1-interacting factor-2; WRN = Werner syndrome helicase (*in* (de Lange, 2004)).

Chromosome ends evade DNA repair and interact with telomerase through association of telomeric DNA with protective and regulatory proteins (Fig.1.6). These are part of the protein complex generally known as shelterin which protects, shapes and associates exclusively with the telomere. Shelterin has six main subunits, TRF1, TRF2, TIN2, Rap1, TPP1 and POT1 which interact with one another and with other non-shelterin proteins (reviewed in (de Lange, 2005)).

TRF2 and TRF1 form homo-dimers containing homologous C-terminal Myb domains specifically capable of binding the double-stranded telomeric DNA. Whilst TRF1 possesses an N-terminal acidic domain TRF2's motif is basic. TRF2 interacts specifically with Rap1 and both TRF2 and TRF1 have TIN2-binding

domains. TIN2 connects both telomeric repeat-binding factors, which contributes to the stabilisation of TRF2 on telomeres, and tethers TPP1/POT1 to TRF2 and TRF1. Several proteins involved in DNA repair associate with components of the shelterin complex. For instance, TRF2 is known to interact with the WRN and BLM helicases, the MRN complex (Mre11/Rad50/Nbs1) and Rad51 which are involved in homologous recombination (HR); ERCC1/XPF which is involved in nucleotide excision repair (NER) and cross-link repair; PARP which is involved in base excision repair (BER) and DNA-PKcs which is involved in non-homologous end-joining (NHEJ). TRF1, on the other end, interacts with tankyrases (1 and 2) known for their role in mitosis.

Shelterin's protective function is mostly performed by TRF2 through stabilisation of the 3'-overhang and formation of the t-loop which is the protective conformation adopted by mammalian telomeres *in vivo* (Griffith *et al*, 1999). TRF2 is capable of remodelling linear telomeric substrates into t-loops *in vitro*. This was demonstrated by incubating a model of linear telomeric DNA with TRF2 and analysing the conformation of the resulting complexes using electron microscopy. It revealed the formation of lasso-like molecules (t-loops), the frequency of which dramatically decreased in the absence of TRF2. Assembly of the telomeric loop by TRF2 was also hindered upon removal of the 3'-overhang by specific nuclease treatment (Griffith *et al*, 1999). In addition, previous work had already revealed that deletion of TRF2 induced end-to-end chromosome fusions due to loss of the single-stranded G-tails, with no disruption of the duplex TTAGGG repeats (van Steensel *et al*, 1998). This suggests that the telomeric repeats alone are not sufficient to ensure telomere integrity and that TRF2 has an essential role in it by maintaining the correct configuration of the 3'-overhang. Furthermore, disruption of the t-loop, by interfering with TRF2 function (van Steensel *et al*, 1998) or with the integrity of the 3'-overhang (Li *et al*, 2003), has been shown to trigger senescence. Expression of TRF2 deletion mutants TRF2$^{\Delta B}$ (lacking Myb domain only) and TRF2$^{\Delta B \Delta M}$ (lacking both its Basic and Myb domains) reduces or almost completely removes the endogenous full-length TRF2 from telomeres, respectively. In the human osteosarcoma tetracyclin-inducible cell line, expression of these mutants is accompanied by growth arrest with characteristics of senescence, as measured by SA-βgal staining and characteristic morphological features, contrarily to what happens when full-length TRF2 is over expressed instead (van Steensel *et al*, 1998). Additionally, human neonatal early passage fibroblasts exposed to a T-oligo, an oligonucleotide homologous to the 3'-overhang sequence TTAGGG, showed a

similar senescent phenotype (Li *et al*, 2003). Cells treated with T-oligo, bearing an exposed telomere 3'-overhang, not only showed SA-βgal activity but also phosphorylation of p53, un-phosphorylation of pRb and elevation of p21^{WAF1} and p16^{INK4a} protein levels consistent with engagement of senescence pathways, as opposed to cells treated with a control bearing a complementary sequence (Li *et al*, 2003). These studies provide evidence that disruption of the t-loop triggers senescence via exposure of the 3'-overhang and suggest that this happens through depletion of protective TRF2 from critically shortened or dysfunctional telomeres. As for TRF1, although it is also involved in the stabilisation of the t-loop its main role seems to be, alongside POT1, in the regulation of telomere length maintenance by controlling the access of telomerase to telomeric DNA via the 3'-overhang (reviewed in (de Lange, 2005)).

Telomerase

Telomerase is the enzyme responsible for maintaining telomere length (Greider & Blackburn, 1985; 1987) and although is it used by most eukaryotes it is just one of the solutions to the end-replication problem found through the course of evolution (de Lange, 2004). For instance, dipteran insects opted for retrotransposition whilst some telomerase-deficient yeast strains turned instead to rolling-circle replication or break-induced replication (BIR)/recombination-dependent replication (RDR)-like pathways. Even some immortalised human cells have been found to use a mechanism of telomere maintenance that does not require telomerase, designated 'alternative lengthening of telomeres' or ALT (Fig. 1.7).

Human telomerase is composed of the telomerase reverse transcriptase enzyme (TERT) and the telomerase RNA component (*TERC*). TERT adds TTAGGG repeats to the telomere by using the 3' overhang as a substrate and TERC as a primer for the DNA synthesis. This is known as the canonical function of telomerase which prevents telomere erosion as a consequence of cell division. However, telomerase also has non-canonical functions which can be divided into those that require telomerase activity but not telomere lengthening and those that require neither telomerase activity nor telomere lengthening (Parkinson *et al*, 2008).
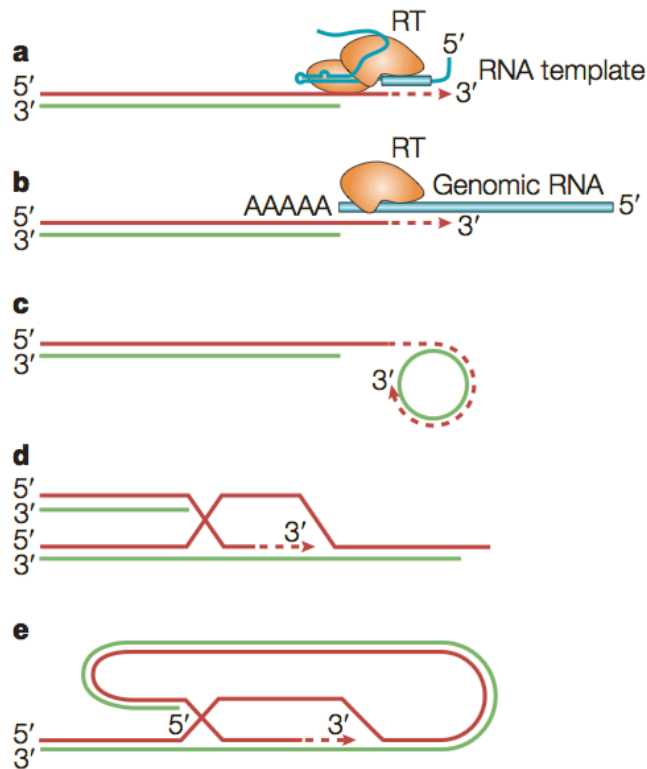
Figure 1.7. Different solutions to the end-replication problem. a. Telomerase, which uses an RNA template (TERC), part of the telomerase complex, for DNA synthesis; **b.** Retrotransposition, where a reverse transcriptase uses genomic RNA as a template (in dipteran insects); **c.** Rolling-circle replication, where the an extrachromosomal circular template is used (in telomerase-deficient *Kluyveromyces lactis*); **d.** BIR/RDR-like pathways, where one telomere uses another telomere as template through strand invasion, and **e.** T-loop formation, by using terminal repeats and extension of the invaded 3' end (possible mechanism for ALT in human cells) (*in* (de Lange, 2004)).

Average telomere length decreases gradually with cell divisions *in vitro* (Harley *et al*, 1990) and *in vivo* with age in proliferative compartments (Lindsey *et al*, 1991; Sharpless & DePinho, 2007). Telomere attrition in normal human cells results in cellular senescence and can be averted by telomerase (Bodnar *et al*, 1998). Ectopic expression of TERT in skin fibroblasts, retinal epithelial cells (Bodnar *et al*, 1998), keratinocytes (Dickson *et al*, 2000) and human skeletal muscle myoblasts (Wootton *et al*, 2003) stabilises telomere length and facilitates cells to acquire unlimited replicative potential without neoplastic transformation (Ouellette *et al*, 1999; Jiang *et al*, 1999). It also extends replicative lifespan of cultured fibroblasts obtained from patients with Werner's syndrome(Wyllie *et al*, 2000). Telomerase activity is low or undetected in normal human somatic cells, however certain stem cells, germ line cells, and most immortal and cancer cell lines are telomerase-positive (Kim *et al*, 1994; Wright *et al*, 1996; Newbold, 1997). In fact, activation of telomerase is one of the events usually required for malignant transformation (Kim *et al*, 1994; Soder *et al*, 1997; Parkinson & Minty, 2007).

The situation in the mouse is quite different. Mouse telomeres are, on average, many times longer than human telomeres and no significant reduction in average size is observed throughout their lifespan (Kipling & Cooke, 1990). Telomerase activity is present in most somatic tissues in the mouse, especially those with high turnover, and its expression seems to be mainly determined by the rate of cell proliferation. This is exemplified in mouse tumours, where telomerase expression is increased with maintenance of basal average telomere length. Furthermore, murine cells increase their telomerase levels and tend to spontaneously immortalise in culture, whilst animals show an increased susceptibility to develop cancer (Kipling, 1997). As telomerase is actively expressed in proliferating tissues and telomeres maintain a constant great size, senescence due to telomere shortening was thought not to be relevant in the mouse.

Telomere dysfunction-induced senescence and ageing

In order to assess the effect of telomere attrition on ageing *in vivo* and for lack of a mammalian-based model system that could mimic human ageing, a telomerase-deficient mouse model was devised. The telomerase knockout mouse (*mTR⁻/⁻* or *Terc⁻/⁻*) carries a deletion of the germline copy of the murine telomerase RNA gene (*mTR*) (Blasco *et al*, 1997). Not surprisingly, given the long murine telomere reserves, the lack of telomerase activity alone was not enough to generate significant ageing phenotypes in these animals (Rudolph *et al*, 1999; Lee *et al*, 1998). However, consecutive generations (G2, G3, G4, G5 and G6) of *mTR⁻/⁻* mice resulting from successive matings of homozygous-null intercrosses exhibited increasingly limiting telomere length, comparable to what occurs naturally in a human setting (Blasco *et al*, 1997; Lee *et al*, 1998).

Late generation (G4 onward) telomerase-deficient mice (*Terc⁻/⁻*) exhibit an age-dependent telomere shortening that results in shortened lifespan and decreased regenerative capacity in the epithelial and haematopoietic systems (Blasco *et al*, 1997; Rudolph *et al*, 1999). Telomerase deficiency and consequent telomere shortening in this mouse model also results in genomic abnormalities, increased apoptosis and senescence, depletion of male germ cells and reduced proliferative capacity in the testes, bone marrow and spleen, suggesting an impairment in stem-cell function in the highly proliferative organs (Lee *et al*, 1998). Additionally it has been shown that *Terc*-null mice with shortened telomeres show an age-dependent dysfunction of the haematopoietic environment causing impairment of B lymphopoiesis and increased myeloid proliferation of transplanted wild-type HSCs from young mice, suggesting a role for telomere attrition also in cell-extrinsic ageing (Ju *et al*, 2007). Finally, recent work (Hewitt *et al*, 2012) suggests that telomere length and integrity are compromised during ageing even in wild-type mice known for expressing telomerase and possessing long telomere reserves. This supports the idea, contrary to what was accepted so far, that telomere attrition and/or dysfunction might be relevant to the ageing process in the mouse after all. In addition to findings obtained in the telomerase-deficient mouse model, several conditions in humans implicate telomeric attrition in organismal ageing.

Various inherited and acquired degenerative disorders suggest a causal role for telomere dysfunction in normal human ageing. Ataxia telangiectasia (AT), Werner's syndrome (WS) and dyskeratosis congenita (DC) are examples of

genetic diseases caused by mutations in genes coding for proteins ATM, WRN and *TERC*/TERT, respectively, with functions related to DNA repair and/or to telomere function (Wyllie *et al*, 2000; Vulliamy *et al*, 2001; Wong *et al*, 2003; Vulliamy *et al*, 2004; Chang *et al*, 2004). These conditions are classified as progeroid syndromes because they are characterised by a range of clinical manifestations that resemble accelerated ageing (Kipling *et al*, 2004; Kirwan & Dokal, 2009). Additionally, cells obtained from patients with DC and WS have shorter telomeres, show reduced replicative potential in culture and are rescued from senescence and readily immortalised following forced expression of telomerase. Neither the *Wrn*-null nor the *Atm*-null mouse models show the classic range of manifestations typical of Werner's or AT. However, when these mice are created on a telomerase-deficient background they present degenerative pathologies associated with accelerated ageing (Wong *et al*, 2003; Chang *et al*, 2004). Furthermore, telomere loss has also been implicated in acquired chronic degenerative diseases characterised by high tissue turnover, such as idiopathic pulmonary fibrosis and liver cirrhosis (Rudolph *et al*, 2000; Wiemann *et al*, 2002; Garcia *et al*, 2007). This has been confirmed in the telomerase-deficient mouse model where telomere dysfunction in *Terc*$^{-/-}$ animals subjected to liver damage resulted in impaired liver regeneration and accelerated development of liver cirrhosis, conditions that were reversed by restoring telomerase activity and telomere function following adenoviral delivery of *Terc* (Rudolph *et al*, 2000).

Telomere dysfunction is at least partly signalled by p53 which seems to exert its anti-proliferative and pro-ageing effects mainly via its transcriptional target p21^{WAF1}. Whilst p53 deletion in late generation telomerase-deficient mice attenuated the cellular and organ defects arising from telomere dysfunction, it also contributed to accelerated tumourigenesis following the establishment of genetic crisis (Chin *et al*, 1999). *p21*^{waf1} deletion in the same experimental model, on the other hand, not only improved stem cell function in both haematopoietic and epithelial compartments it also increased lifespan without contributing to chromosomal instability or cancer formation (Choudhury *et al*, 2007). Over-expression of telomerase can extend the replicative lifespan of several cell strains in culture (Bodnar *et al*, 1998). This, together with the evidence presented from the telomerase-deficient mouse model as well as progeroid and chronic degenerative disorders in humans suggests that dysfunctional telomeres contribute to ageing by limiting stem-cell renewal in proliferative compartments. Testing the role of telomerase in organismal ageing

was therefore the next issue to address but presented a challenge given the well documented cancer-promoting effect of telomerase in the *Tert*-transgenic mouse (González-Suárez *et al*, 2001). Although constitutive expression of telomerase improved wound healing and epidermal stem cell function it also resulted in a decreased lifespan because animals died early from cancer and this was shown to be associated with loss of p53 function (González-Suárez *et al*, 2002). Thus the only way to independently address the role of telomerase expression in organismal ageing was to separate it from its effect on cancer.

For this purpose, Blasco and colleagues devised a novel mouse model constitutively expressing TERT in a cancer-resistant genetic background (Tomás-Loba *et al*, 2008). These tumour-resistant *Tert*-transgenic mice, also known as *Sp53/Sp16/SpArf/TgTert*, result from intercrosses between *TgTert* mice (or *K5-Tert* mice) selectively over-expressing the *Tert* gene in epithelial stem cell compartments due to its expression via the keratin 5 promoter (González-Suárez *et al*, 2001; 2002) and *Sp53* (or 'Super-*p53*') and *Sp16/SpArf* (or 'Super *Ink4a/Arf*') animals carrying extra alleles of the tumour suppressor genes *p53* and a transgenic copy of the entire *Ink4a/Arf* locus (García-Cao *et al*, 2002; Matheu *et al*, 2004). Expression of telomerase in a cancer-resistant background significantly delayed ageing, improved fitness in several epithelia as well as the brain and muscle (organs that do not express *TgTert*) and increased longevity in these animals. This anti-ageing activity was achieved by slowing telomere attrition and by preserving the proliferative potential of stem cells via the combined synergistic action of telomerase and the tumour suppressor genes being over-expressed. It could be argued that these anti-ageing effects could be due to non-canonical functions of telomerase which do not require telomerase elongation activity. However, this has been addressed by Blasco's group when they previously showed that, in contrast with *TgTert* mice, animals over-expressing telomerase but carrying a germline deletion of its catalytic component, that is *TgTert* mice in a *Terc-/-* background, failed to show increased tumourigenesis and increased wound healing (Cayuela *et al*, 2005). This indicates that the *Terc* component of telomerase seems to be required for its function as far as these effects are concerned. It is however still possible that other functions of telomerase, independent of telomerase activity, can also have a beneficial effect on ageing. Given that telomeres are considerably long in mice, regardless the expression of *TgTert*, and that expression of the tumour-suppressor genes seems to also contribute to a slower rate of proliferation, which has been previously associated with decrease incurrence of DNA

damage and better clearance of damaged cells by senescence and/or apoptosis (Matheu *et al*, 2007), it seems likely that telomerase exerts its action by generally preserving telomere health rather than telomere size. Potential causes of telomere dysfunction that might have had their action counteracted by telomerase are damage generated by oxidative stress and DNA damage in the form of DSBs at the telomere.

DePinho and colleagues went further to show that telomerase reactivation in aged telomerase-deficient mice was actually capable of reversing the multi-system degeneration associated with telomere dysfunction (Jaskelioff *et al*, 2011). They have modified late generation *Terc*$^{-/-}$ mice by introducing a knock-in allele encoding a 4-hydroxytamoxifen (4-OHT)-inducible telomerase reverse transcriptase-oestrogen receptor (TERT-ER) under transcriptional control of the endogenous TERT promoter. Telomerase reactivation in G4$^{TERT-ER}$ mice (in the presence of 4-OHT) lead to tissue rejuvenation in organs as diverse as the liver, spleen, testes, brain and even resulted in increased fecundity. As reactivation of telomerase was performed over a short period it did not promote carcinogenesis and thus raises the potential of its use as a telomere rejuvenation strategy at the organismal level.

Since then, the use of telomerase activator TA-65 as a diet supplement in mice has been reported to have beneficial anti-ageing effects (Bernardes de Jesus *et al*, 2011). It resulted in increased telomerase activity with effective rescue of telomere shortening and an increase in health-span indicators such as glucose tolerance, osteoporosis and skin fitness in female adult/old mice, without significantly increasing tumourigenesis. The same research group went on to try telomerase gene therapy using an adeno-associated virus (AAV) of wide tropism administered by injection on their tail-vein (Bernardes de Jesus *et al*, 2012). AAV vectors are very appealing tools for gene therapy and extensive studies in humans attest to their safety and efficacy; they are non-integrative, show poor immunogenicity and a good safety profile as well as the ability to transduce a wide range of tissues, with distinct proliferative capacities. AAV9 mediated expression of mouse *TERT* in adult and old mice also increased health-span and fitness, had an impact on biomarkers of ageing and, more importantly, also increased median lifespan of these animals (Bernardes de Jesus *et al*, 2012). This suggests that the ageing process can be modulated by telomerase at the organismal level and reenforces the role of telomere dysfunction in ageing.

Overall, studies like these (Bernardes de Jesus *et al*, 2011; 2012) using ectopic treatments to modulate ageing or studies in genetically modified mice where clearance of senescent cells has a compelling effect on ageing phenotypes (Baker *et al*, 2011) suggest that interventions in ageing are possible at the organismal level and attest for the contribution of senescent cells to ageing *in vivo*.

The mitochondria connection

Although the decline in stem cell function associated with telomere attrition can account for the reduced regeneration ability in highly proliferative tissues it does not readily explain the telomere-related functional decline in post-mitotic tissues or onset of metabolic disorders.

Although telomere dysfunction in mice resulted primarily in decrease of function in the epithelial and haematopoietic systems (Rudolph *et al*, 1999), reactivation of TERT in this model (late generation *Terc*$^{-/-}$ animals) reversed the generalised ageing-related decline even in organs like the liver, spleen, testes (with an increase in fecundity) and the brain (Jaskelioff *et al*, 2011). Additionally, constitutive expression of telomerase in cancer-resistant mice also improved brain and muscle function (Tomás-Loba *et al*, 2008) and the use of telomerase activators (Bernardes de Jesus *et al*, 2011) or telomerase as gene therapy (Bernardes de Jesus *et al*, 2012) improved metabolic factors such as glucose tolerance and osteoporosis. Finally, although bone marrow failure and epithelial disorders are the defining features of dyskeratosis congenita, one of the human telomere-maintenance disorders, patients also display pulmonary and liver disease as well as mental retardation, deafness and osteoporosis (Kirwan & Dokal, 2009). This evidence indicates that telomere dysfunction affects mitotic, post-mitotic and metabolic ageing.

It is well established that it is the shortest telomere, rather than average telomere length, that triggers telomere dysfunction-induced senescence in cultured cells (Hemann *et al*, 2001). Telomerase targets the shortest telomere keeping cells in cycle both *in vitro* (Bodnar *et al*, 1998) and *in vivo* (Tomás-Loba *et al*, 2008). However, murine telomeres are characteristically long and not in danger of becoming critically short due to constitutive telomerase activity (Kipling & Cooke, 1990; Kipling, 1997) which is also the case for the cancer-

resistant transgenic *Tert* model (Tomás-Loba *et al*, 2008). Also, although senescent human fibroblasts have critically short telomeres, with almost total absence of telomeric repeats in some cases, telomere length is still highly variable (Baird *et al*, 2003). Whereas telomere shortening in primarily precipitated by increased rate of cell division, other factors contribute to accelerated telomere shortening or telomere dysfunction. Besides, telomeres become dysfunctional through loss of their protected status rather than by a complete loss of telomeric DNA (Karlseder *et al*, 2002). Exposure to chronic mild levels of oxidative stress, which is known to promote telomere shortening, was suggested as a possible explanation for the heterogeneity of replicative lifespan of cells in culture (Martin-Ruiz *et al*, 2004).

Mitochondrial dysfunction, characterised by increased production of ROS, a breakdown of membrane potential and activation of mitochondrial biogenesis, has been shown contribute to telomere dysfunction (Passos *et al*, 2007a). Replicatively senescent human fibroblasts, characterised by short telomeres, showed an increase in superoxide levels accompanied by an elevation of mitochondrial mass and mtDNA copy number as well as other features of mitochondrial dysfunction. Reduction of the mitochondrial membrane potential (MMP) or mitochondrial uncoupling, which results in decreased production of mitochondrial superoxide, was found to delay replicative senescence by slowing down oxidative stress-dependent telomere shortening. Thus, mitochondrial dysfunction and superoxide production seem to contribute to telomere loss and TIF formation with induction of TDIS. This is thought to occur via p21^{WAF1}-p38MAPK-TGF-β signalling (Passos *et al*, 2010). Similarly, oncogene-induced senescence was found to contribute to mitochondrial dysfunction and increased ROS production via MAPK signalling (Moiseeva *et al*, 2006) and to contribute to TDIS by accelerating telomeric attrition and by affecting telomere structure (Suram *et al*, 2012). Telomeres, given their G-rich chemistry, are particularly susceptible to oxidative damage and preferred targets for reaction with ROS which can render them permanently dysfunctional (Petersen *et al*, 1998; Hewitt *et al*, 2012).

Conversely, telomere dysfunction has also been shown to contribute to mitochondrial impairment (Sahin *et al*, 2011). Mouse models of telomere dysfunction, exhibiting decline in proliferative and quiescent organs resembling premature ageing, showed repression of mitochondrial regulators PGC-1α and PGC-1β as well as their downstream targets, compromised mitochondrial

biogenesis and function with increase in ROS production, reduction in gluconeogenesis and cardiomiopathy. This was found in both G2 *Terc*^{-/-} and G4 *Tert*^{-/-} models (showing comparable telomere dysfunction) indicating that these phenotypes result from lack of telomerase catalytic activity (canonical) and, therefore, from telomeric compromise. More importantly, forced expression of telomerase or PGC-1α, or germline deletion of p53 in these animals restored the PGC expression network, mitochondrial respiration as well as cardiac and hepatic function. p53 was found to directly repress PGC-1α and PGC-1β therefore establishing a telomere-p53-mitochondria regulatory axis. Since p53 deficiency in mice with dysfunctional telomeres only partially restores PGC levels and mitochondrial function (Sahin *et al*, 2011) this suggests that other pathways might also contribute to mitochondrial and metabolic compromise. Other candidates are p63, sirtuins, the Bmi-p16[INK4a] pathway and p21[WAF1]-dependent signalling (Sahin, 2012).

From these observations an integrated view of ageing (Fig. 1.8) emerged which links the telomere and the mitochondria (Sahin & DePinho, 2012). The central molecule in the telomere-mitochondria axis is p53. Both generalised damage to the DNA in the form of DSBs or specialised damage such as telomere dysfunction signal p53 activation. This indirectly contributes to mitochondrial dysfunction via suppression of mitochondrial regulators PGC-1α and PGC-1β (Sahin *et al*, 2011). Impaired mitochondria function causes increased ROS production and the resulting oxidative stress generates further damage to the DNA (in the form of persistent foci), particularly to the telomeres, eliciting a persistent DDR through p21[WAF1] signalling which will again contribute to mitochondrial compromise (Passos *et al*, 2007a; 2010; Hewitt *et al*, 2012; Fumagalli *et al*, 2012). The vicious cycle that gets established in the cell where genotoxic damage contributes to oxidative damage, and vice-versa, might explain how damage to the telomeres with consequent telomere dysfunction contributes to age-related functional decline in organs without regenerative capacity (Sahin & DePinho, 2012).

In summary, the telomere-p53-mitochondrion model accounts for ageing driven by DNA damage and for the various ageing syndromes and phenotypes described above such as mice with extra copies of p53 ('Super' p53), models of telomere dysfunction (*Terc*-null and Tert-null mice) and models of telomere dysfunction (PGC-1α-null, PGC-1β-null and Bmi-1-null mice) thereby

providing a unified explanation for ageing driven by DNA damage and metabolic pathways (Sahin & DePinho, 2012).
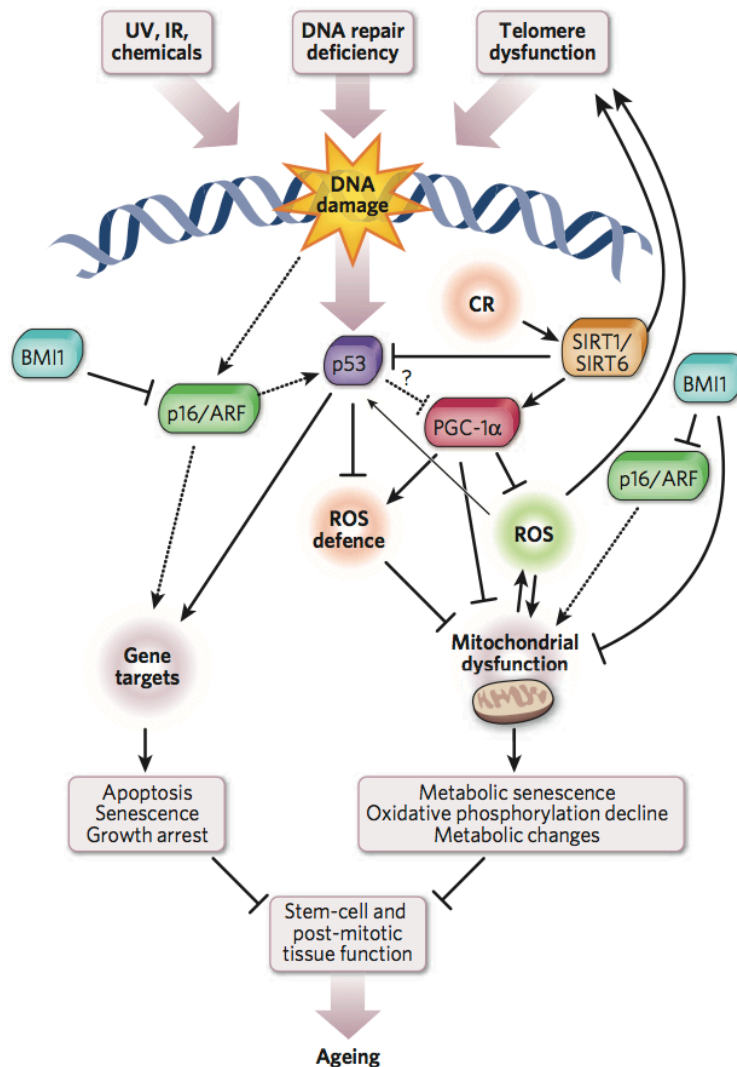
Figure 1.8. The integrated view of ageing linking telomeres and mitochondria. This models suggests reciprocal interaction between telomere dysfunction, p53 activation and mitochondrial dysfunction. Legend: CR = caloric restriction (*in* (Sahin & DePinho, 2010)).

Based on this model, one can predict that interventions where telomere function is restored could also improve or restore mitochondrial activity. It would be interesting to assess whether an improvement in mitochondrial biogenesis and function is observed in animal models where telomere function has been restored, through expression of telomerase, with attenuation of ageing phenotypes, such as *Sp53/Sp16/SpArf/TgTert* mice (Tomás-Loba *et al*, 2008), mice treated with telomerase activator TA-65 (Bernardes de Jesus *et al*, 2011) and mice subjected to telomerase gene therapy through a viral vector (Bernardes de Jesus *et al*, 2012). So far, some interventions known to improve mitochondrial biogenesis and function, such as over-expression of PGC-1α in mice (Wenz *et al*, 2009) or physical activity and the use of resveratrol, a sirtuin activator, in humans (Little *et al*, 2011; Timmers *et al*, 2011) have been shown to reduce age-related decline. Additionally, the development of these or other therapeutic strategies to rejuvenate aged tissue or prevent the onset of ageing disorders, through intervention in components of the p53 pathway for example, could be considered.

The ROS theory of ageing has been challenged on the grounds that in both birds and rodents long-lived species do not exhibit lower levels of oxidative damage in their tissues when compared with short lived species. Parrots that live for 40 years do not have lower levels or oxidative damage or better levels of oxidative defence enzymes than quails that live for 5 years (Montgomery *et al*, 2012). Similarly, naked mole rats (NMRs) that live for 30 years do not have lower levels of oxidative damage than other rodents that live for only 2-3 years (Pérez *et al*, 2009; Lewis *et al*, 2013). However, this can be reconciled if one considers recent evidence showing that telomerase can resolve otherwise irreparable DNA DSBs at the telomere (Suram *et al*, 2012), which are likely caused by ROS during normal ageing. Parrots have higher levels of telomerase than shorter-lived bird species (Venkatesan & Price, 1998; Haussmann *et al*, 2004; 2007) and NMRs have positively selected for genes involved in telomere maintenance (Kim *et al*, 2011). This hypothesis would also explain why ectopic telomerase expression in mouse epithelium can increase both lifespan and healthspan on a cancer-resistant background and reduce telomere damage, despite the fact that mouse telomeres are generally very long (Tomás-Loba *et al*, 2008). Thus, the apparent anomalies within the animal kingdom do not necessarily disprove the oxidative damage theory of ageing for which there is abundant evidence in experimental models such as *Drosophila melanogaster*, *Saccharomyces cerevisiae* and *Caenorhabditis elegans* (Kenyon, 2010; Sohal & Orr, 2012).

However, it will be interesting to test the role of irreparable telomeric DSBs by examining their accumulation during the ageing of NMRs and long-lived birds as compared to their shorter lived relatives.

DNA DSBs and the telomere

Telomeric DNA evades detection by the DNA repair machinery by being protected by the telomeric proteins that form the Shelterin complex. These proteins cap the telomere and shape it into the protective loop that conceals the 3' overhang preventing it from being recognised as a DNA break and processed for repair, as happens on other sites of DNA damage (de Lange, 2005). TRF2 is the shelterin component known to be able to induce the formation of t-loops (Griffith *et al*, 1999) and is thought to be assisted by various recombinational and repair proteins that could promote the strand invasion of the 3'-overhang (de Lange, 2004). The MRE11 complex (containing MRE11, RAD50 and NBS1 proteins), involved in homologous recombination (HR) and RECQ helicases (WRN/BLM), involved in unwinding of the double helix, are likely candidates as they are known to associate with TRF2 (de Lange, 2004).

Structurally, t-loops resemble intermediates in DNA repair pathways, such as the strand-invasion intermediate in homologous recombination (see Chapter 4), and transitional structures in replication-restart events. The t-loop is evolutionarily conserved and is thought to have evolved from an ancient pathway for repair of DNA ends upon collapse of replication forks in prokaryotes called recombination-dependent recombination or RDR (Fig. 1.9). The early steps of RDR resemble t-loop formation and proteins that associate with modern telomeres, such as POT1, RAD51, components of the RAD52 family and the MRE complex, are evolutionarily related to proteins that play a role in RDR (reviewed in (de Lange, 2004)).
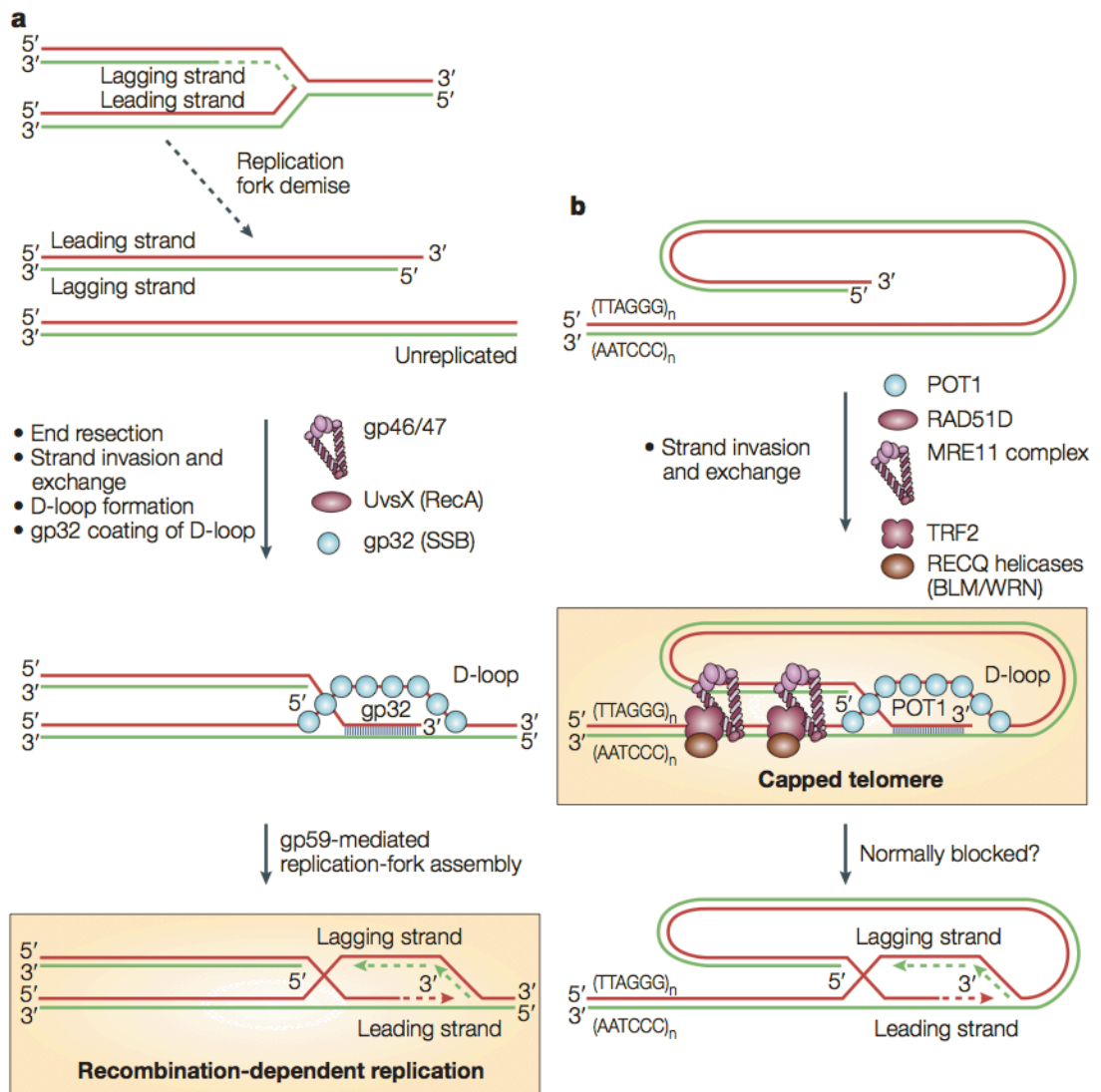
Figure 1.9. T-loop formation resembles RDR. **a.** Recombination-dependent replication (RDR) of phage T4, and **b.** T-loop formation in eukaryotes, where we can see the similarities between a subset of telomeric proteins and some of the RDR factors (*in* (de Lange, 2004)).

Although DNA repair proteins (DNA-PKcs, Ku70/80, ERCC1/XPF, RecQ helicases) associated with the telomere contribute to the formation and stabilisation of the protective telomeric loop they also help process chromosome ends when they get exposed, in an attempt to repair the terminal DNA, which may lead to chromosomal instability (de Lange, 2005). Terminal DNA can get exposed following telomere attrition as a consequence of cell division (Bodnar *et al*, 1998) or following telomere dysfunction via loss of TRF2 and its protected status (van Steensel *et al*, 1998). Telomere dysfunction through inhibition of TRF2 ultimately results in chromosome end-to-end fusions through non-homologous end-joining (NHEJ) between the C-strand of one telomere to the G-strand of another; this involves degradation of the 3'overhang and subsequent telomere end-joining by DNA ligase IV/XRCC4 (van Steensel *et al*, 1998; Smogorzewska *et al*, 2002). Normal cells attempt to prevent chromosomal instability arising from telomere fusions by signalling cell cycle arrest.

Telomere attrition in normal human cells results in cellular senescence and can be averted by telomerase (Bodnar *et al*, 1998) whilst telomere dysfunction via loss of TRF2 can elicit senescence, in human fibroblasts and some cell lines, or apoptosis, in human T lymphocytes and certain p53-deficient cancer cells (van Steensel *et al*, 1998; Karlseder *et al*, 1999). In either case, senescence is induced by alterations in the capped state of the telomere and not by complete loss of telomeric DNA as it was shown that over-expression of TRF2 reduced the senescence setpoint by protecting critically short telomeres from fusion (Karlseder *et al*, 2002). Exposed telomeric DNA leads to cell cycle arrest via activation of ATM-p53 signalling also known as the DNA damage response (DDR).

Telomere uncapping through inhibition of TRF2 or telomere shortening following replicative exhaustion causes telomere dysfunction-induced senescence (TDIS) in normal human fibroblasts (d'Adda di Fagagna *et al*, 2003; Takai *et al*, 2003). Dysfunctional telomeres associate with several DNA damage factors such as 53BP1, H2AX, Rad17, MDC1, NBS1, ATM and MRE11 to form telomere dysfunction-induced foci (TIFs), suggesting that they resemble DNA lesions (Takai *et al*, 2003). In addition, these cells display activated forms of Rad17, ATM, CHK1, CHK2, p53, p21^{WAF1} and H2AX (ɣ-H2AX). The latter is known to recruit checkpoint and DNA repair proteins to sites of DNA damage containing DSBs and ATM to be a signal transducer for DSBs, suggesting that exposed chromosome ends are perceived and processed as a DNA DSB (Takai

et al, 2003; d'Adda di Fagagna *et al*, 2003). ATM activation results in up-regulation of p53 and its transcriptional target p21^{WAF1} followed by G1 arrest (Herbig *et al*, 2004). More importantly, inactivation of the checkpoint kinases (CHK) or of ATM restored cell cycle progression which indicates that firstly, stable arrest requires continuous signalling and secondly, that the signal emitted by dysfunctional telomeres seems similar to the signal generated by IR-induced DSBs and is transduced by the classical DNA damage pathway of senescence (d'Adda di Fagagna *et al*, 2003; Herbig *et al*, 2004). Despite the similarities, telomere dysfunction is a particularly potent cell cycle inhibitor since the presence of a single TIF is capable of causing long-term arrest (Herbig *et al*, 2004). This suggests that the damage signal arising from dysfunctional telomeres is distinct from the signal emerging from DSBs occurring in other areas of the genome and possibly more complex.

DNA double-strand breaks (DSBs) accumulate in human senescent cells and ageing mice suggesting that the accumulation DNA lesions containing unrepairable DSBs may contribute to mammalian ageing (Sedelnikova *et al*, 2004; Wang *et al*, 2009). However, only 20% of the DNA damage foci (ɣ-H2AX) colocalise with telomeres in normal human fibroblasts undergoing senescence (Sedelnikova *et al*, 2004). Permanent DNA lesions differ from transient lesions, where efficient repair occurs, and have recently been characterised as DNA-SCARS or 'DNA segments with chromatin alterations reinforcing senescence' (Rodier *et al*, 2011). Persistent DNA damage foci in these structures fail to associate with certain repair proteins but accumulate activated forms of DDR mediators, particularly H2AX, which sustain both the senescence-associated growth arrest and cytokine secretion. Recent findings, however, show that persistent DDR foci accumulate preferentially at the telomeres in senescent cells and ageing tissues alike (Fumagalli *et al*, 2012; Hewitt *et al*, 2012). This seems to be because while DNA damage in non-telomeric regions of the genome is generally repairable, damage at the telomeres is unrepairable (Fig. 1.10). Telomeres are particularly susceptible to genotoxic stress (Hewitt *et al*, 2012; Suram *et al*, 2012) and telomeric DNA resists repair due to its association with telomeric factor TRF2 (Fumagalli *et al*, 2012). Mammalian TRF2 has been shown to prevent chromosome fusions *in vivo* (van Steensel *et al*, 1998) and, conversely, TRF2 inhibition results in fusions generated by DNA ligase IV-dependent non-homologous end joining, or NHEJ (Smogorzewska & de Lange, 2002). In order to test that telomeres resist DSB repair, Fumagalli *et al* (Fumagalli *et al*, 2012) first used the HO endonuclease inducible system in *S.*

cerevisiae cells to generate DSBs adjacent to areas containing or lacking telomeric repeats. They found that whilst HO-induced DSBs in non-telomeric regions were repaired by NHEJ, DSBs located next to telomeric repeats were not repaired, similarly to what happens in a DNA ligase 4-deleted control strain. Further analysis by ChIP and qPCR showed that the recruitment of DNA ligase IV (the enzyme responsible for the final ligation step in NHEJ) was inhibited in areas with DSBs flanking telomeric repeats as opposed to other DSB sites. Subsequently, the specific involvement of TRF2 was demonstrated by using a system which mimics a telomere containing the telomeric protein TRF2 but lacking telomeric DNA. Authors expressed the LacI-TRF2 fusion protein in cells from a mouse fibroblast line carrying a single integrated I-SceI cleavage site which is flanked by lactose operator (LacO) repeats on one side and tetracycline operator (TetO) repeats on the other. In addition, the expression of the tetracycline repressor fused to yellow fluorescent protein (YFP-Tet) allowed for the visualisation of this locus in the nucleus. I-SceI-induced DNA breaks resulted in a DDR, as measured by co-localisation of YFP-Tet with ɣ-H2AX. Consequently, after a 24h period following I-SceI inactivation to allow for repair, the percentage of DDR-positive cells expressing LacI alone was significantly lower then in cells expressing the LacI-TRF2 fusion protein. In the latter the DDR foci persisted due to lack of repair. This suggests that when TRF2 is ectopically expressed next to a DNA break it inhibits its repair and this seems to be because it inhibits recruitment of repair factors such as DNA ligase IV to the site of damage (Fumagalli *et al*, 2012). Thus it seems that the main factor that turns telomeres into protective structures, by preventing chromosome fusions resulting from exposed DNA, is also what turns them into unrepairable areas of the genome. All this evidence attests for the contribution of telomere dysfunction to organismal ageing.
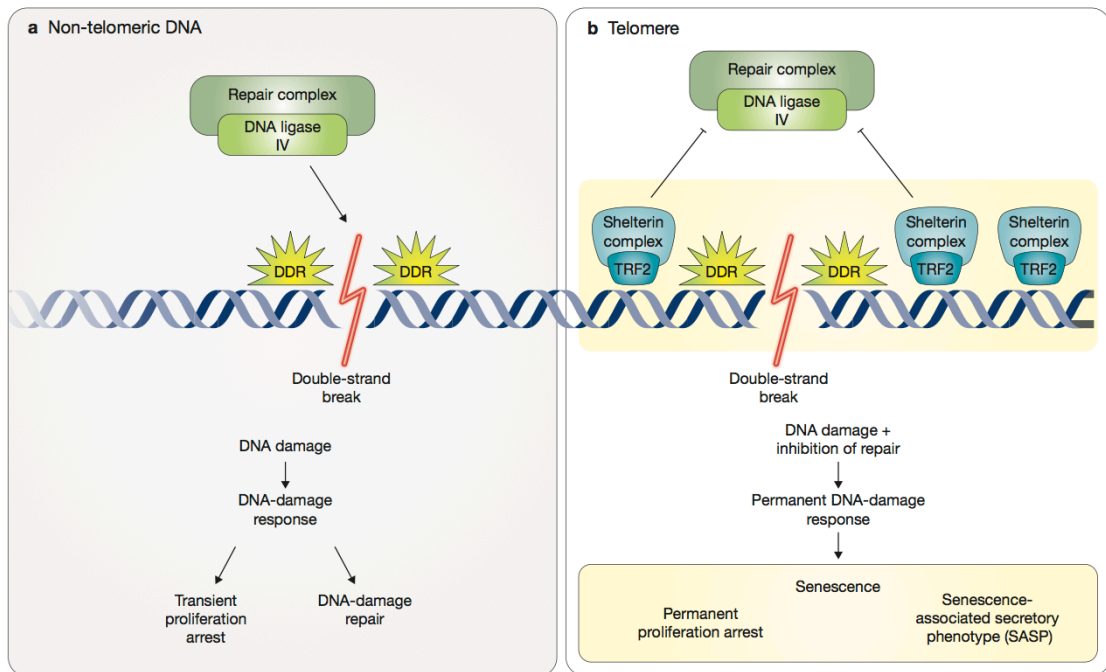
Figure 1.10. Distinction between DNA damage responses at telomeric and non-telomeric sites. a. DNA damage at non-telomeric DNA causes DDR-mediated transient growth arrest since most of the damage is repaired, and **b.** DNA damage at telomeres causes chronic DDR signalling which results in permanent growth arrest and activation of the SASP, since it is irreparable due to inhibition of repair by TRF2 (*in* (van Tuyn & Adams, 2012)).

1.5. Background of the project

In cultured human fibroblasts, telomere dysfunction generated by expression of the dominant-negative mutant of TRF2 (TRF2$^{\Delta B \Delta M}$) is associated with a DNA damage response (DDR) and DNA damage foci that locate to the telomeres (TIFs) (d'Adda di Fagagna *et al*, 2003; Takai *et al*, 2003; Herbig *et al*, 2004). In the skin of ageing primates, 80% of the fibroblasts show markers of senescence but only 15% show telomere-induced foci (Jeyapalan *et al*, 2007) which could indicate that either the remaining 65% are using a telomere-independent mechanism of senescence or that TIFs are just insensitive indicators of telomere-driven senescence *in vivo*.

The effect of telomere uncapping in epidermal keratinocytes is distinct from that observed in fibroblasts. In keratinocytes, dysfunctional telomeres, also generated by depletion of the telomere-binding factor TRF2 via retroviral expression of TRF2$^{\Delta B \Delta M}$, caused a senescent-like cell cycle arrest; however, this was accompanied only by a transient two fold increase in 53BP1 foci and p53 phosphorylation at Serine 15 with no detectable induction of p21^{WAF1}, p53's transcriptional target (Minty *et al*, 2008). The surprisingly subtle DDR observed suggests that the weak DNA damage signal generated by activation of p53 may be sufficient to elicit senescence in keratinocytes, but it can also indicate that damaged telomeres in epidermal cells use an alternative signalling pathway towards senescence. Therefore, other markers were sought. Microarray analysis five days after expression of TRF2$^{\Delta B \Delta M}$ revealed several genes up-regulated by two fold or more. Expression levels for four of these genes (HIST2H2BE, ICEBERG, S100A7 and HOPX) increased with telomere uncapping and decreased with restoration of telomere length via ectopic expression of TERT. This was observed in normal human epidermal keratinocytes expressing TRF2$^{\Delta B \Delta M}$ (NHEK-TRF2$^{\Delta B \Delta M}$) and late passage D17 cells, which suggests regulation by telomerase (Muntoni *et al*, 2003; Minty *et al*, 2008). The D17 cell line (Muntoni *et al*, 2003) is an atypical oral dysplasia lacking functional p16^{INK4a} and p14^{ARF} but retaining wild-type p53. Although possessing an extended lifespan, D17 cells still undergo senescence following considerable telomere erosion close to the end of their replicative lifespan. The data presented by Minty *et al* suggest that HIST2H2BE, ICEBERG, S100A7 and HOPX might be

specific markers for telomere-induced senescence in normal human epidermal keratinocytes. This hypothesis was supported by the down-regulation of the above markers following the ectopic expression of telomerase in D17 in parallel with telomere elongation and immortalisation (Minty *et al*, 2008).

Ideally, biomarkers should be secretable and detectable in body fluids, but lack of specificity for telomere dysfunction is a problem with all the secreted biomarkers identified so far (Jiang *et al*, 2008). The identification of biomarkers that are sensitive indicators of telomere function (be that length or capping status) can be clinically useful as they can be used as indicators of disease progression and, by being mechanism-specific, can be targeted for future anti-ageing strategies (Sahin & DePinho, 2010). The purpose of this study is to assess the specificity of the putative markers of telomere-induced senescence HIST2H2BE, ICEBERG, S100A7 and HOPX and their potential use as biomarkers for TDIS.

1.6. Aims of the project

Initial aims

• Assess if the small induction of DNA damage is enough to cause senescence or to induce the candidate genes.

• Assess if the candidate genes are non-specific markers of any type of growth arrest.

• Assess whether the markers are specific to telomere dysfunction or are non-specific markers of all forms of senescence.

Overall aims of the project

• To assess the specificity of previously identified markers of keratinocyte telomere dysfunction.

• To test their role in telomere-induced keratinocyte senescence.

• To assess their utility in marking telomere dysfunction *in vivo*.

Chapter 2. Materials and Methods.

2.1. Materials

Standard laboratory and cell culture materials (VWR International)

Standard laboratory solutions and chemicals (Sigma-Aldrich)

2.1.1. Biological Materials

Cell strains/lines

Name	Description	ID
BICR-6	Squamous cell carcinoma (hypopharynx)	Cell line
D17	Oral pre-malignant keratinocytes	Cell strain*
NHEK-131	Normal human epidermal keratinocyte strain 131	Cell strain
NHOF-1	Normal human oral fibroblast strain 1	Cell strain
Phoenix A	Phoenix amphotropic packaging cell line	Cell line
Phoenix E	Phoenix ecotropic packaging cell line	Cell line
Retropack ™ PT67	PT67 amphotropic packaging cell line	Cell line
SCC-25	Squamous cell carcinoma	Cell line
SVHFK	SV-40 transformed human foreskin keratinocytes	Cell line
Swiss 3T3	Random bred mouse Swiss 3T3 fibroblasts	Cell line

Table 1. List of cell lines and cell strains. * = cell strain in extended lifespan

Cell culture medium, supplements and other reagents

Name	ID	Company
Adenine hydrochloride	A3159	Sigma
Cholera toxin	9012-63-9	MP Biomedicals
DMEM 4.5 g/L glucose	BE12-604F	Lonza
Donor Adult Bovine Serum (BS)	SH30075.03	Hyclone
EDTA Disodium Salt	E5134	Sigma
Epidermal growth factor (EGF)	E9644	Sigma
Ham's F12	BE12-615F	Lonza
HEPES 1M in 0.85% NaCl	BE17-737E	Lonza
Hyclone Fetalclone II Serum (FCII)	HYC-001-323F	Fisher Scientific
Hydrocortisone hemisuccinate	H2270	Sigma
Insulin	I9278	Sigma
KGM BulletKit	CC-3111	Lonza
L-Glutamine 200 mM	17-605E	Lonza
PBS tablets	BR0014G	Oxoid
Penicillin/Streptomycin	17-602E	Lonza
Transferrin	T1283	Sigma
Trypsin TL Worthington	LS003667	Lorne

Table 2. List of cell culture medium, supplements and other reagents used for cell culture.

Selection agents for gene expression

Name	Conc (ug/mL)	Description	ID	Company
Ampicillin	100	Prokaryotic selection agent	A0166	Sigma
Blasticidin S HCl	8 to 10 (NHEK & D17)	Eukaryotic selection agent	R210-01	Invitrogen
Geneticin (G418)	200 (D17)	Eukaryotic selection agent	11811-023	Invitrogen
Kanamycin sulfate	25	Prokaryotic selection agent	11815-024	Invitrogen
Puromycin dihydrochloride	1 (NHEK) 2 (PhE & NHEK) 2.5 (PT67)	Eukaryotic selection agent	P8833	Sigma

Table 3. List of antibiotics used for drug selection of eukaryotic and prokaryotic cells.

Competent cells

Name	ID	Company
XL1-Blue Competent cells	200249	Stratagene
DH5α Competent cells	From stab culture (12540)	Addgene
Stbl2 ™ Competent cells	10268-019	Invitrogen

Table 4. List of competent *E. coli* cells used for transformation.

Retroviral vectors

Plasmid	Vector backbone	Gene/ Insert	Selection cassette	ID	Provider/PI
pLPC-NMYC	pLPC puro	no insert (EV)	Puromycin	12540	Addgene/ Titia de Lange*
pLPC-NMYC TRF2 deltaB deltaM	pLPC puro	hTRF2	Puromycin	16069	Addgene/ Titia de Lange*
pBabe GFP	pBabe puro	no insert (EV)	Puromycin	-	Cleo Bishop**
pBabe p14^{ARF}	pBabe puro	p14^{ARF}	Puromycin	-	Gordon Peters***
pBabe p16^{INK4a}	pBabe puro	p16^{INK4a}	Puromycin	-	Gordon Peters***
pBabe p53	pBabe puro	p53	Puromycin	-	Gordon Peters***
pGFP-B-RS	pRS	no insert (EV)	Blasticidin	TR30018	Origene
pGFP-B-RS S shRNA anti-HOPX	pRS	non-effective scrambled	Blasticidin	TR30019	Origene
pGFP-B-RS A shRNA anti-HOPX	pRS	shRNA A	Blasticidin	TR319501	Origene
pGFP-B-RS B shRNA anti-HOPX	pRS	shRNA B	Blasticidin	TR319501	Origene
pGFP-B-RS C shRNA anti-HOPX	pRS	shRNA C	Blasticidin	TR319501	Origene
pGFP-B-RS D shRNA anti-HOPX	pRS	shRNA D	Blasticidin	TR319501	Origene

Table 5. List of retroviral vectors used for retroviral transduction. * The Rockefeller University, NY, USA. **BICMS, London, UK. ***Cancer Research UK, London, UK.

Antibodies

Primary antibody anti-human	Host species	Clonality	KDa	Dilution	ID/ Company
GAPDH	Rabbit	Polyclonal	37	1:5000 (WB)	ab9485/ Abcam
HOPX (FL-73)	Rabbit	Monoclonal	20	1:200 (WB) 1:100 (IF)	sc-30216/ Santa Cruz
p16^{INK4a} (C20)	Rabbit	Monoclonal	16	1:200 (WB) 1:1000 (IF)	sc-468/ Santa Cruz
p21^{WAF1} (C70)	Mouse	Monoclonal	21	1:250 (WB)	610233/BD Transducti on Labs
p53 (DO-1)	Mouse	Monoclonal	53	1:250 (WB)	sc-126/ Santa Cruz
TRF2 (clone 4A794)	Mouse	Monoclonal	66	1:500 (WB)	05-521/ Millipore
α-Tubulin	Rabbit	Polyclonal	72	1:1000 (WB)	ab4074/ Abcam
β-Actin	Rabbit	Polyclonal	40	1:1000 (WB)	ab75186/ Abcam

Table 6. List of primary antibodies.

Secondary Ab HRP-conjugated	Host species	Dilution	ID/Company
Anti-mouse IgG	Goat	1:2500	32430/Thermo Scientific
Anti-rabbit IgG	Goat	1:2500	32460/Thermo Scientific
Anti-goat IgG	Sheep	1:10000	A-9452/Sigma- Aldrich

Table 7. List of secondary antibodies used for Western blotting.

Secondary Ab	Description	Host species	ID	Company
Anti-rabbit IgG	Alexa Fluor 488	Goat	A-11008	Invitrogen
Anti-mouse IgG	Alexa Fluor 568	Goat	A-11031	Invitrogen

Table 8. List of secondary antibodies used for Immunocytochemistry.

Other biological materials

• Goat Serum (Dako)

• LB broth (Sigma)

• Milk Powder, <1% fat (Marvel)

2.1.2. Chemical Materials

Chemicals and reagents

Name	ID	Company
2-Mercaptoethanol	M3148	Sigma
DAPI	D3571	Invitrogen
DMSO	D1435	Sigma
Ethanol Absolute	24013	Sigma
Formaldehyde 38% (v/v)	F8775	Sigma
FuGENE6®	11 815 091 001	Roche
Glycerol	G5516	Sigma
Glycine	50046	Sigma
M-PER® Mammalian Protein Extraction Reagent	78501	Thermo Scientific
Methanol	20847.320	VWR
NaCl	27800.360	VWR
Nonidet® P 40 Substitute	74385	Fluka
NuPAGE 20®	NP0002	Invitrogen
PFA	P6148	Sigma
Polybrene®	H9268	Sigma
Restore™ PLUS WB Stripping buffer	46430	Thermo Scientific
Rhodamine B	R-6626	Sigma
SDS sample buffer (4x)	NP0007	Invitrogen
Trizma® base	93350	Sigma
Tween® 20	P1379	Sigma

Table 9. List of chemicals and reagents.

Commercial kits and molecular biology graded reagents

Name	ID	Company
Amersham™ ECL Plus WB Detection System	RPN2132	GE Healthcare
cOmplete® Mini EDTA-free Tablets	04 693 159 001	Roche
DC™ Protein assay	500-0116	Bio-Rad
DyNAmo™ cDNA synthesis kit	F470L	New England Biolabs
HyperLadder ™ V	BIO-33031	Bioline
LightCycler® 480 SYBR Green I Master	04 707 516 001	Roche
Nuclease-free H$_2$O	129114	Ambion
NuPAGE 10% Bis-Tris gels	NP0301BOX	Invitrogen
NuPAGE 4-12% Bis-Tris gels	NP0335BOX	Invitrogen
Plasmid DNA purification maxi kit	12162	Qiagen
Precision Plus Protein™ Standards, Dual Color	161-0374	Bio-Rad
QIAquick PCR purification kit	28104	Qiagen
QIAshredder	79654	Qiagen
RNase-free DNase Set	79254	Qiagen
RNeasy Mini kit	74104	Qiagen
tRNA solution	R4251	Sigma

Table 10. List of commercial kits and molecular biology graded reagents.

Primer sequences

Name	bp	Forward	Reverse
CCNA2	108	CCATACCTCAAGTATTTGCCATC	TCCAGTCTTTCGTATTAATGATTCAG
CCND1	166	CGTGGCCTCTAAGATGAAGG	GTGTTCAATGAAATCGTGCG
HIST2H2BE	134	GGTAGATCCACCCTTATGCTT	TTAAGAGGGGAACACCATGAG
HOPX	84	ACTTCAACAAGGTCGACAAGC	GGGTCTCCTCCTCGGAAA
ICEBERG	175	CTTGCTGGATTGCCTATTAGAG	TTGAGGGTCTTCTTCACAGAG
IVL	83	TGCCTGAGCAAGAATGTGAG	TTCCTCATGCTGTTCCCAGT
p14^{ARF}	66	CTACTGAGGAGCCAGCGTCTA	CTGCCCATCATCATGACCT
p16^{INK4a}	58	CCAACGCACCGAATAGTTACG	GCGCTGCCCATCATCATG
p21^{WAF1}	127	TCACTGTCTTGTACCCTTGTGC	GGCGTTTGGAGTGGTAGAAA
p53	85	AGGCCTTGGAACTCAAGGAT	CCCTTTTTGGACTTCAGGTG
POLR2A	73	GCAAATTCACCAAGAGAGACG	CACGTCGACAGGAACATCAG
S100A7	128	AAAGCAAAGATGAGCAACAC	AAGTTCTCCTTCATCATCGTC
TRF2	105	CCAGATGAAGACAGTACAACCAA	CCAGTTTCCTTCCCCATATTT
TRF2DN	94	GTTGATTTCTGAAGAAGATTTGTT	GTGGAAGTAGAACTTGAGCAC
YAP1	83	CCCAGATGAACGTCACAGC	GATTCTCTGGTTCATGGCTGA

Table 11. List of primer sequences used for qPCR. bp = product length in base pairs.

2.1.3. Other Materials/Equipment

Other Materials	Company
Amersham ECL Hyperfilm ™	GE Healthcare Life Sciences
Immobilon®-FL 0.45 µm PVDF membrane	Millipore
Immobilon®-PSQ 0.2 µm PVDF membrane	Millipore
Immu-Mount	Thermo Scientific
Lab-Tek™ II 8-Chamber Slides	Thermo Scientific
Nalgene® Mr Frosty	Thermo Scientific
Nunc ™ cryovials	Thermo Scientific
Parafilm® M barrier film	Sigma

Table 12. List of other materials.

Equipment	Company
460R bench-top centrifuge	Hettich Rotanta
5415D bench-top centrifuge	Eppendorf
ABI 3730 sequencer*	Applied Biosystems
G-Box transilluminator	Syngene
GSR D1 Cs-137 low dose-rate gamma irradiator**	GSM
J2-MC centrifuge	Beckman-Coulter
Lightcycler® 480 qPCR system	Roche
Megafuge 2.0R centrifuge	Heraeus
Microcentrifuge	Labnet International
NanoDrop ND1000 spectrophotometer	Thermo Scientific
Novex® Mini-Cell WB tanks	Invitrogen
PowerEase 500	Invitrogen
PowerPac 200	Bio-Rad
Synergy HT spectrophotometer	BioTek
Veriti ™ 96-well thermal cycler	Applied Biosystems

Table 13. List of equipment. * Service provided by The Genome Centre, QMUL; ** service provided by QMUL.

2.2. Methods

2.2.1. Cell culture

Routine cell culture was performed in Class II type A laminar flow hoods using aseptic technique. Cells were maintained in standard humidified cell culture incubators, at 37°C and 10% / 90% air CO_2 atmosphere or 5% / 95% air CO_2 atmosphere. Cell pellets were obtained by centrifugation in a Megafuge 2.0R centrifuge (Heraeus). All solutions used in cell culture were isotonic, prepared with calcium- and magnesium-free phosphate buffered saline (PBS). Cells were cryopreserved in 2 mL Nunc™ cryovials (Thermo Scientific) placed in Nalgene® Mr Frosty (Thermo Scientific) containers that allow a 1°C/min cooling rate down to -80°C overnight and then transferred to vapour phase liquid nitrogen storage (-196°C). When required, cells were irradiated using the GSR D1 device (GSM), a Cs-137 low dose-rate research gamma irradiator (service provided by Queen Mary University of London). A list of all cell strains/lines, cell culture medium composition and other reagents used in cell culture can be found in the Materials section under Biological Materials.

Normal Human Epidermal Keratinocytes

NHEK-131 (GIBCO) at 6.8 MPD originate from expansion of primary human keratinocytes, produced from a pool of a minimum of 3 neonatal foreskins. Cells were sourced from the cell bank within the laboratory, thawed rapidly in water at 37°C and co-cultured with lethally irradiated 3T3 'feeder' cells at the correct density in FAD⁻ medium (3 parts DMEM 4.5 g/L glucose, 1 part Ham's F12, 10% (v/v) Hyclone Fetalclone II serum, 20 mM HEPES buffer, 100 U/mL Penicillin, 100 U/mL Streptomycin and 2 mM L-Glutamine, supplemented with 1.8×10^{-4} M Adenine, 5 µg/mL Insulin, 5 µg/mL Transferrin, 0.4 µg/mL Hydrocortisone and 8.4 ng/mL Cholera Toxin). Medium was replenished every third or fourth day with FAD⁺ complete medium (FAD⁻ supplemented with 10 ng/mL EGF). Cells were routinely cultured at 37°C in a 10% CO_2 atmosphere.

Cells were subcultured, at 50-80% confluence, by first removing 'feeders' with 0.02% EDTA and PBS, pipetted vigorously against the dish, followed by disaggregation of the NHEK colonies into single cells, by incubation with 0.1% trypsin / 0.01% EDTA for 10 to 20 minutes at 37°C. Cell pellets were obtained by

centrifugation of single cell suspensions at 800 rpm for 5 min. Cells were cryopreserved in 90% (v/v) Hyclone Fetalclone II serum, 10% (v/v) DMSO at 8-12 MPD.

The number of population doublings (PDs) was calculated based on the formula:

$$PD = 3.32 \times (\log_{10} \text{\# cells harvested} - \log_{10} \text{\# cells seeded})$$

NHEK colonies were revealed in the culture dish (visible with the naked eye) with rhodamine B staining. Cells were first fixed on the cell culture dishes with a solution of 10% (v/v) formalin (3.8% (v/v) formaldehyde) in PBS for 30 min at room temperature, inside a fume hood. After washing with PBS, cells were stained with a 1% (m/v) Rhodamine B aqueous solution for 30 min at room temperature. Plates were thoroughly rinsed with tap water, left to air dry and cloning or plating efficiency was calculated:

$$\text{Cloning efficiency (\%)} = \text{\# colonies obtained} / \text{\# cells seeded} \times 100$$

For irradiation, cells were transported to and from the nearby irradiation facilities in the cell culture dishes, sealed with Parafilm® M barrier film, in a polystyrene box at room temperature. Samples were irradiated at 1.493 Gy/min for 1 min 20 sec for a total dose of 2 Gy, at 1.493 Gy/min for 13 min 23 sec for a total dose of 20 Gy, and at 0.747 Gy/min for 13 min 23 sec for a total dose of 10 Gy. Controls were handled in the same way but received no irradiation.

3T3 and derived cell lines

3T3 cells originally derive from random-bred Swiss mouse embryo cultures. PT67 RetroPack™ cells are a NIH 3T3-derived cell line. 3T3 and derived cell lines were obtained from the cell bank, thawed rapidly in water at 37°C and routinely cultured in 10C medium (90% (v/v) DMEM 4.5 g/L glucose, 10% (v/v) Hyclone donor adult Bovine Serum, 20 mM HEPES, 100 U/mL Penicillin, 100 U/mL Streptomycin and 2 mM L-Glutamine) at 37°C in a 5% CO_2 atmosphere. At 80% confluence, cells were subcultured by rinsing with PBS followed by

incubation with 0.1% trypsin for 5 min at 37°C. Cells were cryopreserved in 90% (v/v) donor adult bovine serum, 10% (v/v) DMSO.

To use as 'feeders', 3T3 or PT67 cells were grown to 100% confluence, trypsinised and re-suspended. Cells were transported on ice as a cell suspension, in BD Falcon™ conical tubes, and irradiated at 1.493 Gy/min for 40 min 11 sec for a total dose of 60 Gy. Irradiated 3T3 cells were frozen at 2.5×10^6 cells/mL and a vial recovered from liquid nitrogen storage each time NHEKs were subcultured. PT67 cells were used freshly irradiated for co-culture with NHEKs during infection.

Phoenix cells (293-derived cell lines)

Phoenix A and E cells were obtained from the cell bank and routinely cultured in Growth Medium (90% (v/v) DMEM 4.5 g/L glucose, 10% (v/v) heat inactivated Hyclone Fetalclone II serum, 100 U/mL Penicillin, 100 U/mL Streptomycin and 2 mM L-Glutamine) at 37°C in a 5% CO_2 atmosphere.

Cells were thawed rapidly at 37°C by holding the vial and gently shaking it in the water bath. As cells started to thaw 1 mL of growth medium (GM) was added immediately and the cell suspension transferred to a 15 mL sterile conical screw cap tube. Additional 2 mL of GM were added to allow osmotic equilibration followed by an extra 10 mL. Cell pellets were obtained by centrifugation at 1000 rpm for 5 min.

Cells were subcultured at 1:4 or 1:5 at 70-80% confluence every 2-3 days for at least a week before being plated for transfection, to maximise transfection efficiency. First they were gently rinsed with PBS (cells do not adhere strongly to the culture dish and therefore detach very easily) and then trypsinised with 0.05% trypsin / 0.01% EDTA for about 30 sec at room temperature. Cells easily detached and were readily pipetted into a single cell suspension by adding GM. Cells were cryopreserved in 90% (v/v) heat inactivated Hyclone Fetalclone II serum, 10% (v/v) DMSO.

Keratinocyte cell lines

Keratinocyte cell lines SCC-25, SVHFK and BICR-6 were obtained from the cell bank and routinely cultured in 10H medium (90% (v/v) DMEM 4.5 g/L glucose, 10% (v/v) Hyclone Fetalclone II serum, 20 mM HEPES buffer, 100 U/mL Penicillin, 100 U/mL Streptomycin and 2 mM L-Glutamine, supplemented with 0.4 µg/mL Hydrocortisone) in the 'feeder' system or in KGM in the 'serum-free system', at 37°C in a 10% CO_2 atmosphere.

Cells grown in the 'feeder system' were subcultured, at 50-80% confluence, by first removing the 'feeders' with 0.02% EDTA and PBS, pipetted vigorously against the dish, followed by disaggregation of the colonies into single cells, by incubation with 0.1% trypsin / 0.01% EDTA for 10 to 20 min at 37°C. Cells grown in the 'serum-free system' were subcultured, at 50-80% confluence, by rinsing 1x with PBS followed by incubation with 0.1% trypsin / 0.01% EDTA for 10 to 20 min at 37°C. Cell pellets were obtained by centrifugation at 800 rpm for 5 min. Cells were cryopreserved in 90% (v/v) Hyclone Fetalclone II serum, 10% (v/v) DMSO.

2.2.2. Immunocytochemistry

Keratinocytes were seeded in Lab-Tek™ II 8-Chamber Slides (Thermo Scientific). Cells were rinsed with PBS and fixed in 4% (v/v) para-formaldehyde (PFA) for 10 min at room temperature. Cells were rinsed with PBS and permeabilised with 0.5% (v/v) NP-40 buffer for 10 min at room temperature.

Non-specific binding sites were blocked by incubating with 10% goat serum in 0.5% NP-40 buffer for 30 min. Incubation with primary antibody (Table 6), diluted in 10% goat serum in 0.5% NP-40 buffer, was performed for 2h at room temperature. Cells were washed 3x for 5 min in 0.5% NP-40 buffer. Incubation with secondary antibody (Table 8), diluted in 10% goat serum in 0.5% NP-40 buffer, was performed for 45 min at room temperature, away from light. Cells were washed 3x for 5 min in 0.5% NP-40 buffer.

Cells were then incubated with DAPI (1:1000 in PBS) for 5 min at room temperature, away from light and washed for 5 min in PBS. Coverslips were mounted with Immu-Mount (Thermo Scientific) and stored in the dark at 4°C.

2.2.3. Gene expression analysis

RNA isolation

Extraction of total RNA was performed using the RNeasy Mini Kit (Qiagen) according to manufacturer's instructions. The kit is based on the use of a high-salt buffer system that selectively binds RNA longer than 200 nucleotides to a silica membrane on a mini spin column. As smaller RNA molecules (rRNA and tRNA) are excluded, the procedure provides an enrichment for mRNA. All centrifugation steps were performed in a 5415D bench-top centrifuge (Eppendorf). Samples were kept on ice.

Growth medium was removed from adherent cells, these were trypsinised and pelleted by centrifugation. Cell pellets were re-suspended in 1 mL of cold PBS (to remove any traces of growth medium), transferred to 1.5 mL eppendorf tubes and the number of cells determined. Cell suspensions were centrifuged for 10 min at 2,500 x g and cell pellets obtained by aspirating supernatants carefully. These were either frozen immediately at -80°C, after removing the supernatant, or processed straight away. Cells were lysed by adding 350 µL RLT buffer (contains 10 µL β-ME per mL of RLT buffer) and vortexing to mix. RLT is a highly denaturing buffer containing guanidine-thiocyanate, which eliminates RNases, and β-ME. Lysates were pipetted directly into QIAshredder (Qiagen) spin columns placed in 2 mL collection tubes and centrifuged for 2 min at full speed. One volume of 70% (v/v) ethanol was added to the homogenised lysates and mixed well by pipetting. The QIAshredder biopolymer-shredding system combined with 70% ethanol ensures ideal binding conditions to the spin column. Samples (up to 700 µL) were then transferred to RNeasy spin columns placed in 2 mL collection tubes, centrifuged for 15 sec at 10,000 x g and flow-through discarded. RNA binds to the silica-membrane in the column and contaminants are removed in subsequent washes. DNase treatment was also performed with the RNase-free DNase Set (Qiagen) to eliminate any genomic DNA contamination.

Buffer RW1 (350 µL) was added to the RNeasy spin column followed by centrifugation at 10,000 x g for 15 sec to wash the spin column membrane and flow-through discarded. A volume of 10 µL of DNase I stock solution was added to 70 µL buffer RDD, mixed by gently inverting the tube and centrifuged briefly

in a micro centrifuge to collect residual liquid from the sides of the tube. The DNase I incubation mix (80 μL) was added directly to the RNeasy spin column membrane, and placed on the benchtop (20–30°C) for 15 min. Buffer RW1 (350 μL) was added to the RNeasy spin column followed by centrifugation at 10,000 x g for 15 sec to wash the spin column membrane and flow-through discarded. Buffer RPE (500 μL) was added to the RNeasy spin column, followed by centrifugation at 10,000 x g for 15 sec to wash the spin column membrane and flow-through discarded. This step was repeated but for 2 min now. The RNeasy spin column was placed in a new 2 mL collection tube and centrifuged at maximum speed for 1 min to eliminate any residual buffer in the sample. Finally, the column was placed in a 1.5 mL collection eppendorf tube, 20 μL to 40 μL of RNase-free water (Qiagen) added to it directly and column centrifuged for 1 min at 10,000 x g to elute RNA. Its concentration and purity was measured using a NanoDrop ND1000 spectrophotometer (Thermo Scientific). RNA concentrations of 200 ng/μL or higher and A260/280 in the 2.00-2.10 range were obtained and indicate good quality RNA.

cDNA synthesis

Purified RNA was reverse transcribed using with Finnzymes DyNAmo^{TM} cDNA synthesis kit (New England BioLabs), which is intended for cDNA synthesis for two-step qRT-PCR for amplicons around 100 bp in length. The reverse transcriptase used (M-MuLV RNase H$^+$) has RNase H activity, thus degrading the RNA template following reverse-transcription. This confers the advantage of facilitating the annealing of primers to the cDNA, when later amplified by qPCR.

cDNA synthesis was performed on a Veriti^{TM} 96-well thermal cycler (Applied Biosystems), using 0.7-1.0 μg purified RNA, 1x RT buffer, 15 ng/μL random hexamer primer set, 10% (v/v) RNase-free H2O, and 10% (v/v) M-MuLV RNase H$^+$ to a final reaction volume of 20 μL, and with the following protocol: 25°C, 10 min for primer extension, 37°C, 30 min for cDNA synthesis, 85°C, 5 min for reaction termination and 4°C hold for cooling the sample. cDNA templates were finally stored at -20°C and diluted in DNase-free water (Qiagen) prior to use.

Primer design

Primers for HOPX, HOP homeobox (NCBI GeneID: 84525), for p21^{WAF1} or CDKN1A cyclin-dependent kinase inhibitor 1A (NCBI GeneID: 1026), for p14^{ARF} or CDKN2A cyclin-dependent kinase inhibitor 2A beta (NCBI GeneID: 1029) and for TRF2 or TERF2 telomeric repeat-binding factor 2 (NCBI GeneID: 7014) were designed using the Roche Applied Science primer design tool. Primers for the dominant negative mutant of TRF2, TRF2DN or TRF2$^{\Delta B\Delta M}$ were designed manually; initial base was G or C and each sequence between 19 and 25 nucleotides long for a T$_m$ between 60°C and 70°C.

$$T_m \text{ (°C)} = G/C \times 4 + A/T \times 2$$

Primers for HIST2H2BE histone cluster 2 (NCBI GeneID: 8349), ICEBERG or CARD18 caspase recruitment domain family member 18 (NCBI GeneID: 59082) and S100A7 or S100 calcium-binding protein A7 (NCBI GeneID: 6278) were previously published (Minty *et al*, 2008). Primers were obtained from Sigma-Aldrich.

Primers for IVL or Involucrin (NCBI GeneID: 3713), for p53 or TP53 tumour protein p53 (NCBI GeneID: 7157), for CCNA2 or Cyclin A2 (NCBI GeneID: 890), for POLR2A or polymerase (RNA) II (DNA directed) polypeptide A (NCBI GeneID: 5430) and for YAP1 or Yes-associated protein 1 (NCBI GeneID: 10413) were kindly donated by Dr Muy-Teck Teh (Institute of Dentistry, QMUL, London, UK). Primers for p16^{INK4a} or CDKN2A cyclin-dependent kinase inhibitor 2A alpha (NCBI GeneID: 1029) were kindly donated by Dr Cleo Bishop (BICMS, London UK) and primers for CCND1 or Cyclin D1 (NCBI GeneID: 595) were kindly donated by Dr Ann-Marie Bergin (Institute of Dentistry, QMUL, London, UK).

All primer sequences (Table 11) were run through the online NCBI Primer-BLAST tool to confirm specificity, binding sites and product length.

Quantitative Polymerase Chain Reaction (qPCR)

Real-time quantitative PCR was performed in the LightCycler 480® qPCR system (Roche Applied Science), using SYBR® Green chemistry. The following protocol was used in the LC480 for all reactions:

Denaturation (Hot Start)

95°C for 5 min

Amplification (45 cycles)

95°C for 10 sec (melting)

65°C for 6 sec (annealing)

72°C for 6 sec (extension)

76°C for 1 sec (acquisition)

Melting Analysis

95°C for 30 sec (melting)

65°C for 30 sec (cooling/annealing)

65°C to 99°C (gradual heating with continuous acquisition)

40°C for 5 sec (cooling/termination)

PCR products were amplified using 5 µL cDNA template, 1x SYBR® Green I Master Mix (Roche Applied Science), 0.7 µM F/R primers and SYBR® Green I H$_2$O, PCR-grade (Roche Applied Science) to a final reaction volume of 50 µL, and purified using the QIAquick™ PCR Purification Kit (Qiagen). A volume of 250 µL of Buffer PB was added to 50 µL PCR sample, mixed and added to a QIAquick™ spin column placed in a 2 mL collection tube. Column was centrifuged at 17,900 x g for 1 min to bind DNA and flow-through discarded. A volume of 700 µL of Buffer PE was added to the column, to wash DNA, centrifuged as before and flow-through discarded. The column was centrifuged for an additional minute to eliminate residual ethanol from buffer PE. Column was then placed in a 1.5 mL micro centrifuge tube and DNA eluted with 40 µL of molecular grade DNase-free water (Qiagen) by centrifuging for 1 min. DNA concentration was measured using a NanoDrop ND1000 spectrophotometer (Thermo Scientific) and the purified product diluted to a concentration of 10^{11} copies of the gene per 2 µL using the following equation:

$$\upsilon = \dfrac{\left[\dfrac{6.02 \times 10^{14}}{(bp)} \times 660\right] \times [DNA] \times 2 \times vol}{10^{11}} - vol$$

= volume required to dilute original DNA stock to obtain a final concentration of 10^{11} copies of the gene per 2 μL

This stock was subsequently diluted, using 25 μg/mL tRNA (Sigma) as a DNA carrier, to prepare a PCR standard dilution series (10^9 to 10^2 copies of the gene per 2 μL). This was used to perform standard curves to achieve absolute quantification for each gene. All dilutions were stored at -20ºC.

qPCR reactions were performed using 2 μL standard/cDNA template, 1x SYBR® Green I Master Mix (Roche Applied Science), 0.5 μM F/R primers and SYBR® Green I H$_2$O, PCR-grade (Roche Applied Science) to a final reaction volume of 10 μL, in LightCycler® 480 96-well plates (Roche Applied Science), in duplicate or triplicate for each sample. Data analysis was performed using LightCycler® 480 relative quantification software (with built-in multiple reference genes normalisation algorithm).

Gel electrophoresis

PCR products were run on a 2.5% (m/v) agarose gel containing 3 μL ethidium bromide, to confirm product size. A total of 4 μL of DNA was mixed with 1 μL DNA loading dye and loaded into the gel. Electrophoresis was conducted at 100 volts for 40 min and gel developed using a G-Box transilluminator (Syngene).

2.2.4. Protein expression analysis

Protein isolation

Growth medium was removed from adherent cells, these were trypsinised and pelleted by centrifugation. Cell pellets were re-suspended in 1 mL of cold PBS (to remove any traces of growth medium), transferred to 1.5 mL

eppendorf tubes and the number of cells determined. Cell suspensions were centrifuged for 10 min at 2,500 x g and cell pellets obtained by aspirating supernatants carefully. These were either frozen immediately at -80ºC, after removing the supernatant, or processed straight away.

Cells were lysed by adding M-PER® Mammalian Protein Extraction Reagent (Thermo Scientific), containing EDTA-free Protease Inhibitor (Roche Applied Science), at a ratio of 100 μL M-PER® Reagent per 1 Million cells, and the mixture pipetted up and down to re-suspend the pellet. Mixture was gently shaken for 10 min at room temperature and cell debris removed by centrifugation at 14,000 x g for 15 min in an 5415D bench-top centrifuge (Eppendorf). Finally, the supernatant was transferred to a new tube and protein lysate either kept on ice for further analysis or stored at -80ºC.

Protein concentration in the samples was determined the colorimetric Bio-Rad DC Protein Assay (Bio-Rad). Working reagent A' was prepared by adding 20 μL of reagent S per 1 mL of reagent A. A total of 3 - 5 dilutions of BSA protein standard containing from 0.2 mg/mL to 2 mg/mL protein were prepared in M-PER® Reagent to generate a standard curve each time the assay was performed. A volume of 5 μl of standards and samples was pipetted into a microtiter plate and 25 μL of reagent A' added into each well. This was followed by the addition of 200 μL reagent B. Plates were gently agitated to mix the reagents and, after 15 min, absorbances were read at 650 nm in a Synergy HT spectrophotometer (BioTek). Samples with amounts of total cellular protein of 20 μg to 40 μg per 20 μL of sample, containing 20% (v/v) SDS sample buffer (Sigma), were boiled on a hot plate at 100ºC for 5 min. Samples ready for Western blot analysis were stored at -20ºC.

Western blotting

Protein in the samples (20 μL) and Precision Plus Protein™ (Bio-Rad) dual colour standards (10 μL) were separated by SDS polyacrylamide gel electrophoresis, under denaturing and reducing conditions, on 10% SDS or 4-12% SDS NuPAGE Bis-Tris pre-cast resolving gels (Invitrogen) at 130 volts on 1x NuPAGE running buffer (Invitrogen). Wet transfer to 0.2 μM or 0.45 μM Immobilon™ PVDF membranes (Millipore), pre-soaked in methanol for 1 min,

was performed on transfer buffer (25 mM Tris, 190 mM glycine and 20% methanol) at 30 volts for 90 min at 4ºC.

PVDF membranes were blocked in 5% low fat milk in Tris-buffered saline and Tween 20 (TBS-T or wash buffer: 1 M Tris, pH 8.0; 5 M NaCl; 0.05% Tween 20) at room temperature for 1h with shaking. Incubation with primary antibodies (Table 6), prepared in 5% low fat milk in TBS-T, was performed for 2h at room temperature or overnight at 4ºC, with agitation, followed by three 5 min washes with TBS-T. Incubation with hrp-conjugated secondary antibodies (Table 7), prepared in 5% low fat milk in TBS-T, was performed for 1h at room temperature with agitation, followed by three 5 min washes with TBS-T. Antigen-antibody complexes were detected by incubating the PVDF membranes with 1 mL Amersham ECL Plus chemiluminescent detection reagent (GE Healthcare Life Sciences) at room temperature for 5 min, followed by detection on Amersham ECL Hyperfilm (GE Healthcare Life Sciences) developed in a dark room on a standard film developer machine.

Densitometry analysis was performed on scanned films using the Java-based image processing software ImageJ (NIH). First, the background is subtracted from the image by applying a suitable rolling ball radius (RBR) and each lane on the blot, containing the band of interest, is then independently selected. Lanes are plotted and the background threshold set. The bands appear as peaks and the area of each peak is then measured. Finally, the relative intensities of the bands of interest are normalised against the values obtained for the corresponding loading control (GAPDH).

2.2.5. Retroviral transduction

A list of all the retroviral vectors, competent bacterial cells and packaging cell lines used can be found in the Materials section under Biological Materials.

Transformation

Super-competent cells (Table 4) were thawed on ice and 100 µL aliquoted into pre-chilled 14 mL BD Falcon polypropylene round-bottom tubes.

Transformations were performed both with and without plasmid DNA using aseptic microbiological technique. A total of 100 ng of plasmid DNA (Table 5) was added to the cells followed by incubation on ice for 30 min. Tubes were then placed in a 42°C water bath for exactly 2 min followed by incubation on ice for 10 min. Four times the volume of preheated LB broth (Sigma) was then added and mixture incubated at 37°C for 1h with shaking at 250 rpm. A 100 µL aliquot of the transformation mixture was plated, using a sterile spreader, on LB agar plates containing the appropriate antibiotic (Table 3) and plates incubated at 37°C overnight.

Plasmid DNA purification

Vectors were prepared using the Plasmid DNA purification maxi kit (Qiagen), according to manufacturer's instructions. The method is based on a modified alkaline lysis procedure and selective binding of plasmid DNA to an anion-exchange resin. All centrifugation steps were performed in a J2-MC centrifuge (Beckman-Coulter).

A single colony was picked from a freshly streaked selective plate and used to inoculate a starter culture of 5 ml LB broth (Sigma) containing the appropriate selective antibiotic (Table 3). The mixture was incubated for 6h at 37°C with shaking at 250 rpm. Glycerol stocks were prepared by adding 700 µL of each vector to the same volume of 60% (v/v) glycerol (Sigma) and stored at -80°C. The starter culture (400 µL) was diluted 1/1000 into selective LB medium in a flask with a volume of at least 4 times the volume of the culture and incubated overnight at 37°C with shaking at 250 rpm. Bacterial cells were harvested by centrifugation at 6000 x g for 15 min at 4°C. The bacterial pellet was lysed in alkaline conditions by re-suspending in 10 mL Buffer P1 followed by mixing with 10 mL Buffer P2 until lysate appeared viscous. Mixture was then incubated at room temperature for exactly 5 min. Genomic DNA, proteins and cell debris were precipitated by mixing immediately with 10 mL of chilled Buffer P3 and incubating on ice for 20 min. They were then removed by centrifugation and in subsequent medium-salt washes. The mixture was centrifuged at 16,000 rpm for 30 min at 4°C and supernatant containing plasmid DNA removed promptly. Centrifugation was repeated at 16,000 rpm for 15 min at 4°C, supernatant containing plasmid DNA again removed promptly and applied to an empty QIAGEN-tip 500 column, pre-equilibrated with 10 mL Buffer QBT.

The supernatant enters the column by gravity flow allowing plasmid DNA to bind the anion-exchange resin in the column, under appropriate low salt and pH conditions. Contaminants such as genomic DNA, proteins and cell debris were removed in two subsequent medium-salt washes with 30 mL Buffer QC. Plasmid DNA was then eluted in 15 mL Buffer QF (a high-salt buffer), precipitated and desalted with 10.5 mL room-temperature isopropanol followed by centrifugation at 14,000 rpm for 30 min at 4°C. The DNA pellet was washed with 5 mL of room temperature 70% (v/v) ethanol (Sigma) and centrifuged at 14,000 rpm for 10 min. The pellet was air-dried for 5–10 min to remove all traces of ethanol and DNA redissolved in 300 µL TE buffer, pH 8.0. Plasmid DNA concentration and purity were measured using a NanoDrop ND1000 spectrophotometer (Thermo Scientific). A260/280 higher than 1.8 was obtained for all vectors, denoting good quality purified plasmid DNA. Vectors were further diluted in Tris-EDTA (TE) buffer to a working concentration of 500 µg/mL and stored at -20°C.

Sequencing

Retroviral vectors were validated by nucleotide sequencing analysis on the ABI 3730 using BigDye® 3.1 chemistry (Applied Biosystems). Plasmids were used at 100 ng/µL and primers at 10 pmol/µL. Primers for the multiple cloning site (MCS) of pBabe vectors were kindly donated by Dr Cleo Bishop (BICMS, London, UK) and their sequences are presented below:

pBabe fwd: 5' CTTTATCCAGCCCTCAC 3' (for the psi packaging signal)

pBabe rev: 5' ACCCTAACTGACACACATTCC 3' (for the SV40 enhancer)

Sequencing data was analysed using 4Peaks software (mekentosj.com) and the identity of the inserts confirmed with the online NCBI's BLASTn database.

Transfection and Infection

Retroviral transduction was used for gene delivery to the target cells. Both indirect and direct strategies were used for infection. The indirect strategy involved production of ectropic virus which was used to generate infectious

amphotropic cell lines; these were then co-cultured with the target cells to deliver the transgenes. The direct strategy involved production of amphotropic virus used to directly infect the target cells via spinfection. Spinfection was performed in a 460R benchtop heated centrifuge (Hettich Rotanta).

Indirect strategy of infection

Transfection (production of ecotropic virus)

Phoenix E cells were seeded at 2×10^5 cells per well (6-well plate) in duplicate, 24h before transfection. Cells were then transfected with 5 µg of plasmid DNA and FuGENE® 6 (1:2.5 ratio). FuGENE® 6 was added drop wise to serum-free medium (DMEM 4.5 g/L glucose, 12.5 mM HEPES buffer), mixed gently and left for 5 min at room temperature. DNA (5 µg) was added, mixed gently and left for 20 min at room temperature. The medium was then aspirated from cells, replaced with the transfection mixture and left to incubate at room temperature for 10 min. Finally, 1 mL of GM was added to the cells and plates returned to the 37°C incubator for 5h. Another 2 mL of GM was then added and cells returned to the incubator for 48h.

At this stage, duplicates were pooled into 10 mm dishes with selective medium (GM containing 2 µg/mL puromycin). At confluence, spent medium was removed, replaced with 1/2 volume of fresh GM and cells incubated at 32°C. Virus was obtained by harvesting the conditioned medium at 48-72h, filtering through a 0.45 µm filter and freezing the viral supernatants immediately at -80°C, in 1mL aliquots.

Infection I (generation of infectious amphotropic cell lines)

PT67 cells were seeded at 2×10^5 cells per well (6-well plate) in duplicate, 24h before infection. Cells were incubated at 37°C for 15 min with polybrene in 10C medium at 5 µg/mL. Supernatants were thawed at room temperature, polybrene (Sigma) added to a final concentration of 5 µg/mL and the mixture added to the cells. The plates were centrifuged at 350 rpm for 1h at 32°C. Cells were then washed with PBS and returned to the 37°C incubator in fresh medium for 48h. At this stage duplicates were pooled into 10 mm dishes with selective

medium (10C medium containing 2.5 µg/mL puromycin). Medium was refreshed every third day until drug-resistant populations of PT67s were obtained. Stocks of these stable cell lines were stored in liquid nitrogen (vapour phase).

Infection II (delivery of transgenes to the target cells)

Infectious PT67 cells were recovered from the cell bank, grown in selective medium (10C containing 2.5 µg/mL puromycin) to confluence and irradiated at 60Gy. One million NHEK-131 were seeded, at equal density, with lethally irradiated 3T3 cells and infectious PT67 cells in 100 mm dishes with FAD⁻ medium for 48h, at which time selective medium (FAD⁺ containing 1.0 µg/mL puromycin) was introduced. All 'feeders' were replaced with 1×10^6 lethally irradiated 3T3 neo/puro^R cells, in selective medium, 48h later. NHEKs were kept on drug selection for the following 72h, at which point selective medium was replaced with FAD⁺, and cells left to grow overnight and harvested the following day.

Direct strategy of infection

Transfection (production of amphotropic virus)

Phoenix A cells were seeded at 1×10^6 cells per 60 mm dish or 2.5×10^6 per 100 mm dish, 24h before transfection. On the day of transfection cells were inspected and dishes selected based on ideal cell density, distribution and absence of clumping.

Cells were transfected at a 1 µg DNA to 2.5 µL FuGENE®6 ratio (1/2.5 ratio) in serum-free medium. First, 10 µL/25 µL (60 mm dish/100 mm dish) of FuGENE® 6 (Roche Applied Science) was added to 550 µL/150 µL S/F medium in a drop wise manner, mixed gently and left at room temperature for 5 min. Then, 4 µg/10 µg of plasmid DNA was added, mixed gently and the mix left at room temperature from 25 to 45 min. Cells were removed from the incubator and the DNA-Fugene mix added to the medium in a drop wise manner. The dish was gently swirled to ensure good distribution before returning cells to the incubator for 24h.

At this point transfection efficiency was assessed by noting fluorescence, transfection medium replaced by half the volume of GM and cells placed in an incubator overnight at 32°C for virus production. Virus was obtained by harvesting the conditioned medium at 48h, 54h, 72h and 78h after transfection. Viral supernatants were collected with a 10 mL syringe, filtered through a 0.45 µm filter and aliquoted into cryovials (1 mL or 2 mL aliquots). These were either used immediately for infection or snap frozen in dry ice and immediately transferred to storage at -80°C. Medium was replenished after each harvest and cells returned to the 32°C incubator until the next time point.

Infection (delivery of transgenes to target cells)

Keratinocytes were seeded at 5×10^4 cells per well with lethally irradiated 3T3s at 1.6×10^5 cells per well, 72h before infection. On the day of infection, 'feeders' were first removed and cells incubated at 37°C for 15 min with FAD medium containing 5 µg/mL polybrene (Sigma-Aldrich). Supernatants were thawed quickly in a 37°C water bath (or used directly after collection), diluted in equal volume of FAD medium and polybrene added to a final concentration of 5 µg/mL. The mixture was added to the cells, plates were returned to the 32°C incubator until 10% / 90% air CO_2 atmosphere was reached and immediately sealed w/ Parafilm® M barrier film. Spinfection was performed in two rounds, at 300 rpm for 1h at 32°C. Cells were washed with PBS and returned to the 37°C incubator in fresh medium until the next infection, 6h later. Cells were washed once again and fresh 'feeders' added in FAD medium. Plates were returned to the 37°C incubator for 24h and FAD replaced with selective medium, containing the appropriate antibiotic. Cells remained in drug selection for 72h at which point medium was replaced with FAD overnight until sample collection.

Chapter 3. Introduction to and establishment of the experimental model.

3.1. Introduction

3.1.1. Background

Fibroblasts have been successfully grown in culture for the first half of the twentieth century and by the 1960s the first human diploid cell strain had been developed (WI-38, (Hayflick & Moorhead, 1961)), followed by others in the next decade (MRC-5, (Jacobs *et al*, 1970) and IMR-90, (Nichols *et al*, 1977)). Growing keratinocytes however, remained a challenge. Early studies (discussed in (Rheinwald & Green, 1975a)) showed that, after disaggregation from skin, epidermal cell growth and maintenance depended on dermal fibroblasts or their products and that keratinocytes would grow in monolayers, but to a very limited extent. The problem was that, while absolutely essential for epithelial colony initialisation, the presence of fibroblasts would also constitute a hindrance as they would overgrow the keratinocytes and take over the culture, rendering sub-cultivation impossible.

3.1.2. Serial sub-cultivation of keratinocytes

Successful serial growth of human keratinocytes in culture was first possible due to the 3T3 cell line. In 1963, Todaro and Green (Todaro & Green, 1963) were working with mouse embryo fibroblasts with the intention of obtaining an immortalised cell line that might be a suitable target for viral transformation. After testing several combinations of inoculation densities and transfer intervals, a unique cell line called 3T3 (3 x 10^5 cells innoculum at a 3 days transfer interval) emerged. 3T3 cells demonstrated a distinctive property, contact inhibition or density-dependent inhibition of growth, which enabled them to arrest growth at confluence and, therefore, to be easily spotted upon successful transformation, as this characteristic would be lost. Later, after isolating epithelial cells from a mouse teratoma (germ line tumour able to differentiate into several somatic tissues), the authors observed that without a background of teratomal fibroblasts epithelial cells grew very slowly, yet when

supplemented with lethally irradiated 3T3 cells they showed exuberant growth in culture (Rheinwald & Green, 1975b). Shortly after, the same procedure was successfully applied to normal human diploid keratinocytes isolated from newborn foreskin and the first human epithelial cell strains were developed (Rheinwald & Green, 1975a).

3T3 cells play a complex role as feeders in supporting the growth of keratinocytes. In general, lethally irradiated 3T3s act as a substitute for mesenchymal fibroblasts while also suppressing proliferation of the contaminating fibroblasts. In fact, irradiated 3T3 proved to be even more effective than irradiated human diploid fibroblasts in their supportive function *in vitro* (Rheinwald & Green, 1975a). However, keratinocyte cell strains and keratinocyte cell lines differ in their dependence upon the 3T3 cells and/or their products, and evolution of mesenchymal independence seems to be acquired upon immortalisation (Green, 1980). The presence of 3T3s is an absolute requirement in both for keratinisation, in cell strains for colony initiation and, in cell lines for colony initiation/growth only at low density. The latter are able to grow if inoculated at high density in complete absence of 3T3s and, for keratinocyte strains, 3T3-conditioned dishes can replace 3T3s in supporting initial colony growth, but are not as effective as the actual 'feeders'. Once colonies are formed, both keratinocyte lines and strains are able to maintain growth in the presence of 3T3-conditioned medium alone but, especially for cell strains, 'feeders' are still a requirement upon sub-cultivation (Rheinwald, 1980). The complex function of 3T3s as 'feeders' seems to be carried out by a combination of secreted soluble products (growth factors), insoluble factors (matrix) deposited on the growth surface and the presence of the cells themselves (support), in close proximity to the keratinocytes (Rheinwald, 1980). 3T3s also remove the keratinocyte cell cycle inhibitor transforming growth factor β or TGF-β (Rollins *et al*, 1989).

The 3T3 system relies not only on the use of lethally irradiated 3T3 cells but also in appropriate growth supplements and ideal growth conditions. The first supplement introduced in the cell culture medium was hydrocortisone (HC) (Rheinwald & Green, 1975a). It constitutes an absolute requirement for colony initiation from single cells in the 3T3 system and it allows colonies to acquire an organised epithelial-like morphology. The first culture conditions (based on DME, 20% FCS and HC, in a 37°C 8% CO_2 atmosphere) allowed cells to reach 50 generations, if obtained from newborn skin (Rheinwald & Green, 1975a). Later,

the introduction of epidermal growth factor (EGF) (Rheinwald & Green, 1977) and cholera toxin (CT) (Green, 1978) enabled extension of culture lifetime to up to 150 generations. EGF (Rheinwald & Green, 1977) also contributes to an increase in colony-forming efficiency (if added once small colonies have formed and not whilst as single cells or it will have the opposite effect). Colonies become larger and less stratified, as EGF contributes to keeping a higher proportion of cells in a dividing state, preventing them from committing to terminal differentiation, or at least delaying them. Its effect, however, will only manifest itself on cells that are still in cycle. Cholera toxin (Green, 1978) acts by increasing the intracellular levels of cAMP, promoting the rate of cell proliferation, thereby increasing the proportion of small cells (dividing fraction) in culture. Further improvements in culture conditions included the addition of Ham's F12 (enabled a reduction in FCS from 20% to 5% or 10%), insulin and adenine (Allen-Hoffmann & Rheinwald, 1984). These resulted in a further increase in colony-forming efficiency to a standard that justified the use of these growth conditions until today.

In parallel to the development of the 3T3 system there were alternative methods being investigated with the objective of dispensing the use of 'feeders'. The first basal nutrient media that allowed serial cultivation of keratinocytes in the absence of a 'feeder' layer or conditioned medium was developed by Peehl and Ham in the 1980s (Peehl & Ham, 1980a). Initially it was based on medium 199 supplemented with 20% FBS, Bovine Pituitary Extract (BPE at 0.15 mg/mL) and HC (10 μg/mL). The authors found that the increase from 0.4 to 10 μg/mL of HC was the determinant factor that allowed for 'feeders' to be absent (Peehl & Ham, 1980a). With the objective of obtaining a more defined system, they later dispensed the use of whole serum by substituting it with small amounts of dialysed FBS protein (1 mg/mL) (Peehl & Ham, 1980b). Also, the superior Ham's F12 replaced basal medium 199 and the introduction of adenine at higher levels (1.8×10^{-4}) and calcium at low concentration (3×10^{-5}) selectively promoted the growth of keratinocytes to the detriment of fibroblasts (Peehl & Ham, 1980b). The final optimised 'serum-free' system which is in use today is designed to support clonal growth of keratinocytes and allows cells to undergo up to 50 generations in culture, if derived from newborn skin (Wille *et al*, 1984). It is based on KBM basal medium (with Ham's F12 and low calcium, 0.1 mM) supplemented with BPE (0.03 mg/mL) EGF (0.1 ng/mL), Insulin (5 g/mL) and HC (0.5 μg/mL) for KGM (keratinocyte growth medium) complete medium.

The development of a 'feeder-free' system for sub-cultivation and clonal growth of keratinocytes was prompted by the need to eliminate confounding effects of another cell type when studying keratinocyte growth and differentiation (Peehl & Ham, 1980a). A study by Wille *et al* (Wille *et al*, 1984) showed that both are regulated by several factors in an integrated manner; insulin, EGF and BPE are more directly related to growth, whilst other growth factors, calcium and serum relate to differentiation. In general, upon growth arrest cells become enlarged and flattened, as they do in the 'feeder' system. However, in the presence of low calcium (0.1 mM), which is the environment in a 'serum-free' system, cells do not stratify or differentiate. This can only be induced by raising the calcium concentration above 0.4 mM (Owens *et al*, 2000). The combination of growth promoting factors such as insulin, EGF and BPE, combined with low calcium keeps cells as a monolayer, in growth phase, away from terminal differentiation. This contrasts with the morphology of the colonies in the 'feeder' system which will be described below.

The early failures in successfully growing keratinocytes *in vitro* were not due to any intrinsic limitation of the keratinocyte as a cell type, but rather to the complex relationship between epidermal cells and fibroblasts (Rheinwald & Green, 1975a; Green *et al*, 1979). Until now no synthetic substitute has been found to completely replace the role of the 3T3 cells as 'feeders'. Despite the development of new systems (serum-free/feeder-free), technically less demanding and user friendly, the 3T3 system is still the cell culture method of choice for growing normal human keratinocytes in use today and the closest to the physiological setting.

3.1.3. Colony morphology and clonality of keratinocytes

The development of the 3T3 system also enabled the isolation of clones of epithelial cells and their characterisation in culture. This is described in a series of studies by Green and colleagues in the 1980s.

Once a single cell is attached to the culture dish and starts dividing a colony is formed. Keratinocytes expand laterally due to cell division as a single layer in direct contact with the surface. In addition, colonies also expand upwards forming layers in consequence of migration of cells from the base that have engaged the program of terminal differentiation. Upon stratification, the

bottom single layer of small compacted cells can easily be perceived as the multiplying front of the colony. All cells in this layer are engaged in cell division, even the ones at the base of the thick multilayered centre, as it was shown by thymidine incorporation assays (Dover & Potten, 1983). The cells of the upper layers are larger and appear flattened, giving the centre of the colony a characteristic appearance, and eventually shed as squames (Rheinwald, 1980). This resembles the morphology/behaviour of normal human skin.

Colonies in culture are, therefore, a heterogeneous mixture of dividing and terminally differentiated cells. Upon sub-cultivation it is possible to isolate single cells and study their ability to form clones and characterise the latter (Barrandon & Green, 1985; 1987). Not surprisingly, it was clear that clonogenic potential was inversely proportional to cell size (Barrandon & Green, 1985). Keratinocytes that are 11 µm or less in diameter will divide and give rise to clones, whilst cells of 12 µm or greater in diameter will irreversibly get larger and terminally differentiate. Interestingly though, highly proliferating clones, originating from the smaller keratinocytes (<11 µm), are capable of giving rise to colonies regardless their diameter. The exception are clones larger than 20 µm which will not divide and have irreversibly committed to terminal differentiation. This shows that whilst the smallest cells are the most clonogenic, it is possible for bigger cells (up to 20 µm) to retain multiplying potential and give rise to cycling progeny of a smaller size.

Further analysis of clones arising from a single cell enabled estimation of their growth potential, based on what colony types they give rise to, and resulted in their characterisation as holoclones, meroclones or paraclones (Barrandon & Green, 1987). Holoclones have the greatest replicative potential and give rise to a high proportion of proliferative colonies with less than 5% of colonies being abortive. Holoclones were originally thought to originate from stem cells. Paraclones, on the other hand, display the shortest replicative lifespan originating colonies that can undergo a maximum of 15 generations by which time they will abort and terminally differentiate. Meroclones are a transitional stage between holoclones and paraclones, and contain a mixture of cells of different replicative potential. The biggest colonies obtained from meroclones are distinctive from proliferative colonies (originated by holoclones) as they display a characteristic wrinkled perimeter in contrast with the regular round edges from the latter.

As fibroblasts (Hayflick, 1965), normal human epidermal keratinocytes display a limited replicative lifespan in culture (Rheinwald & Green, 1975a). Also similarly, the culture lifetime of keratinocytes declines with age of donor (Rheinwald & Green, 1975a). Moreover, there is a shift in the relative frequency of holoclones and paraclones in populations of keratinocytes with age (Barrandon & Green, 1987). Holoclones are the predominant clonal type in populations deriving from newborn skin while paraclones are the most abundant in samples from older donors. Contrarily to what had been initially suggested, replicative senescence, not terminal differentiation or apoptosis, is the process responsible for the eventual exhaustion of replicative potential of keratinocytes with ageing (Norsgaard *et al*, 1996).

3.2. Establishment of experimental model

3.2.1. Choice of *in vitro* model

Normal human epidermal keratinocytes (NHEKs) were chosen as the *in vitro* model for the first part of this study. Since the aim is to work in the context of normal human epidermal ageing the choice of normal cells, with a limited replicative lifespan and thus able to undergo senescence, as opposed to a cell line, which has lost this ability, is suited. Plus, the epidermis is the classical epithelial model, thoroughly characterised and easy to obtain. With the choice of *in vitro* model, the intention is to minimise the introduction of variables due to *in vivo* and *in vitro* ageing.

The fact that cells derive from newborn foreskin should minimise variables due to *in vivo* ageing. Cells are from obviously very young donors, and thus should display optimum colony-forming efficiency and lifespan in culture. In addition, they are expected to possess intact pathways of senescence, with functional, though not activated, p53, p14^{ARF} and p16^{INK4a}. The latter is further guaranteed by the fact that they originate from foreskin, which means cells have not been subjected to UV damage, the main environmental causal agent of skin ageing (Fisher *et al*, 2002).

In order to minimise variables to *in vitro* ageing, cells are used at very early passage (between 8 and 20 MPD which corresponds to about 16 and 30% of the total lifespan, respectively) and cultured in the 3T3 'feeder' system, which delays the induction of p16^{INK4a} (the main effector of senescence in keratinocytes grown on dish) and the appearance of prematurely senescent keratinocytes (Darbro *et al*, 2005). Keratinocytes cultured with 'feeders' show an increased replicative lifespan relatively to cells growing in specialised serum-free medium ('feeder' free system) (Ramirez *et al*, 2001; Rheinwald *et al*, 2002). The 'feeder' system provides optimum conditions for keratinocytes growth, primarily due to the growth factors and mesenchymal/epithelial support provided by the 'feeder' layer, and additionally for the presence of adequate supplements essential for colony-forming ability, normal colony morphology/ stratification and achievement of maximum lifespan (discussed in detail above). Nevertheless, as opposed to previous reports (Ramirez *et al*, 2001),

despite optimum culture conditions provided by the 3T3 system, keratinocytes can still undergo premature senescence via p16^{INK4a} activation following continued expansion in culture and thus do not senesce exclusively via a telomere-dependent mechanism (Dickson *et al*, 2000; Rheinwald *et al*, 2002). The intention is that, by using optimum culture conditions and cells at early passage that have endured a short period of time in culture and therefore have undergone minimised manipulation, a possible bias due to the activation of a telomere-independent pathway of senescence and other undefined effects of ageing are eliminated. Another source of possible experimental bias comes from the use of 3T3s. Keratinocyte cell extracts will contain a residual amount of 'feeders', even though most would be removed by EDTA and washing, so this was accounted for by introducing a 3T3 control in all experiments.

3.2.2. NHEK culture in the 'feeder' system

The successful culture of normal human epidermal keratinocytes (NHEKs) in the 3T3 'feeder' system was established. Colony morphology and cloning efficiency were assessed and the growth conditions optimised. They are described below.

NHEKs and lethally irradiated 3T3s were inoculated into the culture dish as a mixture. The 3T3 cells attach first to the surface and quickly form a monolayer on which the small round keratinocytes rest. These are hardly discernible from the 'feeders' in the first couple of days but about four days following inoculation small colonies start being visible. At this point cells have finally made contact with the surface of the culture dish and, as the colonies expand, keratinocytes push and displace the 'feeder' cells into a compacted 'cuff' which delineates the periphery of each colony (Fig. 3.1.).

Keratinocyte colonies show a typical polygonal epithelial morphology, centrifugal growth and stratification, resembling normal epidermis. Keratinocytes divide from the centre to the periphery, forming a thin layer of small compacted cells that is always visible as a single layer at the edge of the colony. These cells are in close contact with the dish surface and, therefore, are thought to resemble the germinative cells in normal epidermis, harbouring the

potential for cell division. The centre of the colonies appears very thick and composed of stratified layers of flat squamous cells (Fig. 3.1.).

It is also possible to to identify two main types of keratinocyte colonies in culture, abortive and proliferative, reflecting the distinct growth potential of the clone-forming cell they derived from (Barrandon & Green, 1987). Proliferative colonies are bigger, composed of very small cells, and most likely derive from holoclones, whilst abortive colonies are smaller, containing big, flattened, squamous-like cells that aborted growth and terminally differentiated, therefore probably originating from a paraclone (Fig. 3.1.).
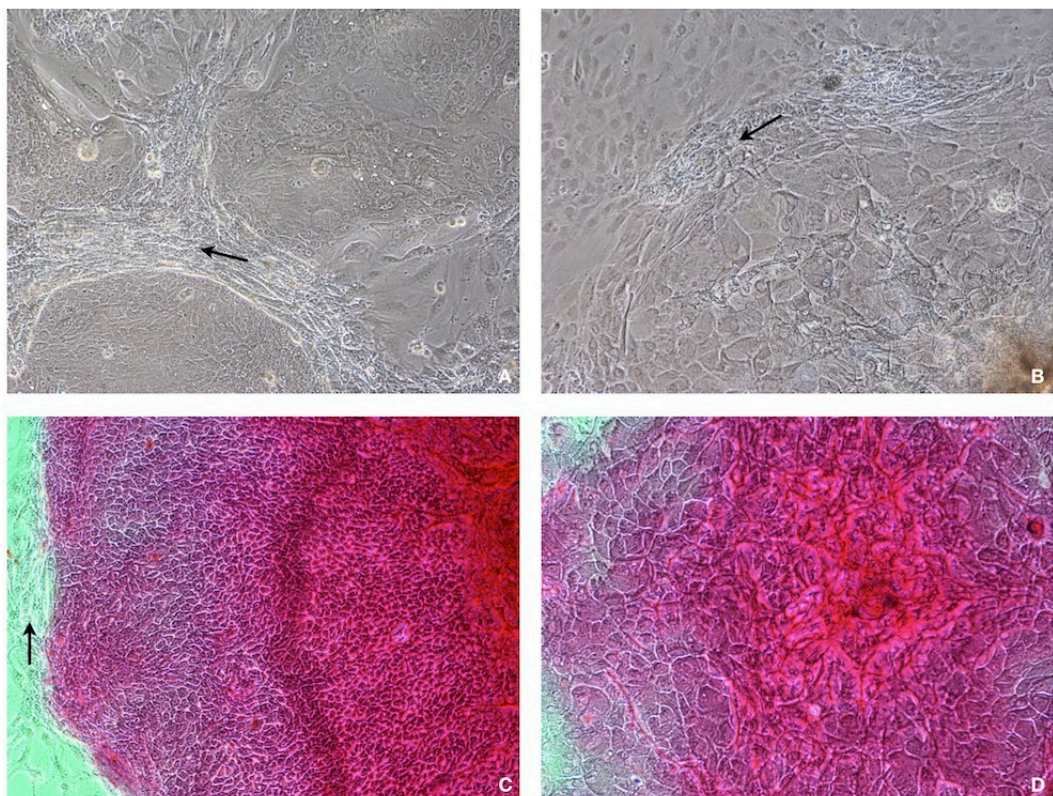
Figure 3.1. Morphology of NHEK colonies in the 'feeder' system. Arrows show the 'cuff' of compacted 'feeders' pushed away by the growing keratinocyte colonies. **A** shows 3 adjacent proliferative colonies and **B** an abortive colony. In **C** and **D** cells were stained with 1% rhodamine B, a dye that binds keratin therefore selectively staining keratinocytes. The staining highlights the pattern of centrifugal growth and stratification as well as the difference in colony size and cell morphology between proliferative (**C**) and abortive (**D**) keratinocyte colonies. NHEKs in **A** were seeded at 5 x 10^4 per 60 mm dish and cultured for 7 days; in B, C and D were seeded at 50 cells per 60 mm dish and cultured for 14 days. These phase contrast images were obtained at 100x magnification.

NHEKs showed the best growth and cloning efficiency if kept in a 10% CO_2/90% air atmosphere as opposed to the conventional 5% CO_2/95% air used routinely in cell culture incubators. For seeding densities as low as 500 and 50 cells per 60 mm culture dish (clonal densities) an optimum 10% cloning efficiency was obtained with 10% CO_2/90% air contrasting strongly with the 4% obtained when cells were maintained in a 5% CO_2/95% atmosphere (Fig. 3.2.).
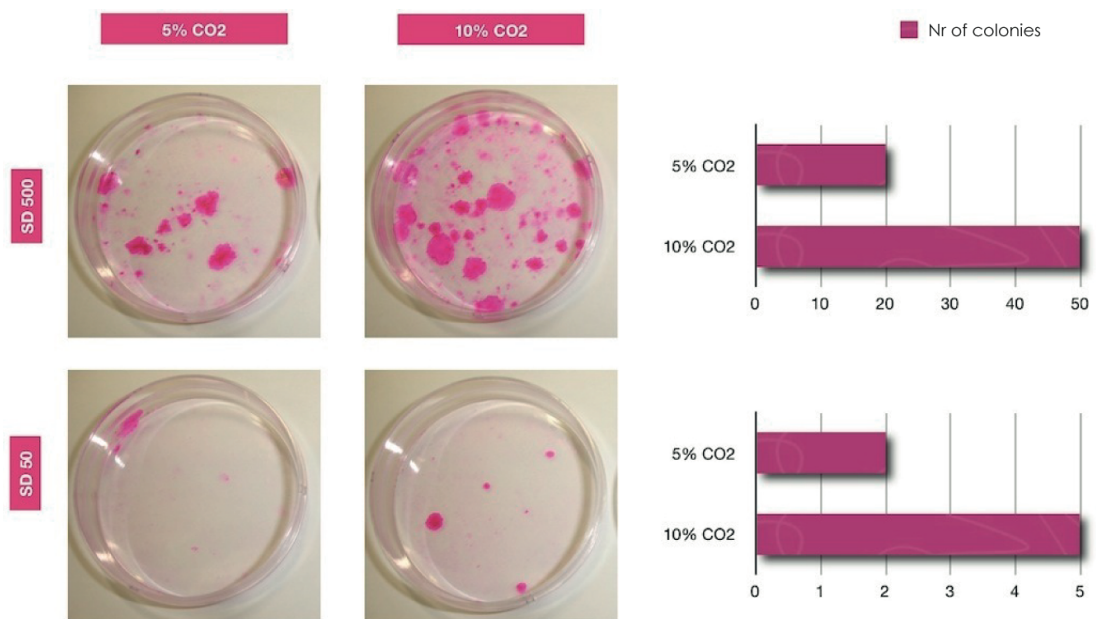
Figure 3.2. Clonogenicity of NHEK cultured in the 'feeder' system. Normal human epidermal keratinocytes show optimum growth in a 10% CO_2/90% air atmosphere. More colonies were obtained with 10% CO_2/90% air compared to 5% CO_2/95% air for the same seeding density (SD), reflecting an optimum 10% plating efficiency for 10% CO_2/90% air as opposed to 4% obtained with 5% CO_2/95% air. NHEK were plated at clonal densities of 50 and 500 cells per 60 mm culture dish and cultured for 14 days, at which point keratinocytes colonies were revealed by staining with 1% rhodamine B.

3.2.3. Primer design

If the cellular part of the work requires the use of a suitable, well established cell culture model, so does the molecular part need to rely on a good basis. The main objective of this study is to perform a transcriptional analysis of four genes that are candidate markers for telomere-induced senescence in keratinocytes. For the results to be reliable it is necessary to understand the requisites for and limitations of gene expression analysis using qPCR. A set of guidelines has been established to ensure homogeneity and accuracy in qPCR experimental design and data analysis and presentation (Bustin *et al*, 2009). Poor choice of primers for qPCR has been put forward as one of the three main causes of technical error that influence assay performance. Others include inadequate sample storage, preparation and nucleic acid quality, as well as inappropriate data and statistical analysis. I will describe here the rationale behind the primer design strategy used for candidate markers HIST2H2BE, ICEBERG, S100A7 and HOPX, for reference genes YAP1 and POL2RA, as well as for TRF2, TRF2$^{\Delta B\Delta M}$, p14^{ARF}, p16^{INK4a}, p53, p21^{WAF1}, Involucrin and Cyclins A2 and D1. For further technical details please refer to the Materials and Methods section (Chapter 2).

To ensure the best qPCR assay performance, good primer design should result in high PCR efficiency (ideally 100%, where every cycle generates double the amount of DNA), specific PCR products with no primer-dimers or other non-specific secondary structures, and no co-amplification of genomic DNA or pseudogenes. Design accounts for characteristics of the primers alone, their spatial interaction with themselves, each other and the template, as well as for location of the annealing sites and amplicon length. Primer size should be 18-30 bp (ideally 19-25 bp), with a GC content of 30-80% (ideally 40-60%) to generate a T_m (melting temperature) of 60-70°C (ideal 64°C) and T_a (annealing temperature) of 58-62°C (ideal 60°C). ΔT_m between forward and reverse primers should be lower than 4°C. Good quality primer design software accounts for nucleotide content and position to prevent occurrence of mismatches with the target DNA, and also checks for complementarity within primers to avoid hairpins. When possible (for multiple exon genes), it is ideal to design intron-spanning primers to avoid co-amplification of genomic DNA (for single exon genes the alternative is to perform DNase treatment on the RNA). Finally, smaller amplicons generate higher PCR reaction efficiencies, the ideal size being 60-120 nucleotides.

The following workflow was used for primer design or analysis. When sequences were already known and obtained from a source, they were first analysed using the NCBI Primer-BLAST tool which predicts the identity of the mRNA amplified, the annealing sites of the primers and product size. When primers were not already available they were designed using the online Roche Universal probe tool. Products were amplified using qPCR and analysed for generation of a single peak, for consistence in T_m and for quality/consistence of standard curves. If qPCR generated a specific, good quality product, primers were accepted. If not, or when primer sequences were not available, they were redesigned or designed from scratch.

HIST2H2BE, ICEBERG, S100A7 and HOPX

These four genes have been put forward as potential specific markers for telomere-induced senescence in normal human keratinocytes and primers for them have been previously described (Minty *et al*, 2008). The objective of this work is to assess their specificity for senescence induced by telomere dysfunction as opposed to senescence induced by other cellular pathways. Previously used primer sequences (Minty *et al*, 2008) were first introduced in the online NCBI Primer-BLAST tool to find out product lengths, annealing sites and specificity for the target. The results obtained are presented below (Figure 3.3).

	Sequence (5'->3')	Length	Tm	GC%
Forward primer	GGTAGATCCACCCTTATGCTT	21	50.93	47.62%
Reverse primer	TTAAGAGGGGAACACCATGAG	21	51.08	47.62%

Products on intended target

Products on allowed transcript variants

Products on potentially unintended templates

Products on target templates

>NM_003528.2 Homo sapiens histone cluster 2, H2be (HIST2H2BE), mRNA

```
product length = 134
Forward primer  1     GGTAGATCCACCCTTATGCTT   21
Template        1649  .....................   1669

Reverse primer  1     TTAAGAGGGGAACACCATGAG   21
Template        1782  .....................   1762
```

	Sequence (5'->3')	Length	Tm	GC%
Forward primer	CTTGCTGGATTGCCTATTAGAG	22	50.84	45.45%
Reverse primer	TTGAGGGTCTTCTTCACAGAG	21	51.10	47.62%

Products on intended target

Products on allowed transcript variants

Products on potentially unintended templates

Products on target templates

>NM_021571.3 Homo sapiens caspase recruitment domain family, member 18 (CARD18), mRNA

```
product length = 175
Forward primer  1    CTTGCTGGATTGCCTATTAGAG   22
Template        80   .....................   101

Reverse primer  1    TTGAGGGTCTTCTTCACAGAG   21
Template        254  .....................   234
```

Figure 3.3. Primer-BLAST analysis for sequences previously used (Minty, 2008) to amplify HIST2H2BE, ICEBERG (or CARD18), HOPX and S100A7. Products from partial alignments are not shown.

	Sequence (5'->3')	Length	Tm	GC%
Forward primer	CTCTTCCACACTAATGACAGAC	22	50.45	45.45%
Reverse primer	TTGTACTCCAGGATTTCCACC	21	51.38	47.62%

Products on intended target

Products on allowed transcript variants

Products on potentially unintended templates

Products on target templates

>NM_001145460.1 Homo sapiens HOP homeobox (HOPX), transcript variant 5, mRNA

```
product length = 205
Forward primer  1     CTCTTCCACACTAATGACAGAC  22
Template        444   ......................  465

Reverse primer  1     TTGTACTCCAGGATTTCCACC   21
Template        648   .....................   628
```

>NM_032495.5 Homo sapiens HOP homeobox (HOPX), transcript variant 1, mRNA

```
product length = 205
Forward primer  1     CTCTTCCACACTAATGACAGAC  22
Template        444   ......................  465

Reverse primer  1     TTGTACTCCAGGATTTCCACC   21
Template        648   .....................   628
```

	Sequence (5'->3')	Length	Tm	GC%
Forward primer	AAAGCAAAGATGAGCAACAC	20	49.39	40.00%
Reverse primer	AAGTTCTCCTTCATCATCGTC	21	49.67	42.86%

Products on intended target

Products on allowed transcript variants

Products on potentially unintended templates

Products on target templates

>NM_176823.3 Homo sapiens S100 calcium binding protein A7A (S100A7A), mRNA

```
product length = 128
Forward primer  1     AAAGCAAAGATGAGCAACAC  20
Template        49    ....................  68

Reverse primer  1     AAGTTCTCCTTCATCATCGTC  21
Template        176   .....................  156
```

>NM_002963.3 Homo sapiens S100 calcium binding protein A7 (S100A7), mRNA

```
product length = 128
Forward primer  1     AAAGCAAAGATGAGCAACAC  20
Template        63    ....................  82

Reverse primer  1     AAGTTCTCCTTCATCATCGTC  21
Template        190   .....................  170
```

Based on Primer-BLAST analysis, all primer sets are specific for the genes in question and should theoretically generate a single product. Primers for HIST2H2BE and ICEBERG amplify a single variant (both genes produce solely one transcript variant). Primers for HOPX amplify transcript variants 1 and 5. Primers for S100A7 amplify S100A7 and S100A7A.

More information on the genes to assess primer design strategy was obtained from the online NCBI Gene tool and gene maps are represented in Fig. 3.15. HIST2H2BE is processed as a single transcript containing a single exon so for this gene it is not possible to obtain primers that span an intron. ICEBERG also generates a single transcript containing 2 exons and an intron. S100A7 and S100A7A are two different genes, each generating a single transcript variant containing 3 exons and 2 introns, however sharing 95% homology (Fig. 3.4). Therefore, with the aforementioned primer set, amplification of S100A7 is accompanied by co-amplification of S100A7A.

Figure 3.4. BLAST analysis for homology between S100A7 and S100A7A transcripts. S100A7 mRNA is 439 bp, S100A7A mRNA is 4279 bp. Query = S100A7; Subject = S100A7A.

Finally, 5 transcript variants have been described for HOPX. Based on the gene map and primer annealing sites, and contrarily to the primer-BLAST prediction, two distinct products should be expected (Fig. 3.5). The forward primer anneals with a common area of exon 1 in variants 3, 1 and 5 while the reverse primer anneals with exon 2 of variant 3 and exon 3 of variants 1 and 5. Therefore, this set of primers should generate 2 products, one for variants 1 and 5 with the same size (205 bp) and a smaller product for variant 3.
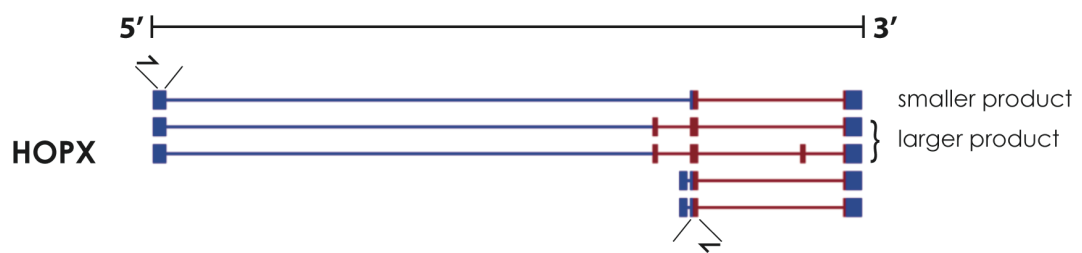
Figure 3.5. Gene map for HOPX and primer annealing sites for sequences previously used (Minty, 2008) to amplify HOPX. Transcript variants 3, 1, 5, 4 and 2 for HOPX are represented, from top to bottom.

All primer sets were tested by qPCR and the sets for HIST2H2BE, ICEBERG and S100A7 originated a single product (single melt curve) with the expected sizes (Fig. 3.17). However, due to the design strategy, directed solely at exons, some genomic DNA contamination was present (around 0.2% genomic DNA present in the final product). Despite limitations in product size (all products larger than 120 nucleotides) and design (not directed at exons spanning an intron) it was decided that the good quality of the products, the good efficiency of the qPCR reaction and the fact that using the same sequences would enable discussion of results in context with work previously published (Minty 2008), these primers were accepted and used for gene expression analysis of HIST2H2BE, ICEBERG and S100A7 (Fig. 3.15).

Contrarily to the primer-BLAST analysis (Fig. 3.3) but as predicted by looking at annealing sites in the gene map (Fig. 3.5), the primer set used for HOPX gave rise to 2 products, one of the predicted length and a smaller, less abundant product. The need for the generation of a single specific product, in addition to the disadvantageously long product size (well larger than 120

nucleotides) generated by this primer set prompted me to design a new set of primers for this gene.

In previous work (Minty *et al*, 2008) the primers used amplified variants 3, 1 and 5. For the new design the decision was not to favour any transcript variants and to design a set that would amplify a common product to reflect all 5 transcripts. This was not possible with an intron-spanning assay, so the design strategy was aimed at a common exon. The Roche Universal probe library generated the following set, that should result in a product of 84 nt. Primer-BLAST analysis confirmed the generation of a single product, common to all variants, with the predicted size (Fig. 3.6 and 3.17). After testing by qPCR this was the set used for gene expression analysis of HOPX (fig. 3.15).

	Sequence (5'->3')	Length	Tm	GC%
Forward primer	ACTTCAACAAGGTCGACAAGC	21	53.31	47.62%
Reverse primer	GGGTCTCCTCCTCGGAAA	18	51.71	61.11%

Products on intended target

Products on allowed transcript variants

Products on potentially unintended templates

Products on target templates

>NM_001145460.1 Homo sapiens HOP homeobox (HOPX), transcript variant 5, mRNA

```
product length = 84
Forward primer  1     ACTTCAACAAGGTCGACAAGC  21
Template        648   .....................  668

Reverse primer  1     GGGTCTCCTCCTCGGAAA  18
Template        731   ..................  714
```

>NM_001145459.1 Homo sapiens HOP homeobox (HOPX), transcript variant 4, mRNA

```
product length = 84
Forward primer  1     ACTTCAACAAGGTCGACAAGC  21
Template        294   .....................  314

Reverse primer  1     GGGTCTCCTCCTCGGAAA  18
Template        377   ..................  360
```

>NM_139212.3 Homo sapiens HOP homeobox (HOPX), transcript variant 3, mRNA

```
product length = 84
Forward primer  1     ACTTCAACAAGGTCGACAAGC  21
Template        523   .....................  543

Reverse primer  1     GGGTCTCCTCCTCGGAAA  18
Template        606   ..................  589
```

>NM_139211.4 Homo sapiens HOP homeobox (HOPX), transcript variant 2, mRNA

```
product length = 84
Forward primer  1     ACTTCAACAAGGTCGACAAGC  21
Template        250   .....................  270

Reverse primer  1     GGGTCTCCTCCTCGGAAA  18
Template        333   ..................  316
```

>NM_032495.5 Homo sapiens HOP homeobox (HOPX), transcript variant 1, mRNA

```
product length = 84
Forward primer  1     ACTTCAACAAGGTCGACAAGC  21
Template        648   .....................  668

Reverse primer  1     GGGTCTCCTCCTCGGAAA  18
Template        731   ..................  714
```

Figure 3.6. Primer-BLAST analysis for new primers designed to amplify all transcript variants of HOPX. Products from partial alignments are not shown.

TRF2 and TRF2$^{\Delta B \Delta M}$

TRF2 or telomeric repeat binding factor 2 is crucial in the establishment of the telomeric complex in mammalian cells. The normal TRF2 gene is composed of 10 exons (Fig. 3.16) and encodes for the TRF2 protein which is composed of three main areas; the N-terminal basic domain, the dimerisation area and the C-terminal Myb domain. The latter is required for binding telomeric DNA.

A specific intron-spanning assay targeting the C-terminal Myb domain was used to design a set of primers which would amplify endogenous functional TRF2. Primers anneal to exons 9 and 10 (Fig. 3.16), area encoding for the Myb domain, and generate a 105 nt product (Fig. 3.7 and 3.17).

	Sequence (5'->3')	Length	Tm	GC%
Forward primer	CCAGATGAAGACAGTACAACCAA	23	52.46	43.48%
Reverse primer	CCAGTTTCCTTCCCCATATTT	21	49.57	42.86%

Products on intended target

Products on allowed transcript variants

Products on potentially unintended templates

Products on target templates

>NM_005652.2 Homo sapiens telomeric repeat binding factor 2 (TERF2), mRNA

```
product length = 105
Forward primer  1      CCAGATGAAGACAGTACAACCAA  23
Template        1431   .......................  1453

Reverse primer  1      CCAGTTTCCTTCCCCATATTT    21
Template        1535   .....................    1515
```

Figure 3.7. Primer-BLAST analysis for sequences designed to amplify TRF2. Products from partial alignments are not shown.

A dominant-negative mutant of TRF2 (TRF2$^{\Delta B \Delta M}$) has been developed (van Steensel *et al*, 1998) which is characterised by lacking both the N-terminal basic and the C-terminal Myb domains. TRF2$^{\Delta B \Delta M}$ cDNA is conveyed in a pLPC plasmid backbone containing a Myc tag contiguous to the insert (Fig. 3.16). The latter contains only the coding regions required to originate the dimerisation domain of TRF2.

The design of a primer set to amplify exogenous TRF2$^{\Delta B \Delta M}$ was performed manually; the forward sequence directed at the Myc tag and the reverse sequence directed at the TRF2$^{\Delta B \Delta M}$ insert (Fig. 3.16). The resulting amplicon was 94 nt in size, confirmed by gel electrophoresis (Fig. 3.17). Primer-BLAST analysis confirmed no endogenous sequences were amplified with this set of primers.

p14^{ARF} and p16^{INK4a}

The gene CDKN2A or cyclin-dependent kinase inhibitor (CDKI) 2A encodes for two important tumour suppressors and main effectors of stress-induced senescence, p14^{ARF} and p16^{INK4a}. Out of the 3 transcript variants described for this locus (fig. 3.16), variant 4 or β encodes for p14^{ARF}, whilst variant 1 or α encodes for p16^{INK4a}. Variant 3 originates a product which is expressed only in the pancreas. Each variant contains 2 introns and 3 exons, with the 2nd and 3rd exons being common between all and the first exon being specific to each of the variants - 1β for p14^{ARF} and 1α for p16^{INK4a}.

A specific assay for variant 4 (p14^{ARF}) was used to design a set of primers which would amplify p14^{ARF}. Primers anneal to exon 1β and exon 2, and span an intron (Fig. 3.16). qPCR analysis confirmed the generation of a single product of the correct size (Fig. 3.17), predicted by Primer-BLAST analysis (Fig. 3.8).

	Sequence (5'->3')	Length	Tm	GC%
Forward primer	CTACTGAGGAGCCAGCGTCTA	21	54.89	57.14%
Reverse primer	CTGCCCATCATCATGACCT	19	51.03	52.63%

Products on intended target

Products on allowed transcript variants

Products on potentially unintended templates

Products on target templates

>NM_058195.2 Homo sapiens cyclin-dependent kinase inhibitor 2A (melanoma, p16, inhibits CDK4) (CDKN2A), transcript variant 4, mRNA

```
product length = 66
Forward primer  1     CTACTGAGGAGCCAGCGTCTA  21
Template        305   ....................  325

Reverse primer  1     CTGCCCATCATCATGACCT  19
Template        370   ...................  352
```

Figure 3.8. Primer-BLAST analysis for sequences designed to amplify p14^{ARF}. Products from partial alignments are not shown.

A primer set for variant 1 (p16^{INK4a}) was available and kindly donated by Dr Cleo Bishop (Blizard Institute, QMUL, London, UK). Based on primer-BLAST analysis (Fig. 3.9), design was aimed at exon 1α and exon 2; this indicates generation of 2 products, an amplicon 332 nt long corresponding to variant 3 and the desired product of 58 nt corresponding to p16^{INK4a} (Fig. 3.16). Since the first is too long and variant 3 is not expressed in keratinocytes, the generation of a single specific product of the correct size, corresponding to variant 1, was confirmed by qPCR (Fig. 3.17).

```
                     Sequence (5'->3')        Length  Tm    GC%
Forward primer  CCAACGCACCGAATAGTTACG  21      54.06 52.38%
 Reverse primer  GCGCTGCCCATCATCATG     18      53.76 61.11%
```

Products on intended target

Products on allowed transcript variants

Products on potentially unintended templates

Products on target templates

>NM_058197.3 Homo sapiens cyclin-dependent kinase inhibitor 2A (melanoma, p16, inhibits CDK4)
(CDKN2A), transcript variant 3, mRNA

```
product length = 332
Forward primer  1     CCAACGCACCGAATAGTTACG  21
Template        325   ....................   345

Reverse primer  1     GCGCTGCCCATCATCATG     18
Template        656   .................      639
```

>NM_000077.3 Homo sapiens cyclin-dependent kinase inhibitor 2A (melanoma, p16, inhibits CDK4)
(CDKN2A), transcript variant 1, mRNA

```
product length = 58
Forward primer  1     CCAACGCACCGAATAGTTACG  21
Template        325   ....................   345

Reverse primer  1     GCGCTGCCCATCATCATG     18
Template        382   .................      365
```

Figure 3.9. Primer-BLAST analysis for sequences designed to amplify p16^{INK4a}. Products
from partial alignments are not shown.

p53

p53 is an important tumour suppressor and central molecule in apoptosis
and senescence. A total of 7 transcript variants have been described for p53
(Fig. 3.16).

A primer set for p53 was available and kindly donated by Dr Muy-Teck
Teh (Institute of Dentistry, QMUL, London, UK). Design was aimed at common
exons 7 and 8 (Fig. 3.16), based on primer-BLAST analysis (Fig. 3.10), and
generated a 85 nt single product reflecting amplification of all variants.

	Sequence (5'->3')	Length	Tm	GC%
Forward primer	AGGCCTTGGAACTCAAGGAT	20	52.62	50.00%
Reverse primer	CCCTTTTTGGACTTCAGGTG	20	50.75	50.00%

Products on intended target

Products on allowed transcript variants

Products on potentially unintended templates

Products on target templates

>NM_001126117.1 Homo sapiens tumor protein p53 (TP53), transcript variant 7, mRNA

```
product length = 85
Forward primer  1     AGGCCTTGGAACTCAAGGAT  20
Template        979   ....................  998

Reverse primer  1     CCCTTTTTGGACTTCAGGTG  20
Template        1063  ....................  1044
```

>NM_001126116.1 Homo sapiens tumor protein p53 (TP53), transcript variant 6, mRNA

```
product length = 85
Forward primer  1     AGGCCTTGGAACTCAAGGAT  20
Template        1052  ....................  1071

Reverse primer  1     CCCTTTTTGGACTTCAGGTG  20
Template        1136  ....................  1117
```

>NM_001126115.1 Homo sapiens tumor protein p53 (TP53), transcript variant 5, mRNA

```
product length = 85
Forward primer  1     AGGCCTTGGAACTCAAGGAT  20
Template        919   ....................  938

Reverse primer  1     CCCTTTTTGGACTTCAGGTG  20
Template        1003  ....................  984
```

>NM_001126114.1 Homo sapiens tumor protein p53 (TP53), transcript variant 3, mRNA

```
product length = 85
Forward primer  1     AGGCCTTGGAACTCAAGGAT  20
Template        1367  ....................  1386

Reverse primer  1     CCCTTTTTGGACTTCAGGTG  20
Template        1451  ....................  1432
```

>NM_001126113.1 Homo sapiens tumor protein p53 (TP53), transcript variant 4, mRNA

```
product length = 85
Forward primer  1     AGGCCTTGGAACTCAAGGAT  20
Template        1294  ....................  1313

Reverse primer  1     CCCTTTTTGGACTTCAGGTG  20
Template        1378  ....................  1359
```

>NM_001126112.1 Homo sapiens tumor protein p53 (TP53), transcript variant 2, mRNA

```
product length = 85
Forward primer  1     AGGCCTTGGAACTCAAGGAT  20
Template        1231  ....................  1250

Reverse primer  1     CCCTTTTTGGACTTCAGGTG  20
Template        1315  ....................  1296
```

>NM_000546.4 Homo sapiens tumor protein p53 (TP53), transcript variant 1, mRNA

```
product length = 85
Forward primer  1     AGGCCTTGGAACTCAAGGAT  20
Template        1234  ....................  1253

Reverse primer  1     CCCTTTTTGGACTTCAGGTG  20
Template        1318  ....................  1299
```

Figure 3.10. Primer-BLAST analysis for sequences designed to amplify all transcript variants of p53. Products from partial alignments are not shown.

p21^{WAF1}

p21^{WAF1} or CDKN1A, cyclin-dependent kinase inhibitor (CDKI) 1A, is the main downstream target of p53. The p21^{WAF1} gene encodes for 2 transcript variants, each containing 3 exons and 2 introns (Fig. 3.15).

A common assay was used to design a single set of primers to amplify both variants. Primers anneal to exons 2 and 3, and span an intron (Fig. 3.15). Amplicon size (127 nt) was just slightly above the recommended maximum of 120 nt and qPCR analysis revealed a single product of good quality. A slight shift in T$_m$ (of about 2°C) was observed between standards and samples, and a minimum amount of primer-dimers was present. Despite these limitations this set of primers was of better quality than other sets previously tested and that we had available. Designing primers for p21^{WAF1} is a challenge as it shares many common areas with other genes, which makes it a difficult gene to obtain a set for with maximum specificity and no unwanted secondary structures or partial annealing happening. Primer-BLAST analysis (Fig 3.11) showed specificity for the product but also over 30 other possible products from partial alignments. Amplicon size was confirmed (Fig. 3.17).

```
                    Sequence (5'->3')        Length  Tm    GC%
Forward primer  TCACTGTCTTGTACCCTTGTGC  22    54.61 50.00%
 Reverse primer  GGCGTTTGGAGTGGTAGAAA   20    52.34 50.00%
Products on intended target
_____

Products on allowed transcript variants
_____

Products on potentially unintended templates
_____

Products on target templates
_____

>NM_000389.3 Homo sapiens cyclin-dependent kinase inhibitor 1A (p21, Cip1) (CDKN1A), transcript
variant 1, mRNA


product length = 127
Forward primer   1     TCACTGTCTTGTACCCTTGTGC   22
Template        462     ....................     483

Reverse primer   1     GGCGTTTGGAGTGGTAGAAA     20
Template        588     ..................       569


>NM_078467.1 Homo sapiens cyclin-dependent kinase inhibitor 1A (p21, Cip1) (CDKN1A), transcript
variant 2, mRNA


product length = 127
Forward primer   1     TCACTGTCTTGTACCCTTGTGC   22
Template        575     ....................     596

Reverse primer   1     GGCGTTTGGAGTGGTAGAAA     20
Template        701     ....................     682
```

Figure 3.11. Primer-BLAST analysis for sequences designed to amplify all transcript variants of p21[WAF1]. Products from partial alignments are not shown.

Cyclins A2 and D1

Cyclins are active regulators of the cell cycle. Both cyclin A2 and D1 generate a single transcript variant, with 8 exons/7 introns and 5 exons/4 introns, respectively (Fig. 3.15.)Primer sets for both cyclins were available and kindly donated by Dr Muy-Teck Teh (Cyclin A2) and Dr Ann-Marie Bergin (Institute of Dentistry, QMUL, London, UK) (Cyclin D1). Primer-BLAST analysis (Fig. 3.12) of the sequences predicted the amplification of a single specific product and qPCR analysis confirmed and attested for the good quality of the amplicon generated and correct amplicon size (Fig. 3.17). It is possible to assess from the BLAST analysis that an intron-spanning assay was chosen for the design. The annealing sites are represented on Fig. 3.15; primers anneal to exons 6 & 7 for CCNA2, and to exons 2 & 3 for CCND1.

	Sequence (5'->3')	Length	Tm	GC%
Forward primer	CGTGGCCTCTAAGATGAAGG	20	52.03	55.00%
Reverse primer	GTGTTCAATGAAATCGTGCG	20	50.83	45.00%

Products on intended target

Products on allowed transcript variants

Products on potentially unintended templates

Products on target templates

>NM_053056.2 Homo sapiens cyclin D1 (CCND1), mRNA

```
product length = 166
Forward primer  1    CGTGGCCTCTAAGATGAAGG    20
Template        533  ....................    552

Reverse primer  1    GTGTTCAATGAAATCGTGCG    20
Template        698  ....................    679
```

	Sequence (5'->3')	Length	Tm	GC%
Forward primer	CCATACCTCAAGTATTTGCCATC	23	51.45	43.48%
Reverse primer	TCCAGTCTTTCGTATTAATGATTCAG	26	51.45	34.62%

Products on intended target

Products on allowed transcript variants

Products on potentially unintended templates

Products on target templates

>NM_001237.3 Homo sapiens cyclin A2 (CCNA2), mRNA

```
product length = 108
Forward primer  1     CCATACCTCAAGTATTTGCCATC    23
Template        1341  .......................    1363

Reverse primer  1     TCCAGTCTTTCGTATTAATGATTCAG    26
Template        1448  ..........................    1423
```

Figure 3.12. Primer-BLAST analysis for sequences designed to amplify CCND1 and CCNA2. Products from partial alignments are not shown.

Involucrin

Involucrin is a marker for terminal differentiation in keratinocytes. The involucrin gene originates a single transcript with only 2 exons and 1 intron (Fig. 3.15). A primer set for involucrin was kindly donated by Dr Muy-Teck Teh. Both primer-BLAST (Fig. 3.13) and qPCR analysis revealed the expected product (Fig. 3.17). Annealing sites are represented in Fig. 3.15 and clearly show that the design was directed at a single exon (exon 2). This is likely to be due to the really small size (only 27 bp) of the first exon, which would make it impracticable to aim for a intron-spanning assay.

```
                    Sequence (5'->3')        Length  Tm    GC%
Forward primer  TGCCTGAGCAAGAATGTGAG  20      52.40 50.00%
Reverse primer  TTCCTCATGCTGTTCCCAGT  20      52.98 50.00%
Products on intended target

Products on allowed transcript variants

Products on potentially unintended templates

Products on target templates

>NM_005547.2 Homo sapiens involucrin (IVL), mRNA


product length = 83
Forward primer  1    TGCCTGAGCAAGAATGTGAG  20
Template        255  ....................  274

Reverse primer  1    TTCCTCATGCTGTTCCCAGT  20
Template        337  ....................  318
```

Figure 3.13. Primer-BLAST analysis for sequences designed to amplify IVL. Products from partial alignments are not shown.

YAP1 and POLR2A

The choice of appropriate reference genes for relative gene expression analysis by qPCR is essential for accurate quantification and reliability of the results (Bustin, 2009). Primer sets for YAP1 (AP1 Yes-associated protein 1) and POLR2A (POLR2A polymerase) were kindly donated by Dr Muy-Teck Teh. YAP1 and POLR2A are 2 of 4 reference genes selected for their highest suitability as reference genes for keratinocytes (Gemenetzidis *et al*, 2009). Gene maps with annealing sites (Fig. 3.16) and primer-BLAST analysis are presented below (Fig. 3.14). Amplicon size was also confirmed (Fig. 3.17).

	Sequence (5'->3')	Length	Tm	GC%
Forward primer	GCAAATTCACCAAGAGAGACG	21	51.87	47.62%
Reverse primer	CACGTCGACAGGAACATCAG	20	53.05	55.00%

Products on intended target

Products on allowed transcript variants

Products on potentially unintended templates

Products on target templates

>NM_000937.3 Homo sapiens polymerase (RNA) II (DNA directed) polypeptide A, 220kDa (POLR2A), mRNA

```
product length = 73
Forward primer   1      GCAAATTCACCAAGAGAGACG   21
Template         1871   ....................   1891

Reverse primer   1      CACGTCGACAGGAACATCAG    20
Template         1943   ...................    1924
```

	Sequence (5'->3')	Length	Tm	GC%
Forward primer	CCCAGATGAACGTCACAGC	19	52.90	57.89%
Reverse primer	GATTCTCTGGTTCATGGCTGA	21	51.87	47.62%

Products on intended target

Products on allowed transcript variants

Products on potentially unintended templates

Products on target templates

>NM_006106.3 Homo sapiens Yes-associated protein 1, 65kDa (YAP1), transcript variant 2, mRNA

```
product length = 83
Forward primer   1      CCCAGATGAACGTCACAGC   19
Template         993    ...................   1011

Reverse primer   1      GATTCTCTGGTTCATGGCTGA   21
Template         1075   .....................   1055
```

Figure 3.14. Primer-BLAST analysis for sequences designed to amplify POLR2A and YAP1.

Products from partial alignments are not shown.
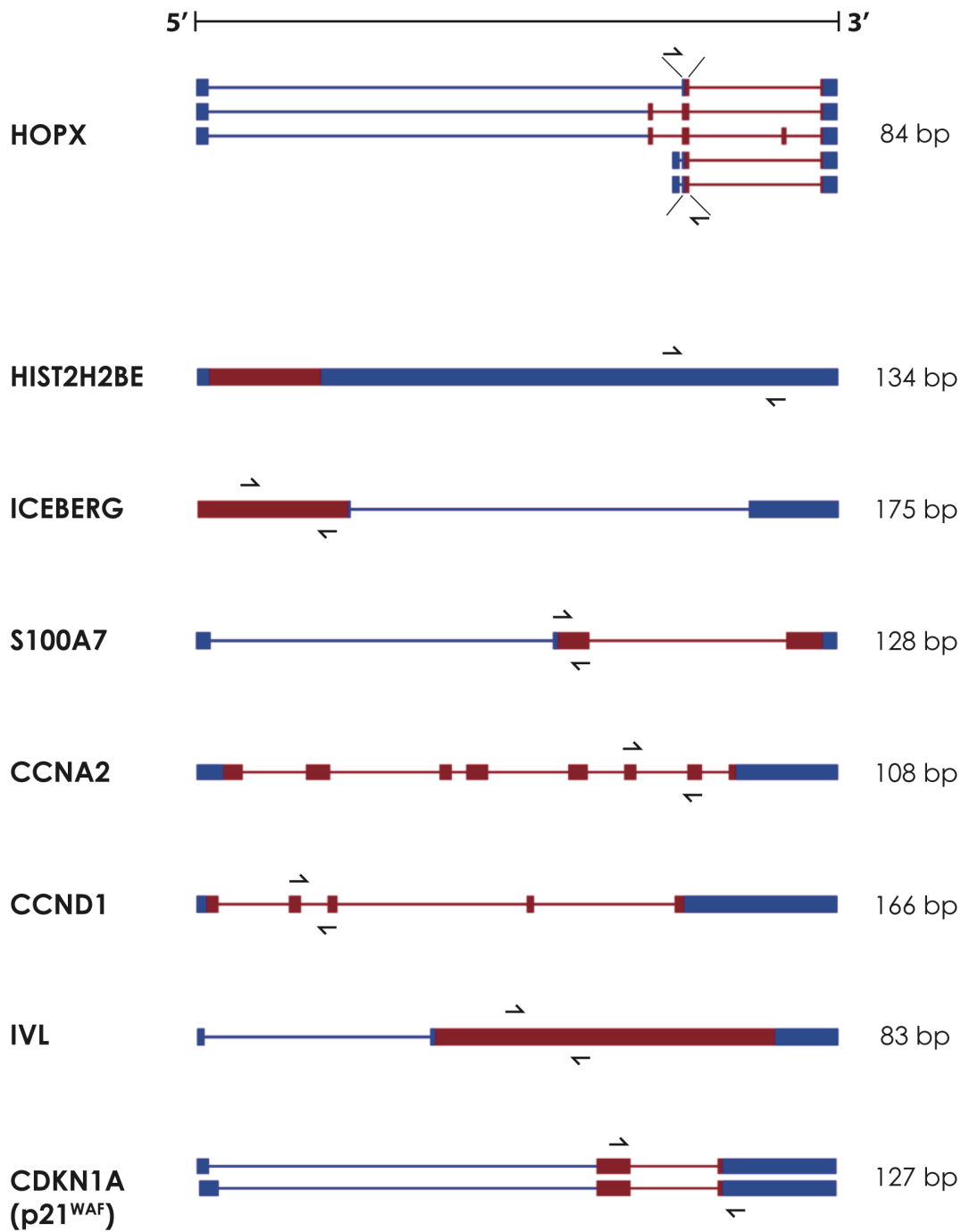
Figure 3.15. Gene maps for HOPX, HIST2H2BE, ICEBERG, S100A7, CCNA2, CCND1, IVL and CDKN1A showing primer annealing sites and product length. Maps represent the transcript variants described in the NCBI database for each gene (boxes = exons; lines = introns; → = fwd primer; ← = rev primer).
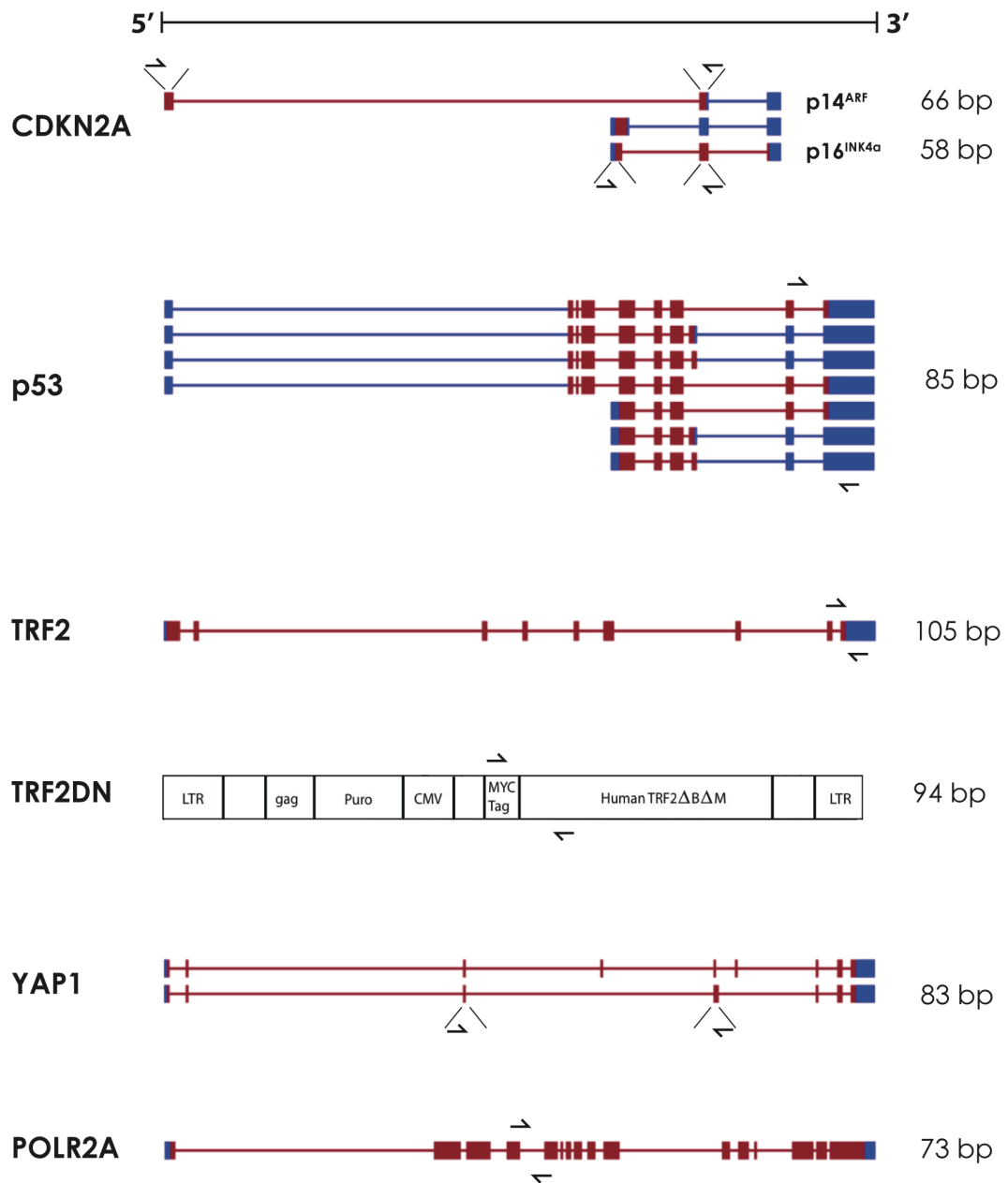
Figure 3.16. Gene maps for CDKN2A, p53, TRF2, TRF2$^{\Delta B \Delta M}$, YAP1 and POLR2A showing primer annealing sites and product length. Maps represent the transcript variants described in the NCBI database for each gene (boxes = exons; lines = introns; → = fwd primer; ← = rev primer) except for TRF2$^{\Delta B \Delta M}$ (exogenous gene) where the retroviral vector, containing the transgene, is represented. TRF2DN = TRF2$^{\Delta B \Delta M}$ (dominant negative mutant of human TRF2 with deletions in the basic and myb domains).
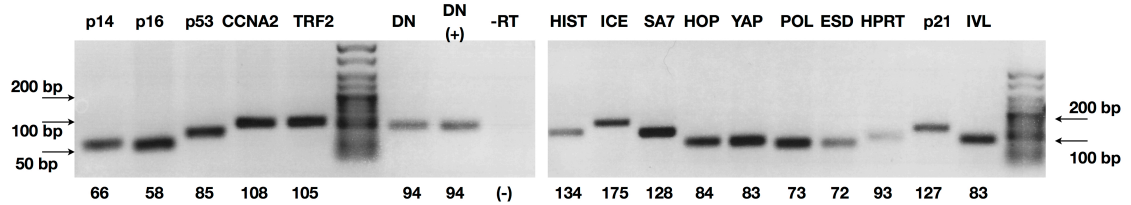
Figure 3.17. Confirmation of PCR product size by gel electrophoresis. qPCR products were run on a 2.5% agarose gel and separated by electrophoresis. All cDNA was reverse transcribed from 1 µg RNA except for DN (+) control where 10 ng of plasmid DNA was used instead. Legend: DN = TRF2$^{\Delta B\Delta M}$; -RT = no reverse transcriptase control; HIST = HIST2H2BE; ICE = ICEBERG; SA7 = S100A7; HOP = HOPX.

cDNA product	Gene name	Transcript variant	mRNA accession #
CCNA2	Cyclin A2 [*Homo sapiens*]	-	NM_001237.3
CCND1	Cyclin D1 [*Homo sapiens*]	-	NM_053056.2
HIST2H2BE	Histone cluster 2, H2be [*Homo sapiens*]	-	NM_003528.2
HOPX	HOP homeobox [*Homo sapiens*]	5 variants	-
ICEBERG	CARD18 caspase recruitment domain family, member 18[*Homo sapiens*]	-	NM_021571.2
IVL	Involucrin [*Homo sapiens*]	-	NM_005547.2
p14^{ARF}	CDKN2A cyclin-dependent kinase inhibitor 2A [*Homo sapiens*]	Variant 4 or β	NM_058195.2
p16^{INK4a}	CDKN2A cyclin-dependent kinase inhibitor 2A [*Homo sapiens*]	Variant 1 or α	NM_000077.3
p21^{WAF1}	CDKN1A cyclin-dependent kinase inhibitor 1A [*Homo sapiens*]	2 variants	-
p53	Tumour protein p53 [*Homo sapiens*]	7 variants	-
POLR2A	Polymerase (RNA) II (DNA directed) polypeptide A [*Homo sapiens*]	-	NM_000937.3
S100A7	S100 calcium binding protein A7 [*Homo sapiens*]	-	NM_002963.3
TRF2	Telomeric repeat binding factor 2 [*Homo sapiens*]	-	NM_005652.2
YAP1	Yes-associated protein 1 [*Homo sapiens*]	2 variants	NM_006106.3

Table 14. Summary of gene information for products amplified by the sets of primers used.

3.3. Discussion

Keratinocytes differ from fibroblasts in their need for mesenchymal support for successful growth in culture. Under appropriate growth conditions sub-cultivation of normal human epidermal keratinocytes is possible for the full range of their lifespan of about 50 - 60 MPD. The establishment of appropriate cell culture conditions for growth is extremely important for this cell type as keratinocytes are particularly sensitive to cell culture stress and will readily activate p16^{INK4a} and engage premature senescence due to inadequate support (Ramirez *et al*, 2001). I have obtained an optimum 10% plating efficiency during sub-cultivation, higher than the reported average of 1 to 5% but within the values obtained for cultures initiated from newborn foreskin (Rheinwald & Green, 1975a). This was possible due to the use of keratinocytes derived from this source, at early passage, combined with the good practice of subculturing cells whilst in exponential growth, the use of a 'feeder' layer and optimised growth conditions.

Epidermal cells constitute a good *in vitro* model for the study of replicative senescence as the epidermis is characterised by a high cell turnover and is, therefore, a truly proliferative tissue *in vivo*. The use of keratinocytes derived from newborn foreskin was aimed at minimising experimental bias due to *in vivo* ageing by ensuring pathways of senescence are intact and not activated by UV damage, for instance. Variables due to *in vitro* ageing were minimised by using cells at very low passage under the lowest possible level of culture stress.

Finally, since this is a gene expression study for the isolation of potentially specific markers for a mechanism of senescence, a great deal of importance was given to primer design. Poor choice of primers for qPCR has been reported as one of the main factors influencing assay performance and, ultimately, data analysis and interpretation (Bustin *et al*, 2009). The rationale behind the strategies used for design, workflow and analysis of primer sets were presented. In general, I aimed at the best possible strategy for design and, when this was not feasible, limitations were presented and accounted for to ensure experimental accuracy.

Chapter 4. Analysis of markers specificity to DNA damage-induced senescence.

4.1. Introduction

4.1.1. DNA damage and repair

Damage to the DNA is a frequent event. It usually affects just one of the strands of the molecule and can result from the action of both endogenous and exogenous agents (reviewed in (Hoeijmakers, 2001)). The most common type of lesions in the DNA are non-bulky alterations to bases, base substitutions or even deletions, as a consequence of spontaneous reactions or reaction with products of normal cell metabolism (Fig. 4.1). Damage can result from methylation due to alkylating agents, oxidation due to ROS (superoxide anions, hydroxyl radicals and hydrogen peroxide), deamination due to loss of the amino group converting cytosine to uracyl and depurination, or loss of purines, due to spontaneous hydrolysis of the N-glycosidic bond resulting in abasic sites. In addition, Ionising radiation (in the form of X-rays or ɣ-rays) can originate breaks in one of the DNA strands, single-strand breaks (ss-breaks or SSBs).

Other agents can cause bulky alterations to the bases which result in both a helical distortion of the DNA duplex and a modification of the DNA chemistry (Fig. 4.1). The most significant of these lesions are pyrimidine dimers (cyclobutane pyrimidine dimers and 6-4 photoproducts) which result from the establishment of covalent bonds between two adjacent pyrimidine bases caused by the UV component of sunlight. Others include bulky chemical adducts and DNA intra-strand cross-links due to reaction with ROS and polycyclic aromatic hydrocarbons.

In addition, despite its high replication fidelity and inherent proofreading ability, DNA polymerase errors can result in insertion of wrong bases during DNA replication resulting in base mismatches, insertions and deletions (Fig. 4.1). Many of these alterations block transcription and also interfere with DNA replication. Therefore, in order to maintain genomic stability and prevent the occurrence of mutations, several mechanisms have evolved to repair DNA damage.

In general, resolution of lesions that affect only one strand of the DNA molecule relies on the intact complementary DNA strand, which can be used as a template for repair. It involves three main steps: excision, re-synthesis and ligation. Briefly, the damaged area is first recognised and excised by nucleases leaving a 'nick' in the faulty DNA strand, a single-strand break (ss-break or SSB). A repair DNA polymerase is then recruited to the area to restore the original sequence, using the complementary strand as a template for synthesis. Finally, the nick left in the sugar-phosphate backbone of the repaired strand is sealed by a DNA ligase. Whilst the re-synthesis and ligation steps use similar enzymes (DNA polymerases and ligases, respectively), the excision step requires specialised nucleases, depending on the modification that occurred in the DNA molecule. From here emerge specialised repair pathways: BER, NER and MMR.
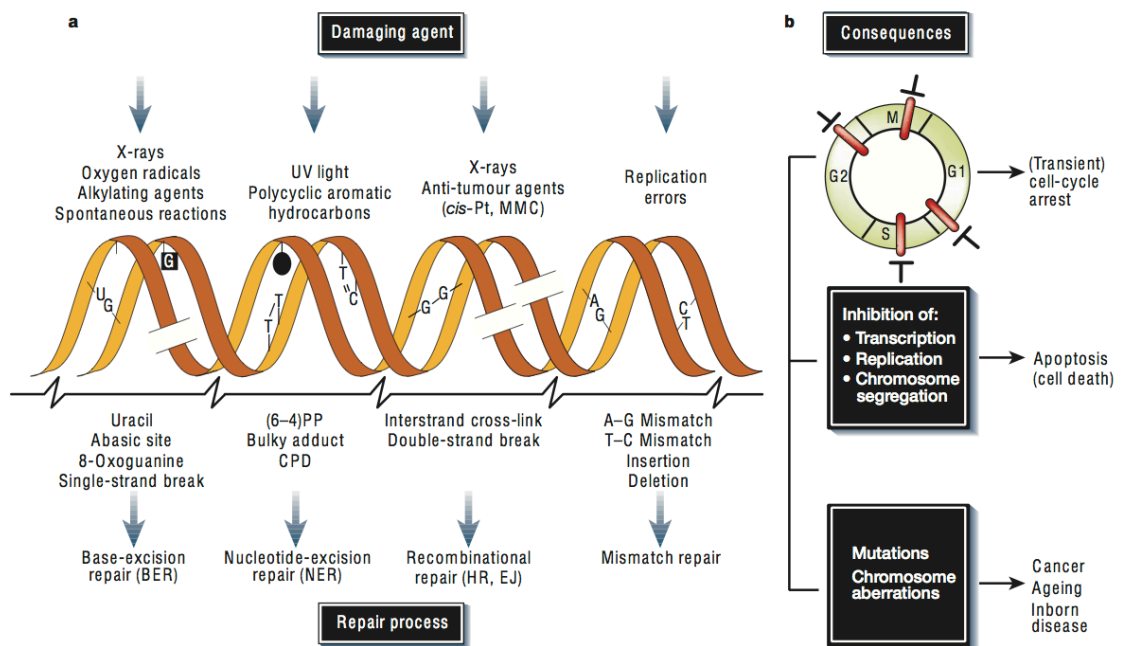
Figure 4.1. Causes of DNA damage, consequences and repair. a. Some of the most common DNA damaging agents, the lesions provoked by them and the mechanisms used for repair; **b.** The acute and permanent effects of DNA damage in the cell. Abbreviations: (6-4)PP = 6-4 photoproduct; CPD = cyclobutane pyrimidine dimer; cis-Pt = cisplatin; MMc = mitomycin C (*in* (Hoeijmakers, 2001)).

Base-excision repair (BER) pathway

The BER pathway (Lindahl & Wood, 1999; Mol *et al*, 1999) corrects lesions arising from the normal cellular metabolism. It is involved in repairing non-bulky modifications to bases in the DNA, resulting from methylation, oxidation, deamination, spontaneous hydrolysis or SSBs. BER operates through two sub-pathways (Fig. 4.2), the "short-patch" (main pathway) and the "long-patch" (backup pathway).

"Short-patch" BER implies the replacement of the damaged base with a single new nucleotide. It is initiated by the action of a DNA glycosylase which flips the base out of the helix and cleaves the N-glycosidic bond between the damaged base and the sugar phosphate backbone of the DNA. This cleavage generates an abasic site in the DNA, which can also arise by the spontaneous

hydrolysis of the N-glycosidic bond. In either case, the abasic site is subsequently processed by APE1 (endonuclease AP1) which cleaves the phosphodiester backbone immediately 5' to the abasic site, resulting in a 3' hydroxyl group and a transient 5' abasic deoxyribose phosphate (dRP). Removal of the dRP is accomplished by the action of DNA polymerase beta (DNA polβ), which adds one nucleotide to the 3' end of the nick and removes the dRP moiety via its lyase activity. The strand nick is finally sealed by the XRCC1-ligase 3 complex, thus restoring the integrity of the DNA.

"Long-patch" BER is employed to repair SSBs or modified bases which are resistant to the lyase activity of DNA polβ. Although it requires many of the same factors involved in the "short-patch" repair, including a DNA glycosylase, APE1 and DNA polβ, it alternatively results in the replacement of approximately 2-10 bases, along with the damaged base, and it is a PCNA-dependent pathway. Single-strand breaks will activate PARP (poly (ADP-ribose) polymerase) and PNK (polynucleotide kinase) which will then bind the SSB, via interaction with the scaffold protein XRCC1, in order to protect and trim the ends for repair synthesis. This involves PCNA (proliferating cell nuclear antigen) and DNA polδ/ε and results in the displacement of the damaged site as part of a DNA "flap" containing 2-10 nucleotides. The oligonucleotide 'overhang' is then excised by endonuclease FEN-1 the sequence sealed by DNA ligase 1.
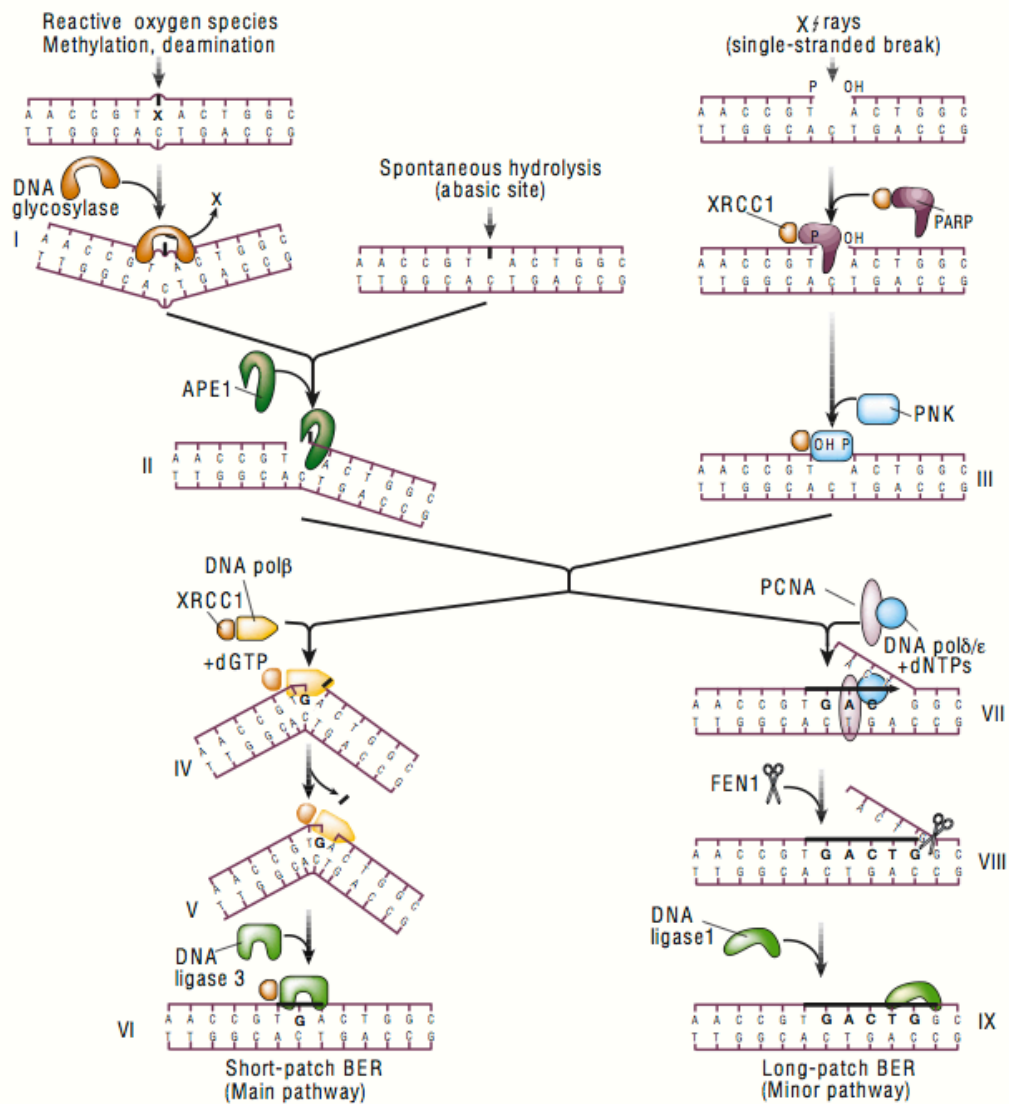
Figure 4.2. Base excision repair (BER) pathways. I. cleavage of damaged base by a DNA glycosylase; **II.** strand incision at the abasic site by APE1 endonuclease; **III.** XRCC!-mediated protection and trimming of SSB ends by PARP and PNK; **IV.** XRCC1-mediated 1-nucleotide gap-filling reaction by DNA polβ; **V.** removal of the 5'-baseless sugar residue by DNA polβ lyase activity; **VI.** sealing by the XRCC1-ligase 3 complex; **VII.** PCNA-mediated repair synthesis (2-10 nucleotides) by DNA polδ/ε; **VIII.** removal of displaced DNA "flap" by FEN1 endonuclease; **IX.** sealing by DNA ligase 1(*in* (Hoeijmakers, 2001)).

Nucleotide-excision repair (NER) pathway

The NER pathway (de Laat *et al*, 1999) is involved in repairing bulky modifications to bases in the DNA, which result in helical distortion and chemical modifications of the DNA duplex. These result, for example, from covalent bonds between bases and hydrocarbons (bulky adducts) or pyrimidine dimers from exposure to UV light, which require removal of the entire nucleotide. The NER process includes damage recognition (by specialised nucleases), local opening of the DNA duplex around the lesion (by DNA helicases), dual incision of the damaged DNA strand, gap repair synthesis and strand ligation. NER also operates through two sub-pathways (Fig. 4.3), the global genome NER (GG-NER), which corrects damage in transcriptionally silent areas of the genome, and the transcription-coupled NER (TC-NER), which repairs lesions on the actively transcribed strand of the DNA. They are fundamentally identical, except in their mechanism of damage recognition.

In GG-NER, the XPC/HHR23B protein complex is responsible for the initial detection of damaged DNA, which is essentially based on recognition of disrupted base pairing rather than of actual lesions. Conversely, damage recognition during TC-NER does not require XPC, but rather is thought to occur when the transcription machinery is stalled at the site of injury. The stalled RNA polymerase complex must then be displaced in order to allow the NER proteins access to the damaged DNA. This displacement is aided by the action of the CSA and CSB proteins, as well as other TC-NER-specific factors. The subsequent steps of GG- and TC-NER proceed in an essentially identical manner. XPA and the hetero-trimeric replication protein A (RPA) then bind at the site of injury and further assist damage recognition. Next, the XPB and XPD helicases, components of the multi-subunit transcription factor TFIIH, unwind the DNA duplex in the immediate vicinity of the lesion. The endonucleases XPG and ERCC1/XPF then cleave one strand of the DNA at positions 3' and 5' to the damage, respectively, generating an approximately 30 base oligonucleotide containing the lesion. This oligonucleotide is displaced, making way for gap repair synthesis (performed by DNA polδ/ε, as well as several replication accessory factors). Finally, the nick in the repaired strand is sealed by a DNA ligase, thus completing the NER process.

Mismatch repair (MMR) pathway

The DNA mismatch repair (MMR) pathway plays an essential role in the correction of replication errors such as base-base mismatches and insertion/deletion loops (IDLs) that result from DNA polymerase mis-incorporation of nucleotides and template slippage, respectively (Hoeijmakers, 2001). Mis-pairs generated by the spontaneous deamination of 5-methylcytosine and hetero-duplexes formed following genetic recombination are also corrected via MMR. The overall process of MMR is similar to the other excision repair pathways (see long-patch BER, and NER), in that the DNA lesion (mismatch or IDL) is recognised, a patch containing the lesion is excised, and the strand is corrected by DNA repair synthesis and re-ligation.
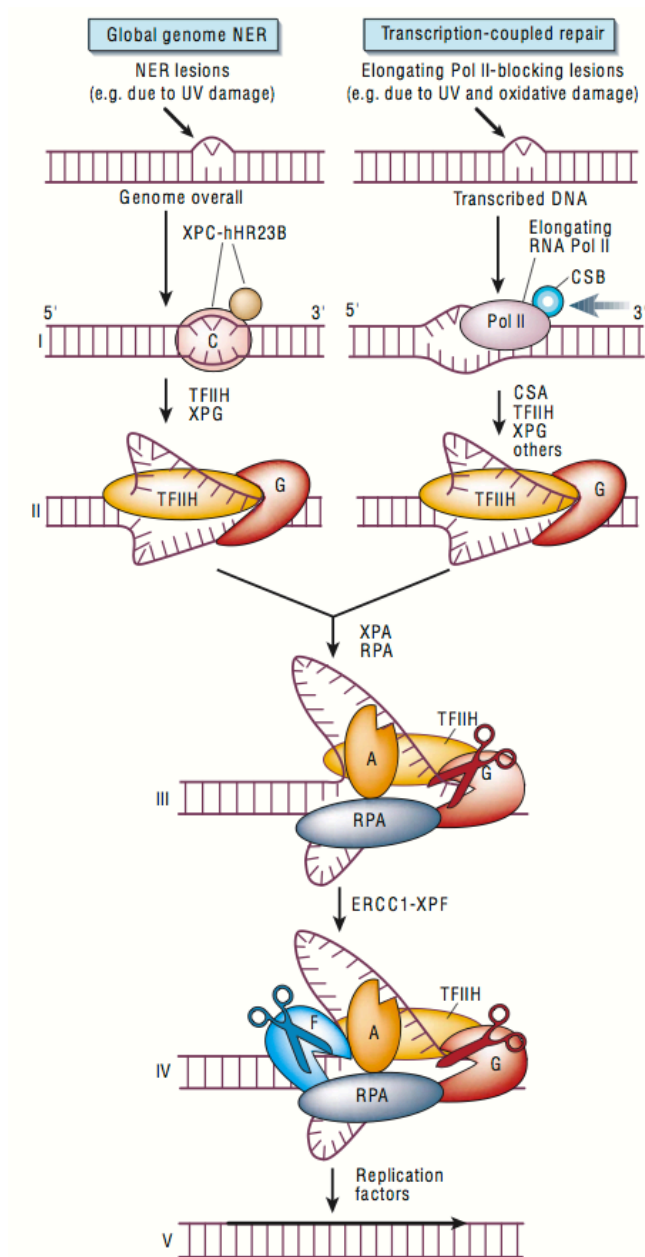
Figure 4.3. Nucleotide excision repair (NER) pathways. I. recognition of helix-distorting lesions by the XPC/HHR23B complex or displacement of stalled RNA pol II by CSA and CSB; **II.** opening of the DNA duplex around the lesion by XPB and XPD helicases, part of the multi-subunit transcription factor TFIIH; **III.** stabilisation of the open intermediate by RPA binding to the undamaged strand; **IV.** incision of the 3' by XPG and of the 5' by ERCC1/XPF endonucleases with generation of a 24-30 oligonucleotide; **V.** gap-filling by the regular DNA replication machinery (*in* (Hoeijmakers, 2001)).

Standard DNA repair pathways (BER, NER and MMR) operate only to repair damage restricted to one of the strands of the double helix. However, there are situations where both strands are broken simultaneously originating DNA lesions called double-strand breaks (ds-breaks or DSBs) that are particularly genotoxic (reviewed in van Gent 2001; Hoeijmakers, 2001), since they pose problems for transcription, replication, and chromosome segregation (Fig.4.1). Damage of this type is caused by a variety of sources including exogenous agents, such as ionising radiation and certain genotoxic chemicals, such as strong oxidising agents and anti-tumour drugs. Also, endogenously generated reactive oxygen species, mechanical stress on the chromosomes and other endogenous processes can result in DSBs. Replication in an area of the DNA already containing a SSB will be converted into a DSB in one of the sister chromatids and DSBs are also naturally occurring intermediate structures during recombination in meiosis and in specific DNA rearrangement events in the immune system such as V(D)J recombination for assembly of Ig or T-cell receptor genes and Ig heavy chain class switching (Fig. 4.1 and 4.4). Since DSBs differ from most other types of DNA lesions in that they affect both strands of the DNA duplex and, therefore, prevent use of the complementary strand as a template for repair, two specialised pathways have evolved to deal with these defects - homologous recombination (HR) and non-homologous end joining (NHEJ) (Fig. 4.4).

The cellular decision as to which pathway to use for DSB repair seems to mainly depend on the stage within the cell cycle at the time of damage acquisition. NHEJ and HR differ in the requirement for an homologous template, in the accuracy of repair and in the phase of the cell cycle each is functional on.
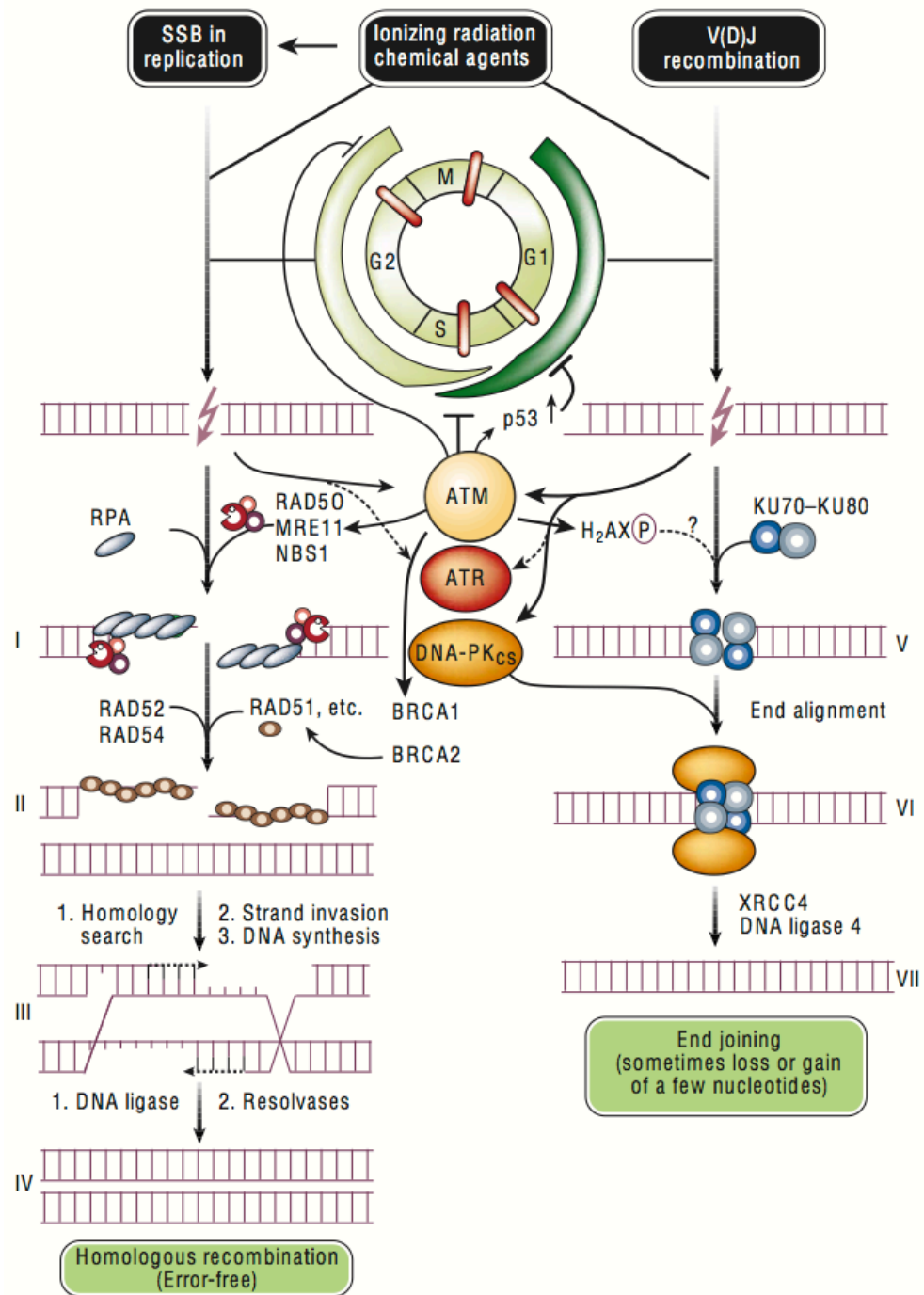
Figure 4.4. Non-homologous end joining (NHEJ) and Homologous recombination (HR). Pathways for DSB repair. **I.** processing of 3'-ssDNA overhangs by the MRE11/RAD50/NSB1 complex; **II.** nucleoprotein filament assembly by RAD5-related proteins; **III.** DNA strand exchange and synthesis; **IV.** ligation and resolving of recombination intermediate; **V.** recognition of free DNA ends by Ku70/Ku80; **VI.** recruitment of DNA-PKcs, XRCC4, DNA ligase 4 and processing factors; **VII.** ; processing and ligation (*in* Hoeijmakers, 2001).

Non-homologous end-joining (NHEJ) pathway

NHEJ (van Gent *et al*, 2001; Hoeijmakers, 2001; Dobbs *et al*, 2010) can operate in any phase of the cell cycle, it is the pathway predominantly used by mammalian cells and usually results in the correction of the break in an error-prone manner with inherent loss or gain of nucleotides. This pathway is also required and regularly used to process DSB intermediates generated through V (D)J recombination. Essential to NHEJ is the activity of the Ku70/Ku80 hetero-dimeric protein. The Ku hetero-dimer initiates NHEJ by binding to the free DNA ends and recruiting other NHEJ factors such as DNA-PKcs (DNA-dependent protein kinase), XRCC4 and DNA Ligase IV to the site of injury. DNA-PKcs becomes activated upon DNA binding, and phosphorylates a number of substrates including p53, Ku and the DNA Ligase IV cofactor XRCC4. Processing factors such as the exo-endonuclease MRN complex (MRE11/Rad50/NBS1), as well as endonucleases FEN-1 and Artemis also get activated and are recruited to the site of injury. They process the DNA ends prior to ligation by Ligase IV in a complex that also includes XRCC4 and Ku (Fig. 4.4. NHEJ).

Homologous recombination (HR) pathway

Unlike NHEJ, HR-directed repair (Haber, 2000; van Gent *et al*, 2001; Hoeijmakers, 2001) corrects DSB defects in an error-free manner, with no loss of nucleotides, using a mechanism that retrieves genetic information from a homologous, undamaged DNA molecule. However, the majority of HR-based repair can only take place when a DSB occurs shortly after DNA has been replicated (in late S and G2) when an undamaged sister chromatid is available for use as a repair template. HR is, therefore, an alternative DSB repair pathway to NHEJ and it is similar to the homologous recombination that occurs during meiosis, except here there is no exchange of genetic material. HR is mediated by the RAD52 group of proteins, including RAD50, RAD51, RAD52, RAD54, and MRE1. Initial response to the DSB involves activation of ATM and one of its downstream targets, NBS1. The exposed DNA ends are first recognised by RAD52 protein and then processed into 3'-end single-stranded DNA (3'-ssDNA) overhangs via the nucleolytic activity of the MRE11/RAD50/NBS1 complex. The newly generated ssDNA ends are bound by RAD51 to form a nucleoprotein filament. RAD51, in conjunction with RPA, RAD52, RAD54, BRCA1, BRCA2, and several additional RAD51-related proteins, serve as accessory factors in filament

assembly and subsequent activities. The RAD51 nucleoprotein filament then searches the undamaged DNA on the sister chromatid for a homologous repair template. Once the homologous DNA has been identified, the damaged DNA strand invades the undamaged DNA duplex in a process referred to as DNA strand exchange. A DNA polymerase then extends the 3' end of the invading strand and subsequent ligation by DNA ligase I yields a hetero-duplexed DNA structure. When this recombination intermediate is resolved, the precise error-free correction of the DSB is complete (Fig. 4.4. HR).

Consequences of DNA damage

All DNA damage repair mechanisms described previously are in place to ensure genomic stability. However, when damage is too extensive and/or repair is not successful this can have varied consequences to the cell. Accumulation of DNA damage can result in mutations that ultimately induce permanent changes towards cancer (Fig. 4.1). Two main types of genetic instability, mutational and chromosomal, have been observed in tumour cells (reviewed in (van Gent *et al*, 2001; Hoeijmakers, 2001).

Mutational instability (MIN) is associated with ss-breaks resulting from point mutations or small deletions and usually arise from defects in the BER pathway. The condition xeroderma pigmentosum, characterised by an an extreme sensitivity of skin to UV-light and a high propensity to skin cancer, is an example of impairment of the NER pathway in which thymine dimers (formed following exposure to UV light) are not repaired.

Chromosomal instability (CIN) relates to extensive rearrangement of chromosomes, mainly as a result of unrepaired DSBs which are particularly genotoxic. Loss of entire chromosomes or chromosome fragments can result in inactivation of tumour-suppressor genes whilst gain or amplification of chromosomal regions can lead to activation of proto-oncogenes, both contributing to genomic instability and tumourigenesis. Chromosomal rearrangements such as translocations, where chromosome arms are exchanged, can also occur. This causes deregulation of gene expression or even fusion between genes that may then acquire oncogenic potential.

Several human syndromes arise from mutations in key genes in the specialised DNA ds-break repair pathways HR and NHEJ and highlight their importance in the maintenance of genomic integrity. Ataxia telangiectasia (AT) is a classic human syndrome characterised by high incidence of chromosomal translocations and predisposition to lymphomas. Patients with AT are extremely sensitive to ionising radiation as they are not able to repair DSBs due to a mutation in the key gene ATM (Ataxia telangiectasia mutated). Nijmegen breakage syndrome (NBS) shows a similar cellular phenotype to AT, characterised by radio-sensitivity but now by a mutation in the NBS1 gene. The latter is a target for phosphorylation by ATM and, consequently, regulates the activity of the MRE11-RAD50-NBS1 complex. Mutations in BRCA1 and BRCA2, genes that are also phosphorylated by ATM, result in susceptibility to breast cancer. Two other conditions, Werner's and Bloom syndromes, are caused by mutations in WRN and BLM genes, respectively, both encoding for DNA-unwinding enzymes from the RecQ helicase family. Interaction of WRN with the Ku hetero-dimer results in increased WRN exonuclease activity whilst a defective BLM gene originates more sister chromatid exchanges in HR.

Cell cycle checkpoints and cell cycle arrest

As DSBs have a high potential for genotoxicity several cell cycle checkpoints are in place to prevent cells from carrying these lesions to their progeny. In eukaryotes, the G1/S and G2/M checkpoints control progression to DNA replication and to mitosis, respectively (Fig. 4.1). Damage to the DNA is acknowledged and signalled so that cell cycle arrests transiently to allow enough time for repair before progression into replication or division. If repair is successful cell cycle is resumed, but if damage is too extensive and/or repair is just not possible the signalling from cell-cycle checkpoints persists to enforce permanent shutdown of the cell.

Cellular fate upon activation of cell cycle checkpoints is dependent on the severity of the DNA damaging agent and on the cell type. In general, normal cells, as opposed to transformed cells, will tend towards senescence as they have intact signalling pathways (Ben-Porath & Weinberg, 2005). Ionising radiation at relatively low doses activates DNA damage signalling resulting in transient cell cycle arrest from which fibroblasts recover. High doses of IR, however, cause persistent signalling and ultimately trigger permanent cell cycle

arrest (Rodier *et al*, 2009). Generally, senescence is induced by lower levels of damage than those required to ensue apoptosis (Ben-Porath & Weinberg, 2005). p53 and ATM/ATR are central proteins in the signal transduction cascade to DNA damage, especially in the response to DSBs, towards apoptosis or cellular senescence (Campisi & d'Adda di Fagagna, 2007). Molecularly, factors such as differences in post-translational modifications, in binding proteins and in transcriptional targets of p53 upon different stimuli, have been implicated in how cells might commit to each of these two possible fates (Ben-Porath & Weinberg, 2005).

4.1.2. DNA damage-induced senescence (p53 pathway)

Damage to the DNA, especially in the form of DSBs, trigger a cascade of events called the DNA damage response (DDR) where p53 is the main effector molecule that ultimately halts cell cycle progression (reviewed in (Campisi & d'Adda di Fagagna, 2007)). Damage to the double helix is first recognised by DNA damage sensors which activate the transducers of signal ATM (Ataxia telangiectasia mutated) and ATR (Ataxia telangiectasia and Rad-3 related), enzymes with protein kinase activity. Sensors include the MRN complex (MRE11/ RAD50/NBS1), which interacts with ATM, and RPA and RFC-like complexes (containing RAD17) that recruit the RAD9/HUS1/RAD1 complex (911 complex), which in turn interacts with ATR. Histone H2AX also localises to sites of damage, is activated via phosphorylation by ATM/ATR or by DNA-PKcs and triggers chromatin modifications that will consequently recruit other proteins. Some will be involved in repair efforts (DNA-end stabilising heterodimers Ku70/80, DNA ligase IV, MRE11 exonuclease, DNA helicase BLM) and others in boosting ATM/ ATR signalling and further transducing the signal. Adaptor proteins such as 53BP1/MDC1 and BRCA1/Claspin mediate the signal from upstream kinases ATM/ATR to downstream kinases CHK2/CHK1, respectively, which ultimately activate their main phosphorylation target, effector protein p53 (Fig. 4.5).
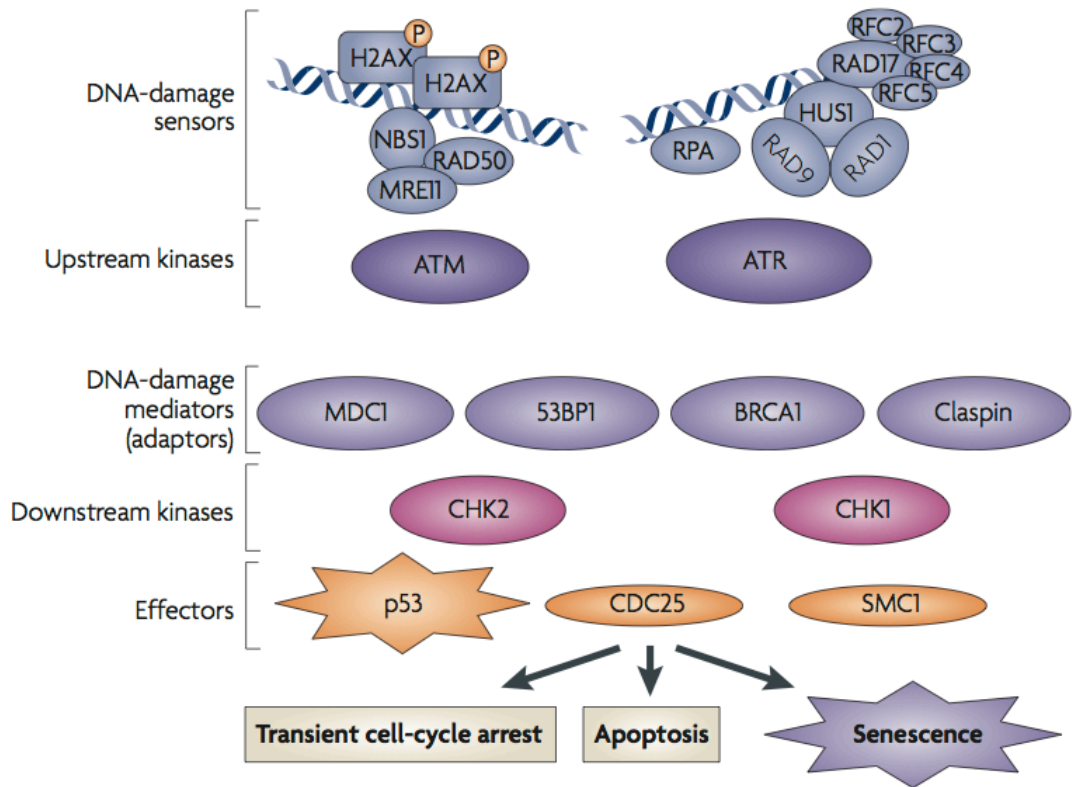
Figure 4.5. The DNA damage response (DDR). 53BP1, p53-binding protein-1; ATM, Ataxia telangiectasia mutated protein; ATR, ATM and Rad-3 related protein; BRCA1, breast cancer type-1 susceptibility protein; CHK1 and CHK2, checkpoint-1 and checkpoint-2 proteins; HUS1, hydroxyurea-sensitive-1 protein; MDC1, mediator of DNA damage checkpoint protein-1; MRE11, meiotic recombination-11 protein; NBS1, Nijmegen breakage syndrome-1 protein; SMC1, structural maintenance of chromosomes protein-1 (*in* (Campisi & d'Adda di Fagagna, 2007)).

127

Upon replicative senescence or following exposure to DNA damaging agents (IR, UV and bleomycin), p53 activation occurs essentially via ATM/ATR-related increase/decrease in phosphorylation at different sites, with p53-phosphoSer15 being the post-translational modification of p53 common to all. Replicative senescent cells, for example, acquire additional distinctive phosphorylation patterns such as an increase at Thr18/Ser376 and decrease at Ser 392 (Webley *et al*, 2000). A comparison between the pattern of changes on phospho-specific p53 epitopes observed in normal human fibroblasts (NHFs) after senescence and following irradiation (UV and IR) is presented in Figure 4.6.
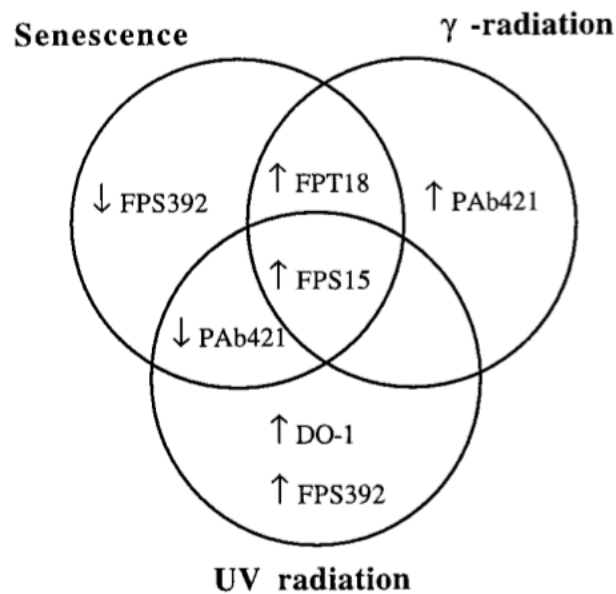
Figure 4.6. Modifications in p53 upon activation by different stimuli. Venn diagram representing the effects of senescence, UV radiation, and IR on phosphospecific p53 epitopes in human diploid fibroblasts. Increase in DO-1 binding relates to a decrease in p53-phosphoSer20 and increase in PAb421 binding relates to a decrease in p53-phosphoSer376 (*in* (Webley *et al*, 2000)).

p53 engages the senescence program, as a consequence of direct damage to the DNA, via its main transcriptional target p21^{WAF1} (CDKN1A), a cyclin-dependent kinase inhibitor (CdkI) which acts a a central regulator of the

G1 checkpoint (reviewed in (Ben-Porath & Weinberg, 2005)). p21^{WAF1} inhibits cell cycle progression directly, either by interfering with CDK2/Cyclin A, CDK4/Cyclin D and CDK6/Cyclin D complexes, required to proceed from G1 (Zhang *et al*, 1994) or by interfering with DNA replication in S phase by interaction with PCNA, the subunit of DNA polδ (Li *et al*, 1994). p21^{WAF1} can also halt cell cycle progression indirectly, by activating pRb via inhibition of CDK2/Cyclin E and CDK1/Cyclin B complexes; pRb, in turn, arrests the cell cycle by binding E2F transcription factor (reviewed in (Campisi, 2005)).

In normal human fibroblasts exposed to DNA strand breaking chemicals, such as bleomycin or actinomycin D, cellular proliferation is permanently halted via DDR with immediate activation of p53 and p21^{WAF1} after damage (Robles & Adami, 1998). p21^{WAF1} signalling is sustained for several days by which point both p53 and p21^{WAF1} levels return to baseline and p16^{INK4a} levels increase. This suggests that p53/p21^{WAF1} initiate the senescence signal while p16^{INK4a} seems to be responsible for maintaining it (Itahana *et al*, 2001; Ben-Porath & Weinberg, 2005). Ionising radiation induces similar activation of the DDR with transient growth arrest after low doses and permanent cell cycle arrest after high doses, but levels of p16^{INK4a} were not assessed (Rodier *et al*, 2009). In replicatively senescent fibroblasts, however, p21^{WAF1} and p16^{INK4a} seem to be independently up-regulated. Single cell analysis showed that the signal from dysfunctional telomeres is transmitted preferentially through ATM/Chk2 accompanied by a characteristic G1 arrest. Stable arrest, however, requires continuous signalling and this pathway did not affect expression of p16^{INK4a}, the delayed induction of which occurs in a telomere- and DNA damage- independent, and apparently stochastic, manner (Herbig *et al*, 2004).

DNA ds-breaks, as visualised by markers of the DDR, accumulate in mouse tissues with age (Wang *et al*, 2009). However, more recently it has become apparent that the unrepaired persistent DSBs (Sedelnikova *et al*, 2004), as visualised by the 53BP1/ɣ-H2AX dual staining and an increase in ɣ-foci size, are the lesions responsible for inducing the expression of a variety of secreted proteins indicative of SASP (Rodier *et al*, 2009). Other markers (Rodier *et al*, 2011) have now defined these unrepairable DSBs as DNA SCARS and it is thought these lesions are a major trigger for senescence *in vivo* (Fumagalli *et al*, 2012). Terminal DNA is not exposed and thus is not recognised and processed

by the cell as a DSB because it is protected by telomeres. These specialised capping structures also ensure that DSB repair pathways HR and NHEJ are not inappropriately activated at chromosome ends, preventing deletion of telomeric DNA, formation of dicentric chromosomes and other serious cell anomalies (reviewed in de (de Lange, 2005)). However, telomeres are also very poor at repairing DSBs, especially in response to oxidative damage (Kruk *et al*, 1995; Petersen *et al*, 1998) and recent data suggests that DDR markers may locate to the telomere because they are a preferential site for unrepaired DSBs (Fumagalli *et al*, 2012; Hewitt *et al*, 2012). In other words, the location of DSBs at telomeres may be a coincidental consequence of poor DNA repair unless they are eliminated by telomerase.

Although it has been shown in human fibroblasts that dysfunctional telomeres are recognised by the DNA damage machinery and trigger a DDR that ultimately results in senescence (d'Adda di Fagagna *et al*, 2003; Takai *et al*, 2003; Herbig *et al*, 2004), telomere dysfunction in human keratinocytes, either via experimental telomere uncapping or via telomere erosion following replicative exhaustion, caused a senescent-like growth arrest accompanied by a very weak DDR (Minty *et al*, 2008). Subsequent microarray analysis revealed several genes induced by telomere dysfunction, and four (HIST2H2BE, ICEBERG, S100A7 and HOPX) apparently regulated by telomerase (Minty *et al*, 2008). These show potential as markers for telomere dysfunction-induced senescence (TDIS).

One possible reason for the differences observed between fibroblasts and keratinocytes could be that the latter are unusually sensitive to telomere uncapping and ensuing DDR. This could mean that some of the candidate biomarkers would also be induced following induction of DNA damage (using ionising radiation, for example) and, consequently, might not be as specific to telomere damage as first realised. Indeed this is a problem with all the secreted biomarkers identified so far (Jiang *et al*, 2008). To investigate HIST2H2BE, ICEBERG, S100A7 and HOPX's specificity as markers for keratinocyte TDIS I started by testing their response to both acute and permanent DNA damage.

4.2. Induction of acute DNA damage

Telomere uncapping via expression of TRF2$^{\Delta B \Delta M}$ generated a surprisingly weak DDR in human keratinocytes that, nevertheless, resulted in senescence and elevation of the four candidate markers (Minty *et al*, 2008). This low level of activation of the p53 pathway was demonstrated by a small increase in p53 phosphorylation at Serine 15 (p53-pS15) and p21^{WAF1} protein levels, accompanied by a low incidence of 53BP1 DNA damage foci. Furthermore, when keratinocytes lacking p16^{INK4a} undergo replicative senescence following telomere erosion, the induction of p53-pS15 and p21^{WAF1} protein is similarly weak (Muntoni *et al*, 2003), showing that the results can be repeated in a natural model of telomere dysfunction-induced senescence. One possible explanation for this is that keratinocytes might be unusually sensitive to the DDR and exit the cell cycle before DNA damage foci can accumulate. Thus, in order to test whether the low level of p53 activation was the factor responsible for inducing the candidate biomarkers normal human epidermal keratinocytes (NHEK) were synchronously irradiated with a relatively low dose of ionising radiation. This should cause a similar number of random DSBs in the DNA (approximately 50 DSBs, (Löbrich *et al*, 1994)) to the number of uncapped telomeres that might be initiated by expression of TRF2$^{\Delta B \Delta M}$ and recognised by the cell as DNA damage.

Keratinocytes were subjected to a relatively low dose (2 Gray) of IR, capable of inducing repairable DNA DSBs, and allowed a short period (6 hours) of recovery for repair. Engagement of the DDR was demonstrated by up-regulation of p21^{WAF1}, the downstream target of p53 and cell cycle inhibitor. Keratinocytes subjected to 2 Gy of IR show a 1.4-fold increase in p21^{WAF1} transcript levels when compared to a non-irradiated control, after a 6hr recovery. Protein levels of p21^{WAF1} show a similar increase whilst total p53 is only mildly elevated (Fig. 4.7). Similar up-regulation of p21^{WAF1} and total p53 has been observed in NHEK with 1 Gy (ɣ-rays) after a 6hr recovery (Minty *et al*, 2008) and in the human diploid fibroblast strain HCA2 with 0.5 Gray (X-rays) following a 2hr recovery period (Rodier *et al*, 2009). p21^{WAF1} has been reported to return to control levels on irradiated cells from 10h to 24h (Rodier *et al*, 2009) as by this point DSBs are thought to have been resolved, therefore eliminating the need for further DDR signalling (transient arrest).
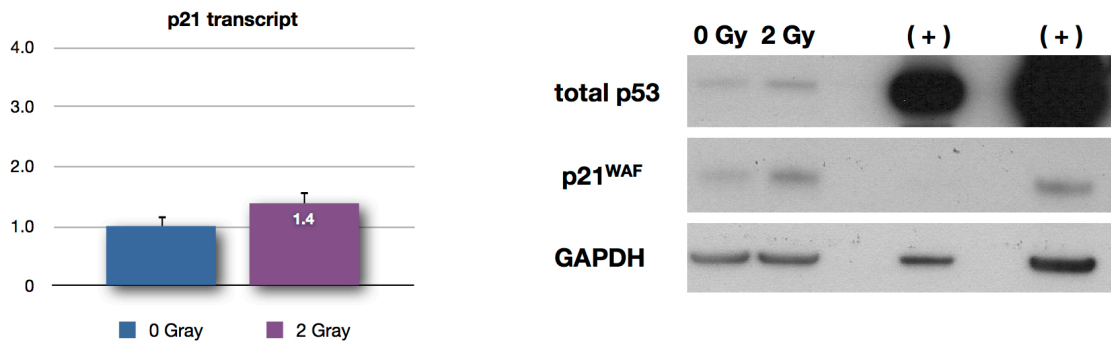
Figure 4.7. Engagement of the DDR following induction of acute DNA damage. p21[WAF1] transcript (graph) and protein (blot) levels in keratinocytes 6 hours following exposure to a relatively low dose (2 Gray) of IR. mRNA levels (fold) were normalised against the non-irradiated control (0 Gray). Results are represented as mean ± s.d. (n=2). Legend: (+) = positive control (SVHFK cell line) - last lane loaded with double the amount of total protein.

Despite induction of p53, via activation of its transcriptional target p21[WAF1], previously elevated to a similar level and accompanied by phosphorylation of p53 at Serine 15 (p53-pS15) in similar experimental conditions (Minty *et al*, 2008), none of the candidate markers showed a significant elevation of their transcript levels 6 hours following exposure to a 2 Gray dose of IR when compared to a non-irradiated control (Fig. 4.8).
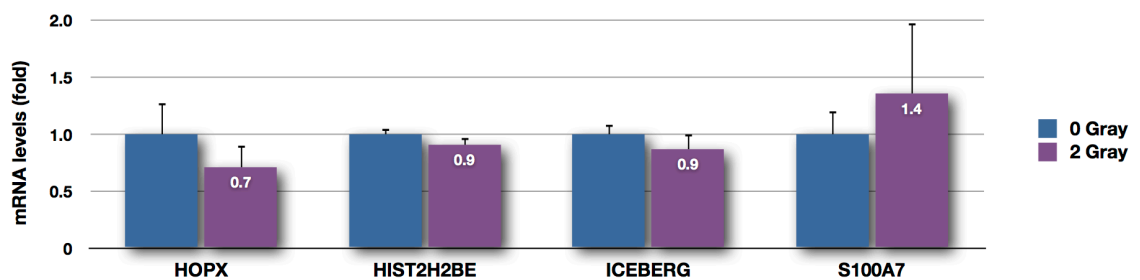
Figure 4.8. Candidate markers response upon induction of acute DNA damage. Gene expression levels of HOPX, HIST2H2BE, ICEBERG and S100A7 in keratinocytes 6 hours following exposure to a relatively low dose (2 Gray) of IR. Values were normalised against the non-irradiated control (0 Gray). Results are represented as mean ± s.d. (n=3).

As expected, given this relatively low dose of IR, the activation of the p53 pathway was transient and did not induce permanent growth arrest via senescence; this is supported by analysis of Cyclins A2 and D1 mRNA which remained at control levels (Fig. 4.9). A 2 Gray dose of ɣ-rays also produced no effect on keratinocyte differentiation following a 6 hr recovery period, as shown by unaltered transcript levels of involucrin (Fig. 4.9).
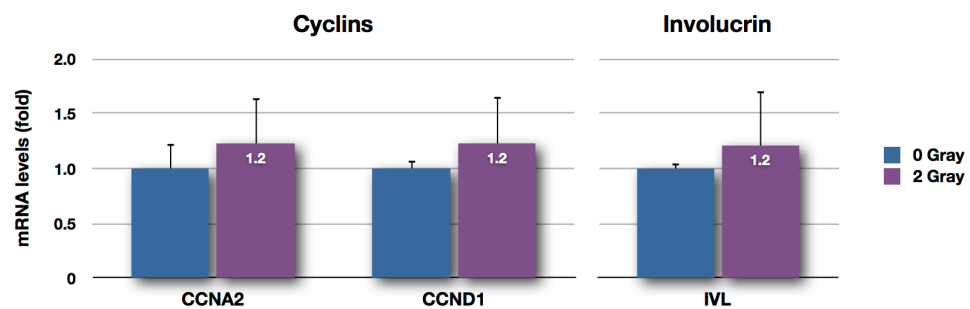
Figure 4.9. Effect of induction of acute DNA damage on cell proliferation and differentiation. Chart shows gene expression levels of Cyclins (A2 and D1) and Involucrin (IVL) in keratinocytes, 6 hours following exposure to a relatively low dose (2 Gray) of IR. mRNA levels (fold) were normalised against the respective non-irradiated control (0 Gray). Results are represented as mean ± s.d. (n=3).

The results indicate that the low level of p53 activation (weak DDR) does not seem to have been the factor responsible for the previously observed induction of the candidate markers.

4.3. Induction of permanent DNA damage

Exposing keratinocytes to a dose of IR that mimics the level of damage to the DNA caused by telomere uncapping generated a similarly low DDR yet did not result in elevation of any of the candidate markers. However, expression of TRF2$^{\Delta B \Delta M}$ induces a senescent-like growth arrest in keratinocytes, despite the low DDR (Minty *et al*, 2008), whilst exposure to such a low dose as 2 Gray of IR does not. I therefore wondered whether a higher level of DNA damage caused by senescence-inducing doses of IR could induce the candidate markers. This is particularly important in view of the recent data implicating unrepairable DSBs in senescence (Rodier *et al*, 2009) and ageing (Sedelnikova *et al*, 2004) and that unrepairable DSBs are preferentially located at the telomeres (Fumagalli *et al*, 2012; Hewitt *et al*, 2012).

To test this, keratinocytes were exposed to high doses (10 and 20 Gray) of IR, capable of generating unrepairable DNA DSBs, and given a 5 day recovery period to resolve any repairable DSBs. Engagement of the DDR was again demonstrated by up regulation of p53's transcriptional target, p21^{WAF1}. Keratinocytes subjected to 10 Gy and 20 Gy show an over 2-fold increase in p21^{WAF1} mRNA levels, when compared to a non-irradiated control, which was accompanied by a similar increase of its protein levels. Total p53, however, was only mildly elevated (Fig. 4.10). It should be noted that p21^{WAF1} levels are constitutively higher in keratinocytes than in fibroblasts because of the well established role of p21^{WAF1} in epidermal differentiation (Macleod *et al*, 1995).

Similar induction of p53 had been previously demonstrated, for comparable doses of IR, with p53-pS15 in addition to elevation of p21^{WAF1} and total p53 (Minty *et al*, 2008; Rodier *et al*, 2009), and persistent 53BP1 foci (Rodier *et al*, 2009). In normal human fibroblasts, p21^{WAF1} signalling was sustained, as doses of this magnitude generate persistent DNA damage foci (PDDF) indicating permanent damage to the DNA through unresolved DSBs (Rodier *et al*, 2009).
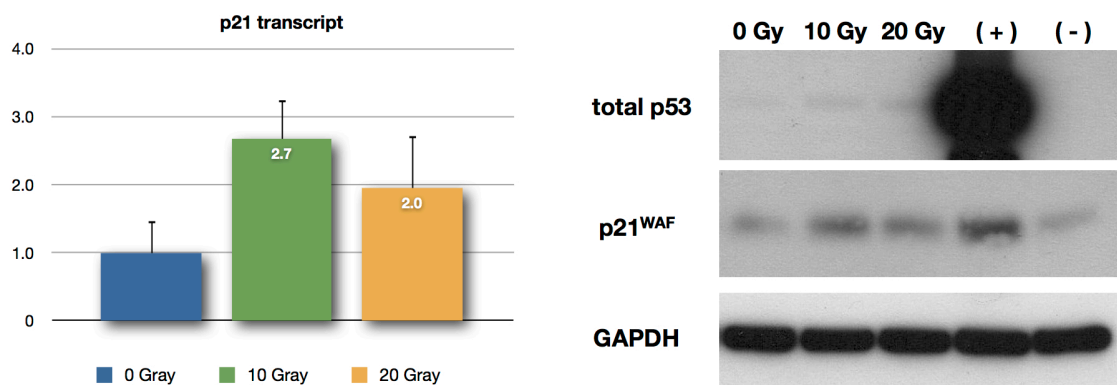
Figure 4.10. Engagement of the DDR following induction of permanent DNA damage. p21^WAF1 transcript (graph) and total p53 and p21^WAF1 protein (blot) levels in keratinocytes, 5 days following exposure to senescence-inducing doses (10 and 20 Gray) of IR. mRNA levels (fold) were normalised against the non-irradiated control (0 Gray). Results are represented as mean ± s.d. (n=2). Legend: (+) = positive control (SVHFK cell line); (-) = negative control (BICR-6 cell line).

Accordingly, I observed that the amount of DNA damage generated and the constitutive DDR signalling that followed seemed to have resulted in growth arrest and senescence. Following exposure to senescence-inducing doses of IR (10 and 20 Gray), the average number of cells obtained 5 days following irradiation was similar to the value obtained for the day 0 control, which suggests a halt in cell division. In contrast, non-irradiated keratinocytes (0 Gray) underwent normal proliferation yielding about 3x the average number of cells by day 5 (Fig. 4.11 Cell yields). In addition, a significant decrease in Cyclin A2 (CCNA2) accompanied by increase in Cyclin D1 (CCND1) transcript levels was observed in irradiated keratinocytes when compared to non-irradiated controls, 5 days following irradiation (Fig. 4.11 Cyclins). Since it is is well established that CCNA2 levels decline in senescent fibroblasts and CCND1 levels increase (Dulić *et al*, 1993) and expression array data suggests that this is also true for keratinocytes (Hunter *et al*, 2006), the growth arrest observed is consistent with senescence.

In addition, since two of the candidate markers (S100A7 and HOPX) have been implicated in terminal differentiation of human keratinocytes (Watson *et al*, 1998; Yang *et al*, 2010) I monitored the expression levels of involucrin (IVL), a marker of later stages of epithelial differentiation (Rice & Green, 1979). This was particularly relevant for keratinocytes exposed to senescence-inducing doses of IR (10 and 20 Gray) and/or that remained for several days in culture. Five days following irradiation, involucrin transcript levels in irradiated keratinocytes were not significantly different from the levels found in non-irradiated cells (Fig. 4.11 Involucrin). This suggests that senescence-inducing doses of IR do not induce terminal differentiation in normal human epidermal keratinocytes. I then decided to assess levels of keratinocyte differentiation markers over the 5-day period between irradiation and recovery. I found, by looking at changes in the non-irradiated controls, that although average transcript levels of IVL remained unaltered, p21^{WAF1} transcript was elevated by over 2-fold in keratinocytes which had undergone 5 days in culture (Fig. 4.11 non-irradiated controls). p21^{WAF1} expression is known to contribute to differentiation-associated growth arrest in keratinocytes (Missero *et al*, 1996) by promoting commitment to the initial stages of differentiation. However, p21^{WAF1} protein becomes down-regulated, both *in vitro* and *in vivo*, at later stages. In fact, p21^{WAF1} sustained expression is thought to act as a negative regulator and suppress terminal differentiation (Di Cunto *et al*, 1998). This suggests that over 5 days keratinocytes were undergoing the initial stages of differentiation.
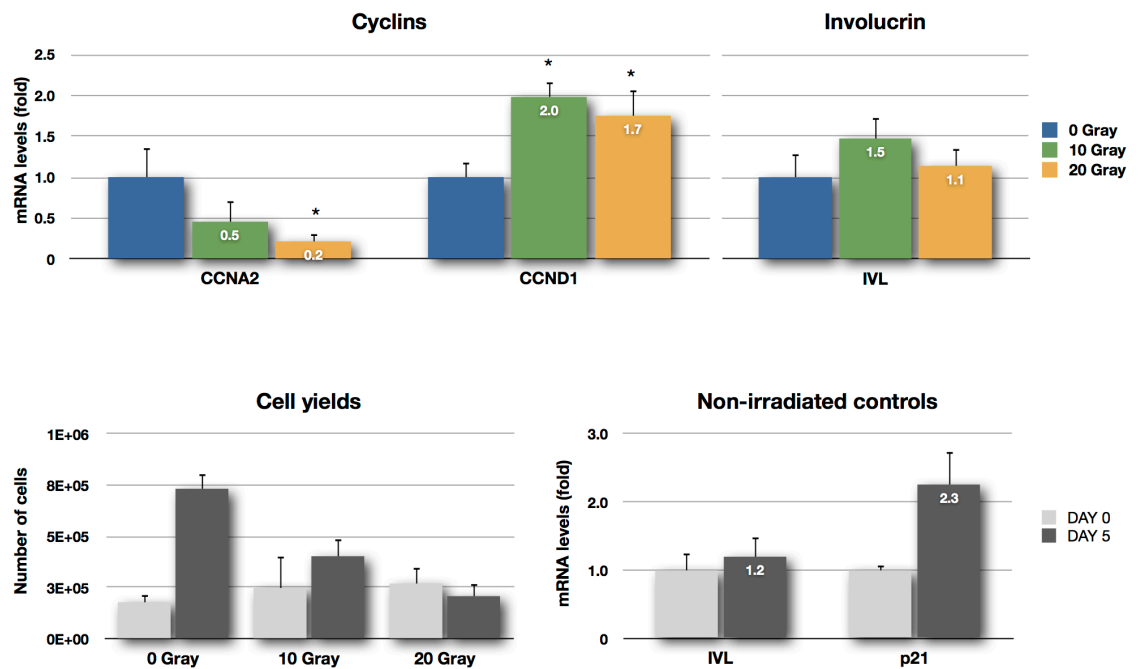
Figure 4.11. Effect of induction of permanent DNA damage on cell proliferation and differentiation. <u>Top chart</u> shows gene expression levels of Cyclins (A2 and D1)and Involucrin in keratinocytes, 5 days following exposure to senescence-inducing doses (10 and 20 Gray) of IR; mRNA levels (fold) were normalised against the respective non-irradiated control (0 Gray). <u>Bottom left chart</u> shows cell yields obtained per treatment (0, 10 or 20 Gray) between day 0 and day 5 whilst <u>bottom right chart</u> shows transcript levels of Involucrin (IVL) and p21[WAF1], in the non-irradiated controls (0 Gray) between day 0 and day 5; values were normalised against the respective day 0 control. Results are represented as mean ± s.d. (n=3); *p<0.05. Statistical significance was calculated by one-way ANOVA followed by Tukey's *post hoc* test.

Despite activation of the p53 pathway of senescence 5 days following exposure to 10 or 20 Gray of IR, candidate markers HOPX, ICEBERG and S100A7 did not show a significant elevation of their transcript levels, when compared to a non-irradiated control (Fig. 4.12). HIST2H2BE, however, demonstrated a dose-dependent elevation of its mRNA levels with ɣ-radiation. I observed an average increase of 1.6-fold and 1.9-fold, 5 days following exposure to doses of 10 and 20 Gray of IR, respectively (Fig. 4.12). Therefore, results show that only one of the markers, HIST2H2BE, was up-regulated by senescing-inducing doses of IR.
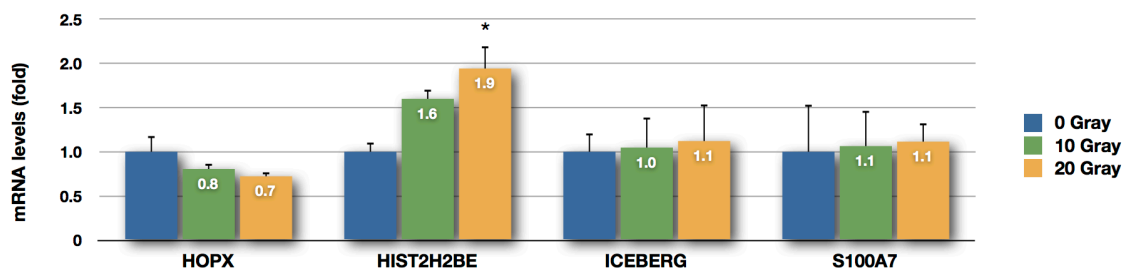
Figure 4.12. Candidate markers response upon induction of permanent DNA damage. Gene expression levels of HOPX, HIST2H2BE, ICEBERG and S100A7 in keratinocytes 5 days following exposure to senescence-inducing doses (10 and 20 Gray) of IR. Values were normalised against the non-irradiated control (0 Gray). Results are represented as mean ± s.d. (n=3); *p<0.05. Statistical significance was calculated by one-way ANOVA followed by Tukey's *post hoc* test.

Although HIST2H2BE was the only gene up-regulated by ɣ-radiation, we observed that, interestingly, all candidate markers were induced by time in culture alone, probably due to cells undergoing the early stages of terminal differentiation as indicated by the increase in p21[WAF1] (el-Deiry *et al*, 1995); see also Fig 4.11). HOPX, HIST2H2BE and ICEBERG transcript levels increased by about 2-fold, and S100A7 by around 8-fold between day 0 and day 5, in the non-irradiated controls (Fig. 4.13). A similar level of induction was found for HOPX, ICEBERG and S100A7 also across the irradiated groups; for HIST2H2BE, this baseline induction was accompanied by an IR-dependent elevation (Fig.4.13).

It is possible that p21^{WAF1} might be regulating the expression of all candidate markers in a differentiation-dependent manner and also HIST2H2BE in a senescence-dependent manner (via the p53 pathway).
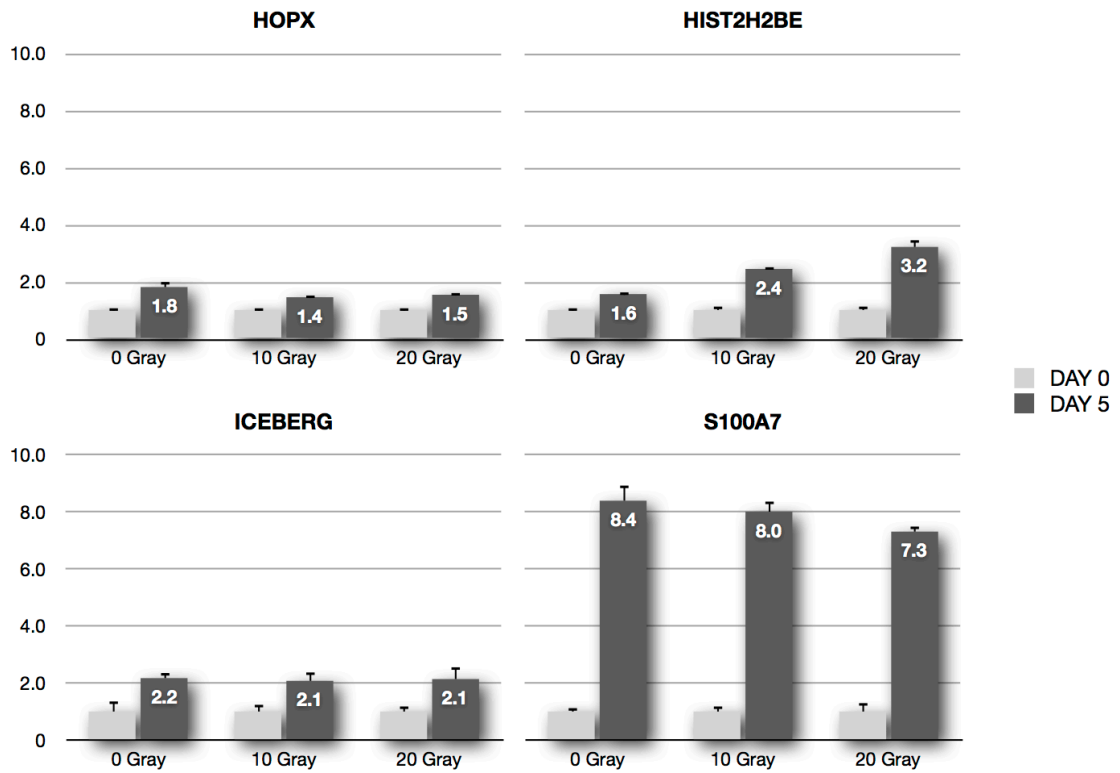
Figure 4.13. Effect of differentiation in the candidate markers gene expression levels. Charts show transcript levels of of HOPX, HIST2H2BE, ICEBERG and S100A7, per treatment (0, 10 or 20 Gray) between day 0 and day 5. Values were normalised against the respective day 0 control. Results are represented as mean ± s.d. (n=3).

4.4. Discussion

Keratinocytes seem to differ from fibroblasts in their response to dysfunctional telomeres. Telomere uncapping as a consequence of expression of the well characterised dominant negative mutant version of the telomeric protein TRF2, TRF2$^{\Delta B\Delta M}$, results in a senescent-like growth arrest accompanied by an unexpectedly weak DNA damage response (DDR). Keratinocytes expressing TRF2$^{\Delta B\Delta M}$ show a characteristic transcriptional profile with up-regulation of genes involved in chromatin remodelling (HIST2H2BE, histone from the H2B family), inflammation (ICEBERG) and terminal differentiation (HOPX and S100A7). I hypothesised that either keratinocytes are extremely sensitive to the DDR or telomere uncapping is mainly being signalled through an alternative pathway to the classical DNA damage p53-dependent senescence pathway.

I tested the first argument by inducing a similar number of repairable DSBs to those predicted by telomere uncapping, with a relatively low dose of IR, and found that none of the candidate markers were induced by acute DNA damage (Section 4.2). This lead me to conclude that the the original elevation of HIST2H2BE, HOPX, ICEBERG and S100A7 expression levels by TRF2$^{\Delta B\Delta M}$ (Minty *et al*, 2008) was not a result of the low level of DDR observed following telomere uncapping.

In order to investigate the second argument, I started by assessing the influence of the activation of the DNA damage pathway of senescence in the candidate markers expression levels. I generated unrepairable DSBs using senescence-inducing doses of IR (Section 4.3) and found that histone HIST2H2BE was the only marker up-regulated as a consequence of permanent DNA damage. This is consistent with recent reports showing that chromatin components, such as H2A and H2B histones, are actively involved in the response to DNA damage. Monoubiquitylation of histone H2B has been identified as an additional post-translational protein modification to ATM-dependent phosphorylation of various cellular targets, part of the DDR (Shiloh *et al*, 2011). H2B histones are ubiquitylated in response to DSBs and promote recruitment of repair proteins (Shiloh *et al*, 2011), such as Rad18 and BRCA1, to the DNA lesions in a RNF168-dependent manner (Panier *et al*, 2012). In addition, impaired histone H2B monoubiquitylation was also recently described as a novel property of cancer cells *in vivo*, reported in breast, colon and lung tumours (Urasaki *et al*, 2012). This indicates that HIST2H2BE is an active player in

the DDR response to generalised DNA damage and, therefore, is not a specific marker for telomere-dysfunction induced senescence. Results also suggest that the original elevation of HOPX, ICEBERG and S100A7 expression levels by TRF2$^{\Delta B \Delta M}$ (Minty *et al*, 2008) cannot be attributed to the activation of p53 via the DNA damage pathway. Therefore, although it was previously shown that the candidate markers are regulated by telomere dysfunction and telomerase (Muntoni *et al*, 2003; Minty *et al*, 2008), they do not appear to be up-regulated by p53.

Recently, several sequential molecular events that distinguish transient from persistent DDR signalling have been identified, following generation of DSBs by IR (Rodier *et al*, 2011). Relatively low doses of ionising radiation result in many small DNA damage foci, the majority of which is resolved within 6 h and the remaining by 24 h. These transient foci contain various repair or adaptor proteins such as MDC1, 53BP1, NSB1 and MRE11, the modified histone ɣH2AX and activated ATM/ATR, indicative of DDR signalling. This shows that active repair is taking place by NHEJ as well as by HR, because cells damaged in S phase show evidence of ssDNA-binding proteins such as Rad51 and RPA70 in addition to DNA synthesis. On the other hand, cells exposed to senescence-inducing doses of IR initially also accumulate many small DNA damage foci and attempt repair over a period of 24 h, where some of the small foci become resolved. However, in these cells some of the foci increase in size (contain more 53BP1) and fail to resolve, with cell cycle arrest occurring within 24 h. In these persistent foci there is no evidence of repair; instead there is a characteristic association between 53BP1 and PML NBs (pro-myelocytic leukaemia protein nuclear bodies) as well as accumulation of activated forms of p53, CHK2 and ɣH2AX. Therefore, authors suggest that these permanent lesions, they designated as DNA-SCARS or 'DNA segments with chromatin alterations reinforcing senescence', do not contain sites of DNA damage but rather harbour stable modifications in chromatin, resulting from excessive damage or failure to repair it, responsible for maintaining the growth arrest.

DNA-SCARS are thought to constitute a reservoir of DDR signalling, including activated p53 and other DDR proteins, essential to the SASP (Rodier *et al*, 2009) as opposed to p53. Ubiquitylated H2B histones are some of the activated chromatin proteins involved in the ATM/CHK2 DDR pathway and in the recruitment of proteins involved in HR repair (Shiloh *et al*, 2011; Panier *et al*, 2012). This might explain the dose-dependent elevation of the candidate

marker HIST2H2BE in response to senescence-inducing doses of IR. DNA-SCARS include TIFs (Takai *et al*, 2003) and foci resulting from both oxidative and oncogenic damage and, although the SASP component is an integral part of these lesions, the growth arrest component can be uncoupled from them in cells with non-functional p53 and pRb senescence pathways (Rodier *et al*, 2011). This means that it is unlikely the other candidate markers might be induced by inflammatory cytokines, such as IL-6, as they are part of the SASP, but other inflammatory pathways upstream of p53 and pRb should not be ruled out. Especially since ICEBERG is known to be induced by pro-inflammatory stimuli, despite its role as negative regulator of IL-1β generation by inhibition of caspase-1 (Humke *et al*, 2000). Similarly S100A7, which is also known as psoriasin for having been firstly isolated from psoriatic skin, has also therefore been linked with inflammatory pathways (Watson *et al*, 1998). In addition, the candidate markers can still be up-regulated by p53, pRb or components of these senescence pathways since neither functional p53 or pRb are required for the formation of DNA-SCARS (Rodier *et al*, 2011).

One interesting find from these experiments was the fact that all candidate markers were elevated just with time in culture. I related this to a natural elevation in p21^{WAF1} expression levels in the already higher basal levels characteristic of keratinocytes due to the role of p21^{WAF1} in terminal differentiation (Missero *et al*, 1996). I hypothesise that senescence driven by telomere dysfunction might have also triggered terminal differentiation in keratinocytes, which could have contributed to the original elevation of the candidate markers (Minty *et al*, 2008).

This hypothesis is supported by the following arguments. Senescent keratinocytes are still capable of undergoing differentiation in culture (Norsgaard *et al*, 1996). Although its expression is p53-dependent in response to DNA damage, p21^{WAF1} is also regulated independently of p53 in normal development of several murine tissues and during cell differentiation; in the latter it is also subjected to post-transcriptional regulation (Macleod *et al*, 1995). I have observed that some of the candidate markers (HOPX, ICEBERG and S100A7) are not regulated by p21^{WAF1} in a p53-dependent manner in response to DNA damage but seem to be regulated in parallel with p21^{WAF1}, independently of p53, during differentiation (HIST2H2BE included). In addition,

two subsequent studies to Minty *et al*'s (Minty *et al*, 2008) have identified terminal differentiation as a phenotype associated with ageing in both melanocytes (Inomata *et al*, 2009) and keratinocytes (Velarde *et al*, 2012) in response to both DSBs and telomere dysfunction.

p21^{WAF1} is responsible for the initial growth arrest preceding terminal differentiation and, although it promotes the commitment of keratinocyte populations to differentiation it also reduces the expression of late differentiation markers, such as loricrin and involucrin, in keratinocytes of the uppermost layers (Missero *et al*, 1996). This is consistent with what I have observed for involucrin transcript which remained at control levels alongside elevation of p21^{WAF1}. Increased expression of p21^{WAF1} has been shown to result in MAPK activation at the transcriptional level in a keratinocyte-specific and cell cycle-independent manner. IGF-1 was the factor upstream of the MAPK signalling cascade identified as responsible for the suppressive effect on terminal differentiation (Devgan *et al*, 2006). Since the candidate markers seem to be influenced by p21^{WAF1} independently of p53 it is, therefore, possible that candidate markers HOPX, ICEBERG and S100A7 might be regulated by any of the MAPK pathways. In fact, it has been recently shown in normal human fibroblasts that the SASP is regulated by p38MAPK via NF-Kβ signalling, independently of the DDR and, thus, of p53 (Freund *et al*, 2011). Consistently, a role for the NF-Kβ pathway in cellular senescence has also recently been reported in fibroblasts (Rovillain *et al*, 2011).

The next priority was to investigate whether the candidate markers might be induced by over-expression of any of the effectors (p14^{ARF}, p16^{INK4a} and p53) of the know pathways of senescence (Chapters 5 and 6). Based on my findings so far, out of the three potential specific markers (HOPX, ICEBERG and S100A7) for TDIS, the homeobox gene HOPX seemed the most interesting candidate. HOPX expression levels were not induced by DNA damage and instead appear to be consistently slightly inhibited by it (Sections 4.2 and 4.3). Also, HOPX has recently been described as a tumour-suppressor gene (Chen *et al*, 2007; De Toni *et al*, 2008; Yamashita *et al*, 2008; Yamaguchi *et al*, 2009) and this is a common feature of genes involved in cellular senescence. I have, therefore, also proceeded to investigate the functional role of HOPX in keratinocyte TDIS (Chapter 7).

Chapter 5. Establishment of an optimal low stress system for retroviral transduction of normal human epidermal keratinocytes to induce senescence by defined genes.

5.1. Introduction

5.1.1. Background

Retroviruses were first discovered in the beginning of the twentieth century, however their full potential as gene delivery vectors only started to be acknowledged in the late 1960s and 1970s, following the discovery of their causal role in cancer and AIDS (Varmus, 1988). These viruses are mobile genetic elements belonging to the family of retrotransposons. They are distinctive from all other viruses for containing an RNA genome that replicates via a DNA intermediate, the provirus, as represented in Fig. 5.1 (Varmus, 1988; C Heiser, 2004a).

The retroviral genome contains three genes, *gag*, *pol* and *env* which encode for all the proteins contained in the virion (Fig. 5.2). The *gag* gene encodes for the structural proteins of the core - matrix, capsid, nucleocapsid and contains the packaging sequence ψ. The *pol* gene encodes for the viral enzymes also contained in the core - protease, reverse transcriptase and integrase. The viral envelope originates from the hosts membrane (lipid bilayer) with additional surface and transmembrane proteins, products of the *env* gene. The receptors and entry co-factors determine the tropism of the retrovirus (Varmus, 1988; C Heiser, 2004a).

The provirus is flanked by two long terminal repeats or LTRs (Fig. 5.2), involved in gene expression, that are composed by the following; region U3, containing the promoter and enhancer; region R, the starting point of transcription in the 5' end and the polyadenylation site in the 3' end; and region U5. In addition, 5'U3 contains a TATA box responsible for recruiting the basal transcription machinery to the promoter and a large number of transcription

factors binding sites. All these features make the retroviral LTR a powerful promoter in driving gene expression (Varmus, 1988; C Heiser, 2004a).
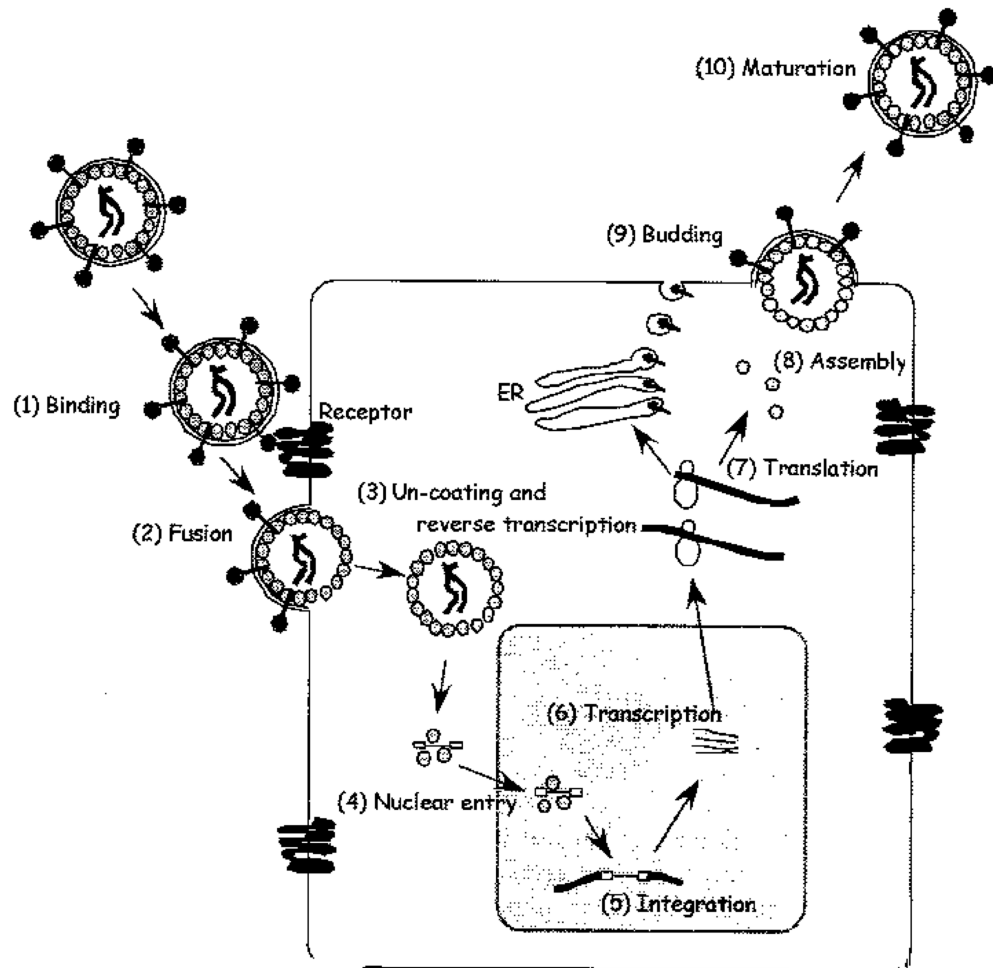
Figure 5.1. The retroviral life cycle. Steps involve 1. <u>Binding</u> to membrane receptors, 2. <u>Fusion</u> to cell membrane, 3. <u>Un-coating</u> and <u>reverse transcription</u> of RNA genome (2 identical single strands), 4. <u>Nuclear entry</u> of DNA intermediate, 5. <u>Integration</u> of provirus, 6. <u>Transcription</u> and 7. <u>Translation</u> into viral proteins, 8. <u>Assembly</u> of viral constituents, 9. <u>Budding</u> through the cell membrane and 10. <u>Maturation</u> of the viral particles (in (C Heiser, 2004a)).

Retroviruses are obligatory intracellular parasites, they thus need to be able to integrate and use the cell's replication, transcription and translation machinery to propagate and be infectious. Simple retroviruses (e.g. MLV) require the host cell to be actively dividing for integration to occur, while

complex retroviruses (e.g. HIV), also called lentiviruses, have developed strategies to overcome this limitation and are able to infect non-dividing cells. Adenoviruses, on the other hand, have a DNA genome and do not integrate in the host's genome or replicate during cell division (C Heiser, 2004a).
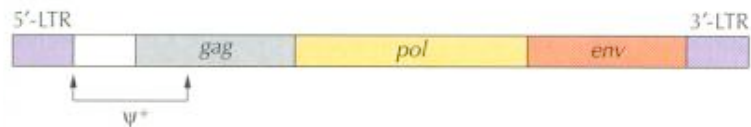
Figure 5.2. The proviral sequence. LTR = Long Terminal Repeat; ψ = psi or packaging signal.

Retroviruses are very efficient tools for gene delivery, especially compared to transfection of naked DNA, with some vectors being able to stably transduce close to 100% of target cells with minimal or no physiological effects on the target cells (Mulligan, 1993). In addition to high transduction efficiency and low toxicity, other advantages of retroviral vectors over non-viral methods and adenoviruses are their genetic stability, due to integration of the provirus in the host's genome, the high expression levels of the transgene, due to their powerful promoter, and the flexibility of their genome which allows varied design strategies (Varmus, 1988). The fact that retroviruses use viral receptors to target the host cell endows them with a great advantage over non-viral methods, cell type specificity. They fuse with the cell membrane, transpose this first barrier and are then effectively uncoated and transported into the cell nucleus. The absolute necessity for the presence of a cellular viral receptor for cell targeting and their specificity to a narrow range of cellular receptors can be a disadvantage (Mulligan, 1993). However, this has been overcome by pseudotyping envelopes from other viruses into a parent retrovirus, therefore broadening the viral tropism (C Heiser, 2004a). Retroviral vectors can only infect cells that are actively dividing (Miller *et al*, 1990). This is an important limitation when compared to adenoviruses and lentiviruses since, as opposed to the latter, they absolutely depend on cellular replication for integration and, consequently, for effective transduction to occur. However, this

also means that they are safer options for the handler (Mulligan, 1993; C Heiser, 2004a).

The main modification in retroviruses that first allowed them to be used safely as vectors for gene delivery was to make them replication-incompetent. Therefore, they integrate the host cell genome but are not infectious because they are missing or have deletions in coding regions required for packaging and virion replication. As a consequence they can now accommodate transgenes and various other sequences of interest which opened up a world of retroviral vector design options in parallel to the development of packaging cell lines.

5.1.2. Retroviral vectors and packaging cell lines

The design of a retroviral vector consists in cloning the retroviral sequence into the multiple cloning site of a plasmid backbone using restriction enzymes. A classical vector must contain the LTRs, the packaging sequence ψ, the polypurine tract (PPT), control elements and the gene of interest, between the two LTRs, under the control of the LTR promoter. Other genes, encoding for selection markers, fluorescent markers or other molecular tags, and even Internal Ribosome Entry Sites (IRES), as well as additional promoters can also be inserted providing a wealth of possible design strategies to suit the objective of the work (C Heiser, 2004a). For example, CMV promoters are more powerful in driving gene expression than MLV promoters. Each promoter will allow for generation of separate transcripts encoding for transgene and selection marker, for instance, each with distinct expression levels. IRES vectors however, allow for both transgene and selection marker or fluorescent tag to be generated as a single transcript. This greatly reduces the probability of loss of expression of each insert independently and allows for generation of clones where the level of expression of the tag/marker should directly reflect the expression level of the transgene. This makes IRES vectors superior to conventional ones. Whilst the retroviral vector provides the gene(s) of interest and essential *cis* elements for packaging, reverse transcription and integration, the packaging cell line provides the helper genome (*gag*, *pol* and *env*), that encodes for the viral proteins, in *trans* (Fig. 5.3) (Nolan lab website).

The concept of packaging cell lines was born from the observation that cells carrying a virus with a defective ψ would produce replication-incompetent viruses (C Heiser, 2004a) and revolutionised the use of retroviral vectors for gene transfer (Mulligan, 1993).
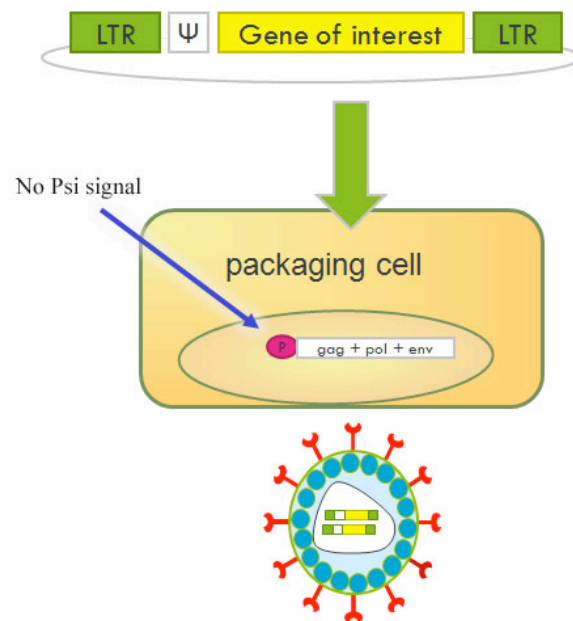
Figure 5.3. Contribution of the retroviral vector and the packaging cell line for viral production. The retroviral vector provides the gene(s) of interest and essential *cis* elements for packaging, reverse transcription and integration. The packaging cell line provides the helper genome (*gag*, *pol* and *env*), which encodes for the viral proteins, in *trans* (LTR = Long Terminal Repeat; ψ = psi or packaging signal).

The first packaging cell line ψ-2 was based on NIH-3T3 cells and MLV with a deletion in ψ and, obviously, limited tropism for murine cells (Mann *et al*, 1983). Several other ecotropic lines followed with tropism for avian and some mammalian cells and the first amphotropic cell line ψ-AM was developed in the 1980s. All first generation packaging cell lines were very efficient in producing retroviruses with high-titer (10^7 U/mL), but their major limitation was the generation of replication-competent helper viruses as a consequence of recombination events (Miller *et al*, 1990; C Heiser, 2004a).

The next improvements focused on introducing multiple deletions in the helper genome and on reducing homology between the latter and the vector construct (Miller *et al*, 1990; C Heiser, 2004a). Therefore, second generation packaging cell lines (e.g. PA317) carry deletions in the splice donor site and in the 3'LTR in addition to deletions in ψ, already present in the previous cell lines (Miller, 2002). This strategy did not affect the titer and greatly reduced the probability of generating replication-competent retroviruses as two recombinant events would be required for this to occur.

An additional refinement was introduced to guarantee helper-free vectors (Miller *et al*, 1990; Miller & Chen, 1996; C Heiser, 2004a). Third generation packaging cell lines (ψ-CRE, ψ-CRIP, GP+E-86, GP+*env*AM12, RetroPack PT67) carry a split helper genome which means that the *gag-pol* regions are separated from the *env* region . Three recombination events would be required for helper-viruses to be generated, which makes this extremely unlikely to occur. The viral genes can also be controlled using heterologous control elements (other than the LTR and poly-A) which greatly decreases the homology between helper and vector sequences. PT67 cells (Miller & Chen, 1996) are based on 10A1 MLV genome and have the particularity of producing vectors that use multiple receptors for cell entry. They contain the alternative receptor Glvr-1, in addition to the amphotropic receptor Ram-1, thus presenting an important advantage over the best amphotropic packaging cell lines in infecting human cells.

The latest generation packaging cell lines (BOSC23 and Phoenix) include several other refinements. Phoenix (Swift *et al*, 2001), as their predecessor BOSC23, were generated by introducing constructs expressing retroviral functions into 293T cells (Pear *et al*, 1993). The latter derive from the HEK 293 immortal cell line, developed in 1977 after transformation of human embryonic kidney cells *in vitro* with adenovirus type 5 DNA (Graham *et al*, 1977). These cells have been used extensively since, for their ability to be easily transfected, and originated the 293T cell line after insertion of the SV40 T-antigen mutant gene (DuBridge *et al*, 1987). Both BOSC23 and Phoenix systems are bipartite and capable of carrying episomes for rapid generation of high titer stocks of helper-free retroviruses (Pear *et al*, 1993) although Phoenix lines do not demonstrate loss of titer over time, as did BOSC23, and are more stable due to a bipartite helper genome built with a good choice of promoters driving the expression of *gag-pol* (RSV) and *env* (CMV) (Nolan lab website). By using the *gag-pol* and

env regions separately and from two different viruses, homology between them was eliminated therefore preventing the generation of replication competent retroviruses. This was previously possible in a bipartite genome originating from the same virus if three homologous recombinational events occurred (Miller *et al*, 1990). By using non-Moloney promoters there is also less probability of recombination with the introduced retroviral construct carrying the transgene. In addition, it is possible to monitor *gag-pol* production via the expression of a surface marker (IRES-CD8) and to select Phoenix cells expressing *gag-pol* and *env* via two co-selectable markers (Nolan lab website).

5.1.3. Gene delivery

The retroviral vector needs to be delivered to the packaging cell line for retroviral production. Gene delivery can be achieved by chemical and physical methods and is referred to as transfection. The lipid-based system FuGENE® 6 for transfection of mammalian cells constitutes an example of the many new lipid formulations/recipes that delivered improvements in transfection efficiency, compared to early chemical methods for DNA delivery like calcium phosphate and DEAE-dextran (Luo & Saltzman, 2000). The latter are based on the formation of complexes between the respective chemical and the DNA which are then in direct contact with the cells and subsequently internalized by endocytosis. DEAE-dextran and calcium phosphate methods are equally simple but more cytotoxic; calcium phosphate renders only a 50% transfection efficiency and, due to variation in the sizes of the calcium phosphate-DNA complexes, originates poor reproducibility between experiments; DEAE-dextran results in a much higher transfection efficiency, has good reproducibility but requires low or no serum in the growth medium and during transfection (Luo & Saltzman, 2000; C Heiser, 2004b).

The main limitations of the lipid-based methods are the still poor understanding of the lipid-DNA complexes and the variations in the formulation as a consequence of the fabrication process (Luo & Saltzman, 2000). Generally, a successful DNA delivery system should promote the contact with the cell membrane, mediate the uptake of the DNA by the cell via endocytosis, protect the DNA from degradation by endosomic/lysosomic enzymes and cytoplasmic nucleases, and finally should allow the dissociation of the DNA from the

condensed complexes for effective entry into the nucleus (Luo & Saltzman, 2000; C Heiser, 2004b). Once in the nucleus, the transfection efficiency is now solely dependent on the composition of the gene expression system (Luo & Saltzman, 2000). A plasmid construct is an episome and therefore does not integrate in the cell's genome and replicates independently, resulting only in transient gene expression. Despite being a transient system, it should still render a good expression level as these plasmids carry the SV40 bi-directional origin of replication (ORI) and therefore have a higher rate of episomal replication in cells expressing the SV40 large T antigen (Pear *et al*, 1993), which is the case of Phoenix, for example, as they are derived from the 293T cell line.

5.2. Establishment of experimental model

5.2.1. Overview of and choice of retroviral delivery systems

HOPX, HIST2H2BE, ICEBERG and S100A7 showed potential specific markers of telomere-driven senescence as they were up-regulated following telomere uncapping ensued from expression of TRF2$^{\Delta B \Delta M}$; this, however, seemed to occur independently of a DDR (Minty *et al*, 2008). In fact, HOPX, ICEBERG and S100A7 were not even elevated by the strong DDR generated by senescence-inducing doses of IR which results in activation of p53 and its transcriptional target p21^{WAF1} (Chapter 4). However, the response to IR might differ from direct over-expression of p53 since it triggers distinct molecular events towards activation of the p53 pathway. I am, therefore, interested in further investigating how the candidate markers are regulated by each of the main effectors of senescence independently, especially when these are over-expressed in normal keratinocytes.

To test this, I aim to manipulate newborn foreskin keratinocytes to ectopically express p53 (Sugrue *et al*, 1997), p16^{INK4a} (McConnell *et al*, 1998) and p14^{ARF} (Dimri *et al*, 2000) as well as the dominant negative mutant form of the telomere-binding protein TRF2 (TRF2$^{\Delta B \Delta M}$) to artificially uncap telomeres (van Steensel *et al*, 1998). The intention is to obtain pure populations of keratinocytes that are selectively undergoing senescence either via the p53/pRb common pathway, the telomere-independent pathways (p14^{ARF}/p53 and p16^{INK4a}/pRb) or via the telomere-p53-dependent pathway and observe the candidate

markers response in each independent system of senescence. In addition, I aimed to introduce the transgenes into keratinocytes without causing undue cellular stress as this would be likely to induce p16^{INK4a} and cause an unacceptable background of spontaneous senescence (Ramirez *et al*, 2001). Since the main objective is to obtain early downstream markers of telomere dysfunction in keratinocytes, the best suited system of delivery of the transgenes would be one in which it is possible to achieve high expression levels in a short period with maximum efficiency.

As opposed to normal cells, cell lines such as HEK 293 and its variant 293T are particularly easy to transfect (Graham *et al*, 1977; Pear *et al*, 1993) and were the base for the development of several packaging cell lines aimed at generating retroviral particles in high titre for successful transduction of normal cells (Swift *et al*, 2001). In the case of normal keratinocytes, it is very difficult to achieve stable transfection with plasmid constructs, however close to 100% success has been reported with retroviral vectors (Garlick *et al*, 1991; Mathor *et al*, 1996; Levy *et al*, 1998). These have been thoroughly used for their safety in handling, high transduction efficiency and low toxicity to the target cells. Retroviral gene delivery systems have previously been employed with success to over-express p16^{INK4a} in the TIG-3 strain of human diploid fibroblasts (McConnell *et al*, 1998) and p14^{ARF} in WI-38 (Dimri *et al*, 2000), both using pBabe-puro vectors. Similarly, they have also been used to ectopically express TRF2$^{\Delta B\Delta M}$ in IMR-90 and WI-38 using pBabe-puro and pLPC-puro vectors (Smogorzewska & de Lange, 2002), and in NHEK using pLPC vectors sub-cloned into the IRES vector pMIG (Minty *et al*, 2008).

The main challenge with past attempts to transduce normal human keratinocytes has been achieving long-term expression of the transgenes. This might have been due to early arrest of LTR-driven gene expression, which might call for keratinocyte-specific enhancers and further improvements in vector design, or to a general difficulty in targeting holoclones, with consequent loss of the transgene with cell division (discussed in (Levy *et al*, 1998)).

Early strategies to transduce keratinocytes involved three steps: transfection of the retroviral vector into an ecotropic packaging cell line for transient production of retroviral particles; infection of an amphotropic cell line that will stably produce virus; and infection of keratinocytes by co-culture with the virus-producing amphotropic cells. Garlick *et al* used a 3rd generation eco

packaging cell line (ψ-CRE), and 1st (ψ-AM), 2nd (PA-317) and 3rd (ψ-CRIP) amphotropic packaging cell lines. Keratinocytes were co-cultured with infectious producer lines as feeders under G418 selection (Garlick *et al*, 1991). Later, Mathor *et al* turned to 3rd generation both eco (GP+E-86) and amphotropic (GP+envAM12) packaging lines and keratinocytes were now co-cultured with a 1:2 mixture of lethally irradiated 'feeders' and infectious producer cells, still under G418 selection. They achieved an improvement in the number of generations the transgenes were expressed for and high transduction efficiencies (Mathor *et al*, 1996).

Subsequently, further improvements were introduced in the delivery strategy, as opposed to refinement of the existing retroviral vectors, in order to obtain better results (Levy *et al*, 1998). Levy *et al* used pBabe-puro vectors where the transgene was placed under the control of the LTR promoter, as it previously rendered high expression levels, whilst the SV40 promoter directed puromycin expression. Puromycin was chosen as the selectable marker as it rapidly killed non-transduced controls with no harmful effects on transduced keratinocytes, as opposed to G418 which revealed greater cell-toxicity and reduced efficiency in killing uninfected cells. In addition, latest generation transfection reagents as well as 3rd generation eco (GP+E-86) and amphotropic (GP+*env*AM12) packaging cell lines were preferred to earlier methods. The amphotropic line was infected more successfully with 48-72h viral supernatants and then these infectious cells were used as 'feeders' in co-culture to infect keratinocytes. This optimised protocol is the most efficient method reported until now for transduction of normal keratinocytes (Fig. 5.4.).

In previous work from our lab (Minty *et al*, 2008) this last strategy was adapted to selection by FACS for expression of TRF2$^{\Delta B \Delta M}$ in keratinocytes. pLPC vectors were sub-cloned into the IRES vector pMIG with GFP as a marker. This made it possible to accurately select populations of keratinocytes expressing high and low levels of the transgene as this directly reflected high and low GFP signal. Although the use of a superior retroviral vector as well as latest generation packaging cell lines (Phoenix E and Retropack PT67) resulted in high levels of gene expression in a short time frame it also came with limitations (Minty, 2007). FACS sorting introduces a greater deal of physical stress to the cells and keratinocytes are known for being particularly sensitive to physiological/external stressors. Cells can respond by undergoing apoptosis (Frisch & Francis, 1994) or by expressing p16^{INK4a} prematurely and undergoing

senescence (Ramirez *et al*, 2001), which will result in cell loss or introduction of experimental bias. Additionally, the preparation of the cells for sorting and the procedure itself resulted in greater cell losses and introduction of contamination, consequently with the same outcome. As this indirect strategy is also technically demanding and time consuming, a more direct strategy for infection of keratinocytes using amphotropic supernatants was tested, yet resulted in poor infection rates (as low as 3%) (Minty, 2007). In accordance with this, Levy *et al* had already observed that producer lines generated by retroviral infection originate higher viral titres than lines obtained by transfection (Levy *et al*, 1998).
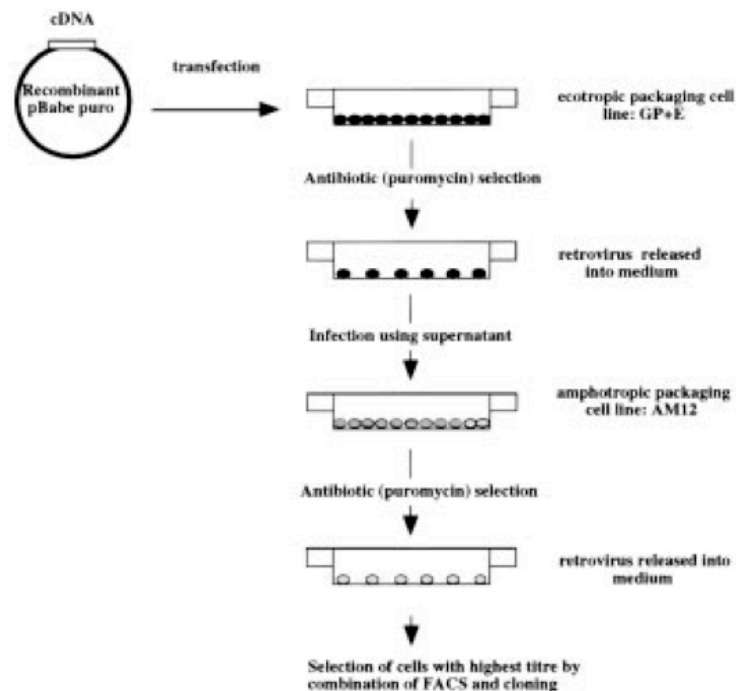
Figure 5.4. Schematic representation of the protocol used for obtaining amphotropic cell lines producing virus in high titre. This indirect strategy involves transfection of the retroviral vector into an ecotropic packaging cell line (GP+E). Virus produced from these cells was used to infect another producer line (AM12), now to generate amphotropic viral particles. The amphotropic producer cells with highest titre were then used as 'feeders' in co-culture to infect normal keratinocytes (in (Levy *et al*, 1998)).

Based on the alternatives, I have decided to use the original pBabe-puro (Stott *et al*, 1998; McConnell *et al*, 1998; Dimri *et al*, 2000) and pLPC-puro (Smogorzewska & de Lange, 2002) retroviral vectors, transduce the keratinocytes via the indirect strategy of infection (Levy *et al*, 1998; Minty *et al*, 2008) and isolate transduced populations of NHEK using drug selection (Levy *et al*, 1998). This should be the most straightforward approach to obtain efficient transduction of NHEK, cultured in the 'feeder' system, in a short period and with the least deleterious effects on the cells.

5.2.2. Indirect strategy for infection of keratinocytes (via ecotropic virus)

In pBabe-puro vectors, the transgenes p53, p14^{ARF}, p16^{INK4a} and the GFP tag are under the control of the 5'LTR while the SV40 promoter drives the expression of puromycin. In pLPC-puro N-myc constructs, the 5'LTR controls puromycin expression and both TRF2$^{\Delta B \Delta M}$ and the Myc tag are under the control of the CMV promoter. Maps of the plasmid backbones used are presented below (Fig. 5.5).
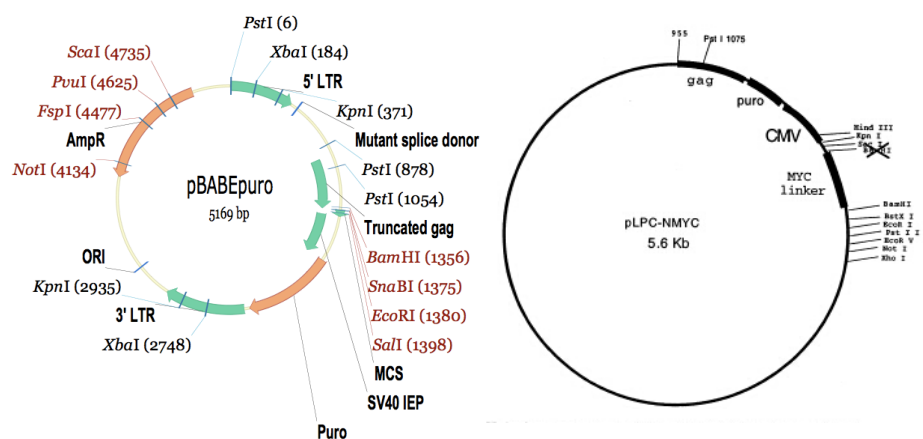
Figure 5.5. Maps of empty vectors pBabe-puro and pLPC N-myc puro. Both vectors contain the required retroviral LTRs, a truncated *gag* gene carrying the packaging signal ψ, a gene for puromycin resistance, an additional promoter (SV40 internal early promoter for pBabe and CMV promoter for pLPC) and multiple cloning sites (MCS) where transgenes can be inserted.

Vectors were transfected into Phoenix Eco cells using a lipid-based transfection reagent (FuGENE®6) reported to have a good transfection efficiency. Because the plasmid constructs are introduced as episomes, and therefore do not integrate in the genome and replicate independently, this results in transient gene expression with high levels within 48-96 hours following DNA transfection. Transient transfection allows for rapid generation of supernatants containing high titre infectious viral particles, which were collected within this time frame. The cationic polymer polybrene was added to the viral supernatants for its ability to heighten infection efficiency by increasing the virus adsorption rates (Davis *et al*, 2002). The virions produced by Phoenix Eco have an ecotropic envelope and can, therefore, infect murine cells like the amphotropic Retropack PT67s. Infection, followed by drug selection, resulted in the generation of stable PT67 lines continuously producing infectious viral particles carrying an amphotropic envelope. The outline for the experimental design is represented in Fig. 5.4, except for the use of later generation producer lines. Finally, infection of NHEK was performed by co-cultivation with lethally irradiated infectious PT67 which, by being in close contact with the recipient cells, promote efficient transmission of the virus particles.

Early attempts to optimise the transduction protocol were unsuccessful and presented many challenges. Initially I was only able to obtain a pBabe-puro empty vector control, which by lack of a fluorescent tag made transduction efficiency difficult to monitor. It meant that success or failure could only be assessed post-infection of the amphotropic producer line followed by a week long process of drug selection and would be solely based on the rate of cell survival. I later acquired the desired pBabe-puro GFP empty vector control which permitted a visual assessment of transfection/infection efficiencies at any stage of the process. As Levy *et al* (Levy *et al*, 1998) have previously observed, it was clear that the transfection of the first producer line was the determinant step of the whole procedure. Optimisation of Phoenix E seeding density and good cell culture practice were essential to guarantee ideal cell distribution, without formation of clumps, and cells in active proliferation. Successful transfection also assured that drug selection time on transfected cells was minimised generating good quality viral supernatants within 72h. Subsequent optimisation of PT67 seeding density for infection allowed for generation of amphotropic producer lines stably expressing the transgenes. Originally ,

infectious PT67 lines, obtained in this manner, were treated as regular 'feeder' cells, that is to say they were lethally irradiated, stored in liquid N and revived just before culture. The first attempt to infect keratinocytes was performed by co-culture of NHEK with 1 Million irradiated PT67-GFP or PT67-p16, obtained directly from the cell bank. It became clear that PT67s are not as robust as 3T3s and do not recover well from frozen. As a consequence, the 'feeder' layer was too sparse resulting in small and abortive keratinocyte colonies in all experimental groups. Cells were then stained for p16^{INK4a} and, as expected, all experimental groups stained positive, indicating cells started expressing p16^{INK4a} due to culture stress (Fig. 5.6). Two questions arose from this that needed addressing; first, I wondered whether keratinocytes were in stress just because the PT67 layer was sparse or if PT67 are generally unsuitable as 'feeders' and NHEK absolutely require irradiated 3T3s in culture for growth; and second, if the infection procedure was actually successful and NHEK co-cultured with PT67-p16 were expressing endogenous and/or exogenous p16^{INK4a}.
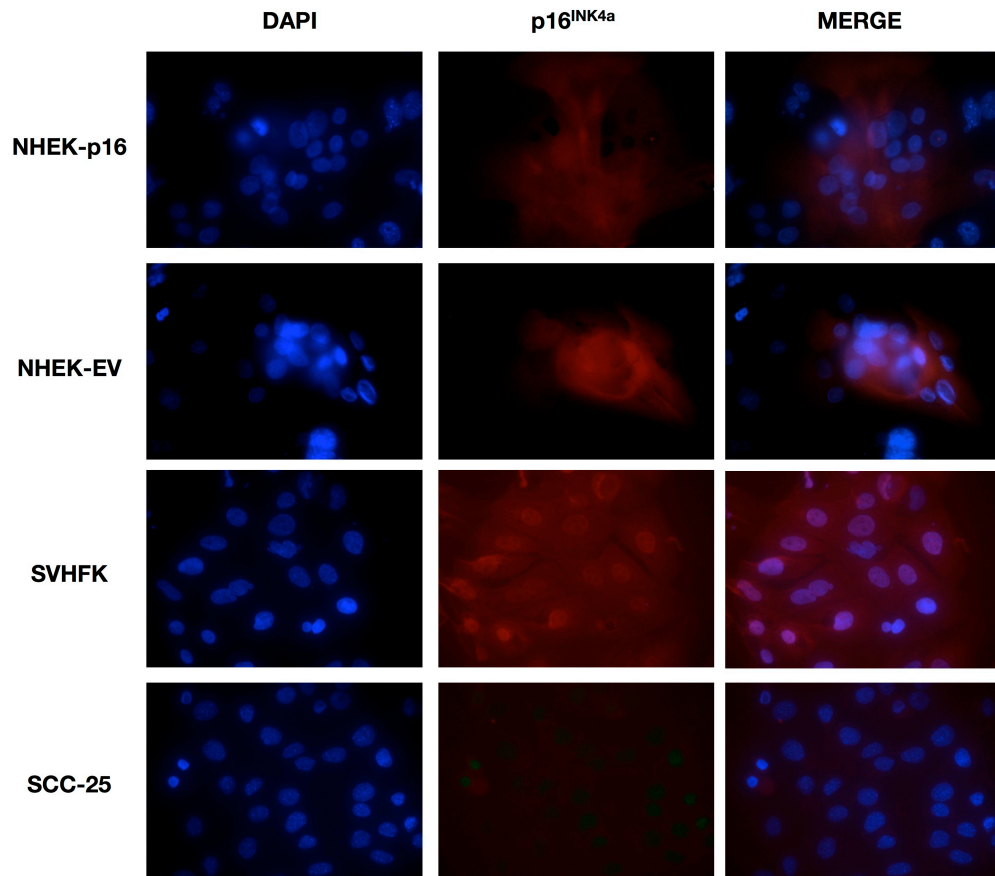
Figure 5.6. Expression levels of p16^{INK4a} in transduced NHEK. NHEK transduced with empty vector control (NHEK-EV) and p16^{INK4a} (NHEK-p16) were immunostained with an antibody against p16^{INK4a} (red). DNA was counterstained with DAPI (blue). Merged images are shown in the right panels. SVHFK cell line was used as a positive control and SCC-25 as a negative control. Photos were taken at 600x magnification.

At this stage it was important to consider the limitations of transducing normal keratinocytes with $p14^{ARF}$, $p16^{INK4a}$, p53 and $TRF2^{\Delta B\Delta M}$ for this study. The nature of the transgenes, the aim for early time points and the need to prevent keratinocytes from entering premature senescence in culture via $p16^{INK4a}$ determine experimental design. All transgenes are being introduced to induce senescence in keratinocytes and are, therefore, expected to inhibit proliferation. This means that upon co-culture with infectious PT67s as 'feeders' followed by a 48h period required for gene expression, transgenes will be expressed causing cells to arrest. Based on this alone, ideally NHEK should be seeded at high density for infection as they are allowed merely 2 days to grow following infection, to make sure sufficient cells can be obtained. However, in order to achieve high infection rates, lower densities (clonal, ideally) at time of infection are preferred as this maximises contact with infectious producer cells and would also mean less cell death following drug selection later on. There will, therefore, have to be a compromise between these two factors to ensure high enough infection rates that will also render sufficient cell yields. Plus, as I am aiming for early time points, drug selection cannot be carried out for too long which highlights again the importance of high infection efficiency. By ensuring a reduced number of non-transduced cells drug selection would cause less cell death and, consequently, would render the desired higher yields of transduced cells.

Two experimental approaches were devised to answer the questions arisen from the afore mentioned optimisation attempts (Fig. 5.7). In the first (Fig. 5.7 method 1) the idea was to replicate the original protocol that had been successful (Levy *et al*, 1998) in order to confirm if infection had indeed occurred. Therefore, NHEK were seeded at clonal density with 1 Million freshly irradiated infectious PT67; this also to test whether poor recovery had been the cause for previous failure. In the second (Fig. 5.7 method 2), 3T3 'feeders' were introduced to account for the possibility that PT67, even at the correct density, might not be sufficient to provide feeder support to the keratinocytes. If this was the cause of failure in infection then the first system will originate again abortive colonies, despite NHEK density. Therefore, in the second method I introduced 10^6 instead of 10^5 NHEK as this would reproduce the seeding densities I needed to work with to obtain adequate cell yields following the induction of senescence.
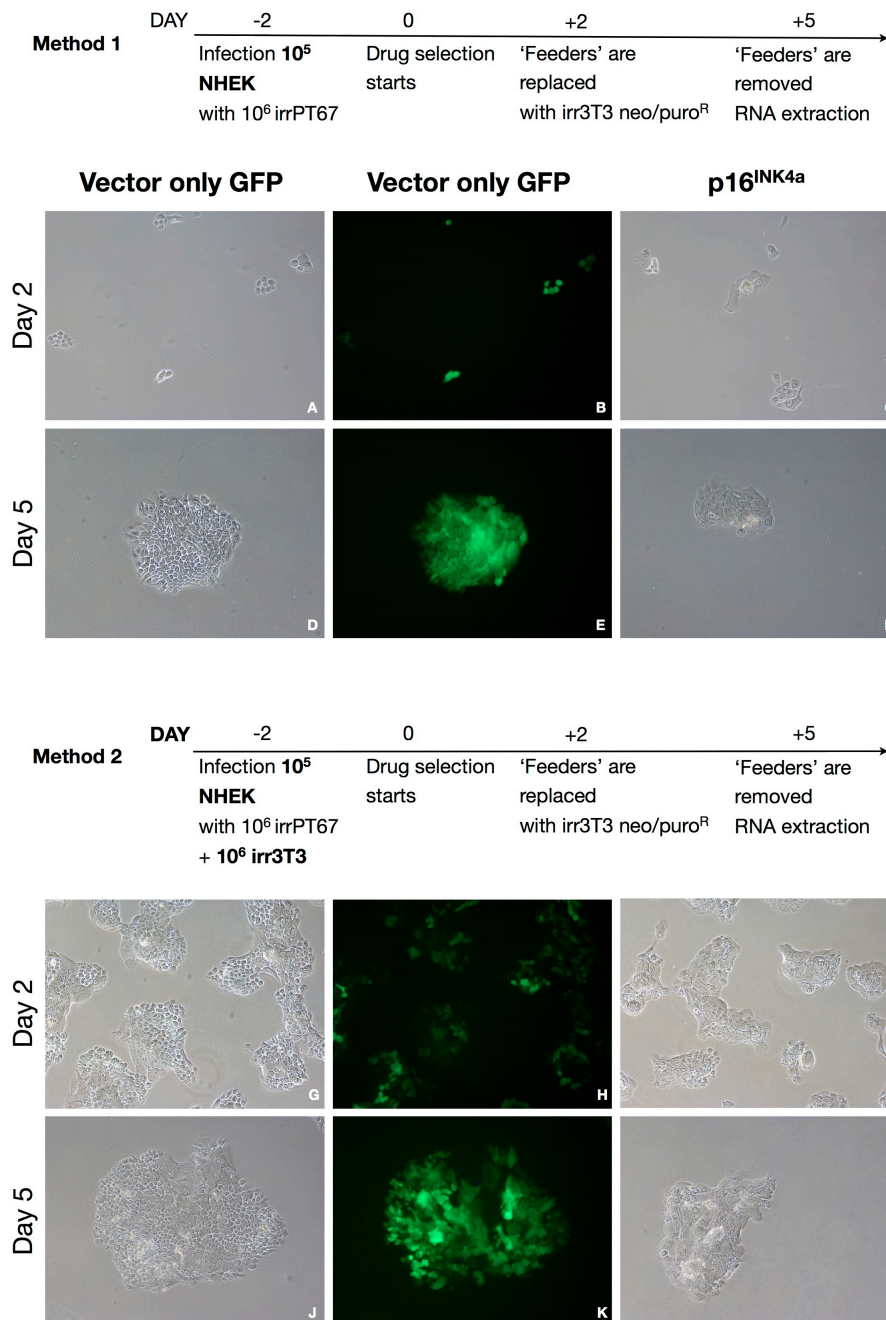
Figure 5.7. Assessment of two methods used for retroviral transduction of normal human epidermal keratinocytes. Phase contrast images of NHEK colonies ectopically expressing GFP-flagged empty vector control (left and centre columns) and p16^{INK4a} (right column) at two time points (day 2 and day 5). Early passage NHEKs (around 10 MPD) were co-cultured at clonal density with infectious PT67 packaging cells (method 1) and at high density with infectious PT67 packaging cells with 'feeders' (method 2), and drug selected with puromycin 48h later for a total culture time of 5 days. Photos were taken at 100x magnification after removing 'feeders'.

In both experimental methods (Fig. 5.7 diagrams of experimental design), infection corresponded to co-culture of NHEK with infectious freshly irradiated PT67s (day -2) followed by a 48h period to allow gene expression. At this point (day 0) drug selection was introduced (1 μg/mL puromycin) and 'feeders' were removed and replaced with irradiated 3T3 puromycin resistant 48h later (day 2). Cells remained under drug selection until day 5, by which time there was 100% cell death in the mock control, 'feeders' were removed and NHEK processed for RNA collection.

With the use of an empty vector expressing GFP it was possible to visually assess transduction efficiency by observing fluorescence (Fig. 5.7 B, E and H, K). Also, obtaining puromycin-resistant proliferative colonies in the EV control (Fig. 5.7 D and J) as opposed to abortive puromycin-resistant colonies in the p16^{INK4a} group suggests infection was successful. Seeding keratinocytes at clonal density (method 1) originated fewer and smaller colonies with infection rates reaching 100% as early as 2 days after introduction of puromycin (Fig. 5.7 A and B) and at the end of the experiment, when colonies were bigger, on day 5 (Fig. 5.7 D and E). Coherently, when NHEK were seeded at high density (method 2) resulting colonies are bigger and more numerous. Consequently infection rates are not as high (about 50%) 2 days after introducing drug selection (Fig. 5.7 G and H). However, by day 5 close to 100% transduced cells were obtained, as observed by fluorescence in the GFP empty vector control (Fig. 5.7 J and K). Seeding NHEK at higher densities has the disadvantage of generating pseudo colonies, that is colonies arising from individual clones that merge due to proximity during growth. This may allow for non-transduced cells (not expressing GFP) in the centre of the pseudo colony to remain sheltered by the outer cells and escape drug selection (Fig. 5.7 J and K). Despite a slight decrease in transduction rate this is preferable, since high density at seeding ensures a higher yield of transduced cells in the p16^{INK4a} experimental group (Fig. 5.7 I and L) when compared to the group seeded at clonal density (Fig. 5.7 C and F). Following the drug selection period, colonies expressing p16^{INK4a} were generally smaller and abortive; cells looked enlarged with a classical senescent appearance (Fig. 5.7 F and L), whilst colonies expressing GFP empty vector only were generally bigger and proliferative, containing small cells with a high nuclear/ cytoplasm ratio (Fig. 5.7 D and J).

Results also showed that, provided they were expanded beforehand and used freshly irradiated, infectious PT67s alone were suitable as 'feeders' and could successfully support the growth of keratinocyte colonies (Fig. 5.7 D and E). These appeared as healthy as colonies where irradiated 3T3s were introduced in addition to infectious PT67, in co-culture with NHEK (Fig. 5.7 J and K). Nevertheless, the latter modification was extended to the generation of all other systems of senescence in keratinocytes via expression of p14^{ARF}, p53 and TRF2$^{\Delta B \Delta M}$. This was to assure that despite possible experimental variation arising from PT67 cell density during infection, resulting transduced NHEK colonies would not prematurely express p16^{INK4a} and become abortive due to lack of proper 'feeder' support. Additionally, p16^{INK4a} expression levels were assessed by qPCR to ensure they remained at control levels in all experimental groups except in NHEK ectopically expressing it.

The optimised protocol was extended to all other constructs (Fig. 5.8). Five days following expression of transgenes cell yields for p53 and p16^{INK4a} were lower (by approximately half) than for the empty vector control, which suggests cell division arrest. Additionally, the morphological appearance of the colonies was consistent with senescence for both transgenes (Fig. 5.8 p53 and p16^{INK4a}). Although similar numbers of keratinocytes expressing EV and p14^{ARF} were obtained, the larger colonies expressing the latter have a mosaic-like pattern with some cells appearing to be senescent whilst others seem proliferative (Fig. 5.8 p14^{ARF} top). This suggests p14^{ARF} might not be as potent an inducer of senescence in keratinocytes as p16^{INK4a} and is consistent with the fact that p14^{ARF} has been shown not to accumulate when human keratinocyte senesce (Munro *et al*, 1999). In the case of TRF2$^{\Delta B \Delta M}$ this strategy for infection seems to not have worked, as colonies expressing the transgene proliferated more than colonies expressing the corresponding EV (not shown).
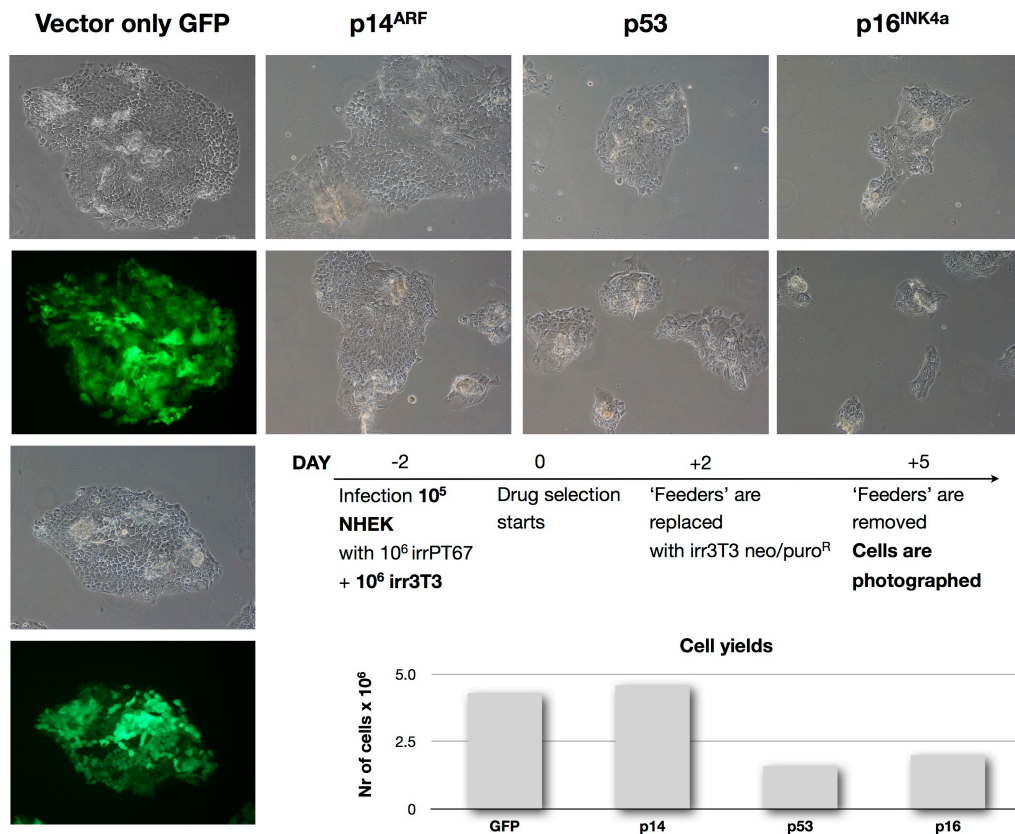
Figure 5.8. NHEK transduced with all transgenes via an indirect strategy of infection. Phase contrast images of NHEK colonies ectopically expressing GFP-flagged empty vector control (left column), p14^{ARF}, p53 and p16^{INK4a} at day 5. Early passage NHEKs (around 10 MPD) were co-cultured at high density with infectious PT67 packaging cells and 'feeders', and drug selected with puromycin 48h later for a total culture time of 5 days (diagram of experimental design). The graph represents the number of cells obtained on day 5 for each experimental group. Photos were taken at 100x magnification after removing 'feeders'.

Expression of all transgenes was confirmed by qPCR analysis (Fig. 5.9 transgenes). A decrease in CCNA2 transcript levels was also observed in keratinocytes over-expressing p14^{ARF}, p16^{INK4a} and p53, which is consistent with senescence, but not for TRF2$^{\Delta B \Delta M}$ where CCNA2 was actually elevated relatively to the empty vector control, indicating cells were actively proliferating (Fig. 5.9 CCNA2). CCND1 transcript was only elevated in keratinocytes over-expressing p16^{INK4a} (Fig. 5.9 CCND1) which, in conjunction with decrease in CCNA2, reiterates induction of senescence. Levels of CCND1 in cells expressing the other transgenes remained at control levels. These results indicate that p16^{INK4a} was the most effective inducer of senescence in normal keratinocytes, followed by p53 and p14^{ARF}, based on the level of reduction in CCNA2 accompanied by elevation of CCND1 obtained following their expression. Results also show that this infection strategy was unsuccessful for TRF2$^{\Delta B \Delta M}$, with the transgene being expressed at a level (4-fold) that seemed insufficient to trigger senescence in NHEK.

Early studies (van Steensel *et al*, 1998) using an inducible system to express TRF2$^{\Delta B \Delta M}$ in a human fibrosarcoma cell line have reported 'leaky expression' of TRF2$^{\Delta B \Delta M}$, based on immunofluorescence analysis. A fraction of the induced cells, which did not show morphological alterations consistent with senescence and no expression of SA-β Gal, coincidently expressed very low levels of TRF2$^{\Delta B \Delta M}$. This difference was apparently subtle enough not to be noticed by Western blot analysis. Later, in normal human keratinocytes, it was observed that although expression levels of TRF2$^{\Delta B \Delta M}$ are high initially they decrease over time with some colonies being able to reverse the phenotype by down-regulating TRF2$^{\Delta B \Delta M}$ expression and resuming proliferation (Minty *et al*, 2008). It is worth mentioning that in the last study cells were not subjected to selective pressure. I have conducted a time point study and observed a gradual decrease in protein levels of TRF2$^{\Delta B \Delta M}$ in keratinocytes maintained under selective pressure, with maximum levels 5 days following expression of the transgene and minimum at day 13, when the experiment was terminated (Fig. 5.10).
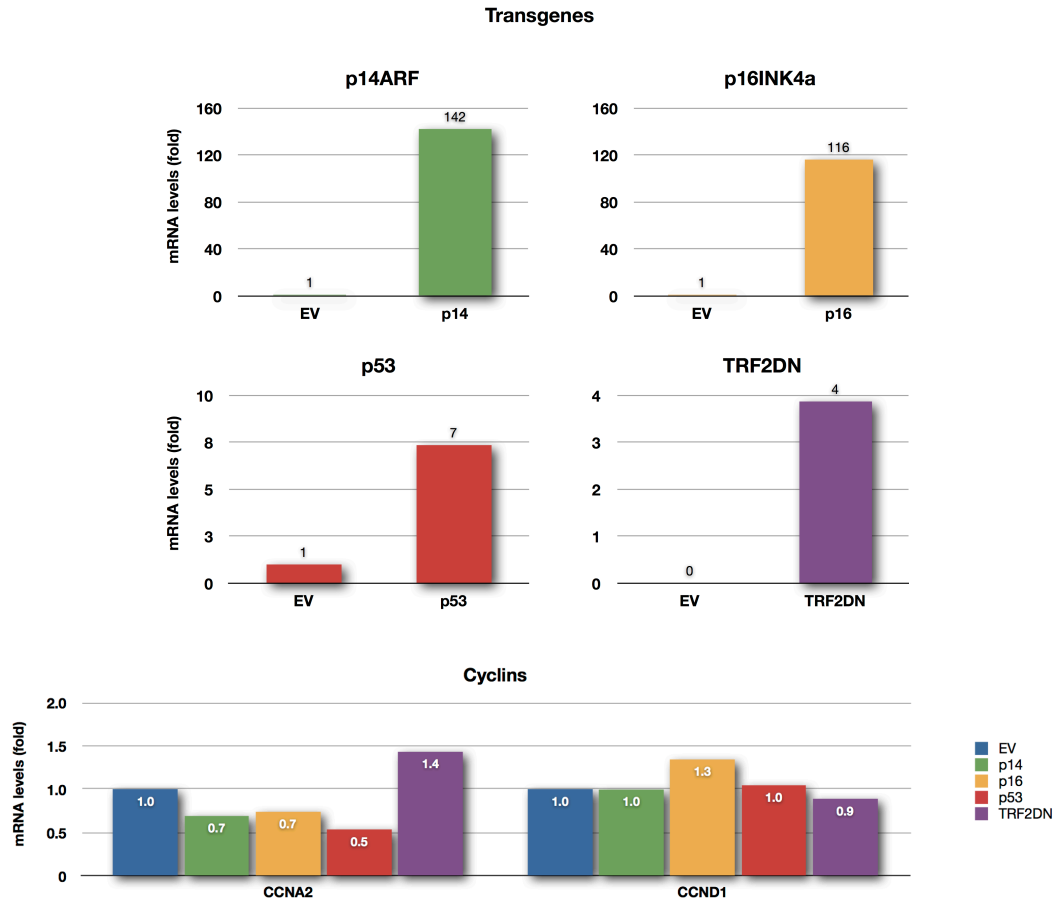
Figure 5.9. Gene expression levels of transgenes and Cyclins in NHEK transduced via an indirect strategy of infection. Graphs represent transcript levels of transgenes p14[ARF], p16[INK4a], p53 and TRF2$^{\Delta B \Delta M}$ as well as cyclins A2 (CCNA2) and D1 (CCND1) in keratinocytes ectopically expressing empty vector control (EV), p14[ARF], p16[INK4a], p53 and TRF2$^{\Delta B \Delta M}$. Values are normalised against the respective empty vector control (n=1).
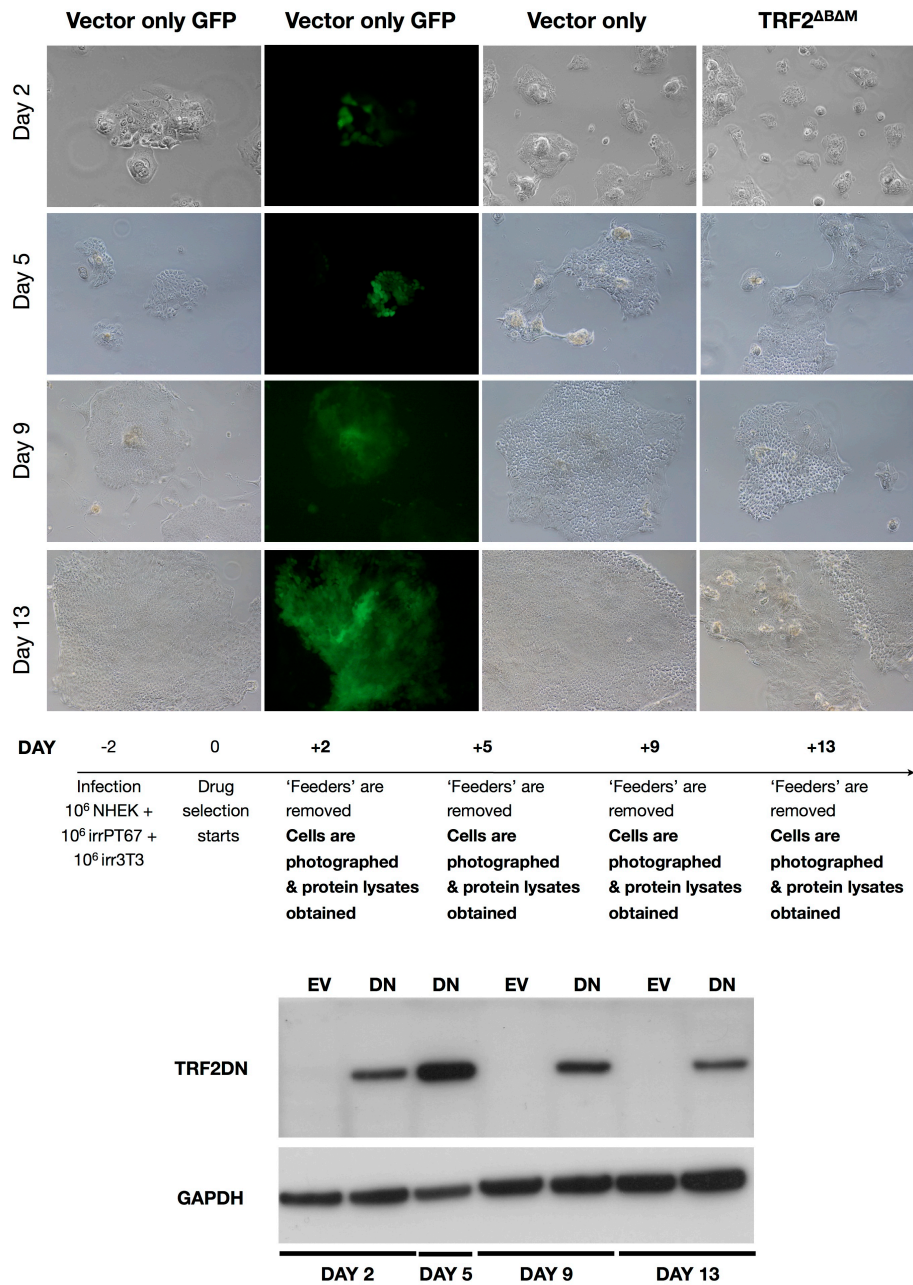
Figure 5.10. Time point analysis of TRF2$^{\Delta B \Delta M}$ expression levels in NHEK following retroviral transduction. Phase contrast images of NHEK colonies (top panel) expressing GFP-flagged empty vector control plus empty vector control (EV) and TRF2$^{\Delta B \Delta M}$ (DN). EV and DN share the same vector backbone. GFP-flagged EV was included to assess transduction efficiency. Early passage NHEKs (around 10 MPD) were co-cultured with infectious PT67 packaging cells and 'feeders', and drug selected with puromycin 48h later for a total culture time of 13 days (diagram of experimental design). Photos were taken at 100x magnification after removing 'feeders'. Protein lysates were collected at day 2, 5, 9 and 13 for western blot analysis (bottom panel).

These levels of expression, however, were not sufficient to elicit a phenotype. This suggests that expression levels of TRF2$^{\Delta B \Delta M}$ need to surpass a certain threshold to be capable of inducing senescence and that ideal time for analysis is 5 days following transduction, when expression is at its peak and before cells start down-regulating it. I reasoned that the process of transfection of TRF2$^{\Delta B \Delta M}$ into Phoenix cells was the root of the problem, generating lower titre viral supernatants. Original protocols include drug selection on the transfected Phoenix cells in order to maximise viral titre. If this can possibly be advantageous in the case of constructs carrying transgenes that are somehow beneficial to the target cells, this is not the case with TRF2$^{\Delta B \Delta M}$. I have indeed observed that both p53 and TRF2$^{\Delta B \Delta M}$ have a harmful effect on the producer Phoenix cells following prolonged periods of drug selection. The combination of the transgenes and the selective pressure acts as a hindrance. I therefore thought that by optimising transfection and using the Phoenix system as the transient system it is and by collecting concentrated viral supernatants as early as 48h up to 76h post-transfection with no drug selection on the producer cells, viral titre might actually be improved, especially in the case of the TRF2$^{\Delta B \Delta M}$ construct. In addition, by eliminating the second producer line and generating amphotropic virus from Phoenix A which could infect NHEK directly, I might prevent a 'dilution' effect in the expression of TRF2$^{\Delta B \Delta M}$. Direct strategies for infection of normal epidermal keratinocytes have been reported to have poor success rates ((Minty, 2007) and discussed in (Levy *et al*, 1998)). Nevertheless, as in the case of Levy *et al*'s (Levy *et al*, 1998) attempt to achieve long-term expression of the integrin gene in keratinocytes, I thought it was just a question of optimising the steps towards obtaining the maximum expression of deleterious genes in a short time frame.

5.2.3. Direct strategy for infection of keratinocytes (via amphotropic virus)

Since the aim was to obtain good quality amphotropic virus to infect NHEK directly, Phoenix A cells were transfected based on Roche's Fugene6 original manufacturer protocol for maximum efficiency. Also, volume of growth medium was reduced prior to overnight incubation at 32°C so that

concentrated viral supernatants could be obtained 48-78 hours post-transfection, thereby eliminating the drug selection step on the transfected Phoenix cells. Due to technical limitations (heated centrifuge only holds 6-well plates) experimental design for the subsequent infection had to change to be adapted to 6-well plates; NHEK seeding density was optimised for infection in wells (5×10^4 NHEK + 1.6×10^5 irr3T3 per well) as well as the concentration of puromycin (kill curve revealed 2.0 µg/mL was ideal). In order to obtain enough cells for analysis, each construct was expressed in a total of 12 wells (2 plates per construct) per experiment, which should yield around 0.5 Million transduced senescent NHEK at the end of the experiment.

The main advantage of co-culture with infectious 'feeders' in the previous indirect strategy is the close contact between these and the NHEK which maximises exposure of the latter to the viral particles for a period of 48h. In this new direct strategy, infection is performed by centrifugation at 350 rpm for 1 hour at 32°C so, although both centrifugation and temperature maximise viral uptake, contact time with the virus is a lot shorter. Therefore, I thought that by subjecting keratinocytes to more than one round of spinfection with freshly collected supernatants I might be able to increase infection efficiency. Supernatants have the highest viral titre 48h to 72h after transfection and can be collected every 6 hours. I thus compared infection rates between one or several rounds of infection (up to 3 rounds) using EV-GFP supernatants collected at 48h, 54h and 72h (Fig. 5.11). One round of infection resulted in up to 50% of cells expressing GFP, per colony; colonies showing close to 100% fluorescence were rare. With two or three rounds of infection however, infection rates were higher with more than half of the cells per colony expressing GFP; several colonies showed close to 100% fluorescence and colonies with no GFP signal were the exception.
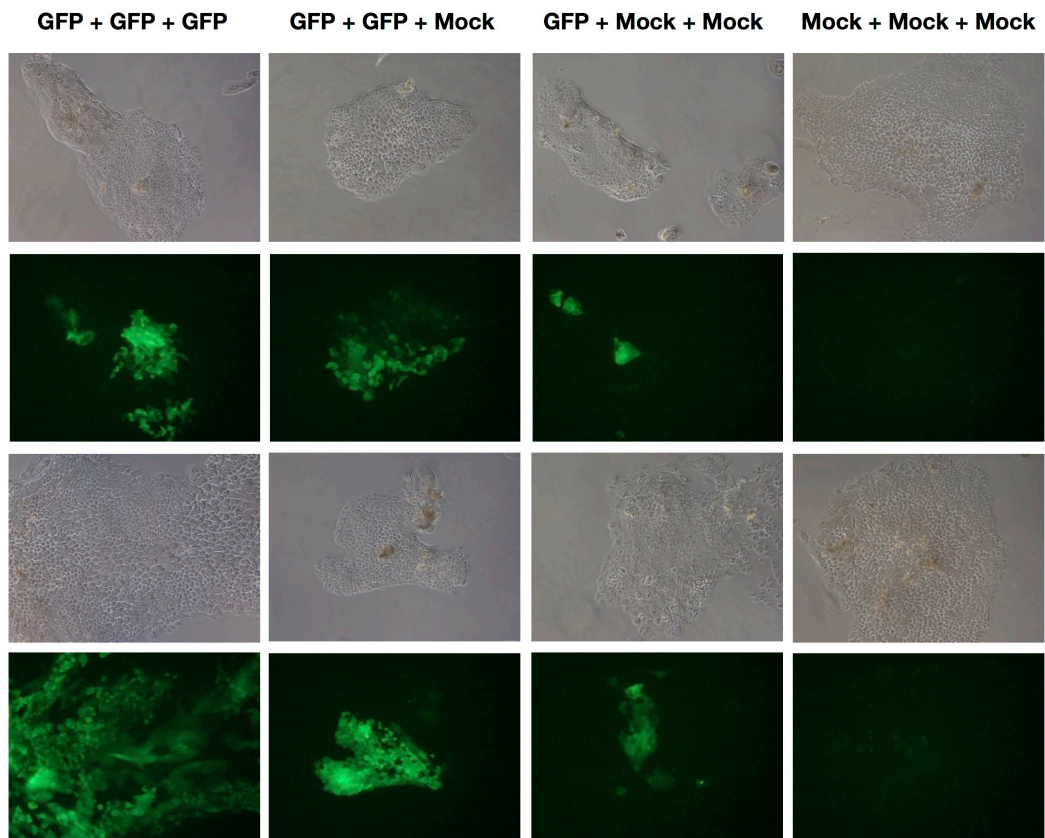
Figure 5.11. Assessment of NHEK transduction efficiency following one or more rounds of infection. Phase contrast images of NHEK colonies ectopically expressing GFP-flagged empty vector following 1 (GFP + Mock + Mock), 2 (GFP + GFP + Mock) or 3 (GFP + GFP + GFP) rounds of infection. Control mock infections were performed using the same procedure but without viral supernatants. Early passage NHEKs (around 10 MPD) were infected with retroviral supernatants using spinfection and cultured for a total of 8 days, without drug selection. Photos were taken 8 days after the first infection, at 100x magnification, after removing 'feeders'.

Since there was no apparent difference between using two or three rounds of infection, I opted for adapting the infection protocol to two successive infections with a 6 hour interval between them. Using 2 rounds also has the advantage of not depriving the keratinocytes of 'feeders' for a period longer than 8 hours, whilst 3 rounds are likely to cause stress to the target cells by being without 'feeders' for period of 24h. Prior to spinfection NHEK cultures were prepared by removing 'feeders' to promote contact of the virus with the keratinocytes. Additionally, plates were gassed, at 32ºC, until a 10% CO_2 atmosphere was obtained and immediately sealed to ensure these conditions were maintained during spinfection to prevent culture stress. Following infection, NHEK were allowed a gene expression time of 24h after which drug selection was introduced (2 µg/mL puromycin) and cell extracts collected 5 days later. This method was extended to all constructs and proved to be very successful for all, especially $TRF2^{\Delta B \Delta M}$ (Fig. 5.12 diagram of experimental design).

In general, five days following expression of the transgenes, the number of cells obtained expressing $p14^{ARF}$, $p16^{INK4a}$, p53 or $TRF2^{\Delta B \Delta M}$ was about half of the number obtained for the respective empty vector control (Fig. 5.12 graph). This observation, combined with the senescent appearance of the NHEK colonies suggests proliferation arrest (Fig. 5.12 photos).

Quantitative PCR analysis confirmed over-expression of all transgenes in all NHEK populations (Fig. 5.13). It is well established that CCNA2 levels decline in senescent fibroblasts and CCND1 levels increase (Dulić *et al*, 1993) and expression array data suggests that this is true for keratinocytes also (Hunter *et al*, 2006). Analysis also revealed a decrease in CCNA2 transcript levels, sometimes accompanied by increase in CCND1, when compared to the respective empty vector control, which is consistent with senescence (Fig. 5.14).
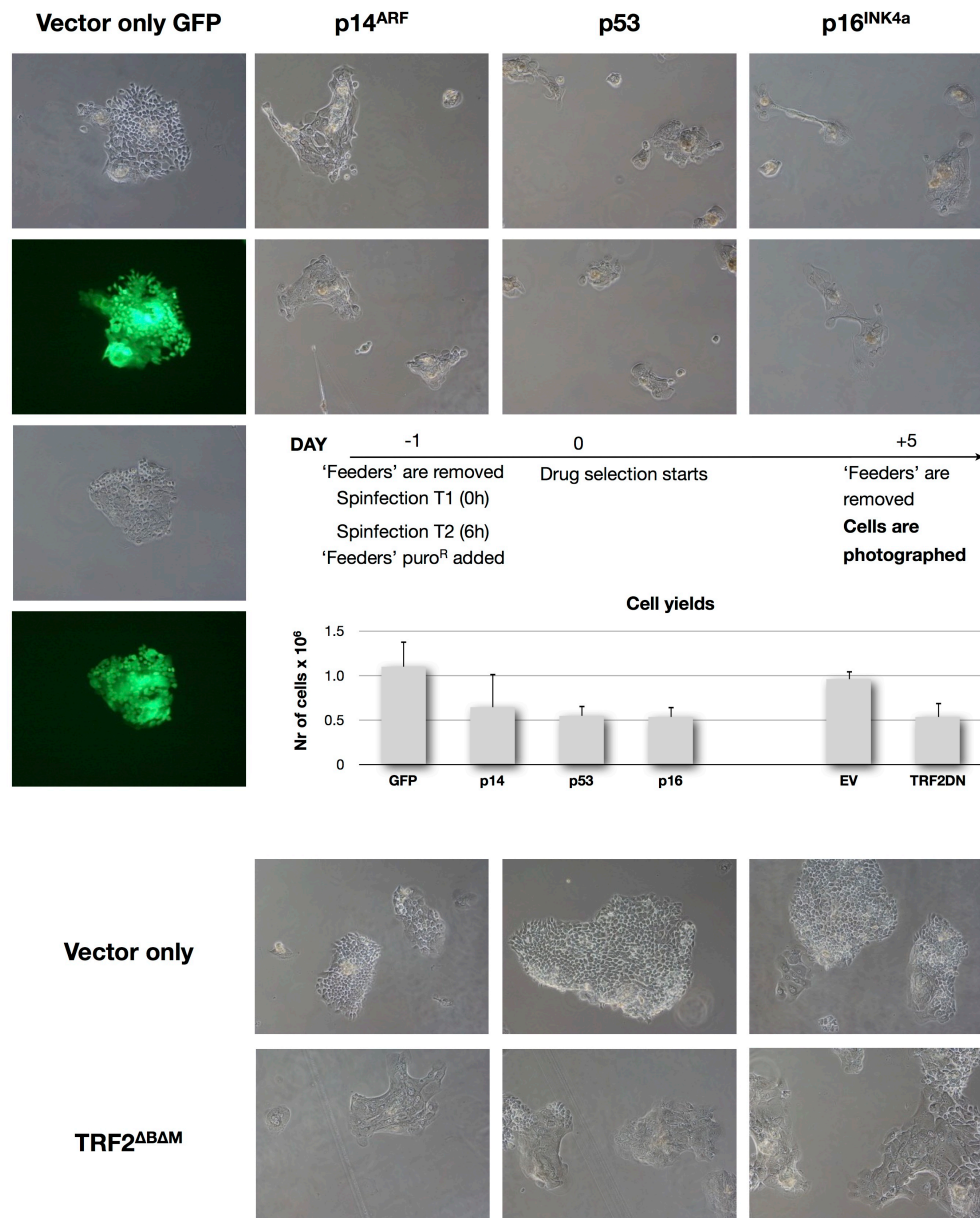
Figure 5.12. NHEK transduced with all transgenes via a direct strategy of infection. Phase contrast images of NHEK colonies ectopically expressing GFP-flagged empty vector control, $p14^{ARF}$, p53 and $p16^{INK4a}$ (columns); empty vector control and $TRF2^{\Delta B \Delta M}$ (rows), at day 5. Early passage NHEKs (around 10 MPD) were infected with retroviral supernatants using spinfection, and drug selected with puromycin 24h later for a total culture time of 5 days (diagram of experimental design). Graphs represent the number of cells obtained on day 5 for each experimental group (n = 2; bars show st dev). Photos were taken at 100x magnification after removing 'feeders'.
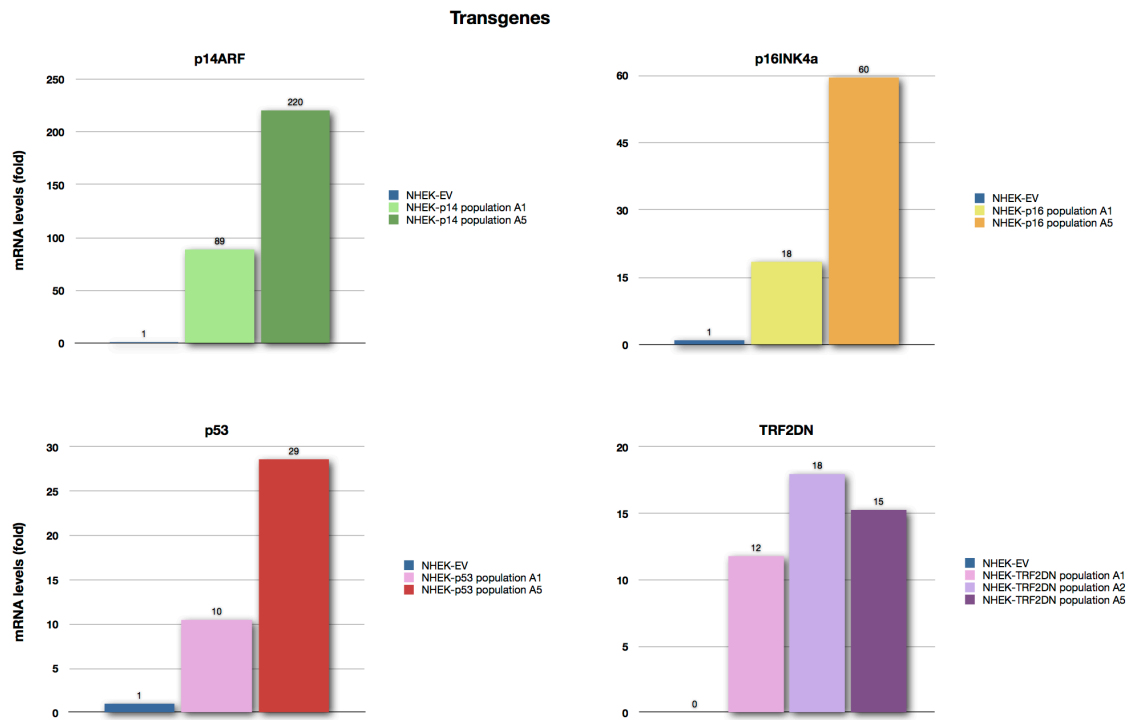
Figure 5.13. Gene expression levels of transgenes in NHEK transduced via a direct strategy of infection. Graphs represent transcript levels of transgenes p14^{ARF}, p16^{INK4a}, p53 and TRF2$^{\Delta B \Delta M}$ in populations of keratinocytes ectopically expressing empty vector control (EV), p14^{ARF}, p16^{INK4a}, p53 and TRF2$^{\Delta B \Delta M}$. Values are normalised against the respective empty vector control.
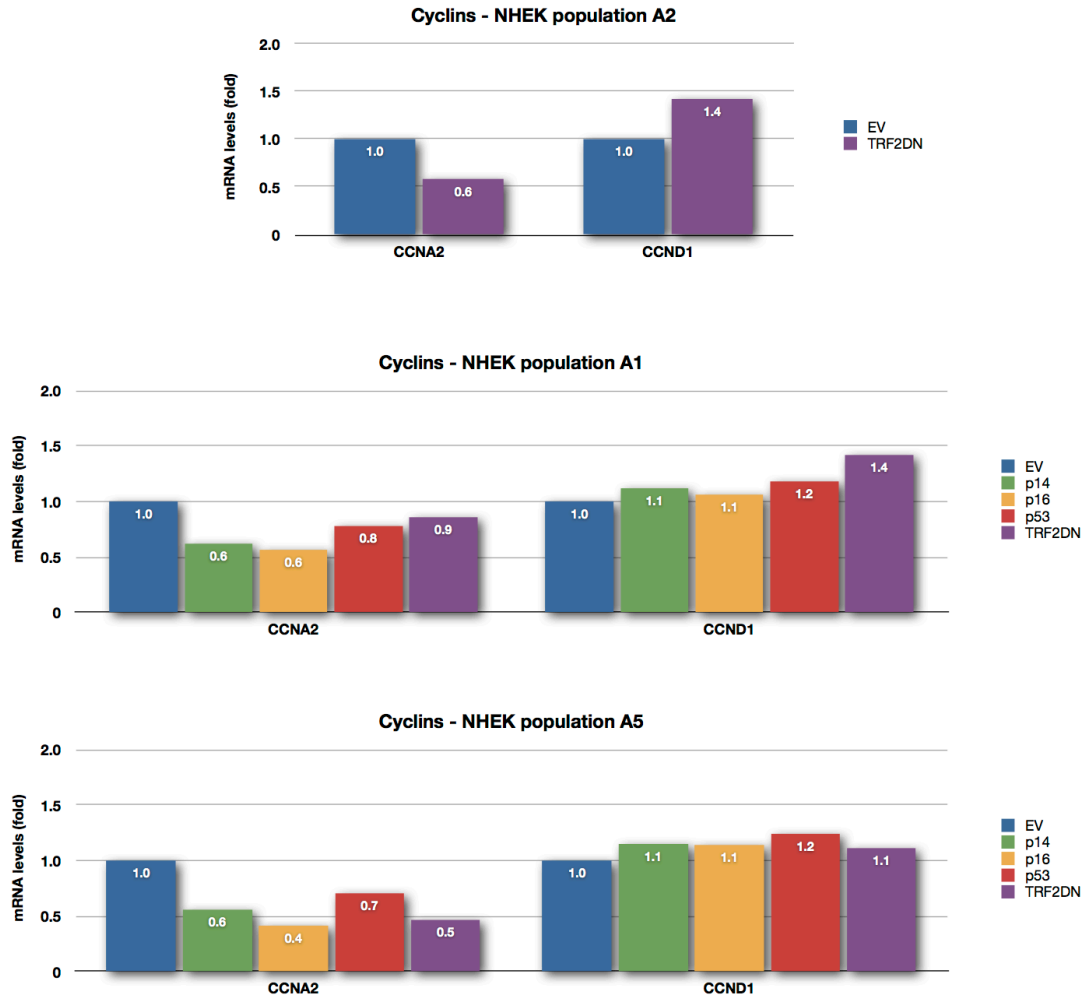
Figure 5.14. Gene expression levels of cyclins in NHEK transduced via a direct strategy of infection. Graphs represent transcript levels of cyclins A2 (CCNA2) and D1 (CCND1) in populations of keratinocytes ectopically expressing empty vector control (EV), p14^{ARF}, p16^{INK4a}, p53 and TRF2$^{\Delta B \Delta M}$. Values are normalised against the respective empty vector control.

In the conditions tested, an overview of the two strategies for transduction of keratinocytes showed that a direct strategy for infection was generally more effective than an indirect one (Tables 15 and 16).

	LOW	MEDIUM	HIGH
TRF2$^{\Delta B\Delta M}$	A1 (12-fold)	A5 (15-fold)	A2 (18-fold)
p14^{ARF}	A1 (89-fold)	EA (142-fold)	A5 (220-fold)
p16^{INK4a}	A1 (18-fold)	A5 (60-fold)	EA (116-fold)
p53	A1 (10-fold)	EA (7-fold)	A5 (29-fold)

Table 15. Summary of levels of expression (LOW, MEDIUM or HIGH) of p14^{ARF}, p16^{INK4a}, p53 and TRF2$^{\Delta B\Delta M}$ in NHEK populations expressing the transgenes, obtained via a direct strategy (A1, A2 and A5) and via an indirect strategy of infection (EA). Legend: A = amphotropic; EA = ecotropic/amphotropic.

	LOW	MEDIUM	HIGH
TRF2$^{\Delta B\Delta M}$	-/40% (12-fold)	50%/- (15-fold)	40%/40% (18-fold)
p14^{ARF}	40%/- (89-fold)	30%/- (142-fold)	40%/- (220-fold)
p16^{INK4a}	40%/- (18-fold)	60%/- (60-fold)	30%/30% (116-fold)
p53	20%/20% (10-fold)	50%/- (7-fold)	30%/20% (29-fold)
	↓**CCNA2/CCND1**↑	↓**CCNA2/CCND1**↑	↓**CCNA2/CCND1**↑

Table 16. Summary of induction levels of cyclins CCNA2 and CCND1 in NHEK populations expressing LOW, MEDIUM or HIGH levels of p14^{ARF}, p16^{INK4a}, p53 and TRF2$^{\Delta B\Delta M}$.

This was the case especially for TRF2$^{\Delta B\Delta M}$ as effective expression levels of the construct, high enough to engage senescence, were only obtained with the direct infection strategy. Out of the 3 NHEK populations obtained, A1 resulted in the lowest expression level of TRF2$^{\Delta B\Delta M}$ (12-fold), still higher than the previous 4-fold in NHEKs infected with an indirect strategy. A1 keratinocytes down-regulated CCNA2 by 10% and up-regulated CCND1 by 40%, whilst in EA keratinocytes CCNA2 was up-regulated and CCND1 remained at control levels which indicates proliferation rather than arrest. In NHEK populations A2 and A5 higher levels of expression, 15-fold and 18-fold respectively, were obtained resulting in a 40-50% down-regulation of CCNA2, accompanied by 40% increase in CCND1 for A5.

For all the other transgenes two additional NHEK populations were obtained, using the direct infection strategy. A5 resulted in the highest expression levels for p14^{ARF} and p53, while A1 resulted in the lowest. Despite this, in all cases a reduction in CCNA2 was observed, accompanied by elevation of CCND1 in the case of p53 when expressed at the highest levels. As for p14^{ARF} it was interesting to notice that a consistent 30-40% down-regulation of CCNA2 occurred despite the level of expression of this transgene in keratinocytes; it is worth noticing that these vary from 89-fold to 220-fold.

As for p16^{INK4a}, this transgene constitutes the exception with the highest expression levels achieved with the indirect infection strategy which rendered a 116-fold elevation of its transcript, followed by 30% decrease in CCNA2 and increase in CCND1. However, in A1 and A2 keratinocytes p16^{INK4a} was still induced by 18-fold and 59-fold accompanied by a convincing 40-50% decrease in CCNA2 transcript, which is consistent with senescence.

In conclusion, I found that generally the highest the expression level obtained for the transgene the most profound was the influence on the cyclins, with more effective induction of senescence. As I found there was intra- and inter-experimental variation in expression, as a consequence of experimental variation or infection strategy used, populations of transduced keratinocytes were not pooled. Instead they were analysed individually based on LOW, MEDIUM, or HIGH expression levels of each effector of senescence.

5.3. Discussion

I have been trying to investigate the specificity of candidate markers HOPX, HIST2H2BE, ICEBERG and S100A7 to telomere-dysfunction induced senescence (TDIS). Although they are all induced telomere dysfunction and seem to be regulated by telomerase (Muntoni *et al*, 2003; Minty *et al*, 2008), HOPX, ICEBERG and S100A7 are not elevated as a result of p53 activation and ensuing DDR following exposure to senescence-inducing doses of IR (Chapter 4). I cannot however exclude possible induction of the markers by other forms of activation of p53, or by other main effectors of senescence, such as p14^{ARF} and p16^{INK4a}. The latter is particularly important as premature senescence by induction of p16^{INK4a}, also known as 'stress or aberrant signalling-induced senescence' (STASIS), is the main competitor mechanism to replicative senescence via telomere shortening or TDIS in cultured keratinocytes (Rheinwald *et al*, 2002). Therefore, to further investigate the effect of activation of the main pathways of senescence in the candidate markers, I aimed to use retroviral transduction for establishing stable populations of keratinocytes ectopically over-expressing p53 (Sugrue *et al*, 1997), p16^{INK4a} (McConnell *et al*, 1998), p14^{ARF} (Dimri *et al*, 2000) or the dominant negative mutant form of the telomere-binding protein TRF2 (TRF2$^{\Delta B \Delta M}$) to artificially uncap telomeres (van Steensel *et al*, 1998).

Given the challenge that normal keratinocytes present as target cells for gene delivery I based my experimental approach on a successful indirect strategy for infection, which has previously been reported for these cells (Levy *et al*, 1998). Briefly, it is based first on the production of ectropic retroviral particles which are used to infect an amphotropic packaging cell line thereby stably expressing the transgene of interest. The latter is then used as a 'feeder' layer to infect normal keratinocytes which become stably transduced following selective pressure. Our group has previously adopted this approach to fluorescence-activated cell sorting (FACS) as a means of selection of transduced cells by cloning the original retroviral vector (expressing TRF2$^{\Delta B \Delta M}$ in this case) into an IRES vector expressing a GFP tag (Minty, 2007; Minty *et al*, 2008). Despite the good expression levels, which resulted in a senescent-like phenotype from expression of the transgene, the process of cell sorting was a cause of undue stress to the cells and presented other limitations. I have,

therefore, opted for using the original retroviral vectors, pBabe-puro for expression of p53, p16^{INK4a} and p14^{ARF} or pLPC-NMYC-puro for expression of TRF2$^{\Delta B \Delta M}$, given their reported efficiency and low toxicity of the drug selection agent in normal human epidermal keratinocytes (Levy *et al*, 1998).

Nevertheless, I found that the transduction efficiency using the previous strategy was greatly influenced by the transgene being expressed. Despite being effective for the empty vector construct expressing solely the GFP tag and for p16^{INK4a}, the strategy rendered low levels of expression for p14^{ARF}, p53 and particularly for TRF2$^{\Delta B \Delta M}$. I found that p14^{ARF}, p53 and TRF2$^{\Delta B \Delta M}$ all affected the performance of the first packaging line (Phoenix), especially if this was also subjected to drug selection. Also, that the use of a second producer line had a sort of 'diluting' effect in the expression of TRF2$^{\Delta B \Delta M}$ which was probably made worse by the longer time required for drug selection when compared with sorting by FACS. Whichever the explanation(s), by the time keratinocytes were transduced, the levels of expression obtained for TRF2$^{\Delta B \Delta M}$ were not high enough to induce a senescent-like arrest, using this strategy. Since this is an exogenous dominant negative mutant which depletes telomeres of its endogenous functional TRF2, it is not surprising that it would be selected against by the cells and in fact TRF2$^{\Delta B \Delta M}$'s expression has been characterised as 'leaky' (van Steensel *et al*, 1998). I found that in order to elicit senescence a certain threshold level of expression needed to be surpassed and this is consistent with the findings of others (J. Jacobs - personal communication). The emergence of revertant keratinocyte colonies following down-regulation of TRF2$^{\Delta B \Delta M}$ expression levels has also previously been reported (Minty *et al*, 2008).

Given the previous observations I went back to basics and decided to challenge the pre-conception that normal human keratinocytes are difficult cells to transduce directly. Since the nature of the transgenes, especially TRF2$^{\Delta B \Delta M}$, required a straightforward approach with as few intermediate steps as possible I have decided to use the highly efficient and latest generation Phoenix system to produce amphotropic viral particles without drug selection for optimum titre 2 to 3 days following transfection. These were then used to directly infect keratinocytes in two consecutive rounds of infection, performed on the same day (6 hours apart) with an optimised low speed centrifugation method, in order to promote viral uptake thereby hopefully increasing infection rates and maximising expression levels of the constructs. Selective pressure was also introduced earlier in order to prevent unwanted variants to take over the

culture, especially cells which might have lost the transgene whilst still retaining the puromycin cassette, and to obtain levels of expression of the constructs high enough to generate a phenotype in five days time. This was a limitation I needed to account for, considering my general experimental approach when compared with the superior expression system consisting of an IRES vector combined with FACS sorting, previously used by our lab (Minty *et al*, 2008). I found that this direct strategy of infection was the only successful method capable of generating a senescent-like phenotype following the expression of TRF2$^{\Delta B\Delta M}$, as demonstrated by decrease in Cyclin A2 transcript and colony-forming efficiency analysis. Overall, this approach generated the highest expression levels of the constructs (with the exception of p16^{INK4a}), despite some inter-experimental variation, which in turn was associated with a stronger phenotype (exception for p14^{ARF}).

From a technical point of view, these manipulations were extremely challenging and given the limitations of working with both normal keratinocytes and transgenes which halt proliferation and induce deleterious effects on the cells one would have to agree with others (Levy *et al*, 1998) in thinking that an inducible system applied to keratinocytes is much warranted and long overdue. Despite the challenges, the optimisation of both infection strategies towards obtaining a low stress system for retroviral transduction of NHEK allowed me to obtain populations of keratinocytes expressing defined levels (divided into low, medium or high) of the inducers of senescence p14^{ARF}, p16^{INK4a}, p53 and TRF2$^{\Delta B\Delta M}$. These senescent populations will serve as models in the assessment of the effect that activation of the various cellular pathways of senescence might have on the candidate markers for keratinocyte TDIS (Chapter 6).

Chapter 6. Analysis of markers specificity to other forms of senescence.

6.1. Introduction

6.1.1. Pathways of senescence

p53 and pRb are the main effectors of senescence and are activated through independent, although also interacting, molecular pathways (Fig. 6.1). These are selectively or mutually induced by various stimuli and the engagement of each pathway can be both cell type-specific and species-specific. Intrinsic and extrinsic stimuli act simultaneously in a population of normal growing cells thereby resulting in a mosaic effect where the senescence program is being engaged by distinct pathways in different cells (Ben-Porath & Weinberg, 2005; Campisi & d'Adda di Fagagna, 2007).
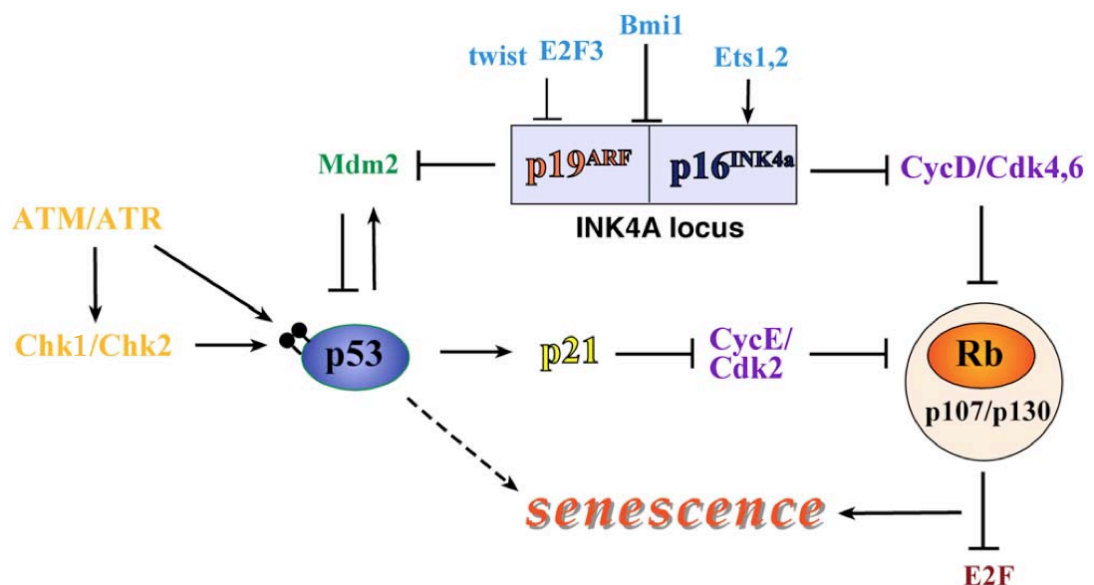
Figure 6.1. Molecular pathways of senescence. p53 and pRb are the central effectors of senescence (adapted from (Ben-Porath & Weinberg, 2005)).

The p53/p21^WAF1 pathway

p53 mediates the response to DNA damage, telomere dysfunction and oxidative stress (Fig. 6.2). As discussed previously (Chapter 4) p53 is the central protein in the classical DNA damage pathway of senescence activated by stimuli that generate a DDR (Ben-Porath & Weinberg, 2005). In consequence of exposure to DNA damaging agents such as ionising radiation (Di Leonardo *et al*, 1994), DNA strand breaking chemicals (Robles & Adami, 1998) or endogenous insults such as dysfunctional telomeres (d'Adda di Fagagna *et al*, 2003; Takai *et al*, 2003; Herbig *et al*, 2004) and ROS (Moiseeva *et al*, 2006), normal human fibroblasts activate ATM/ATR and CHK2/CHK1. These are the upstream regulators of p53 that transmit the DNA damage signal and mediate the post-translational activation of p53 through phosphorylation, mainly at the Serine 15 site (p53-pS15). p53 then triggers several downstream transcriptional targets of which p21^WAF1 is the most pivotal, acting as the principal mediator of p53-dependent senescence (Di Leonardo *et al*, 1994; Brown *et al*, 1997).

p21^WAF1 is, along with p16^INK4a, a cyclin-dependent kinase inhibitor (CDKI). However, as opposed to p16^INK4a, it interacts with a range of CDK/Cyclin complexes, therefore acting as an important regulator of the cell cycle. For instance, by inhibiting CDK2 activity and thus disrupting CDK2/Cyclin E complexes, it suppresses phosphorylation of pRb and, therefore, its inactivation. In its hypo-phosphorylated form, pRb is active and enforces senescence by inhibiting the transcription of E2F1 target genes, required for cell-cycle progression (Ben-Porath & Weinberg, 2005; Campisi & d'Adda di Fagagna, 2007). The p53-p21^WAF1-pRb pathway can be triggered by oxidative stress (Itahana *et al*, 2003) and in consequence of chronic stimulation of the anti-proliferative cytokines such as Interferon β, which acts by increasing intracellular ROS (Moiseeva *et al*, 2006). Although p53 can activate senescence by triggering the parallel RB pathway through p21^WAF1 (Fig. 6.2), p53/p21^WAF1 alone can induce senescence independently from the RB family primarily by interfering with CDK2/Cyclin A complexes (Smogorzewska & de Lange, 2002). However, cells that senesce exclusively via p53/p21^WAF1 can resume growth following inactivation of the p53 pathway but eventually arrest with characteristics of crisis (Beauséjour *et al*, 2003).
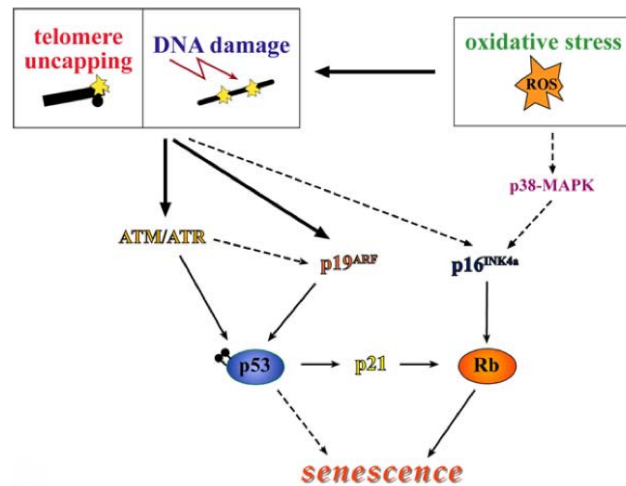
Figure 6.2. Endogenous stimuli that engage p53. In human cells, telomere uncapping and general DNA damage activate primarily p53, via the ATM/ATR kinases, and secondarily p16^{INK4a}. Oxidative stress can result in damage to DNA and accelerate telomere shortening, triggering p53, but can also activate p16^{INK4a} via p38-MAPK. In the mouse, these stimuli preferentially activate p53 via ARF (*in* (Ben-Porath & Weinberg, 2005)).

The nature of p53 activation/stabilisation depends on the triggering stimuli. Replicative senescence and DNA damaging agents, such as IR, UV and bleomycin, activate the p53 pathway via post-translational modifications in p53 (Webley *et al*, 2000; Minty *et al*, 2008). Although phosphorylation at Serine 15 also contributes to stabilisation of p53 by disruption of MDM-2 binding (Shieh *et al*, 1997), not a significant increase in total p53 was observed in NHFs following senescence or exposure to any of these DNA damaging agents (Webley *et al*, 2000) or in NHEKs subjected to IR (Minty *et al*, 2008). Over-expression of wild-type p53 (in p53-deficient cells) however, engages the pathway essentially via stabilisation of the molecule with ensuing increase in p21^{WAF1} and MDM-2 expression levels (Sugrue *et al*, 1997). MDM-2 (also known as HDM-2 to distinguish from the murine homologue mdm-2) is an E3 ubiquitin ligase whose function is to functionally inactivate p53 by promoting its proteolytic degradation in the nucleolus. Upon senescence, p53 activation/stabilisation induces MDM-2 which, in turn, negatively regulates p53 expression (Dimri *et al*, 2000; Ben-Porath & Weinberg, 2005).

Whilst in human cells general damage to the DNA is detected and signalled through upstream kinases ATM/ATR, other physiological stressors are signalled to p53 by its other upstream regulator ARF.

The p14/p53 pathway

ARF (p14^{ARF} in humans and p19^{arf} in mice) regulates the stress-dependent pathway that activates p53 (Fig. 6.3) and plays a central role in response to physiological stressors in mouse cells. It is up-regulated in rodent fibroblasts (Kamijo *et al*, 1997) and in human fibroblasts (Dimri *et al*, 2000) upon senescence. In contrast, p14^{ARF} does not seem to be involved in keratinocyte senescence (Munro *et al*, 1999). p14^{ARF} is also activated by ectopic expression of oncoproteins such as activated MYC, RAS and RAF, and by supra-physiological mitogenic signals such as E2F1 and E1A (Serrano *et al*, 1997; Dimri *et al*, 2000; Itahana *et al*, 2001). Phosphorylation of p53 following DNA damage caused by IR does not involve ARF but apparently ARF also contributes to p53 stabilisation in these situations (Ben-Porath & Weinberg, 2005).

ARF stabilises p53 and directs its accumulation by sequestering the E3 ubiquitin ligase MDM-2 in the nucleolus (Fig. 6.1), therefore preventing p53 from being targeted for proteolytic degradation (Sherr, 1998; Stott *et al*, 1998; Dimri *et al*, 2000). Over-expression of p14^{ARF} in normal human fibroblasts results in elevation of p53 total protein to levels higher than those found in replicatively senescent cells; this is followed by an increase in p21^{WAF1} protein levels (Dimri *et al*, 2000). Expression of oncogenic RAS in normal human cells also results in stabilisation of p53 and premature senescence (Serrano *et al*, 1997).

Several molecules act as regulators of p14^{ARF} (Fig. 6.1). Transcription factor E2F1, which regulates cell cycle progression by either trans-activating target genes needed for DNA synthesis or by binding the active form of pRb, Cyclin A and MDM-2, is also an activator of p14^{ARF} (Dimri *et al*, 2000). E2F3 and Twist, on the other hand, act as repressors of the p14^{ARF} protein (Ben-Porath & Weinberg, 2005). The *INK4a* locus, which encodes for both p14^{ARF} and p16^{INK4a}, is controlled by upstream regulators such as Bmi-1, a member of the Polycomb family (Itahana *et al*, 2003) and CBX7 (Gil *et al*, 2004) which repress both products and are down-regulated at senescence.
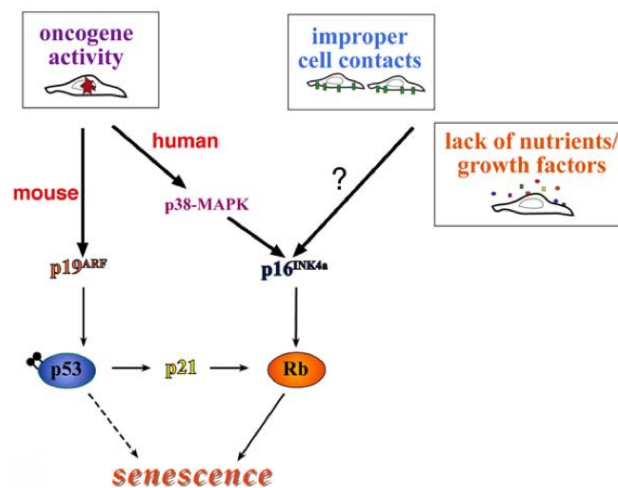
Figure 6.3. Endogenous and exogenous stimuli that activate products of the *INK4a* locus, p14^ARF and p16^INK4a. In mice, ARF regulates the stress-dependent pathway which activates p53, however in humans this role is taken primarily by p16^INK4a with activation of pRb (*in* (Ben-Porath & Weinberg, 2005)).

The p16^INK4a/pRb pathway

The p16^INK4a/pRb pathway acts in parallel to the p53 pathway and seems to have a redundant role as it responds to all the stresses that activate p53 but to a lesser extent. For instance, following DNA damage (Di Leonardo *et al*, 1994) and telomere damage (d'Adda di Fagagna *et al*, 2003; Herbig *et al*, 2004) senescence is mediated by p53 and usually accompanied by expression of p21^WAF1. However, both DNA damage and dysfunctional telomeres can also induce p16^INK4a (Fig. 6.2), although with delayed kinetics (Robles & Adami, 1998; Stein *et al*, 1999; Smogorzewska *et al*, 2002; Jacobs & de Lange, 2004). The p16^INK4a/pRb pathway seems to act as a second barrier to proliferation of cells with severe DNA damage that are at risk of undergoing malignant transformation and is, therefore, redundant to the p53 pathway (Bartkova *et al*, 2005; Gorgoulis *et al*, 2005). It is, however, the pathway of choice in response to stresses such as activated oncogenic or mitotic proteins, nutrient/growth factor deficiency, and improper cell-cell and cell-matrix contacts (Ben-Porath & Weinberg, 2005) (Fig. 6.3).

p16[INK4a] is, along with p21[WAF1], a CDKI and specifically inhibits the activity of cyclin-dependent kinases 4 and 6 (CDK4/CDK6), therefore inactivating complexes with Cyclin D. As a consequence, it suppresses the phosphorylation and inactivation of pRb allowing the latter to repress E2F transcriptional targets and halt cell cycle progression (Narita *et al*, 2003). Over-expression of p16[INK4a] in early passage human diploid fibroblasts induces premature senescence which is accompanied by accumulation of pRb in its hypo-phosphorylated form (McConnell *et al*, 1998). p16[INK4a] is selectively up-regulated in aged human skin (Ressler *et al*, 2006) and has a particularly important role in human keratinocyte senescence (Munro *et al*, 1999; Rheinwald *et al*, 2002). However, it is unclear whether p16[INK4a] operates independently of the p14[ARF]/p53 pathway, as disruption of p16[INK4a] function alone does not result in a significant extension of NHEK replicative lifespan (Rheinwald *et al*, 2002; Haga *et al*, 2007). However, BMI-1, which inactivates p14[ARF] and p15[INK4b] in addition to p16[INK4a] (Jacobs *et al*, 1999) is much more effective in extending keratinocyte replicative lifespan than knock-down of p16[INK4a] alone (Maurelli *et al*, 2006; Haga *et al*, 2007).

p16[INK4a] is activated in situations of stress and is responsible for premature stress-induced senescence, also known as 'stress or aberrant signalling-induced senescence' or STASIS. In human epithelial cells (especially mammary epithelial and keratinocytes) p16[INK4a] spontaneously starts being expressed just with time in culture under standard conditions. This phenomenon, also known as cell culture stress or 'culture shock', can be delayed by using 'feeder' layers for culture growth, but cells will still undergo p16[INK4a]-dependent and telomere-dependent senescence later on (Ramirez *et al*, 2001; Rheinwald *et al*, 2002). However, the precise signals that activate p16[INK4a], independently of DSBs are unclear.

Oncogenes such as activated RAS and oxidative stress also induce p16[INK4a]-dependent senescence. In human cells, RAS activates p53 and p16[INK4a] in parallel, but p16[INK4a] has a more prominent role in oncogene-induced senescence (Serrano *et al*, 1997; Brookes *et al*, 2002), at least in the absence of DSBs. Oncogenic RAS can activate p16[INK4a] by phosphorylating and activating Ets transcription factors; p38-MAPK proteins mediate activation of both p53 and p16[INK4a] in RAS-induced senescence (Iwasa *et al*, 2003). Oxidative stress activates p16[INK4a] also through p38-MAPK in some cells (Forsyth *et al*, 2003), but in certain cell strains the p53/p21[WAF1] pathway is activated instead (Itahana *et al*, 2003). Oncogene-induced senescence in cancer precursor lesions such as

dysplastic nevi show a mosaic pattern of p16^{INK4a} expression, however associated with indicators of a DDR (Suram *et al*, 2012).

Additionally, expression of p16^{INK4a} has been shown to directly correlate with several markers of keratinocyte migration and to inversely correlate with genes involved in terminal differentiation (Darbro *et al*, 2005). Senescent keratinocytes *in vitro* expressing p16^{INK4a} often co-express the ɣ2 chain of laminin 5 and exhibit an increase in directional mobility (Natarajan *et al*, 2006). This has been associated with the early stages of invasion in SCCs and with the wound healing process in normal epithelia via generation of non-dividing motile cells (Natarajan *et al*, 2003). The inhibitor of epithelial cell proliferation TGF-β is one of the molecules known to be expressed in wounded epithelium and its chronic signalling is known to induce senescence by promoting p16^{INK4a}/pRb heterochromatin formation (Zhang & Cohen, 2004). Chromatin state is a regulator of p16^{INK4a}; treatment with histone deacetylase inhibitors (HDACIs) acts as a positive regulator (Munro *et al*, 2004) whilst chromatin remodelling gene Bmi-1 acts as a negative regulator (Itahana *et al*, 2003). Bmi-1 is down-regulated at senescence and its over-expression results in extension of the replicative lifespan of human fibroblasts via suppression of the p16^{INK4a}/pRb senescence pathway (Itahana *et al*, 2003).

p16^{INK4a}/pRb can establish self-maintaining senescence-associated heterochromatin which is thought to contribute to the irreversibility of the cell cycle arrest upon senescence (Funayama & Ishikawa, 2007). As opposed to what happens with the p53 pathway, cells that have engaged the p16^{INK4a}/pRb pathway for several days cannot resume growth despite ensuing inactivation of p16^{INK4a}, pRb or p53 (Itahana *et al*, 2003). Loss of p16^{INK4a}/pRb in human mammary epithelial cells alternatively engages the p14^{ARF} pathway partly because E2F also stimulates p14^{ARF} expression (Zhang *et al*, 2006). Up-regulation of p16^{INK4a} during senescence inhibits Cyclin D/CDK4/CDK6-mediated phosphorylation of pRb. In its active, hypo-phosphorylated form, pRb recruits heterochromatin-forming proteins to E2F target promoters resulting in distinct chromatin structures called senescence-associated heterochromatin foci (SAHF). This condensed chromatin state prevents E2F from accessing its promoters thereby silencing target genes, such as cyclin A (CCNA2), required for cell cycle progression (Narita *et al*, 2003).

6.1.2. Telomere dysfunction-induced senescence

Telomere shortening, as a consequence of cell division, is the molecular event thought to lie behind the phenomenon of replicative senescence. Due to the end-replication problem, cells lose around 100bp, out of the 15Kb reserve length of telomeric DNA, per population doubling (Harley *et al*, 1990; Bodnar *et al*, 1998). Replicative senescence is triggered by the shortest dysfunctional telomere as opposed to the average telomere length of a population of cells (Hemann *et al*, 2001). Telomere length analysis in fibroblasts (STELA) confirmed gradual telomere shortening consistent with losses through end-replication and close to total loss of telomeric repeats at senescence (Baird *et al*, 2003).

TRF2 is an essential telomeric protein responsible for inducing the protective t-loop conformation characteristic of the telomeric complex (de Lange, 2002). Over-expression of TRF2 accelerates telomere shortening yet delays the onset of senescence by allowing cells to proliferate beyond the normal senescence set-point of 6 to 7Kb (Karlseder *et al*, 2002). It is possible that a critically short telomere may no longer be able to bind enough TRF2 to acquire a protective capped state and thus will emit a dysfunctional signal that triggers senescence (Karlseder *et al*, 2002). Therefore, what makes a telomere dysfunctional is not the complete loss of telomeric DNA but rather its capped status (Blackburn, 2000).

Telomere-dependent senescence can be studied by growing normal cells in culture until they are 'old', i.e., have reached their replicative limit or by inducing prematurely dysfunctional telomeres in 'young' cells, i.e., that have undergone only a few divisions. TRF2 is, along with TRF1, a telomeric DNA-binding protein (Fig. 6.4). The normal TRF2 allele encodes for a sequence composed of an N-terminal basic domain, in contrast with the acidic motif found in TRF1; a dimerisation area that allows binding of other TRF2 molecules to form functional homo-dimers as well as binding of accessory proteins (Rap1, TIN2 and TPP1); and, finally, a characteristic C-terminal Myb domain, similar to the one found in TRF1, strictly required for binding telomeric DNA (reviewed in (de Lange, 2005).
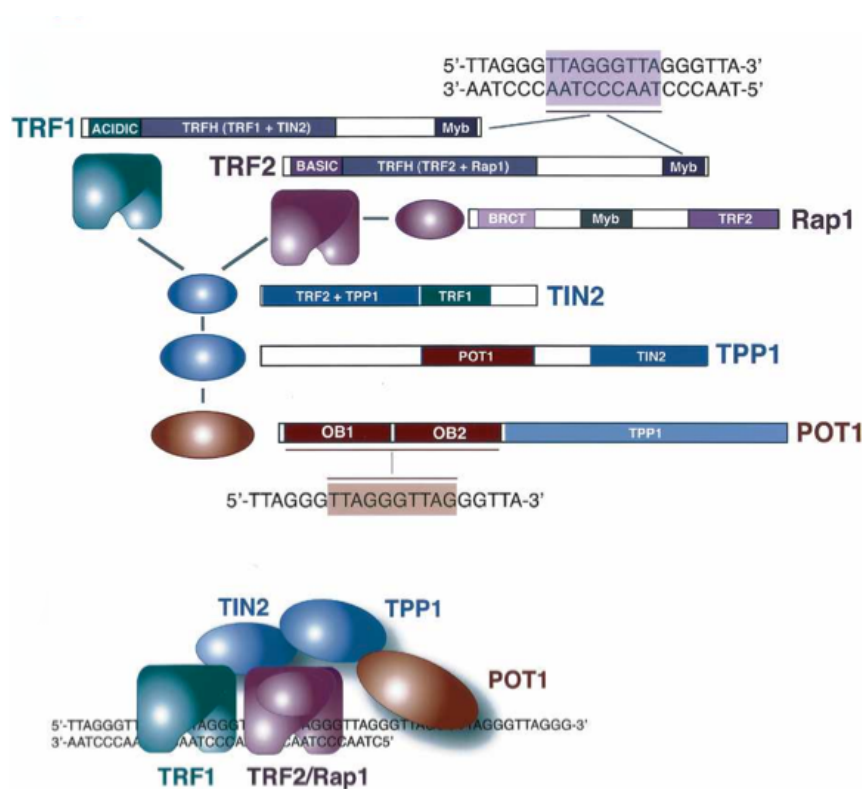
Figure 6.4. Telomere-binding proteins TRF1 and TRF2. Schematic representation of TRF1 and TRF2 domain structures with binding sites to accessory proteins (Rap1, TIN2, TPP1 and POT1) and to telomeric DNA (top). Assembly of the human telomeric complex showing interactions between telomeric proteins, TRF1 and TRF2, and accessory proteins as well as with telomeric DNA (bottom) (*in* de Lange, 2005).

Two TRF2 mutants have been developed to disrupt TRF2 protective function at the telomere (van Steensel *et al*, 1998). The TRF2$^{\Delta B}$ mutant lacks the basic domain whereas TRF2$^{\Delta B \Delta M}$ (TRF2DN or TRF2 dominant negative) lacks both the basic and Myb domains (Fig. 6.5). The latter acts as a strong dominant negative mutant for its ability to dimerise with endogenous TRF2 whilst carrying an absent telomeric DNA-binding domain.
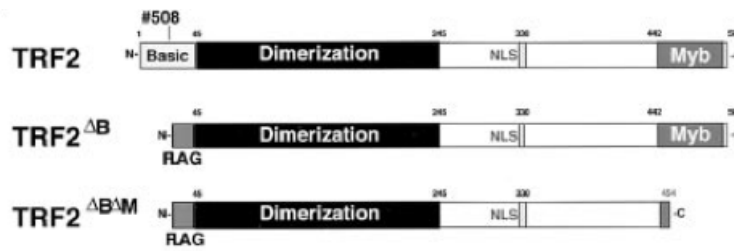
Figure 6.5. Human TRF2 deletion mutants. Schematic representation of full-length human TRF2 and mutants lacking the basic domain, TRF2ᐃB or both the basic and the Myb domains, TRF2ᐃBᐃM (*in* van Steensel, 1998).

TRF2ᐃBᐃM sequesters endogenous full-length TRF2 into defective dimers that are incapable of binding the telomere, therefore depleting it from TRF2 complexes and, ultimately, exposing the telomeric DNA. This results in growth arrest accompanied by phenotypical characteristics of senescence (van Steensel *et al*, 1998). The main advantage of using this system as opposed to replicative exhaustion is that senescence can be induced prematurely in normal cells that have undergone only a few divisions thereby minimising the chance of accumulation of any other cellular changes (Smogorzewska & de Lange, 2002). There is, however, debate on whether acute induction of telomere dysfunction truly mimics senescence occurring naturally via replicative exhaustion or merely elicits a phenotype evocative of crisis in normal cells (Herbig *et al*, 2004). Although chromosome end-fusions were reported for IMR-90 cells (Smogorzewska & de Lange, 2002), TRF2ᐃBᐃM-expressing NHEK did not show any evidence of anaphase bridges and were, therefore, senescent and not in crisis (Minty *et al*, 2008).

The cellular consequences of telomere dysfunction vary between species and, within the same species, differ between cell types. In mouse cells, experimental uncapping of telomeres primarily engages the p53 pathway of senescence whilst in human cells it engages both p53 and p16^{INK4a}/pRb (Smogorzewska & de Lange, 2002). Within the latter, expression of TRF2ᐃBᐃM induces apoptosis in certain mammalian cell types, such as T-lymphocytes and p53-competent cancer cell lines (Karlseder *et al*, 1999), and senescence in both fibroblasts (Smogorzewska & de Lange, 2002) and keratinocytes (Minty *et al*, 2008).

Dysfunctional telomeres trigger a classical DNA damage response in human diploid fibroblasts (Takai *et al*, 2003; d'Adda di Fagagna *et al*, 2003; Herbig *et al*, 2004). The first observation was that following expression of TRF2$^{\Delta B \Delta M}$, many of the 53BP1 foci generated colocalised with the telomere. These were referred to as telomere-dysfunction induced foci or TIFs (Takai *et al*, 2003) and also contained several other DNA damage response factors. The fact that indicators of a DDR such as 53BP1, Mre11 and the phosphorylated forms of ATM, H2AX and Rad17 were present at dysfunctional telomeres suggested that these might be perceived by the cell as sites of DNA damage (Takai *et al*, 2003). In addition to activated H2AX (ɣ-H2AX), which also colocalised with DNA damage checkpoint protein Mdc1 and DSB repair factor NBS1, there was evidence for activation of upstream protein kinases ATM and ATR, their downstream transducer kinases CHK1 and CHK2, and target proteins Rad17, Mdc1, p53 plus its transcriptional target p21^{WAF1}. This indicates the generation of a DDR followed by engagement of the p53/p21^{WAF1} pathway of senescence similarly to the well characterised response elicited by DSBs following exposure to IR (d'Adda di Fagagna *et al*, 2003). Single-cell analysis further confirmed that the signal from uncapped telomeres is transmitted primarily via ATM and CHK2, with ATR taking this role and processing the signal mainly via CHK1 in cells depleted of ATM. In addition, the signal activates p53 and p21^{WAF1} causing G1 arrest without influencing p16^{INK4a} expression (Herbig *et al*, 2004). Importantly, this can happen without the total loss of TRF2 from most fibroblasts telomeres, suggesting that the physiological uncapping of telomeres does not require total TRF2 depletion, or that DSBs can occur at the telomere in the absence of telomere shortening or uncapping, as it has recently been demonstrated (Hewitt *et al*, 2012; Fumagalli *et al*, 2012).

In normal epidermal keratinocytes, telomere uncapping results in a senescent-like arrest although accompanied by a surprisingly low DDR (Minty *et al*, 2008). This is characterised by a number of 53BP1 foci which is much lower than the number obtained following exposure to as low a dose of IR as 2 Gray and accompanied by a coherently mild phosphorylation of p53 at Serine 15. In addition, total p53 and p21^{WAF1} protein levels remained at control levels. Although this contrasts with what was previously reported for normal human fibroblasts (Herbig *et al*, 2004), it is very similar to what has been reported for the keratinocyte dysplasia line D17 upon telomere erosion following serial passage to senescence (Muntoni *et al*, 2003). D17 cells are mortal but have a mutation in the *INK4a* locus which makes them both p14^{ARF} and p16^{INK4a}-deficient while

retaining functional wild-type p53. As a consequence they are unable to senesce via these pathways but do so via the p53 pathway alone. Induction of p16^{INK4a} has been reported in fibroblasts as a late event succeeding the initial DDR as a result of telomere dysfunction (Jacobs & de Lange, 2004) but in both replicative senescent fibroblasts (Herbig *et al*, 2004) and TRF2$^{\Delta B \Delta M}$-expressing keratinocytes (Minty *et al*, 2008) p16^{INK4a} becomes up-regulated in a stochastic, telomere- and DNA damage-independent manner with increasing replicative age.

6.2. Over-expression of the main effectors of senescence

Genes HOPX, ICEBERG and S100A7 show potential as markers for telomere dysfunction-induced senescence since they were up-regulated in keratinocytes with dysfunctional telomeres (via forced expression of TRF2$^{\Delta B \Delta M}$ or via natural telomere uncapping) and their expression returned to control levels following ectopic expression of telomerase (Muntoni *et al*, 2003; Minty *et al*, 2008). Moreover, these candidate markers were not affected by induction of general DNA damage in the form of repairable or unrepairable DSBs (Chapter 4). HOPX, ICEBERG and S100A7 were not elevated in response to induction of p53 following exposure to ionising radiation so it is possible that, in keratinocytes, dysfunctional telomeres might be signalled differently from DSBs and not through the classical DNA damage pathway of senescence as happens in fibroblasts (Takai *et al*, 2003; d'Adda di Fagagna *et al*, 2003; Herbig *et al*, 2004). Although these data and previous work (Minty *et al*, 2008) indicate that these genes do not appear to be regulated by p53, I wondered whether direct over-expression of p53 or of the other two main effectors of senescence, p14^{ARF} and p16^{INK4a}, would induce the candidate markers.

To test this, retroviral gene transfer was used to generate models of keratinocyte senescence. Cell cycle inhibitors p14^{ARF}, p16^{INK4a}, p53 and the dominant negative version of TRF2, TRF2$^{\Delta B \Delta M}$ were independently over-expressed in NHEKs via retroviral transduction. Keratinocytes were either infected indirectly, by co-culture with infectious packaging cell lines producing retroviral particles capable of infecting human cells or, alternatively, by being exposed directly to amphotropic viral supernatants (Chapter 5). Retroviral

vectors were allowed a 24h (direct strategy) or 48h (indirect strategy) expression time before NHEKs were placed under drug selection. Populations of keratinocytes selectively senescing via each of the main pathways of senescence (p14^{ARF}/p53 pathway, p53 pathway and p16^{INK4a}/pRb pathway) and via telomere dysfunction were obtained and analysed 5 days after infection. The response of the candidate markers (via gene expression analysis) in each of the classical models of senescence was compared to the model of telomere dysfunction-induced senescence.

Delivery of the transgenes to the keratinocytes was at the first instance visually confirmed by the high percentage of fluorescence (close to 100%) obtained in the GFP-expressing empty vector control and by the distinct phenotypical appearance of the cells/colonies expressing p14^{ARF}, p16^{INK4a}, p53 and TRF2$^{\Delta B \Delta M}$ when compared to the empty vector control (Chapter 5). Levels of expression of the transgenes were assessed by qPCR. These varied between experiments and also depended on the strategy used for delivery. For instance, I have found that TRF2$^{\Delta B \Delta M}$ was only expressed at levels high enough to induce senescence via a direct strategy of infection. Similarly, this strategy generally resulted in higher expression levels for p14^{ARF} and p53. For p16^{INK4a}, however, delivery via an indirect strategy of infection proved to be more successful (Chapter 5). As a result, distinct populations of keratinocytes selectively over-expressing the transgenes at LOW, MEDIUM or HIGH levels were obtained. The transcriptional profiles of each NHEK population are presented in Figures 6.6 to 6.9.

Figure 6.6. Transcriptional profile of populations of normal human epidermal keratinocytes expressing TRF2$^{\Delta B \Delta M}$ at different levels. Keratinocyte populations expressing TRF2$^{\Delta B \Delta M}$ at LOW (12-fold), MEDIUM (15-fold) and HIGH (18-fold) were analysed by qPCR for induction of transcript levels of candidate markers (HOPX, HIST2H2BE, ICEBERG and S100A7), cyclins (CCNA2 and CCND1) and effectors of senescence (p14^{ARF}, p16^{INK4}, p53 and TRF2$^{\Delta B \Delta M}$). TRF2 mRNA levels were also assessed to confirm they remain unaltered by expression of its dominant negative mutant TRF2$^{\Delta B \Delta M}$ (TRF2DN). Results are expressed in fold mRNA levels normalised against the respective empty vector (EV) control. Legend: EV = NHEK expressing empty vector control; DN = NHEK expressing TRF2$^{\Delta B \Delta M}$.

Figure 6.7. Transcriptional profile of populations of normal human epidermal keratinocytes expressing p14^{ARF} at different levels. Keratinocyte populations expressing p14^{ARF} at LOW (89-fold), MEDIUM (142-fold) and HIGH (220-fold) were analysed by qPCR for induction of transcript levels of candidate markers (HOPX, HIST2H2BE, ICEBERG and S100A7), cyclins (CCNA2 and CCND1) and effectors of senescence (p14^{ARF}, p16^{INK4}, p53 and TRF2$^{\Delta B \Delta M}$). TRF2 mRNA was also assessed to confirm it remains at control levels. Results are expressed in fold mRNA levels normalised against the respective empty vector (EV) control. Legend: EV = NHEK expressing empty vector control; p14 = NHEK expressing p14^{ARF}.

Figure 6.8. Transcriptional profile of populations of normal human epidermal keratinocytes expressing p16^{INK4a} at different levels. Keratinocyte populations expressing p16^{INK4} at LOW (18-fold), MEDIUM (60-fold) and HIGH (116-fold) were analysed by qPCR for induction of transcript levels of candidate markers (HOPX, HIST2H2BE, ICEBERG and S100A7), cyclins (CCNA2 and CCND1) and effectors of senescence (p14^{ARF}, p16^{INK4}, p53 and TRF2$^{\Delta B\Delta M}$). TRF2 mRNA was also assessed to confirm it remains at control levels. Results are expressed in fold mRNA levels normalised against the respective empty vector (EV) control. Legend: EV = NHEK expressing empty vector control; p16 = NHEK expressing p16^{INK4}.

Figure 6.9. Transcriptional profile of populations of normal human epidermal keratinocytes expressing p53 at different levels. Keratinocyte populations expressing p53 at LOW (10-fold), MEDIUM (7-fold) and HIGH (29-fold) were analysed by qPCR for induction of transcript levels of candidate markers (HOPX, HIST2H2BE, ICEBERG and S100A7), cyclins (CCNA2 and CCND1) and effectors of senescence (p14^{ARF}, p16^{INK4}, p53 and TRF2$^{\Delta B \Delta M}$). TRF2 mRNA was also assessed to confirm it remains at control levels. Results are expressed in fold mRNA levels normalised against the respective empty vector (EV) control. Legend: EV = NHEK expressing empty vector control; p53 = NHEK expressing p53.

Successful delivery of the retroviral vectors and over-expression of the main effectors of senescence p14^{ARF}, p16^{INK4a} and p53 as well as expression of the dominant negative mutant TRF2$^{\Delta B \Delta M}$ resulted in a large reduction in CFE (colony-forming efficiency). Cloning efficiency was reduced by 50% with p14^{ARF} and by at least 75% with p16^{INK4a}, p53 and TRF2$^{\Delta B \Delta M}$, when compared to the respective empty vector control (Figure 6.10). Also, in addition to the distinct phenotypical appearance of the cells/colonies upon senescence (Chapter 5) a significant decrease in transcript levels of Cyclin A2 (CCNA2) accompanied by elevation of Cyclin D1 (CCND1) was observed in keratinocytes expressing at least MEDIUM or HIGH levels of the transgenes, which is consistent with senescence (Figures 6.6 to 6.9). Taken together this shows that the transduced cells went on to exit the cell cycle rather than terminal differentiate or die.
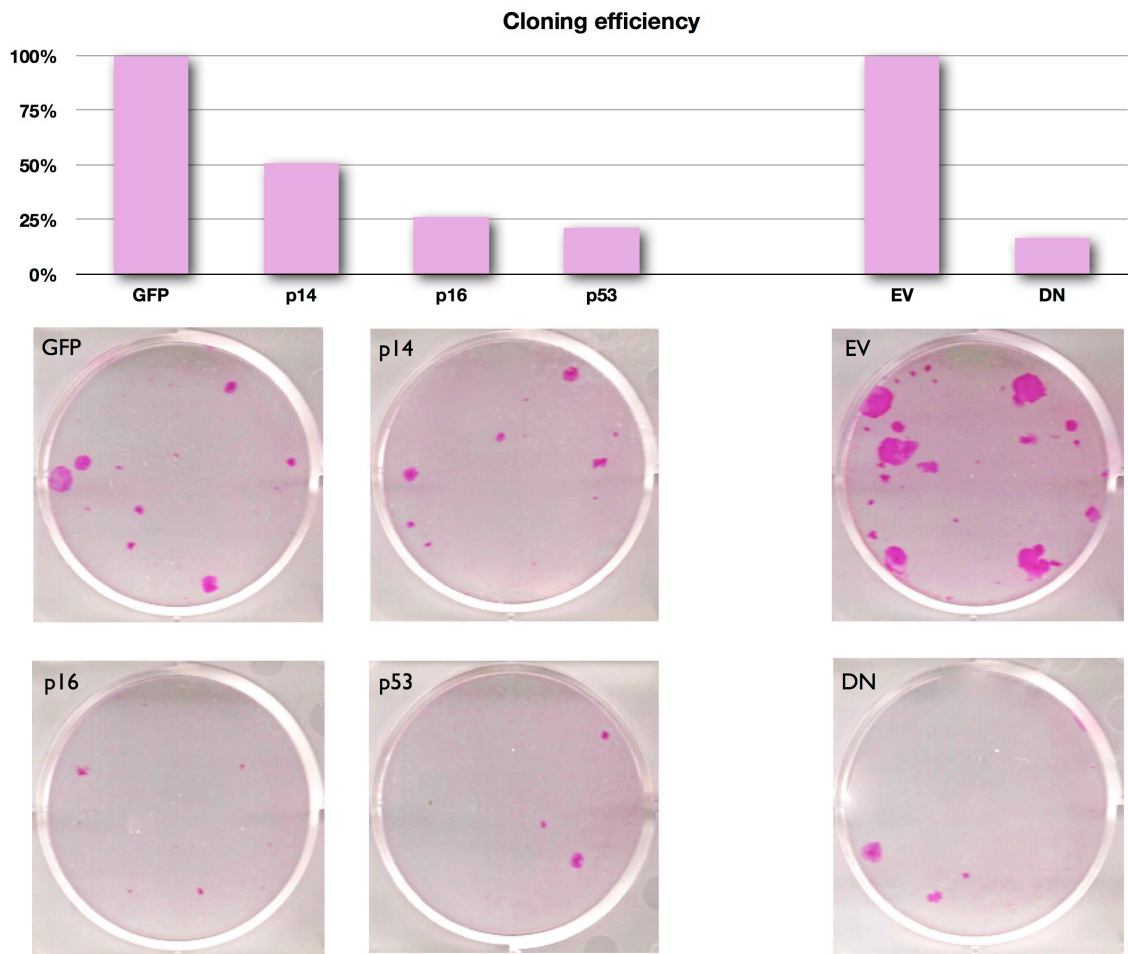
Figure 6.10. Analysis of cloning efficiency of NHEK transduced with p14^ARF, p16^INK4α, p53 and TRF2^ΔBΔM. NHEK were transduced via a direct strategy of infection and, 48h later, trypsinised and seeded at clonal density (7×10^3 cells per 6-well plate). Cells were cultured for 2 weeks under drug selection and finally fixed and stained with rhodamine B to reveal keratinocyte colonies. Cloning efficiency, displayed as percentage and normalised against the respective EV control, was calculated by dividing the total number of colonies obtained per well by the total number of cells seeded per plate (7,000). Photos show wells representative of the results obtained for each construct. GFP = empty vector control for p14^ARF, p16^INK4, p53; EV = empty vector control for TRF2^ΔBΔM (DN).

In general, the level of expression of the transgene correlated directly with the level of reduction in CCNA2/elevation in CCND1, so there seems to be a threshold level of expression above which senescence seems to be engaged. This was most evident with TRF2$^{\Delta B\Delta M}$ and has previously been reported in fibroblasts (van Steensel *et al*, 1998). Levels of expression of TRF2$^{\Delta B\Delta M}$ of 4-fold did not result in cell cycle arrest as cells proliferated as well as the empty vector control (experiments described in Chapter 5). An 11-fold expression level, however, resulted in a mild decrease (10%) in CCNA2 yet 40% elevation of CCND1 whereas 15-fold and 18-fold levels resulted in a convincing 50% reduction in CCNA2 and 40% decrease in CCNA2/40% increase in Cyclin D1, respectively (Figure 6.6). Over-expression of p16^{INK4a} by 18-fold resulted in a 40% decrease in CCNA2, 59-fold augmented it to 60% and, finally, 116-fold caused a 30% reduction in CCNA2 accompanied by the same elevation in CCND1 (Figure 6.8). Elevation of p53 by 7-fold resulted in a 50% decrease in CCNA2 and a similar expression level of 10-fold resulted in poorer reduction of CCNA2 (just 20%) followed by a mild increase in CCND1 (also 20%). Over-expression of p53 by 28-fold, however, reduced CCNA2 by 30% and CCND1 maintained a mild elevation (Figure 6.9). The exception to the direct correlation between expression of the transgene and effective cell cycle arrest was p14^{ARF}. Regardless being over-expressed at a LOW (89-fold), MEDIUM (142-fold) or HIGH (220-fold) level it resulted always in 30-40% reduction of CCNA2 alone (Figure 6.7). I have considered, therefore, that MEDIUM and HIGH levels of expression of the transgenes were capable of inducing senescence in NHEK (exception for p53 where 7-fold reduced CCNA2 to a higher level than did 10-fold).

Each candidate marker responded differently to over-expression of each of the known effectors of senescence (Figures 6.6 to 6.9). As demonstrated before (Minty *et al*, 2008), all candidate markers were elevated upon telomere dysfunction-induced senescence in keratinocytes via expression of TRF2$^{\Delta B\Delta M}$ (Fig. 6.6). Interestingly, whilst high doses of IR with consequent activation of p53 only induced HIST2H2BE (Chapter 4), direct over-expression of p53, depending on the level, did induce some of the other markers (Fig. 6.9). A 7-fold induction of p53 induced both HOPX and HIST2H2BE by 40%. A 4x higher expression level (28-fold), however, induced HIST2H2BE and S100A7 by 1.5-fold,

and HOPX and ICEBERG by over 2-fold and 3-fold, respectively. p14^{ARF} induced only HOPX and HIST2H2BE, by around 50% (Fig. 6.7) whilst p16^{INK4a} did not cause significant elevation of any of the markers (Fig. 6.8). The average transcript levels of the candidate markers HOPX, HIST2H2BE, ICEBERG and S100A7 between populations of keratinocytes expressing the transgenes at MEDIUM and HIGH levels are summarised in Figure 6.11.
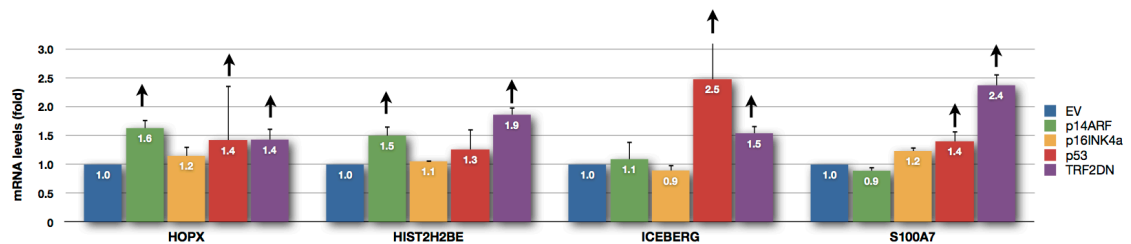
Figure 6.11. Transcript levels of HOPX, HIST2H2BE, ICEBERG and S100A7 in keratinocytes transduced with p14^{ARF}, p16^{INK4a}, p53 and TRF2$^{\Delta B\Delta M}$. Gene expression levels of the candidate markers (HOPX, HIST2H2BE, ICEBERG and S100A7) were normalised against the respective empty vector control (EV) and averaged (n=2) between populations of NHEK expressing MEDIUM and HIGH levels of the transgenes (p14^{ARF}, p16^{INK4}, p53 and TRF2$^{\Delta B\Delta M}$). Bars represent standard deviation and arrows induction of the markers.

HOPX was induced, in average, at a higher level by p14^{ARF} (1.6-fold) and p53 (1.8-fold) than by TRF2$^{\Delta B\Delta M}$ (1.4-fold). HIST2H2BE was also induced by p14^{ARF} (1.5-fold) and p53 (1.4-fold), however at a lower level than by TRF2$^{\Delta B\Delta M}$ (1.9-fold). ICEBERG was significantly induced by p53 (2.4-fold) whilst S100A7 was not. Both ICEBERG and S100A7 were also not induced by p14^{ARF} or p16^{INK4a} yet were elevated by 1.5-fold and 2.4-fold, respectively, following expression of TRF2$^{\Delta B\Delta M}$. Nevertheless, expression of the dominant negative mutant of TRF2 resulted in generally lower (by about 1-fold) levels of expression of the candidate markers than what had been previously reported using a different technique for retroviral transduction (Minty *et al*, 2008). Minty *et al* obtained an elevation of 2.5-fold for HOPX versus 1.4-fold, 2.4-fold for HIST2H2BE versus 1.9-fold, 2.8-fold for ICEBERG versus 1.5-fold and 3.5-fold for S100A7 versus 2.4-fold, therefore demonstrating that relative levels between markers are similar. HOPX, HIST2H2BE

and ICEBERG are elevated to a similar level (about 1.5-fold) following expression of TRF2$^{\Delta B\Delta M}$, whilst S100A7 is always about half to 1-fold higher (Fig. 6.11).

Results from the retroviral transduction experiments suggest that S100A7 is the most promising candidate as a specific marker of telomere dysfunction-induced senescence as it was not induced by over-expression of the main effectors of senescence yet was selectively elevated following telomere uncapping via expression of TRF2$^{\Delta B\Delta M}$.

6.3. Discussion

I have been investigating the hypothesis that telomere dysfunction in keratinocytes might be signalled through an alternative pathway to the classical p53-dependent senescence pathway activated in response to generalised DNA damage. As a consequence of expression of the dominant negative mutant version of the telomere protection factor 2, TRF2$^{\Delta B\Delta M}$ in newborn human epidermal keratinocytes (Minty *et al*, 2008) a weak DDR ensued and the senescent-like arrest that followed was accompanied by a characteristic transcriptional profile with up-regulation of genes involved in chromatin remodelling (HIST2H2BE, histone from the H2B family), inflammation (ICEBERG) and terminal differentiation (HOPX and S100A7). These genes show potential as markers for keratinocyte TDIS.

So far I have shown that the weak DDR was not the factor responsible for the induction of any of these genes and that a strong DDR, activated in response to extensive DNA damage following exposure to senescence-inducing doses of IR, was only responsible for inducing the histone HIST2H2BE (Chapter 4). Despite being regulated by telomere dysfunction and telomerase (Muntoni *et al*, 2003; Minty *et al*, 2008), this suggests that HOPX, ICEBERG and S100A7, are apparently not regulated by p53, at least, not via the DNA damage pathway of senescence. However, since the nature of p53 activation depends on the triggering stimuli it is still possible that p53 or the other main effectors of senescence might be at play.

In order to assess the influence of the activation of each of the main pathways of senescence (p14^{ARF}/p53 or p53/p21^{WAF1} or p16^{INK4a}/pRb) in the

expression of the candidate markers I have used retroviral transduction to over-express $p14^{ARF}$, $p16^{INK4a}$ and p53 in keratinocytes, as well as expression of $TRF2^{\Delta B\Delta M}$ as a model for telomere dysfunction (Chapter 5).

Activation of p53 has been reported to occur as a consequence of telomere uncapping (Takai *et al*, 2003; d'Adda di Fagagna *et al*, 2003; Herbig *et al*, 2004) or following exposure to IR (Di Leonardo *et al*, 1994) through phosphorylation of the molecule at the Serine 15 site and, at least in keratinocytes, IR does not cause considerable elevation of p53 transcript or stabilisation of the protein, within five days (Minty *et al*, 2008). Whilst HIST2H2BE was the only candidate marker elevated in response to senescence-inducing doses of IR, HOPX and ICEBERG were also induced by direct over-expression of p53 using retroviral vectors. This may be because with this manipulation p53 activation occurs due to stabilisation of the molecule rather than due to post-transcriptional modifications.

Over-expression of $p14^{ARF}$ also resulted in up-regulation of HIST2H2BE and HOPX probably because $p14^{ARF}$ also contributes to stabilisation of p53. ARF acts by sequestering the E3 ubiquitin ligase MDM-2 in the nucleolus thereby preventing p53 from being targeted for proteolytic degradation (Sherr, 1998; Stott *et al*, 1998; Dimri *et al*, 2000). This can easily be confirmed by looking at protein levels of total p53 in keratinocytes transduced with $p14^{ARF}$. It is however unlikely that activation of $p14^{ARF}$ might have been the factor responsible for the original induction of the markers (Minty *et al*, 2008); first, because $p14^{ARF}$ is known not to play a role in keratinocyte senescence (Munro *et al*, 1999) and second, since the other two candidates, ICEBERG and S100A7, did not seem to be affected by over-expression of $p14^{ARF}$. Since all the aforementioned manipulations resulting in activation of p53 (Di Leonardo *et al*, 1994; Sugrue *et al*, 1997; Dimri *et al*, 2000) also result in activation of $p21^{WAF1}$, p53's transcriptional target, this data suggests that HIST2H2BE, HOPX and ICEBERG are regulated by $p21^{WAF1}$ in a p53-dependent manner. As S100A7 was the only candidate marker whose expression levels seemed unaffected by direct over-expression of either $p14^{ARF}$ or p53, or by p53 activation following irradiation (Chapter 4), S100A7 does not seem to be regulated by p53. Nevertheless, S100A7 seems to be regulated by $p21^{WAF1}$, however in a p53-independent manner, more likely related to the process of terminal differentiation in keratinocytes (Chapter 4).

Finally, over-expression of p16^{INK4a} did not cause elevation in transcript levels of any of the candidate markers. The frequency of expression of p16^{INK4a} increases in keratinocytes during serial passage in culture (Rheinwald *et al*, 2002) and in human skin with age (Ressler *et al*, 2006). The p16^{INK4a}-dependent pathway of senescence is therefore the main competitor mechanism to telomere dysfunction-dependent senescence in keratinocytes (Ramirez *et al*, 2001; Rheinwald *et al*, 2002). These data suggest they operate independently and p16^{INK4a} was not a contributing factor in the up-regulation of the candidate markers. Also, since all genes seem to be affected by terminal differentiation and since p16^{INK4a} causes growth arrest without an effect on differentiation (Di Cunto *et al*, 1998) this is consistent with our findings.

Some secreted proteins are induced by CDKI ectopic expression (McConnell *et al*, 1998) but many are not (Coppe *et al*, 2011) and instead require activation of the NF-KB pathway (Freund *et al*, 2011), which is often activated in fibroblast senescence (Rovillain *et al*, 2011; Vaughan & Jat, 2011). I have not tested the role of NF-KB directly or any candidate upstream regulators of p16^{INK4a} other than IR. However, NF-KB is activated by DSBs (Freund *et al*, 2011) and IR causes DSBs but does not induce the expression of HOPX, ICEBERG or S100A7 (Chapter 4). Therefore, it seems unlikely that NF-KB activation or its upstream transcriptional regulator p38 would induce any of these candidate biomarkers of telomere dysfunction.

Genes HOPX, HIST2H2BE, ICEBERG and S100A7 were put forward as potential markers for TDIS in normal human epidermal keratinocytes since their expression levels were elevated following telomere dysfunction and returned to normal upon ectopic expression of telomerase (Minty *et al*, 2008). I have investigated the specificity of the four candidate markers to DNA damage-induced senescence (Chapter 4) and to other forms of senescence (Chapter 6) in relation to telomere dysfunction-induced senescence (TDIS). Overall, results suggest that S100A7 is the most promising candidate as a specific marker of TDIS as it was the only gene selectively elevated following telomere uncapping via expression of TRF2$^{\Delta B \Delta M}$ and not by senescence-inducing doses of IR or by over-expression of p14^{ARF}, p16^{INK4a} or p53.

S100A7 (or psoriasin) is a member of the S100 family, first isolated from psoriatic skin (Madsen *et al*, 1991). Its up-regulation has been associated with abnormal terminal differentiation, pathogenesis of inflammatory skin disease

and progression of breast, bladder and skin cancer (Celis *et al*, 1996; Moubayed *et al*, 2007). In addition, S100A7 has also been shown to be severely down-regulated in immortal keratinocytes (immortal dysplasias and carcinomas) that have p53 and p16^{INK4a} dysfunction and which express telomerase (Parkinson, unpublished data), and in the D17 keratinocyte dysplasia, which has functional p53 but lacks the products of the *INK4a* locus, p14^{ARF} and p16^{INK4a}, and has not activated telomerase (Muntoni *et al*, 2003; Minty *et al*, 2008). The growth arrest associated with senescence following expression of its main effectors p53 and p16^{INK4a} has been shown to be uncoupled from the SASP (Coppe *et al*, 2011). In fact, p53 activation (Coppé *et al*, 2008) and ectopic expression of p21^{WAF1} or p16^{INK4a} (Coppe *et al*, 2011) were found to restrain the SASP in epithelial cells. Neither p53 activation (Chapter 4), p53 or p16^{INK4a} over-expression (Chapter 6) restrained S100A7 expression like they do the rest of the senescence secretome which suggests that S100A7 regulation seems to occur independently from the inflammatory cascade. Although PAI, a component of the senescent secretome, has been shown to be transcriptionally up-regulated by p16^{INK4a} (McConnell *et al*, 1998) this does not seem to be the case for S100A7 in keratinocytes. This is in agreement with previous findings on how p16^{INK4a} does not induce the main components of the SASP (Coppe *et al*, 2011). Finally, the fact that p16^{INK4a} expression has been directly associated with genes involved in keratinocyte migration during senescence, wounding and micro-invasive dysplasia as opposed to genes associated with terminal differentiation (Natarajan *et al*, 2003; Darbro *et al*, 2005; Natarajan *et al*, 2006) might also explain why S100A7 was not up-regulated by over-expression of p16^{INK4a}.

The ideal biomarker should be cell type- and mechanism-specific as well as a secreted molecule for ease of detection. The secreted biomarkers identified so far for telomere dysfunction are also induced by generalised DNA damage (Jiang *et al*, 2008) and thus not mechanism-specific. This might be because when telomeres become critically short they are reinterpreted as DSBs and processed as such (Takai *et al*, 2003; d'Adda di Fagagna *et al*, 2003). Keratinocytes, however, seem to respond differently to telomere dysfunction and selectively up-regulate S100A7 following TDIS. Therefore, this gene shows great potential as a biomarker for TDIS since it is also keratinocyte-specific and a secreted molecule which shows no elevation in the serum of patients with psoriasis (Anderson *et al*, 2009).

Chapter 7. Analysis of the functional role of homeobox gene HOPX in TDIS.

7.1. Introduction

Following the work in Chapter 4 a decision was made to proceed with the functional analysis of a lead candidate downstream effector of keratinocyte telomere dysfunction-induced senescence (TDIS). The homeobox gene HOPX was chosen as the lead candidate marker based on the results obtained at the time and also because there was evidence for its role as a tumour suppressor gene.

Upon telomere uncapping, and associated low DDR, HOPX was up-regulated in normal human epidermal keratinocytes (Minty *et al*, 2008). I further showed that, although HOPX is induced by telomere dysfunction it does not seem to be influenced by either a weak or a strong DDR, following induction of DNA damage in keratinocytes (Chapter 4). Consistent with this is the fact that HOPX has also been shown to be severely down-regulated in immortal keratinocytes expressing telomerase and lacking functional p53 and p16^{INK4a} (E. K. Parkinson, unpublished microarray data). These findings suggest HOPX might be regulated by telomerase but not by p53. However, HOPX also showed some down-regulation in a cell line (D17 dysplasia, (McGregor *et al*, 2002)) that lacks p16^{INK4a} and p14^{ARF} but possesses functional p53 and normal levels of telomerase (Muntoni *et al*, 2003; Minty *et al*, 2008). Importantly, elevation of HOPX transcript following telomere uncapping in D17 was reversed by ectopic expression of telomerase (Muntoni *et al*, 2003; Minty *et al*, 2008). So, the fact that HOPX does not seem to be regulated by p53, at least not via the DDR, suggests that dysfunctional telomeres in keratinocytes might be signalled through an alternative pathway to the classic DNA damage pathway, used to signal telomere damage in fibroblasts (Takai *et al*, 2003; d'Adda di Fagagna *et al*, 2003; Herbig *et al*, 2004). HOPX is even more interesting as it has recently been described as a tumour-suppressor gene (Chen *et al*, 2007; De Toni *et al*, 2008; Yamashita *et al*, 2008; Yamaguchi *et al*, 2009), a characteristic shared by several genes involved in cellular senescence. I intend to proceed with functional analysis of HOPX by attempting its stable knockdown using retroviral-delivered short hairpin RNAs (shRNAs) to generate short interfering RNA (siRNA).

By ablating its function I aim to assess whether HOPX is actively involved in the TDIS pathway in keratinocytes.

HOPX belongs to the group of *HOX* genes, well known for their role in embryogenesis and development, which are characterised by containing a 60 aminoacid domain required for DNA binding. HOPX is, however, an unusual homeobox gene as it encodes for a homeodomain protein that does not bind DNA, acting instead by binding the serum response factor (SRF) as a means to regulate transcriptional activity and it was first associated with modulation of cardiac development (Chen *et al*, 2002; Kook & Epstein, 2003; Kook *et al*, 2006). Post-natal expression of HOPX occurs normally in several terminally differentiated organs such as the heart and the brain, as well as in skeletal muscle and epithelia. Studies show its involvement in the late stages of terminal differentiation in both the lens (Vasiliev *et al*, 2007) and the skin (Yang *et al*, 2010), and in the induction of skeletal muscle differentiation (Kee *et al*, 2007). In mice, up-regulation of HOPX is associated with an increase in differentiation and results in the development of severe cardiac hypertrophy and fibrosis (Kook *et al*, 2003). HOPX is also up-regulated in senescence, namely in normal epidermal keratinocytes undergoing TDIS (Minty *et al*, 2008). Conversely, HOPX down-regulation generally is associated with proliferation and has been reported in lung cancer (Chen *et al*, 2003; 2007), head and neck squamous cell carcinoma (Lemaire *et al*, 2004), choriocarcinoma (Asanoma *et al*, 2004), uterine endometrial cancer (Yamaguchi *et al*, 2009) and gastric cancer (Ooki *et al*, 2010). In contrast, HOPX seems to be over-expressed in thyroid carcinoma (Pauws *et al*, 2004). Recent studies show that transcriptional silencing of HOPX during malignant transformation is a result of hyper-methylation of its promoter (Yamaguchi *et al*, 2009; Ooki *et al*, 2010). HOPX knockdown in HPV-immortalised keratinocytes treated with anti-viral drugs (I. Paterson,   University of Bristol, personal communication) and in immortalised human endometrial cells (Yamaguchi *et al*, 2009) results in accelerated proliferation, whilst the forced expression of HOPX in keratinocyte lines has the opposite effect, i.e., slowing down proliferation (I. Paterson,   University of Bristol, personal communication). Based on this body of evidence HOPX has been recently classified as a tumour-suppressor gene.

RNA interference (RNAi)

The process of gene silencing was first observed in plants (Napoli *et al*, 1990) but only understood and characterised several years later as RNA interference (RNAi). This coincided with the discovery that dsRNA (double-stranded RNA), containing a pair of both sense and anti-sense strands of the target mRNA, was the inducer of effective gene silencing in both *C. elegans* (Fire *et al*, 1998) and mammalian cells (Elbashir *et al*, 2001). RNAi is thought to have evolved as a protective cellular mechanism against dsRNA viruses and other mobile genetic elements such as transposons, especially in nematodes, insects and plants. However, in addition to its role in mRNA degradation, RNAi has a more complex role as it is also involved in regulation of transcription, translation, chromatin structure and genomic integrity (Medema, 2004; Kim & Rossi, 2007). RNA silencing pathways are conserved in eukaryotes, from yeast to plants and mammals, and have been since characterised (reviewed in (Medema, 2004; Kim & Rossi, 2007)).

The siRNA pathway mediates port-transcriptional gene silencing via effector short interfering RNA molecules (siRNAs). These are small double-stranded complementary RNA molecules with dinucleotide 3' overhangs resulting from processing of exogenous larger dsRNA by the RNase III enzyme Dicer. siRNAs mediate mRNA cleavage by activating the RNA-induced silencing complex (RISC). The sense strand of the double-stranded siRNA is first cleaved by the endonuclease component Argonaute 2 (AGO2) freeing the anti-sense strand which guides RISC to the fully complementary target mRNA. Following cleavage this is finally degraded by exonucleases. siRNAs can also mediate transcriptional gene silencing through chromatin modifications such as histone methylation (Fig. 7.1 left).

The miRNA pathway is involved in gene regulation during development and differentiation and acts through effector micro RNAs (miRNAs). These are small RNAs (around 22nt in length) which, as opposed to siRNAs, derive from a single transcript folded into a ds-hairpin containing loops. The endogenous long primary transcript (Pri-miRNA) is transcribed by RNA polII in the nucleus and processed by the Drosha/DGCR8 microprocessor complex into stem-loop precursors (pre-miRNA) around 70 nt long. These are exported to the cytoplasm by dsRNA-binding protein Exportin 5 (XPO-5) where they are processed into miRNAs by the Dicer/TRBP/PACT complex. Instead of being cleaved by AGO2, due to imperfect sequence complementarity, the miRNA sense or passenger strand is unwound and discarded through RISC's helicase activity. The

remaining mature miRNA anti-sense strand then binds 3' untranslated regions (3'UTRS) in the target mRNA through RISC activation which directs translational repression and mRNA degradation in cytoplasmic P-bodies (Fig. 7.1 right). The choice between achieving gene silencing through block of transcription, translation or via direct transcript degradation is thought to depend not on the nature of the RNAi effectors (whether they are siRNAs or miRNAs) but on the degree of complementarity between the interference molecules and the target mRNA.
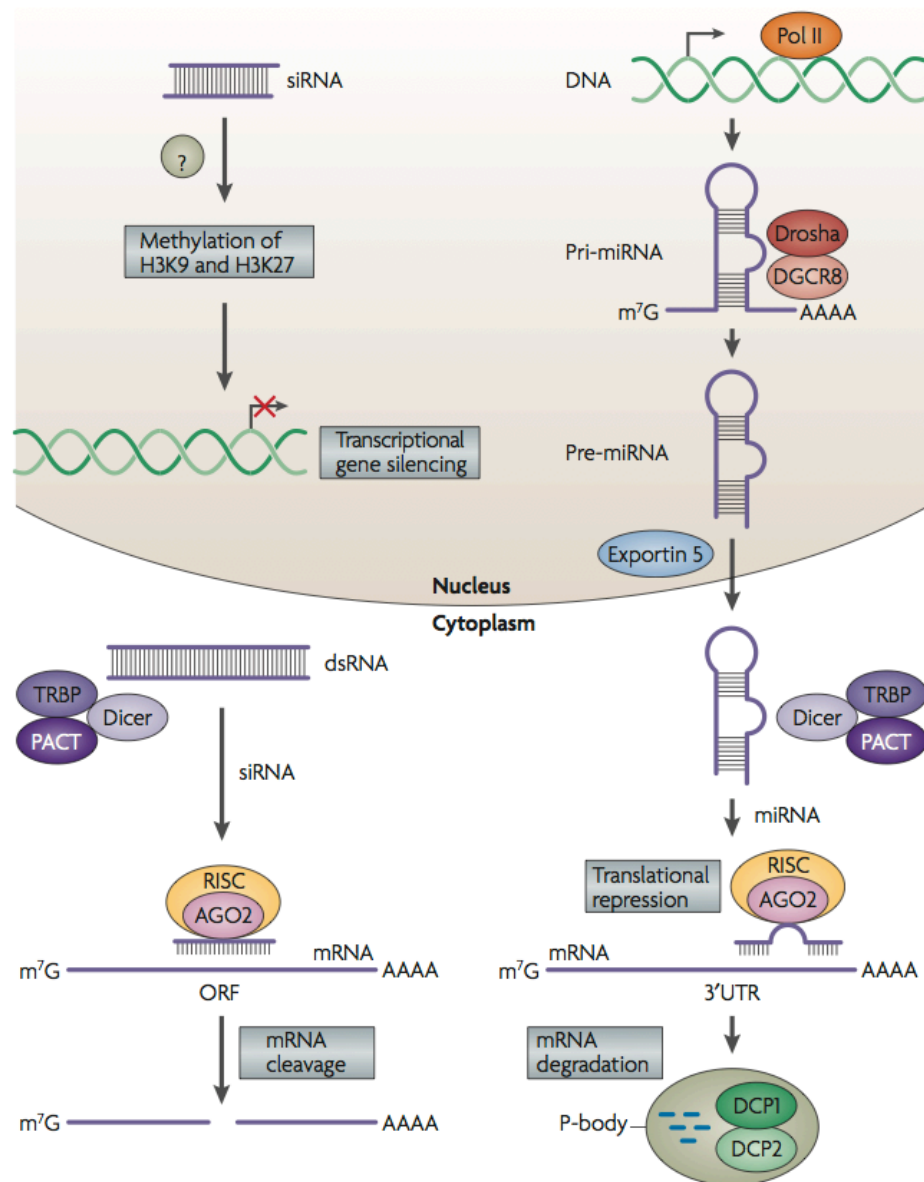
Figure 7.1. RNA interference (RNAi) pathways in mammalian cells. siRNA pathway (left) and miRNA pathway (right). Legend: TRBP = TAR RNA-binding protein (TRBP); PACT = protein activator of protein kinase PKR (PACT); AGO2 = Argonaute 2; RISC = RNA-induced silencing complex (RISC); DGCR8 = DiGeorge syndrome critical region gene 8; DCP1 and DCP2 = de-capping enzymes 1 and 2; H3K9, histone 3 lysine 9; H3K27, histone 3 lysine 27; m7G, 7-methylguanylate; ORF, open reading frame (*in* (Kim & Rossi, 2007)).

Several RNAi effector molecules have been developed for use as gene silencing tools (Medema, 2004; Kim & Rossi, 2007). Early on it became clear that large dsRNA could not be used to generate siRNA in mammalian cells since sequences larger than 30 base pairs would trigger an interferon inflammatory response which ultimately resulted in non-specific gene silencing through generalised block in protein synthesis (Williams, 1997). However, it was soon discovered that short interfering dsRNA sequences (siRNAs) could be successfully used instead (Elbashir *et al*, 2001). Synthetic siRNAs are introduced directly via transfection either unmodified or containing chemical modifications to improve stability (Fig. 7.2 a). Although this results in a transient knock-down of the target gene, lasting just up to 6 days, the strategy is very effective since high copy numbers of siRNAs are obtained in the cell. Effector siRNAs can also be generated indirectly in cells transduced with vectors expressing short hairpin RNAs (shRNAs) since these are processed into functional siRNAs by Dicer through the endogenous RNAi pathway (Fig. 7.2 b). In this case stable knock-down of the target gene is achieved due to continuous expression of the shRNA and, therefore, siRNA production in the target cell. Despite having the advantage of being used to transduce primary or non-dividing cells, especially with the use of retroviral, adenoviral or lentiviral systems, shRNAs are less effective than siRNAs in mediating gene silencing as they generate fewer siRNA molecules. Drug selection on the various vector-based systems will have a similar effect. Therefore, in order to achieve effective gene silencing through a vector-based system, the choice of a target sequence efficiently recognised by the few copies of siRNAs generated is an essential consideration in hairpin design.
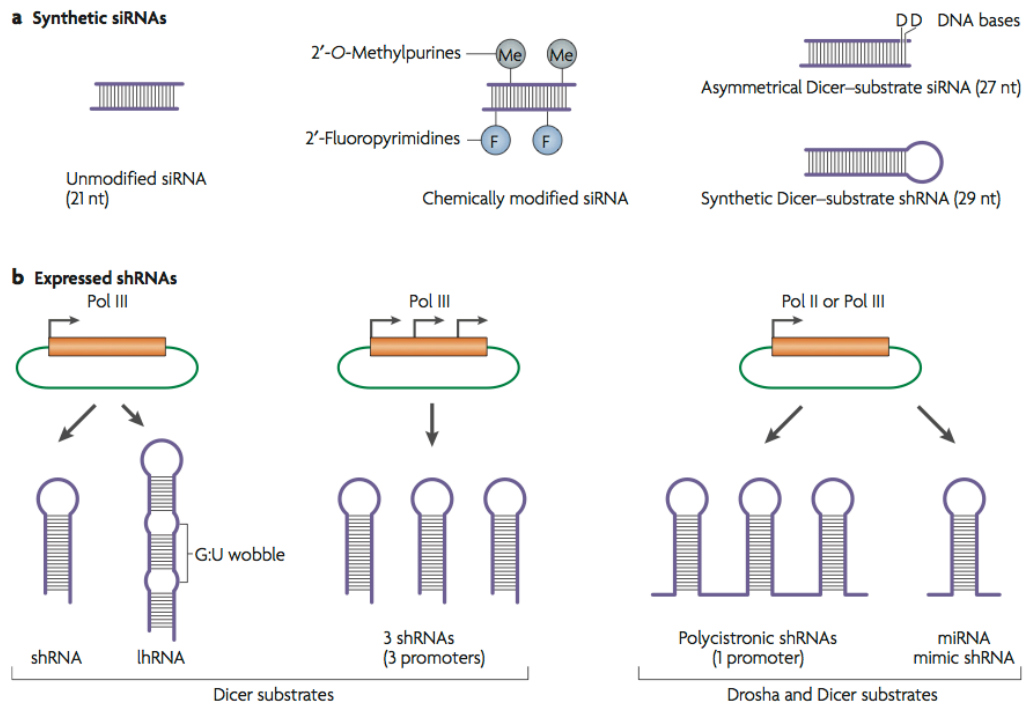
Figure 7.2. Overview of various RNAi effector molecules used as gene silencing tools. Synthetic siRNAs (a) and expressed shRNAs (b) (*in* Kim, 2007).

In order to proceed with HOPX functional analysis and further investigate its role in keratinocyte TDIS I opted for a retroviral vector-based system for expression of shRNAs designed to silence HOPX transcript. The aim was to induce stable knock-down of HOPX in two keratinocyte models of TDIS. The first is based on artificial telomere uncapping, through expression of the dominant-negative mutant version of telomere-binding factor TRF2 (TRF2$^{\Delta B \Delta M}$), in newborn early passage normal human epidermal keratinocytes. The second, a model of natural telomere uncapping, consists of an oral keratinocyte dysplasia line (D17) characterised by deletion of the *INK4a* locus, wild type functional p53 and a finite, although extended, lifespan. If HOPX is essential to keratinocyte TDIS its ablation should block or mute telomere-dysfunction induced senescence thereby extending replicative lifespan. If this strategy succeeds, a new pathway from dysfunctional telomeres to senescence would be identified. Ultimately, the objective would be to demonstrate this *in vivo*.

7.2. Establishment of experimental model

The choice of a retroviral-based shRNA system for silencing HOPX expression in normal keratinocytes was appropriate given the objectives of this work and despite shRNAs' overall lower efficiency when compared to siRNAs'. As a general rule, cell strains are difficult to transfect directly with plasmid DNA and keratinocytes are a particularly challenging cell type. One of the most successful systems for the expression of transgenes in normal human epidermal keratinocytes involves transduction with retroviral vectors (Levy *et al*, 1998). In addition, since the predicted phenotype following HOPX KD in keratinocyte TDIS models is the bypass of senescence checkpoints and, thus, extension of replicative lifespan, effective KD needs to be maintained for several days or weeks. Stable knock-down using shRNA is therefore preferable to transient KD via siRNA.

Based on the preceding considerations I obtained a set of commercially designed shRNAs against human HOPX (Origene) conveyed in pGFP-B-RS vectors, which are based on a pRS plasmid backbone (Fig. 7.3). pGFP-B-RS constructs contain a GFP cassette under the control of a CMV promoter. As the GFP sequence does not get integrated with the retroviral vector, fluorescence is used solely to monitor transfection efficiency (transfection control). Also, since I intended to super-infect keratinocytes with TRF2$^{\Delta B\Delta M}$ and this construct is associated with a puromycin selection marker (pLPC N-MYC vector - see Chapter 5), I opted for a retroviral construct containing an alternative selection marker, blasticidin (BSD). In addition to being a driver of selective pressure for gene expression (in this case shRNA expression), resistance to blasticidin should also provide information on the transduction rate of the target cells. Within the retroviral vector, the blasticidin resistance cassette (BSDr) is under the control of an SV40 promoter, whereas the human U6 promoter directs shRNA expression. The shRNA cassette consists of a 29bp target specific sequence, a 7bp loop and another 29bp reverse complementary sequence followed by a termination sequence (TTTTTT) located immediately downstream to stop transcription by RNA pol III.

Figure 7.3. Map of shRNA cloning vector pGFP-B-RS. The GFP cassette is under the control of a CMV promoter. In the retroviral construct, an SV40 promoter drives expression of the blasticidin-resistance cassette (BSD^r), whilst the human U6 promoter directs shRNA expression. The shRNA cassette consists of a 29bp target specific sequence, a 7bp loop and another 29bp reverse complementary sequence followed by a termination sequence (TTTTTT) located immediately downstream to stop transcription by RNA pol III.

The various commercially obtained hairpins (shRNA sequences A, B, C and D) were assessed and the best two selected for the least off-target effects and highest knock-down efficiency. Origene's hairpin design predicted that at least one of the four constructs should produce more than 70% knock-down (72h post-transfection), provided a minimum transfection efficiency of 80% is achieved. This was a rather optimistic prediction since most vector-based systems render only around 50% maximum KD efficiency, as opposed to 80% or higher obtained with siRNAs. Although the design of these shRNA constructs was directed against a maximum number of transcriptional variants at this gene locus (based on Origene's datasheet), the fact that multiple alternatively spliced transcript variants (at least 5 so far) were identified for HOPX could influence target specificity and reduce KD efficiency. Nevertheless, an efficient level of KD for human HOPX was previously reported using these constructs in immortal oral keratinocytes (Ian Paterson, University of Bristol, personal

communication). In addition to the specific anti-HOPX shRNAs, a hairpin containing a scrambled shRNA sequence non-specific to HOPX was also provided, to control for KD background (scrambled control). An empty vector control was included as an additional negative control for KD and as a reference for normal gene expression level and phenotype.

To assess the quality of the hairpins, shRNA constructs were first transduced into normal human epidermal keratinocytes (NHEK) via a direct strategy of infection through generation of amphotropic retroviral particles (see Chapter 5). Briefly, pGFP-B-RS plasmid constructs containing shRNA sequences A, B, C or D, the shRNA scrambled sequence (scrambled control, S) or vector only (empty vector control, EV) were transfected into the amphotropic Phoenix packaging cell line (Phoenix A cells). Infectious retroviral particles were collected 48h following transfection and used to directly infect keratinocytes cultured in the 'feeder' system via spinfection (see Chapter 2). Drug selection (8µg/mL blasticidin, based on kill curve) was introduced 24h after infection and level of KD assessed 12 days later.

The transfection efficiency was higher than 80% for all constructs as observed by levels of fluorescence. This, consequently, resulted in good infection rates given the low number of keratinocytes that succumbed to drug selection and a good number of successfully transduced healthy colonies. Blasticidin proved to be a very efficient selection agent, causing 100% cell death in the mock control within just 3 days and exhibiting very low toxicity on the transduced cells given the lack of any visible deleterious effects, when compared to non-transduced cells (mock control). The level of knock-down, inferred from reduction in HOPX protein levels in the cells transduced with the shRNAs, was assessed by western blot followed by densitometry analysis against the background generated by the scrambled control. By normalising against the scrambled control I ensured it is solely the target specific KD that is being calculated. shRNA sequences A and B resulted in the highest level of HOPX KD, 50% and 32% respectively, whilst C and D generated less than 20% and less than 10% KD, respectively (Fig. 7.4 HOPX KD in NHEK). Hairpins A and B were, therefore, the most effective and selected (out of the possible 4) to induce HOPX KD in both models of TDIS.
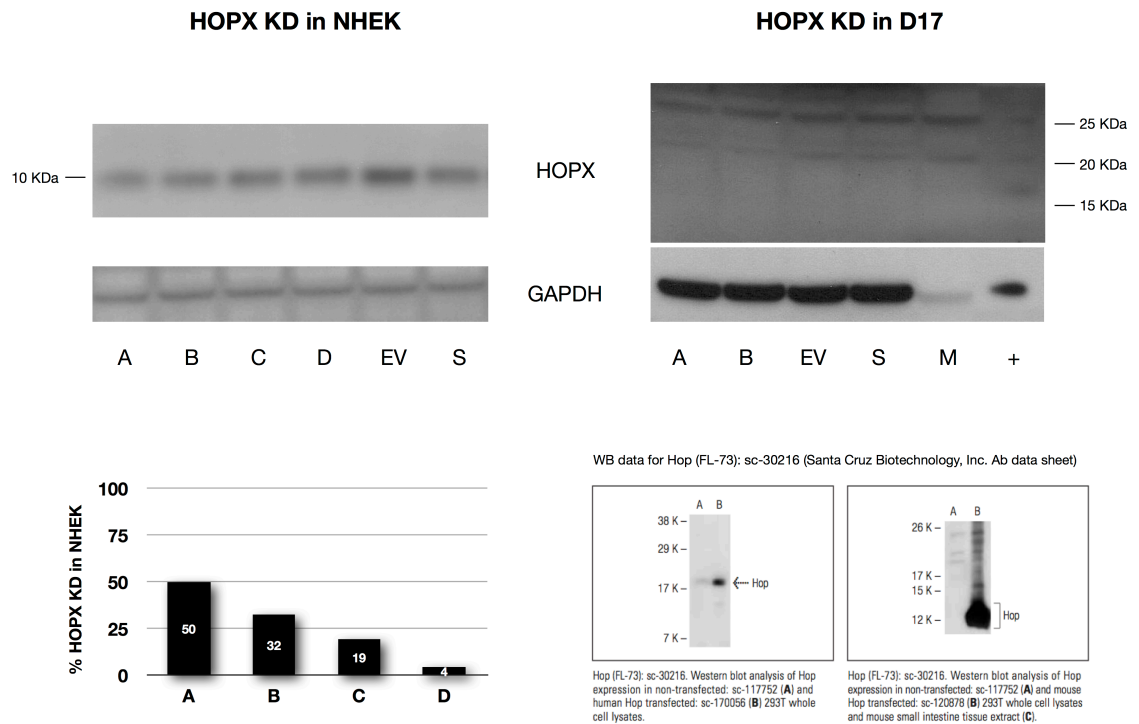
Figure 7.4. Assessment of the level of HOPX knockdown induced by shRNA systems. HOPX KD in NHEK (left) and in D17 oral keratinocyte dysplasia (right). Densitometry analysis was performed in NHEK using Image J software and results normalised against GAPDH. Level of KD obtained by the hairpins was calculated in relation to the scrambled control and plotted as a percentage. A, B, C and D correspond to 4 different shRNA hairpin sequences. EV and S are the empty vector control and scrambled control, respectively. M (mock control) corresponds to mock infection. + = human HOPX positive control sc-170056 (293T lysate).

Next, shRNA sequences A and B were used to attempt HOPX knockdown in the keratinocyte oral dysplasia D17 (Fig. 7.4 HOPX KD in D17), using the same procedure described for NHEK. Whilst western blot analysis in NHEK revealed a single (and what seems to be) specific band for HOPX at 10 KDa, in D17 generated several apparently unspecific bands. I have obtained products corresponding to 20, 22 and 25 KDa which were also present in the positive control used (293T lysate recommended by Santa Cruz Biotechnology). Of note was also the fact that that the HOPX signal in NHEK was a lot stronger than in D17 as can be seen by the higher level of background in D17 blots due to double the exposure time for these films. HOPX has been shown to be down-regulated in D17 (Hunter *et al*, 2006). It is, therefore, possible that the bands

obtained for D17 were unspecific and the product of specific size was not detected due to low levels of expression of HOPX protein in these cells. However, Santa Cruz Biotechnology (Fig 7.4), did report band sizes of approximately 20, 22 and 25 KDa in human cells. The data sheet suggests that the most specific band generated with this antibody against HOPX corresponds to 20KDa. Whichever the case, the signal of bands at 20 and 25 KDa did seem to have been affected by the expression of the hairpins, with sequence A generating a greater signal reduction, followed by sequence B (as I previously observed and measured in NHEK). Consequently, I have not been able to accurately assess and measure the level of HOPX KD in D17 following expression of hairpins A and B.

The overall distinct migration pattern observed in D17 (NHEK do not generate any additional bands of higher molecular weight) hints that different HOPX isoforms might be selectively expressed in keratinocytes originating from oral and epidermal tissues. A total of 5 transcript variants encoding for 3 distinct protein isoforms (NCBI Gene database ID: 84525), as a result of alternative splicing patterns and expression controlled by 2 distinct promoters (Yamashita *et al*, 2008), have been described so far for the human HOPX gene (Fig. 7.5). According to the NCBI database, variants 2, 3 and 4 encode for protein isoform b, variant 1 for isoform a and variant 5 for isoform c.
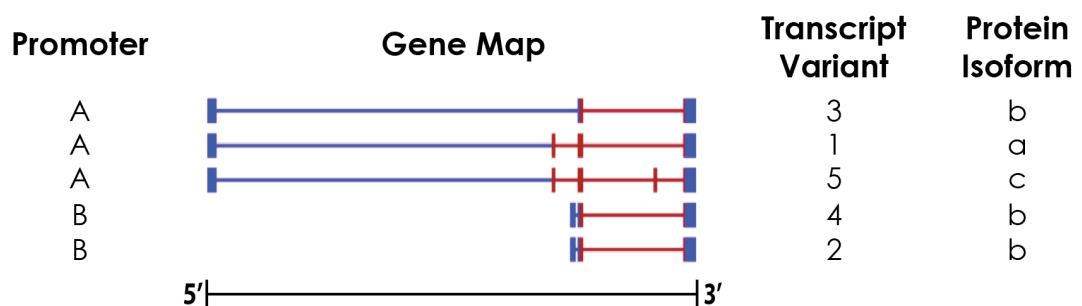
Figure 7.5. Gene expression products described for the human HOPX locus. Isoform a = 91aa (10.4 KDa); isoform b = 73aa (8.3 KDa); isoform c = 112aa (12.5 KDa). Legend: coding region; untranslated region.

My western blot data suggests that protein isoform a, product of expression of splice variant 1, is the predominant HOPX isoform in epidermal keratinocytes and two recent studies have reported similar results (Yang *et al*, 2010; Obarzanek-Fojt *et al*, 2011). I also predict that an isoform of higher molecular weight might be the main one expressed in oral keratinocytes and others (K. Hunter, University of Sheffield, personal communication) have found that in fact protein isoform c, product of transcript variant 5, is the main HOPX isoform found in keratinocytes of oral origin. Therefore, since epidermal keratinocytes seem to predominantly express HOPX protein isoform a and oral keratinocytes isoform c, an shRNA design strategy directed specifically at transcript variant 1, in case of NHEK, and at transcript variant 5, in case of D17, could possibly result in higher KD efficiency. Finally, given the difficulty in detecting protein levels of HOPX in D17, knock-down could alternatively be assessed by looking at reduction of transcript (by qPCR analysis) rather than of protein levels, following expression of shRNAs.

Next I investigated the distribution of HOPX at the cellular level, anticipating the possibility of extending this analysis to human tissue. I have, therefore, optimised the staining conditions in cultured keratinocytes for a commercial antibody against HOPX which has been reported in the literature (Ooki *et al*, 2010). Predominant nuclear staining was selectively obtained in normal keratinocytes (NHEK) in contrast with a squamous cell carcinoma (SCC) line expressing telomerase (SCC-25), used as negative control. I have also observed some cytoplasmic staining mainly in cells at the centre of the colony in NHEK, as opposed to low background cytoplasmic levels displayed in SCC-25 (Fig. 7.6). Recent studies in normal human epidermal keratinocytes confirm a nuclear localisation for HOPX (Yang *et al*, 2010) but also migration of the protein to the cytoplasm during terminal differentiation (Obarzanek-Fojt *et al*, 2011). This is coherent with the fact that NHEK colonies grow from the centre to the periphery and stratify at the centre of the colony as a result of the normal program of differentiation, active in cells cultured in the 3T3 'feeder' system. Therefore, HOPX is mainly present in the nucleus but can also be found in the cytoplasm of normal epidermal keratinocytes occupying stratification areas.
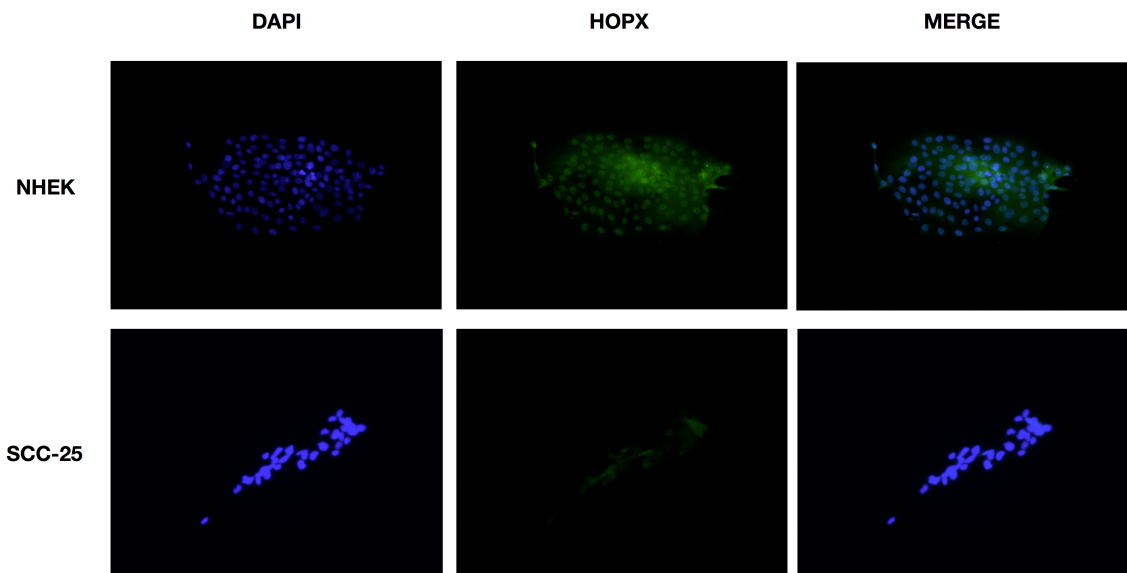
Figure 7.6. Optimisation of immunocytochemistry conditions for detection of HOPX protein at the cellular level. Staining shows predominant nuclear localisation for HOPX in NHEK, but also some protein present in the cytoplasm of a subset of cells (mainly at the centre of the colony). In contrast, the SCC-25 cell line used as a negative control shows low levels of cytoplasmic staining for HOPX. Legend: NHEK = normal human epidermal keratinocytes; SCC-25 = squamous cell carcinoma cell line 25.

7.3. Functional analysis of HOPX

I intended to conduct a functional analysis of HOPX in keratinocyte TDIS in three stages. The first would involve the use of shRNA constructs against HOPX followed by superinfection with the well characterised dominant negative mutant of TRF2 (TRF2$^{\Delta B \Delta M}$) in order to induce senescence via telomere dysfunction. If HOPX is a key intervenient in the signalling pathway from dysfunctional telomeres to senescence, HOPX knock-down should block or mute premature telomere-driven senescence, in newborn keratinocytes used at early passage, by allowing cells to resume proliferation. Re-entry of the keratinocytes into the cell cycle can be assayed by Ki67 staining. The second stage would be to extend this to a natural epithelial model of telomere dysfunction, the oral dysplasia D17 which is characterised by having deletions in the *INK4a* locus therefore resulting in inactive p14^{ARF} and p16^{INK4a} proteins, despite retaining functional p53 (McGregor *et al*, 2002). This means that these oral keratinocytes show an extended lifespan (maximum reported of 45 MPDs) but are still capable of undergoing senescence through replicative exhaustion. Therefore, the D17 dysplasia is mortal but does not undergo premature STASIS via p16^{INK4a}, senescing only as a consequence of telomere erosion at the end of its replicative lifespan or via other p53-activating stimuli. Further extension of D17's replicative lifespan as a consequence of HOPX knock-down would solidify its role in keratinocyte TDIS. Finally, the third stage would be to demonstrate an age-related increase of HOPX expression in older human skin, when compared to young skin, especially in pools of senescent cells characterised by dysfunctional telomeres.

Due to technical difficulties in expressing TRF2$^{\Delta B \Delta M}$ in keratinocytes using an indirect strategy for retroviral transduction (described in Chapter 5), I decided to proceed straight to the D17 dysplasia. Late passage (> 40 MPDs) D17 oral keratinocytes were transduced with amphotropic retroviral particles carrying shRNA sequences A or B against HOPX, the shRNA scrambled sequence (scrambled control, S) or vector only (empty vector control, EV) and subjected to drug selection (10 μg/mL blasticidin) 24h after infection. A mock infection, using the exact same procedure but with supernatants from non-transfected Phoenix A cells, was conducted in parallel as a control (mock control, M). I have also applied the same experimental procedure to D17 cells expressing the catalytic subunit of telomerase, TERT. Since TERT expression

restores telomere length and these cells have no p16^{INK4a} checkpoint, TERT is sufficient to immortalise D17 keratinocytes (Muntoni *et al*, 2003). Therefore, I expected HOPX knock-down to have no effect on the predicted proliferation pattern for D17-TERT cells.

Assuming a KD efficiency of 50% for hairpin A and 32% for hairpin B in D17s, as I previously demonstrated in NHEK (Section 7.2), in case of a potential role of HOPX in keratinocyte TDIS, I expected a stronger phenotype in D17 expressing shRNA A than shRNA B. Confirmation of reduction of both mRNA, by qPCR analysis, and protein levels, by western blotting and densitometry analysis, was not conducted for this experiment due to time constraints and technical difficulties in detecting HOPX protein in D17s (Section 7.2). Preliminary results (Fig. 7.7), resulting from a single experiment, show firstly some variation in maximum replicative lifespan between D17 and D17-neo cells (EV control for the TERT construct) with the first undergoing a maximum of 43 MPDs and the latter 46 MPDs. This difference is unlikely due to possible induction of premature senescence from exposure to the drug selection agent as cells in the mock control for both populations, which were not exposed to blasticidin, show a matching replicative limit. The D17-neo population underwent a maximum number of PDs that matches the maximum reported for this oral dysplasia, of around 45 MPDs (McGregor *et al*, 2002). The exception in the D17 population were cells expressing hairpin B, which underwent 3 additional population doublings when compared to D17s expressing all other shRNA constructs and mock control (46 MPDs versus 43 MPDs). However, the fact that hairpin A did not cause the same effect in D17s and that the extension of lifespan matches the limit obtained in neoEV-expressing D17 cells, regardless which shRNA construct they were expressing, suggests that the lifespan extension in D17s might not be related to expression of the hairpin. Basically, the increase was modest and did not surpass the maximum reported for this cell line and might just reflect variation within the cell population. As expected, D17-neoTERT keratinocytes went over the maximum replicative lifespan by more than 20 population doublings suggesting immortalisation via ectopic expression of telomerase. These cells, containing repaired telomeres, were not affected by expression of either of the hairpins against HOPX. Therefore, so far, the data suggest that HOPX might not have a functional role in keratinocyte TDIS.
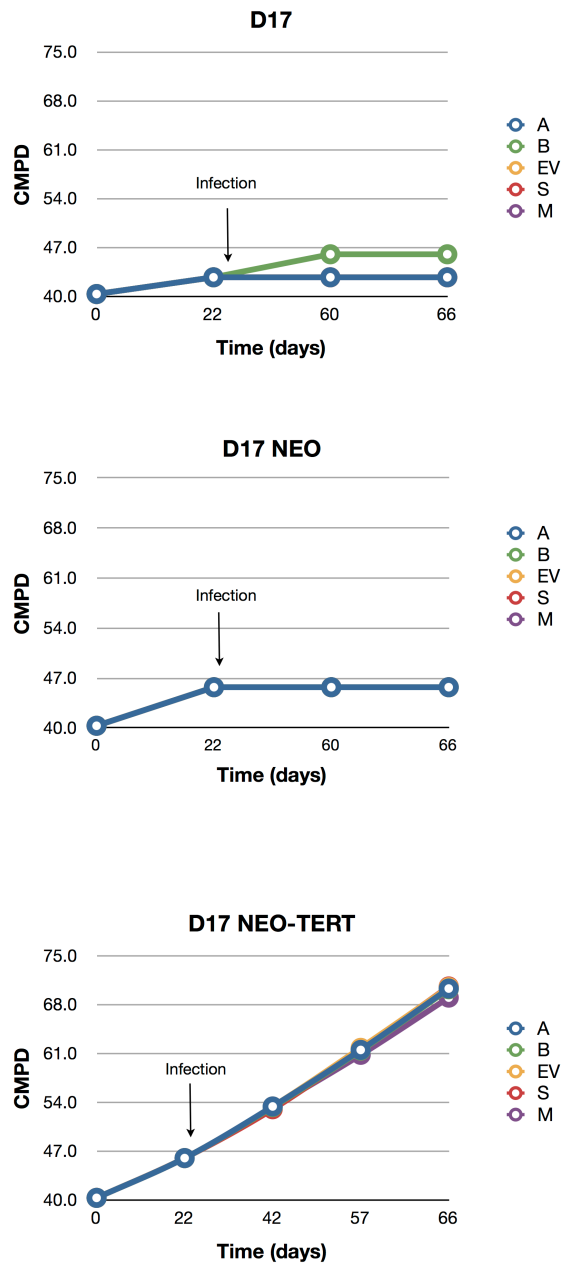
Figure 7.7. Effect of HOPX knockdown in the replicative lifespan of oral keratinocyte dysplasia D17. Hairpin containing shRNA sequence B caused extension of the replicative lifespan in D17 by 3 MPD but did not affect TERT-expressing D17 keratinocytes. D17 and D17-TERT expressing keratinocytes, at 40 MPDs, were transduced with retroviral vectors expressing shRNA constructs (A and B) against HOPX, vector only (EV) or scrambled (S) control and drug selected with blasticidin. A mock (M) infection control, not subjected to drug selection, was also included. Legend: CMPD = cumulative mean population doublings; Time = time in culture; Infection = indicates introduction of the shRNA constructs by retroviral transduction.

However, it was not possible to state conclusively that ablation of HOPX function did not have an effect at the cellular level. First, there is the question of whether the shRNA sequences used caused the same level of KD in D17 as they did in NHEK and second, whether this level of KD is sufficient to elicit a phenotype. Unless I had access to a positive control for HOPX KD where enough of the transcript is targeted to deplete the cellular levels of protein enough to ablate function and generate a cellular phenotype, it would be difficult to distinguish between a truly negative result and a technical limitation. As it is apparent that different transcript variants are expressed predominantly in either epidermal or oral keratinocytes, a more targeted hairpin design to the relevant mRNA sequence might improve KD efficiency. An alternative might also be to try and use siRNAs in very nearly senescent D17s followed by assessment of re-entry in the cell cycle by staining for Ki67, and of senescence, by staining for SA-β galactosidase. Cells originating from a dysplasia line should be more receptive to transfection than normal keratinocytes and siRNAs are more efficient KD tools, but the fact that this is is a transient system will make if difficult to retain a phenotype for more than a week. The difficulty in detecting the low levels of HOPX protein levels present in oral dysplasias would still remain a challenge. This can be circumvented by using qPCR analysis to assess the decrease in transcript instead. The use of this method to assess KD is not as accurate though since reduction in mRNA levels does not always reflect an equivalent reduction in protein levels. Therefore, to conclusively determine the role of HOPX in keratinocyte TDIS additional experiments and possibly a different experimental approach may be required.

To assess the role of HOPX in TDIS *in vivo* consent has been requested at the beginning of the project for the use of samples of human skin obtained from bat-ear corrections and other facial and ear procedures such as mastoidectomy, meatoplasty and tympanoplasty. These were to be collected from Hospitals under the jurisdiction of the Greater Glasgow Health Board and snap frozen in liquid nitrogen, prior to storage and use. The intention would be to assess HOPX by indirect immunofluorescence (ICC) using the antibody we have acquired and for which an ICC procedure was optimised (Fig. 7.5). In some experiments some sections were to be double stained for HOPX and 53BP1 to assess the relative sensitivity of the two methods. The actual age of each sample would be assessed using SAHF and Mcm antibodies as above.

Since authorisation was not granted for the use of human skin obtained from biopsies, I have established a collaboration with Dr Utz Herbig's lab (New Jersey, NY, USA) to investigate the abnormal expression of HOPX in human tissue containing epidermal cells harbouring dysfunctional telomeres.

Dr Herbig had samples of epidermis flanking melanotic naevi, where most cells are undergoing TDIS, and lab member Neetu Razdan examined the expression of HOPX in these samples at my request (Fig. 7.8). Although melanocytes (Fig. 7.8 red) in the dysplastic naevi have dysfunctional telomeres (Suram *et al*, 2012), as assessed by the colocalisation of DNA damage foci with the telomeres (Takai *et al*, 2003), they do not express HOPX, as they show staining only at background levels. In these samples, we found that HOPX expression was mainly confined to the keratinocytes in the upper layers of the epidermis (Fig. 7.8 green in top and bottom rows), observation that is consistent with previous reports of HOPX distribution in the skin (Yang *et al*, 2010). However, HOPX-positive keratinocytes were also present in unusual locations of the epidermis (Fig. 7.7 green middle row) flanking nevi. This stochastic distribution in other layers of the epidermis raises the possibility that HOPX might be specifically expressed in keratinocytes undergoing TDIS. Therefore, it would be interesting to test whether the cells expressing HOPX in the lower layers of the epidermis also contain telomere dysfunction-induced DNA damage foci (TIF). This analysis is ongoing.
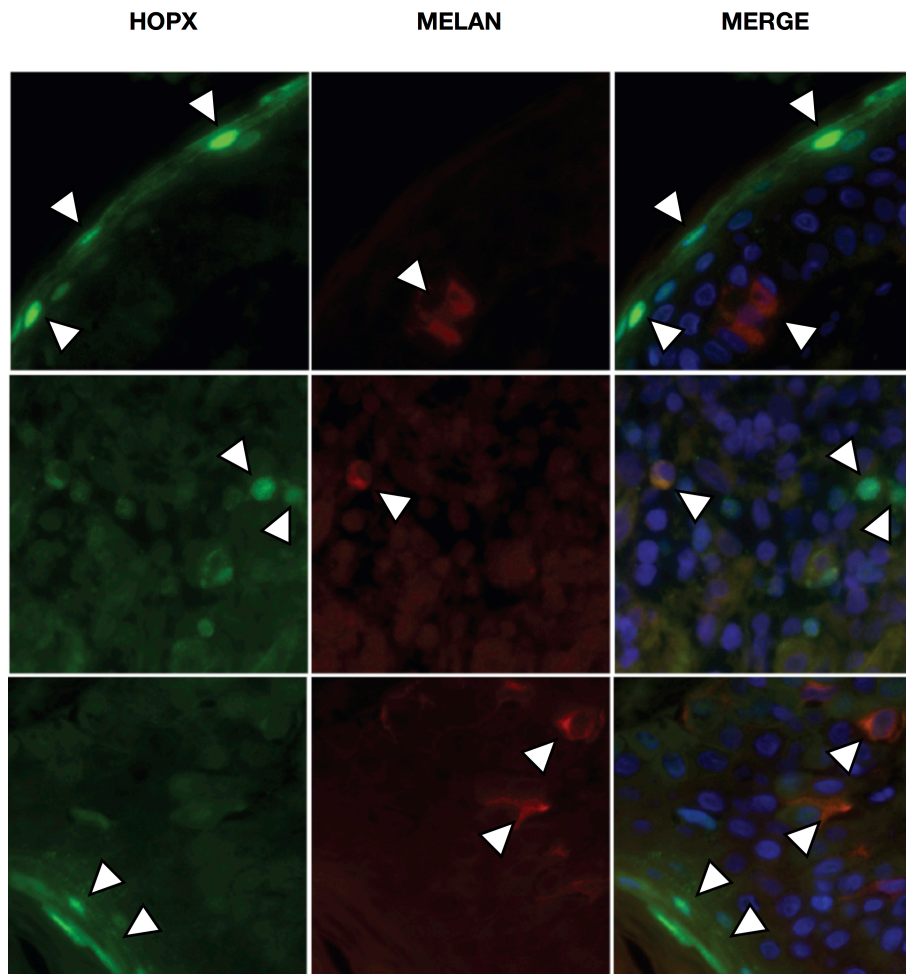
Figure 7.8. Expression of HOPX protein in dysplastic melanotic naevi. Staining revealed HOPX expression (mainly nuclear) predominant in cells of the upper layers of the epidermis (left panels top and bottom) but also in other locations (left centre). Melanocytes are revealed in red and do not express HOPX (centre panels). Legend: HOPX; MelanA; DAPI. Work conducted by Neetu Razdan under the supervision of Dr Utz Herbig (Herbig's lab, UMDNJ, New Jersey, USA).

7.4. Discussion

Genes HOPX, HIST2H2BE, ICEBERG and S100A7 showed potential as specific markers for telomere dysfunction-induced senescence (TDIS) in keratinocytes (Minty *et al*, 2008) since their expression levels were elevated following telomere uncapping, and associated weak DDR, but returned to control levels following ectopic expression of telomerase. The main objective of the present work was to further assess their specificity to TDIS as opposed to DNA damage-induced senescence and other forms of senescence, and then select the lead candidate for further investigation.

Following the initial assessment of the candidates response to DNA damage-induced senescence I found that HOPX, ICEBERG and S100A7 were not induced either by a weak or a strong DDR ensued by low or high levels of DNA damage, respectively (Chapter 4). Whilst ICEBERG and S100A7 transcript remained at control levels, however accompanied by some inter-experimental variation, the amount of HOPX transcript was inversely proportional to the intensity of DNA damage being generated. Therefore, HOPX levels showed a consistent reduction trend with DNA-damage induced senescence contrasting with the previously observed elevation trend with telomere dysfunction-induced senescence. Based on these initial results HOPX seemed like the most interesting candidate to follow. However, both HOPX and S100A7 were particularly interesting genes from the beginning as their expression levels are also severely down-regulated in immortal keratinocytes (immortal dysplasias and carcinomas) that have p53 and p16^{INK4a} dysfunction as well as activated telomerase (E. K. Parkinson, unpublished microarray data). HOPX took precedence when several recent reports emerged confirming its role as a tumour-suppressor gene.

I started by assessing the potential functional role of HOPX in TDIS. I hypothesised that if HOPX plays an essential role in the pathway signalling dysfunctional telomeres towards growth arrest by senescence, the ablation of HOPX function should delay, prevent or reverse the establishment of the senescence program. The intention was first, to attempt stable KD of HOPX in newborn low passage NHEK expressing TRF2$^{\Delta B\Delta M}$, an artificial model of telomere dysfunction, and see if the senescent phenotype could be reversed in these cells. Then I would proceed to a natural model of telomere dysfunction, oral keratinocytes from the dysplasia line D17 which have dysfunctional p14^{ARF} and

p16^{INK4a} (due to deletion in the *INK4a* locus) but retain functional p53 and normal expression levels of telomerase. These cells are mortal and senescence naturally via telomere shortening at the end of their slightly extended replicative limit; I would investigate whether HOPX KD could further extend the replicative lifespan of these cells.

Stable KD of HOPX was established in NHEK by expression of shRNAs via retroviral transduction. However, the best hairpin rendered just a maximum of 50% reduction in HOPX protein levels in NHEK. Concomitantly, due to technical difficulties in expression of TRF2$^{\Delta B\Delta M}$ in NHEK using a previously reported successful transduction strategy in keratinocytes (Levy *et al*, 1998) I had to first optimise this technique to the required experimental conditions for this construct (Chapter 5). Therefore, I decided to proceed directly to the keratinocyte D17 dysplasia. This came with its own set of technical challenges. Western blotting analysis revealed several bands for HOPX protein none of which matching the predicted size of the protein isoforms and, since HOPX is down-regulated in oral dysplasias, I suspected the bands obtained were unspecific and the antibody used could not detect the low levels of HOPX protein in D17 cells. Nevertheless, I have transduced D17s with the two best hairpins against HOPX, previously optimised in NHEK. Results indicated that HOPX KD may extend D17 replicative lifespan very slightly and did not affect the growth of D17 ectopically expressing telomerase which have, therefore, repaired their telomeres. The observed increase was, however, not noteworthy or consistent (between 2 populations of D17). This could be because HOPX has no active role in a signalling pathway signalling dysfunctional telomeres in keratinocytes towards senescence. Alternatively, it might be because the amount of KD obtained, with the experimental strategy used, was not high enough to ablate HOPX function to a level capable of generating a cellular phenotype. Therefore, these results are inconclusive in what concerns the functional role of HOPX in keratinocyte TDIS.

HOPX homeobox is a relatively recently identified gene. The literature and gene databases are not always in agreement in terms of information regarding its transcript variants and protein isoforms. New data is now emerging faster due to the recent interest in HOPX for its tumour suppressor activity and this has also prompted the development of new, and hopefully more specific and efficient, experimental tools such as antibodies, siRNAs and shRNAs. For instance, since it has become apparent that epidermal and oral keratinocytes

predominantly express different HOPX transcript variants which result in distinct protein isoforms, RNAi efficiency could be greatly improved by targeting the relevant mRNA sequence. Therefore, an improvement in experimental design by acquiring more specific tools should allow us to generate conclusive results in future.

The final aim was to assess the lead candidate as a potential *in vivo* marker for TDIS in keratinocytes. Although HOPX is not a secreted protein, its potential specificity to TDIS would be very appreciated as it could be used to identify telomere-driven senescent cells *in vivo*. The original intention was to compare HOPX expression in skin from young and old persons. However, I was unable to acquire the skin samples for analysis and instead established a collaboration with Herbig's lab for the analysis of HOPX expression in melanocytic naevi. In these benign skin lesions most cells display hallmarks of TDIS (Suram *et al*, 2012) such as DDR foci that colocalise with dysfunctional telomeres (TIF) and high levels of heterochromatic proteins (macroH2A). Although the dysfunctional telomeres in melanocytes are not critically short and retain TRF2 they are fragile due to the accumulation of telomeric DNA lesions and stochastic telomere attrition, resulting from replication stress associated with oncogene-induced senescence (OIS). We have found that HOPX was not expressed in melanocytes of naevi but only in keratinocytes of the upper layers of the epidermis and stochastically in keratinocytes of the supra-basal layers. Dr Herbig (personal communication) has also observed that the presence of keratinocytes with dysfunctional telomeres in these naevi is sporadic and apparently unrelated to ageing. This could mean that telomere dysfunction is not the major driving force behind keratinocyte stem cell ageing, but equally could be related to the fact that senescent keratinocytes may have a short tenure in the epithelium as a result of terminal differentiation (Chapter 4) or as a result of clearance by the innate immune system (Xue *et al*, 2007).

These results are inconclusive regarding a functional role of HOPX in keratinocyte TDIS or its use as a specific marker for TDIS *in vivo*. Nevertheless, whilst HOPX might not be actively involved in the pathway that signals dysfunctional telomeres in keratinocytes, its up-regulation seems to be specific to telomere dysfunction-induced senescence (TDIS) as opposed to DNA damage-induced senescence (Chapter 4) or STASIS, stress or aberrant signalling-induced senescence (Chapter 5). HOPX has been associated with terminal differentiation in cardiac (Kook & Epstein, 2003) and skeletal muscle

(Kee *et al*, 2007), in the lens (Vasiliev *et al*, 2007) and in the skin (Yang *et al*, 2010; Obarzanek-Fojt *et al*, 2011). In epidermal keratinocytes I also observed this association (Chapter 4) and HOPX is also known to induce other terminal differentiation markers in the epidermis (Obarzanek-Fojt *et al*, 2011). Therefore, if TDIS ultimately engages the terminal differentiation program in keratinocytes this will place the stem cell pool under increased replicative stress and stem cells are known to be prone to poor clonal growth with increasing age perhaps as a result of premature transit cell differentiation or senescence. Impaired stem cell function contributes indirectly to epidermal stem cell ageing.

Chapter 8. General Discussion and Future Perspectives.

Cellular senescence and *in vivo* ageing

A connection between the process of replicative senescence in cultured cells and organismal ageing was first proposed by Hayflick and Moorhead in the 1960s (Hayflick & Moorhead, 1961) and the nature of this relationship has been a matter of extensive investigation over the following decades. The prevalence of senescent cells has been shown to directly correlate with chronological age in animal models (Jeyapalan *et al*, 2007; Janzen *et al*, 2006) and in humans (Dimri *et al*, 1995; Ressler *et al*, 2006). Telomere dysfunction is relevant to epithelial ageing as its causal role has been demonstrated in mice (Lee *et al*, 1998; Rudolph *et al*, 1999) and also because telomeres are shorter in the epidermis of older humans (Lindsey *et al*, 1991; Nakamura *et al*, 2002; Sugimoto *et al*, 2006). In fact, human telomeres shorten with age in several human tissues where, by definition, the stem cells are responsible for the telomere length of the tissue (reviewed in (Sharpless & DePinho, 2007)). However, whether overall telomere length correlates with chronological age has been a controversial matter. Whilst some report a low rate of telomere loss with ageing in the epidermis apparently due to telomerase activation (Krunic *et al*, 2009), several groups report consistent tissue-specific loss of telomeric DNA with age in human skin, both in the epidermis and dermis, and oral epithelium (Lindsey *et al*, 1991; Nakamura *et al*, 2002; Sugimoto *et al*, 2006). Of note is that the methodology used by these groups to measure telomere length varies from southern blotting to *in situ* hibridisation, but techniques such as STELA, which can detect the shortest telomeres in a cell population, has not yet been applied to human epidermis. However, mean telomere length is a poor indicator of the telomere status of a tissue since the shortest telomere is capable of triggering senescence (Hemann *et al*, 2001). Furthermore, telomeres may not need to be critically short to contribute to ageing as Tomás-Loba *et al* have shown that TERT targeted to the epidermis improved lifespan and health span of cancer-resistant mice and that this was associated with increased telomere function (Tomás-Loba *et al*, 2008). The mechanism by which dysfunctional telomeres cause senescence is not completely clear. Identification of more specific markers for TDIS can aid the treatment of epithelial ageing as they can be potential targets for therapeutic intervention.

Ideally, *in vivo* markers should be cell- and mechanism-specific as well as non-invasive to facilitate early detection and allow for prompt therapeutic intervention. Reliable bio markers for telomere dysfunction are lacking and the ones identified so far are not specific as they are also up regulated by DSBs in non-telomeric DNA and infection (Jiang *et al*, 2008). Telomere-associated DSBs can be detected as DNA damage foci, also known as telomere dysfunction-induced foci or TIFs (Takai *et al*, 2003) but such complexes may be transient and insensitive indicators of telomere dysfunction (Jeyapalan *et al*, 2007). Firstly, because the complete loss of a telomere may not score as a TIF, merely a DSB and also, because as TIFs do not accumulate with age in human epidermis (U. Herbig, personal communication), they are unlikely to be reliable indicators of telomere dysfunction in this cell type. Secondly, previous work from our group has shown that experimental telomere uncapping following the ectopic expression of TRF2$^{\Delta B \Delta M}$ or following replicative senescence does not result in a dramatic increase in DNA damage foci (Minty *et al*, 2008) or a strong DDR (Muntoni *et al*, 2003; Minty *et al*, 2008).

In addition, the cell cycle inhibitor p16^{INK4a} is a robust biomarker of ageing in human skin (Ressler *et al*, 2006) and, using a novel approach to delete p16^{INK4a}-positive cells in the *BubR1* progeroid mouse model, Baker *et al* (Baker *et al*, 2011) showed that several age-related phenotypes such as muscle weakness, fat loss and cataracts were delayed when p16^{INK4a}-positive cells were deleted and all but cataracts were reversed when p16^{INK4a}-positive cells were deleted in aged animals. However, when human keratinocytes were induced to senesce following the expression of TRF2$^{\Delta B \Delta M}$ no acute induction of p16^{INK4a} was observed, suggesting that the initial events following telomere uncapping do not induce p16^{INK4a}.

Keratinocyte stem cell ageing

Although it is agreed that human skin thins and shows diminished function with chronological age it has been suggested that this is not the result of keratinocyte stem cell ageing but only due to mesenchymal ageing (Stern & Bickenbach, 2007; Giangreco *et al*, 2008). Epithelial stem cells do not get depleted with increasing age *in vivo* (Martin *et al*, 1998b; Giangreco *et al*, 2008). However, their function does appear to become impaired, as evidenced by a reduced clone size following damage by ionising radiation in murine intestine (Martin *et al*, 1998a; 1998b), and this may contribute to tissue deterioration. Thus, epithelial stem cells under-perform in response to injury and at least some of this is likely to be due to accumulation of DNA damage (Velarde *et al*, 2012) and to the intrinsic properties of the aged human keratinocytes themselves (Barrandon & Green, 1987) and not only to the senescence of the mesenchyme (Giangreco *et al*, 2008). In the haematopoietic system, the action of the senescence effector p16^{INK4a} regulates stem cell ageing through the stem cells themselves and also through the mesenchyme (Janzen *et al*, 2006; Sharpless & DePinho, 2007). In experiments using the p16^{INK4a} knockout mouse it has been shown that stem cells retain their function better when p16^{INK4a} is absent (Sharpless *et al*, 2001) and although no epidermal stem cell ageing phenotype has been reported in p16^{INK4a}-deficient mice this could be explained by the report that p15^{INK4b} compensates for p16^{INK4a} in the epidermis of these animals (Krimpenfort *et al*, 2007). It has been hypothesised that silent changes in the stem cells manifest themselves only when asymmetric divisions generate transit amplifying (progenitor) cells, whereupon p16^{INK4a} directs premature senescence and reduced tissue function ((Sharpless & DePinho, 2007) and Fig. 8.1).
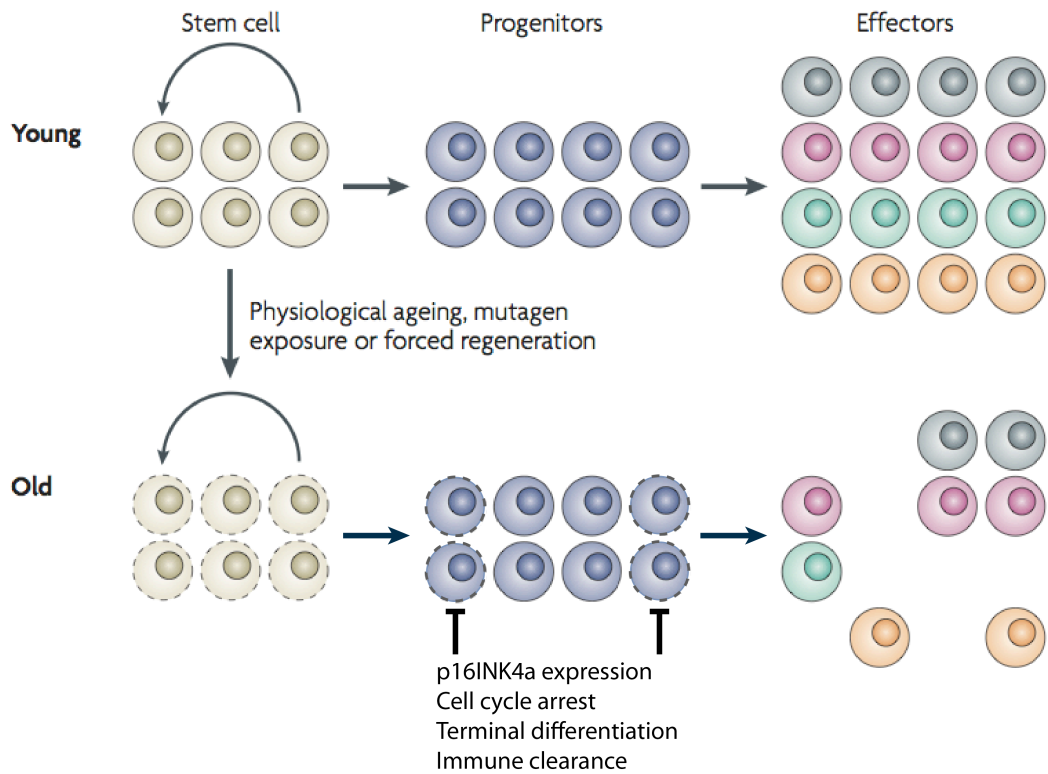
Figure 8.1. *INK4a* **expression and stem cell ageing.** Impaired stem cell function is manifested in the stem cells reduced ability to originate functional progenitors. With ageing, and upon asymmetric division, p16[INK4a] expression directs premature senescence thereby removing cells from the progenitor pool and consequently affecting the regenerative capacity of the tissue. Premature senescence can also be driven by DNA damage or telomere dysfunction which can lead to terminal differentiation and immune clearance with a similar outcome for the renewing capability of the tissue (adapted from (Sharpless & DePinho, 2007)).

p16^{INK4a}- (Ressler *et al*, 2006; Waaijer *et al*, 2012) SA-βGal (Dimri *et al*, 1995) positive keratinocytes do accumulate with age in human skin but they are generally singletons and limited to the basal layer (Fig. 8.2) rather than in groups or columns. This suggests that p16^{INK4a} expression does not lead to terminal differentiation of the keratinocytes expressing it and, furthermore, that they have a short tenure in the epidermis. This could be explained on the grounds that senescent cells are known to be targeted by both the innate (Xue *et al*, 2007; Ventura *et al*, 2007) and adaptive (Kang *et al*, 2011) immune system and thus may turn over rapidly.
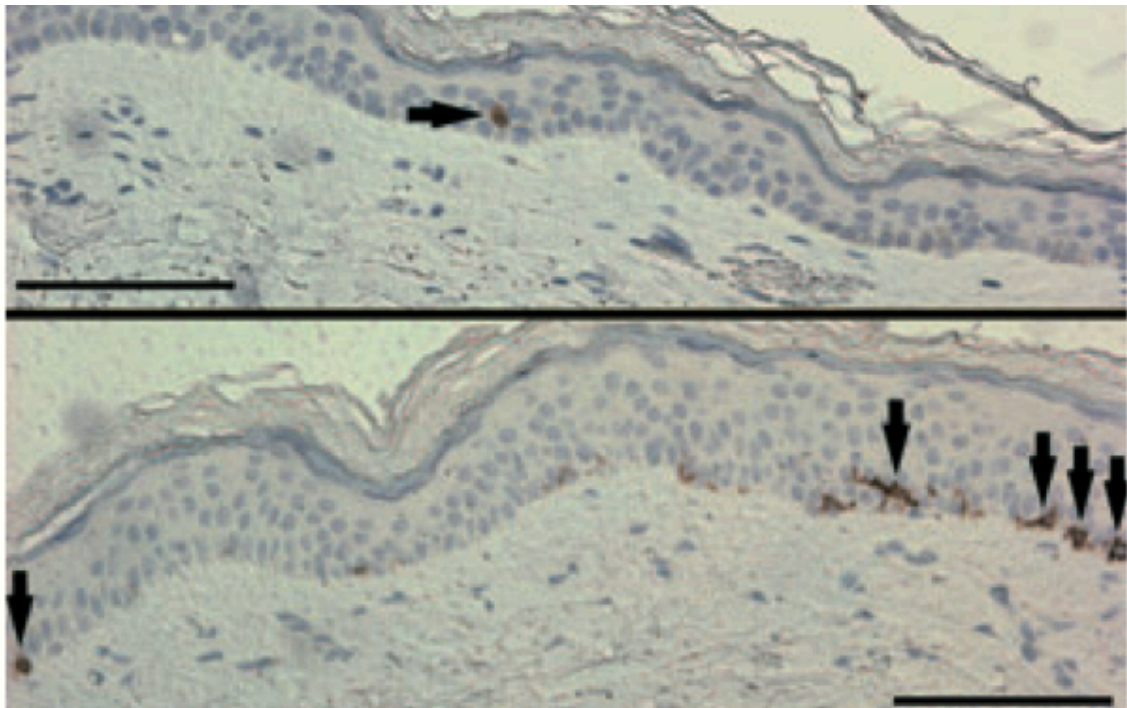
Figure 8.2. p16^{INK4a} expression in human epidermis. p16^{INK4a}-positive cells (arrows) accumulate as singletons in the epidermis of older persons (bottom panel) when compared to younger persons (top panel) and are confined to the basal layer (*in* (Waaijer *et al*, 2012)).

An increase in p16^{INK4a} expression with serial passage in culture correlated with keratinocyte clonal exhaustion and p16^{INK4a} inactivation was shown to be required, in addition to hTERT expression, in order to achieve immortalisation (Rheinwald *et al*, 2002). Although p16^{INK4a} knock-down alone is not sufficient to extend replicative lifespan in most cases (Rheinwald *et al*, 2002) this may be due to technical insufficiency and poor knockdown (Maurelli *et al*, 2006). For instance, we have found (Parkinson, unpublished results) that the use of the transcriptional repressor of the *INK4a* locus Bmi-1 as opposed to shRNAs against p16^{INK4a} has proved more efficient in sustaining p16^{INK4a} inactivation, supporting the findings of others (Maurelli *et al*, 2006; Haga *et al*, 2007). Since Bmi-1 knocks down both products of the *INK4a* locus, p14^{ARF} and p16^{INK4a}, and nearly all immortal keratinocytes in neoplasia have deletions of *INK4A* both *in vitro* (Munro *et al*, 1999) and *in vivo* (Reed *et al*, 1996) this suggests that the co-deletion of p14^{ARF} and p16^{INK4a} may be a requirement for immortalisation.

Admittedly, it is possible that p16^{INK4a} and not telomere dysfunction might be the major contributor to stem cell ageing in the epidermis. As shown by immunocytochemistry analysis, p16^{INK4a} expression directly correlates with donor age in human skin *in vivo* and, conversely, Bmi-1 was significantly down-regulated with increasing age (Ressler *et al*, 2006). Inactivation of p16^{INK4a} *in vitro*, using an anti-sense strategy, in cells retaining high proliferative potential and not in transient amplifying keratinocytes blocks clonal evolution, averts senescence and retains keratinocytes in the stem cell compartment (Maurelli *et al*, 2006). Also in both physiological and premature ageing Bmi-1 down-regulation and expression of p16^{INK4a} were shown to strongly correlate, with Bmi-1 over-expression resulting in reduced p16^{INK4a} activity and increase in clonogenicity (Cordisco *et al*, 2009). These data suggests that in epidermal cells inactivation of p16^{INK4a} accompanied by expression of Bmi-1 are necessary to maintain stemness and that the opposite results in clonal exhaustion and senescence during ageing. Finally, the expression of p16^{INK4a} in the epidermis (but not the dermis) is a strong indicator of physiological age (Waaijer *et al*, 2012). However, I could find no evidence that experimental uncapping of telomeres in human keratinocytes was capable of inducing the p16^{INK4a} transcript (Chapter 6), which generally correlates with p16^{INK4a} protein levels (Hara *et al*, 1996).

Telomere dysfunction-induced senescence and DSBs

Recently, a strong association between the accumulation of permanent damage to the DNA and the processes of senescence and ageing has been established (Sedelnikova *et al*, 2004; Fumagalli *et al*, 2012; Hewitt *et al*, 2012) suggesting that unrepairable DSBs have a causal role in mammalian ageing.

In normal human cell strains, of both mesenchymal and epithelial origin, the incidence of ɣ-H2AX foci and of SA-β gal-positive cells increases towards the end of their replicative lifespan. Similarly, the same trend for cryptogenic ɣ-foci is observed with increasing age in several murine tissues. They colocalise with several repair proteins and, therefore, mark persistent DNA lesions containing irreparable DSBs (Sedelnikova *et al*, 2004). DNA DSBs also accumulate following radiotherapy in mice (Le *et al*, 2010) and in fibrosis in humans (Pitiyage *et al*, 2011), where they are associated with senescence. Terminal DNA normally goes undetected by the cells' DNA repair machinery because it is organised in a protective nucleoprotein complex which prevents exposure of chromosomal ends (de Lange, 2005). However, telomeric DNA can become exposed and processed as a DSB following telomere shortening or telomere dysfunction (d'Adda di Fagagna *et al*, 2003; Takai *et al*, 2003). As a consequence of the end-replication problem telomeres become gradually shorter after each cell division and it has been observed that in replicatively senescent fibroblasts critically short telomeres associate with DNA damage foci and trigger a DDR which results in senescence (d'Adda di Fagagna *et al*, 2003). Similar results were obtained in normal fibroblasts containing long telomeres but that have been rendered dysfunctional due to ectopic expression of the dominant negative mutant TRF2$^{\Delta B \Delta M}$, which strips telomeres off the endogenous telomere protection factor TRF2, essential for the formation of the protective telomeric loop (Takai *et al*, 2003; d'Adda di Fagagna *et al*, 2003).

These two areas were linked when it was shown that although DSBs do not particularly associate with the telomeres in replicatively senescent cells (Sedelnikova *et al*, 2004) or in ageing murine tissues (Wang *et al*, 2009), unrepairable DSBs do (Fumagalli *et al*, 2012; Hewitt *et al*, 2012). As previously demonstrated (Rodier *et al*, 2011), these two groups confirmed that the continuous DDR signalling which is responsible for sustaining the permanent cell cycle arrest associated with senescence, triggered in normal human fibroblasts

by IR-induced genotoxic stress, arises from persistent DNA damage foci which mark permanent DNA lesions. What was interesting was that these unrepairable DSBs, originating from genotoxic (Fumagalli *et al*, 2012; Hewitt *et al*, 2012) or oxidative (Hewitt *et al*, 2012) stress, were preferentially located at the telomeres. Moreover, irreparable damage to the telomeres was shown to occur in both mitotic and post-mitotic tissues *in vivo*, such as mouse neurons following whole body irradiation, as well as in neurons and hepatocytes of baboons (Fumagalli *et al*, 2012) and murine hepatocytes and enterocytes (Hewitt *et al*, 2012) with physiological ageing, and to correlate with senescence. A connection between telomere damage and ageing had only previously been reported in fibroblasts originating from the skin of baboons (Herbig *et al*, 2006). This occurs independently of telomere length and seems related instead to the fact that telomeres are specialised structures which resist DNA repair and are also particularly sensitive to damage (Fumagalli *et al*, 2012; Hewitt *et al*, 2012).

Both the structure of telomeric DNA and the telomere-associated protein TRF2 prevent DNA repair (Fumagalli *et al*, 2012). In yeast, when telomeric repeats were experimentally engineered adjacently to a DSB, the recruitment of DNA ligase IV to that area was impaired, inhibiting repair. Similarly, in mouse cells carrying the LacI-TRF2 fusion protein placing TRF2 next to a DSB site also specifically inhibited repair and resulted in the accumulation of persistent ɣ-H2AX foci. This is consistent with previous studies where it was shown that TRF2 prevents the occurrence of chromosome end-to-end fusions *in vivo* (van Steensel *et al*, 1998). The mechanism by which this occurs was demonstrated *in vitro* to be inhibition of ligase IV-mediated NHEJ as cells where telomeres were depleted of TRF2, by over-expression of the mutant TRF2$^{\Delta B \Delta M}$, displayed an increase in telomere fusions (Smogorzewska & de Lange, 2002). Later, it was further confirmed *in vitro* that telomere-associated proteins such as TRF2 and RAP1 directly inhibit both DNA-PK and ligase IV-mediated end-joining (Bae & Baumann, 2007). In sum, exposure of telomeric DNA resists repair and, therefore, triggers sustained DDR signalling by activation of the DNA damage checkpoint (Fumagalli *et al*, 2012). It has been argued (Fumagalli *et al*, 2012) that telomeres have evolved as specialised structures to protect the ends of linear chromosomes from end-to-end fusions by inhibiting NHEJ and that, as a consequence, became irreparable areas of the genome.

Telomeres are not only poor at repair but also preferred targets for certain types of DNA damage (Hewitt *et al*, 2012). They have been shown to be

particularly sensitive to oxidative stress (Petersen *et al*, 1998; Hewitt *et al*, 2012), radiation-induced (Hewitt *et al*, 2012) and drug-induced (Suram *et al*, 2012) genotoxic stress as well as oncogenic stress (Suram *et al*, 2012). This can be because telomeres repair UV lesions (Kruk *et al*, 1995) and ss-breaks (Petersen *et al*, 1998) less efficiently and do not repair DSBs (Fumagalli *et al*, 2012; Hewitt *et al*, 2012). It can also be for the fact that guanine triplets, which are part of the TTAGGG telomeric repeat, are particularly susceptible to oxidative modifications (Oikawa *et al*, 2001). Also, higher levels of ROS found in senescent fibroblasts seem to correlate with telomeric ɣ-H2AX foci (Passos *et al*, 2007a). More recently, it has also been shown that telomeres are hypersensitive to oncogene-induced and drug-induced replication stress (Suram *et al*, 2012). Since telomeric regions seem to be more sensitive to stress that other areas of the genome it has been argued that telomeres could have evolved as specialised sensors of DNA damage to enforce the senescence program (van Tuyn & Adams, 2012).

In all, this recent work (Fumagalli *et al*, 2012; Hewitt *et al*, 2012; Suram *et al*, 2012) suggests that in normal fibroblasts, as far as genotoxic stress is concerned, only DNA damage at the telomeres causes senescence since it is irreparable and, therefore, capable of triggering persistent DDR signalling. Unrepairable, but not repairable DSBs, induce the chronic expression of a variety of secreted proteins, such as cytokines, growth factors and proteases, known as the SASP or 'senescence-associated secretory phenotype' (Coppé *et al*, 2008; Rodier *et al*, 2009). The permanent DNA lesions thought to be responsible for sustaining the damage-induced growth arrest and SASP have been characterised and termed DNA-SCARS or 'DNA segments with chromatin alterations reinforcing senescence (Rodier *et al*, 2011). The secretome is largely (Freund *et al*, 2011) but not exclusively (McConnell *et al*, 1998) dependent on NF-Kβ signalling, which is associated with senescence (Rovillain *et al*, 2011; Vaughan & Jat, 2011). For instance, senescence induced by ectopic expression of p21^{WAF1} and p16^{INK4a} did result in activation of the plasminogen activator inhibitor (PAI-1) at the transcriptional level (McConnell *et al*, 1998). In fact, the SASP seems to be uncoupled from the senescence-associated cell cycle arrest (Rodier *et al*, 2011). Although p53 is required to initially trigger growth arrest (Campisi & d'Adda di Fagagna, 2007), the classical effectors of senescence p53 and p16^{INK4a} are neither required (Coppé *et al*, 2008) or in most cases sufficient (Coppe *et al*, 2011) to elicit a functional SASP.

TDIS in epidermal keratinocytes induces a weak DDR and induces markers of terminal differentiation

Telomere dysfunction, induced by expression of TRF2$^{\Delta B \Delta M}$, in normal human epidermal keratinocytes resulted in senescence and was accompanied by a weak DDR and a characteristic transcriptional profile (Minty *et al*, 2008). This included genes involved in chromatin remodelling (HIST2H2BE, a histone from the H2B family), inflammation (ICEBERG or CARD18, a caspase recruitment domain family member) and terminal differentiation (HOPX, an atypical homeobox gene and S100A7, a calcium binding protein of the S100 family) that showed potential as specific markers for TDIS in keratinocytes. This is because they were up-regulated by artificial telomere uncapping and natural telomere erosion, and down-regulated by telomere recapping following ectopic expression of telomerase (Muntoni *et al*, 2003; Minty *et al*, 2008). However, it was possible that the weak DDR was enough to trigger senescence and induce terminal differentiation in keratinocytes, as previously reported for melanocytes (Inomata *et al*, 2009) and HSCs (Wang *et al*, 2012). To test this hypothesis and to test the specificity of the candidate markers for TDIS I have tested the influence that other inducers of senescence such as radiation-induced DNA damage, p14^{ARF}, p16^{INK4a} and p53 might have on their expression levels.

The effect of the senescence effectors on candidate markers expression levels

Normal human epidermal keratinocytes were exposed to doses of ionising radiation capable of generating acute or permanent damage to the DNA (Chapter 4) or transduced with retroviral constructs expressing p14^{ARF}, p16^{INK4a}, p53 or TRF2$^{\Delta B \Delta M}$ (Chapter 6). Whilst S100A7, HOPX or ICEBERG were not induced by repairable or unrepairable DSBs (Chapter 4) or by the effector of senescence p16^{INK4a} (Chapter 5), ICEBERG and HOPX were induced by p53 and p14^{ARF} when these were ectopically expressed at higher levels (Chapter 5). The levels of initial growth arrest, as assessed by reduction in CCNA2 expression levels (Chapter 5) and irreversible growth arrest, as assessed by cloning efficiency (Chapter 6) were nearly identical following expression of each of the main effectors of senescence. Thus, S100A7 seems to be the most specific early

marker for telomere dysfunction in keratinocytes since it was selectively induced by telomere uncapping via expression of TRF2$^{\Delta B \Delta M}$ (Minty *et al*, 2008) and Chapter 6) and not by DSBs (Chapter 4) or by over expression of p14^{ARF}, p53 or p16^{INK4a} (Chapter 6). This is important because p16^{INK4a}-positive cells accumulate in the epidermis of elderly individuals (Ressler *et al*, 2006) and their number in the skin has been shown to inversely correlate with younger biological age in the offspring of long-lived humans (Waaijer *et al*, 2012). A recent paper reporting how glucocorticoids suppress the SASP and NF-Kβ signalling without affecting the senescence-associated growth arrest (Laberge *et al*, 2012) allied to the fact that keratinocyte growth medium contains hydrocortisone might explain the weak DDR following telomere uncapping in keratinocytes and why SASP components such as inflammatory cytokines were not detected in the microarray analysis of keratinocytes expressing TRF2$^{\Delta B \Delta M}$ despite the growth arrest (Minty *et al*, 2008). It is thus possible that most of the DDR is a consequence of the SASP and NF-Kβ signalling and also that the induction of S100A7, the most promising marker, may also be independent of the inflammatory cascade. This is in general agreement with recent data showing that the senescence effectors in general and p16^{INK4a} in particular do not induce the SASP (Coppe *et al*, 2011; Rodier *et al*, 2011). This raises the question of what upstream pathways activating p16^{INK4a} and p53, other than DSBs, regulate S100A7 (see future plans).

TDIS and terminal differentiation

Dysfunctional or critically short telomeres activate a DDR which triggers cell cycle arrest through senescence in fibroblasts (Takai *et al*, 2003; d'Adda di Fagagna *et al*, 2003; Herbig *et al*, 2004). However, our previous work showed that telomere dysfunction induced by TRF2$^{\Delta B \Delta M}$ in normal epidermal keratinocytes and by replicative senescence in the D17 keratinocyte dysplasia stopped cells from dividing but surprisingly did not induce high levels of DSBs or, in either case, a strong DDR (Muntoni *et al*, 2003; Minty *et al*, 2008). Instead, markers of terminal differentiation were induced and their expression was reversed by telomerase (Minty *et al*, 2008). This is in line with a recently reported link between stem cell ageing and terminal differentiation in response to DNA damage and telomere dysfunction (Inomata *et al*, 2009; Wang *et al*, 2012; Velarde *et al*, 2012).

In mice, irreparable DSBs, induced by IR, caused melanocyte stem cells (MSCs) to prematurely differentiate into mature melanocytes which ultimately resulted in hair greying, the most common ageing phenotype (Inomata *et al*, 2009). Additionally, both IR and telomere dysfunction result in an induction of lymphoid differentiation in favour of myeloid differentiation of murine HSCs. Lymphoid competent HSCs seem to be more sensitive to incremental DNA damage which affects their differentiation potential and ultimately limits their repopulation capacity (Wang *et al*, 2012). ATM deficiency protected MSCs from premature differentiation (Inomata *et al*, 2009). Baft and p21^{WAF1} KD independently rescued the repopulation capacity of telomere dysfunctional or irradiated HSCs and their over expression impaired HSC function in response to both ageing and DNA damage, in murine and human cells (Wang *et al*, 2012). This had previously been reported for p21^{WAF1} in telomere dysfunctional HSCs (Choudhury *et al*, 2007). These studies point to the existence of a 'stemness checkpoint', ATM-dependent in MSCs (Inomata *et al*, 2009) and Batf- and p21^{WAF1}-dependent in HSCs (Wang *et al*, 2012), which sensitises stem cells to terminal differentiation upon accumulation of DNA damage thus removing them from the stem cell pool. Finally, ageing phenotypes of the skin such as reduced mitochondrial activity, senescence and reduced thickness of the epidermis have also been associated with DNA damage and induction of terminal differentiation (Velarde *et al*, 2012). Using a mouse model of *Sod2* deficiency, which results in mitochondrial oxidative stress, it has been demonstrated that impaired mitochondrial function induces DNA damage and senescence but not apoptosis. The reduction in the number of cells and thickness of the epidermis has been associated with a decrease in proliferation due to senescence combined with an increase in terminal differentiation. It has early on been demonstrated in human keratinocytes that senescent cells are still capable of undergoing terminal differentiation (Norsgaard *et al*, 1996).

Although these studies (Inomata *et al*, 2009; Wang *et al*, 2012; Velarde *et al*, 2012) suggest that terminal differentiation is a likely outcome of senescence resulting from activation of DNA damage checkpoints, I have found that the low levels of DSBs induced by telomere uncapping in epidermal keratinocytes (Minty *et al*, 2008) or irreparable DSBs caused by senescence-inducing doses of IR were not capable of inducing the candidate markers HOPX or S100A7, which are associated with terminal differentiation. Therefore, although telomere dysfunction in keratinocytes, induced by ectopic expression of TRF2$^{\Delta B\Delta M}$, seems to ultimately commit cells to terminal differentiation this does not seem to be

due to DNA damage signals at the telomere but rather due to other properties of the dysfunctional telomere itself (Fig. 8.1). In this case keratinocytes will exfoliate and thus have a short tenure in the epidermis and it might explain why senescent cells expressing indicators of telomere dysfunction TIFs, do not accumulate in this compartment with age. This last hypothesis is not supported by the lack of supra-basal SA-β Gal staining in the suprabasal layers of aged epidermis (Dimri *et al*, 1995). However, senescent cell loss by other mechanisms such as immune clearance (Fig. 8.1) could contribute to epidermal ageing indirectly, as the stem cells are placed under additional replicative stress, which in turn will result in further telomere shortening, damage and dysfunction and telomere shortening is seen in squamous epithelia with age (Lindsey *et al*, 1991; Nakamura *et al*, 2002; Sugimoto *et al*, 2006). This correlation was first demonstrated in hepatocytes subjected to chronic damage where constant attempts at regeneration and consequent high cell-turnover resulted in accelerated telomere shortening and senescence (Wiemann *et al*, 2002). At the cirrhosis stage hepatocytes show significantly reduced proliferation ability and mesenchymal cells take over forming the characteristic fibrotic scar tissue.

However, telomeres do not need to be strikingly shortened to contribute to ageing. Telomerase targeted to the epidermis reduces TIFs and extends both lifespan and healthspan of mice (Tomás-Loba *et al*, 2008) and telomerase-activating drugs can do the same (Bernardes de Jesus *et al*, 2011; 2012). The TERT protein is known to possess non-canonical functions (Parkinson *et al*, 2008), however, Tomás-Loba *et al* (Tomás-Loba *et al*, 2008) presented evidence that even long telomeres possessed DSBs that were removed by telomerase in line with the recent reported ability of telomerase to resolve otherwise unrepairable DSBs at the telomeres (Suram *et al*, 2012). This is thus thought to occur through canonical telomerase functions. Although telomeres do shorten in mice with age (Sharpless & DePinho, 2007) it is unlikely that they ever get critically short to the point of exposing the DNA double strand, nevertheless they do show an increase in TIFs, which is reduced by the expression of telomerase (Tomás-Loba *et al*, 2008). This may be connected with the recent report that telomerase can resolve unrepaired DSBs at the telomere (Suram *et al*, 2012) and so telomeres may not need to be short to direct ageing-related phenotypes. In humans epidermal TIFs do not increase with age (U. Herbig, personal communication) and the reason for this discrepancy is not clear. The heterogeneous nature of the human population coupled with an inadequate population size may offer one explanation but also the failure of epidermal keratinocytes to demonstrate

DSBs when telomeres are uncapped (Minty *et al*, 2008) and the possible short tenure of senescent basal keratinocytes in humans (Dimri *et al*, 1995) may also be relevant.

S100A7 as a marker for TDIS

In order to determine the actual contribution of TDIS to epidermal ageing and to effectively distinguish it from p16^{INK4a}-induced senescence it will become necessary to find reliable indicators of telomere functional status in the epidermis. S100A7 is a promising marker since it seems to be keratinocyte-specific, mechanism-specific and because it is also a secreted protein. S100A7, also known as psoriasin, was first identified as a protein abundantly expressed in keratinocytes originating from psoriatic skin (Madsen *et al*, 1991). Besides skin inflammation, its up-regulation has since been reported at the early stages of various carcinomas such as SCC of the bladder (Celis *et al*, 1996), SCC, BCC and precancerous lesions of the skin (Moubayed *et al*, 2007). It is recently emerging as a good non-invasive marker of squamous cell and large cell lung cancer (Zhang *et al*, 2008) since its expression in the lung seems independent from differentiation and inflammation and seems to decrease during progression to invasive carcinoma. As SCCs harbour cells with short and dysfunctional telomeres (Gordon *et al*, 2003) and this may be an early event because the breakdown of senescence occurs only in late dysplasia (McGregor *et al*, 2002; Natarajan *et al*, 2003) it is possible that this is another situation where S100A7 elevation is linked to keratinocyte TDIS. The work I have presented in this thesis supports our earlier findings (Minty *et al*, 2008) which suggest that S100A7 is TDIS-specific and elevated in the early stages of senescence (chapters 4 and 6). In addition, the fact that it is secreted in blood, urine and saliva and that although it is elevated in psoriatic skin (Madsen *et al*, 1991) it is not in sera of patients with psoriasis (Anderson *et al*, 2009) makes it a promising biomarker. I have also established that the main senescence effectors do not induce S100A7 and, indirectly, that NF-Kβ is not likely to be required. However, since NF-Kβ acts downstream of DSBs, the next aim will be to test other upstream activators of p16^{INK4a} and p53 other than DSBs and to investigate S100A7 expression in the context of neoplasia and ageing.

General perspectives for the causal role of senescence in ageing

There is now considerable evidence that senescence can cause tissue (Baker *et al*, 2011) and organismal ageing (Tomás-Loba *et al*, 2008) and also that senescence may limit stem cell function (Janzen *et al*, 2006; Krishnamurthy *et al*, 2006; Sharpless & DePinho, 2007). However, and as discussed in detail above, as stem cells numbers do not diminish with age it is still very unclear how ageing stem cells contribute to tissue dysfunction. One hypothesis is that defects in stem cells may remain silent until differentiation takes place whereupon poor regenerative capacity and wound repair may be attributable to transit cell dysfunction.

It is well established that expression of senescence markers such as SA-β gal and p16[INK4a] is associated with organismal ageing (Dimri *et al*, 1995; Ressler *et al*, 2006). p16[INK4a] is a hallmark of senescence in human cells and a robust biomarker of ageing in human skin (Ressler *et al*, 2006). Furthermore, p16[INK4a] expression in the epidermis (but not the dermis) has been shown to actually reflect the physiological age of the individual (Waaijer *et al*, 2012). Thus, the relevance of p16[INK4a]-dependent senescence to organismal ageing is now unquestionable. However, the contribution of p16[INK4a]-independent senescence, namely p53- and telomere-related senescence, to ageing of proliferative compartments such as the epidermis is still a controversial matter.

Congenital defects in components of the telomerase complex (Vulliamy *et al*, 2001; Garcia *et al*, 2007; Kirwan & Dokal, 2009) and chronic diseases in humans characterised by rapid telomere shortening (Wiemann *et al*, 2002), support a connection between telomere dysfunction and ageing. In contrast, although murine ageing has many similarities with human ageing it originally appeared to occur independently of telomere length. Mouse telomeres are on average longer than human telomeres (Kipling & Cooke, 1990) due to a background level of telomerase expression in murine tissues (Kipling, 1997). The telomerase-knockout mouse (Blasco *et al*, 1997) provided a model system to study the effects of telomere dysfunction and these animals demonstrated features of premature ageing in several proliferative compartments (Lee *et al*, 1998; Rudolph *et al*, 1999; Allsopp *et al*, 2003; Choudhury *et al*, 2007). Although p53 deficiency rescued some of the phenotype it did not extend lifespan of these animals due to increased tumourigenesis (Chin *et al*, 1999). However, loss of p21[WAF1], p53's transcriptional target, partially extended longevity without

tumour development (Choudhury *et al*, 2007). More interestingly, in a recently developed mouse model endowed with a cancer-resistant background (Tomás-Loba *et al*, 2008) TERT over-expression improved fitness of proliferative compartments and increased lifespan, undoubtedly demonstrating the importance of telomere maintenance in the context of mammalian ageing. Finally, since telomeres have been recently characterised as specialised DNA structures which are both particularly susceptible to damage (Hewitt *et al*, 2012; Suram *et al*, 2012) and resistant to repair (Fumagalli *et al*, 2012), persistent DNA damage capable of inducing senescence seems to mainly emanate from the telomeres. This occurs irrespectively of telomere length and is corrected by expression of telomerase. All this evidence highlights the importance of TDIS in the context of ageing and raises new questions on how telomere dysfunction contributes to human ageing.

In addition, telomere dysfunction is not necessarily associated with TIFs or a DDR (Muntoni *et al*, 2003; Minty *et al*, 2008) suggesting that signals other than the DDR originate from the telomere but whether these are required for senescence and ageing is yet to be established. Nevertheless, the markers of keratinocyte telomere dysfunction that I have characterised in this thesis, especially S100A7, may have the potential to identify cells with telomere dysfunction in human tissues and body fluids.

Future plans

The underlying hypothesis of my thesis is that tissue- and mechanism-specific markers of telomere dysfunction exist and that S100A7 appears to be such a marker. I have established that S100A7 expression does not seem to be induced by the main effectors of senescence, p14, p16 and p53. Indirectly, these findings indicate that S100A7 should also not be regulated by NF-Kβ. However, since NF-Kβ acts downstream of DSBs, I would in future like to test whether other upstream activators of p16^{INK4a} and p53 other than DSBs, such as TGF-β, ROS and HDACs, could regulate S100A7 expression. Furthermore, since previous work in the D17 dysplasia suggested that S100A7 is regulated by TERT (Minty *et al*, 2008) I would also like to show that S100A7 protein is up-regulated in D17 with senescence and is down-regulated by expression of telomerase in these cells. Finally, I would like to extend this work to clinical samples (tissue/ serum/saliva) in order to further investigate S100A7 expression in the context of neoplasia and ageing. I would expect S100A7 to be expressed in pre-malignancy and ageing associated with telomere dysfunction, and to be down-regulated in neoplasia.

Chapter 9. References

Allen-Hoffmann BL & Rheinwald JG (1984) Polycyclic aromatic hydrocarbon mutagenesis of human epidermal keratinocytes in culture. *Proc Natl Acad Sci USA* **81:** 7802–7806

Allshire RC, Dempster M & Hastie ND (1989) Human telomeres contain at least three types of G-rich repeat distributed non-randomly. *Nucleic Acids Res* **17:** 4611–4627

Allshire RC, Gosden JR, Cross SH, Cranston G, Rout D, Sugawara N, Szostak JW, Fantes PA & Hastie ND (1988) Telomeric repeat from T. thermophila cross hybridizes with human telomeres. *Nature* **332:** 656–659

Allsopp RC, Morin GB, DePinho R, Harley CB & Weissman IL (2003) Telomerase is required to slow telomere shortening and extend replicative lifespan of HSCs during serial transplantation. *Blood* **102:** 517–520

Anderson K, Wong J, Polyak K, Aronzon D & Enerbäck C (2009) Detection of psoriasin/S100A7 in the sera of patients with psoriasis. *British Journal of Dermatology* **160:** 325–332

Asanoma K, Kato H, Inoue T, Matsuda T & Wake N (2004) Analysis of a candidate gene associated with growth suppression of choriocarcinoma and differentiation of trophoblasts. *The Journal of reproductive medicine* **49:** 617–626

Aspinall R (2003) Aging of the Organs and Systems Aspinall & Richard (eds) Kluwer Academic Pub

Bae NS & Baumann P (2007) A RAP1/TRF2 complex inhibits nonhomologous end-joining at human telomeric DNA ends. *Mol Cell* **26:** 323–334

Baird DM, Rowson J, Wynford-Thomas D & Kipling D (2003) Extensive allelic variation and ultrashort telomeres in senescent human cells. *Nat Genet* **33:** 203–207

Baker DJ, Wijshake T, Tchkonia T, Lebrasseur NK, Childs BG, Sluis BV de, Kirkland JL & Deursen JMV (2011) Clearance of p16Ink4a-positive senescent cells delays ageing-associated disorders. *Nature***:** 1–6

Barrandon Y & Green H (1985) Cell size as a determinant of the clone-forming ability of human keratinocytes. *Proc Natl Acad Sci USA* **82:** 5390–5394

Barrandon Y & Green H (1987) Three clonal types of keratinocyte with different capacities for multiplication. *Proc Natl Acad Sci USA* **84:** 2302–2306

Bartkova J, Horejsí Z, Koed K, Krämer A, Tort F, Zieger K, Guldberg P, Sehested M, Nesland JM, Lukas C, Ørntoft T, Lukas J & Bartek J (2005) DNA damage response as a candidate anti-cancer barrier in early human tumorigenesis. *Nature* **434:** 864–870

Bartkova J, Rezaei N, Liontos M, Karakaidos P, Kletsas D, Issaeva N, Vassiliou L-VF, Kolettas E, Niforou K, Zoumpourlis VC, Takaoka M, Nakagawa H, Tort F, Fugger K, Johansson F, Sehested M, Andersen CL, Dyrskjot L, Ørntoft T, Lukas J, et al (2006) Oncogene-induced senescence is part of the tumorigenesis barrier imposed by DNA damage checkpoints. *Nature* **444:** 633–637

Beauséjour CM, Krtolica A, Galimi F, Narita M, Lowe SW, Yaswen P & Campisi J (2003) Reversal of human cellular senescence: roles of the p53 and p16 pathways. *EMBO J* **22:** 4212–4222

Ben-Porath I & Weinberg RA (2005) The signals and pathways activating cellular senescence. *Int J Biochem Cell Biol* **37:** 961–976

Bernardes de Jesus B, Schneeberger K, Vera E, Tejera A, Harley CB & Blasco MA (2011) The telomerase activator TA-65 elongates short telomeres and increases health span of adult/old mice without increasing cancer incidence. *Aging Cell* **10:** 604–621

Bernardes de Jesus B, Vera E, Schneeberger K, Tejera AM, Ayuso E, Bosch F & Blasco MA (2012) Telomerase gene therapy in adult and old mice delays aging and increases longevity without increasing cancer. *EMBO Mol Med* **4:** 691–704

Blackburn EH (2000) Telomere states and cell fates. *Nature* **408:** 53–56

Blackburn EH & Gall JG (1978) A tandemly repeated sequence at the termini of the extrachromosomal ribosomal RNA genes in Tetrahymena. *J Mol Biol* **120:** 33–53

Blasco MA, Lee HW, Hande MP, Samper E, Lansdorp PM, DePinho RA & Greider CW (1997) Telomere shortening and tumor formation by mouse cells lacking telomerase RNA. *Cell* **91:** 25–34

Bodnar AG, Ouellette M, Frolkis M, Holt SE, Chiu CP, Morin GB, Harley CB, Shay JW, Lichtsteiner S & Wright WE (1998) Extension of life-span by introduction of telomerase into normal human cells. *Science* **279:** 349–352

Brookes S, Rowe J, Ruas M, Llanos S, Clark PA, Lomax M, James MC, Vatcheva R, Bates S, Vousden KH, Parry D, Gruis N, Smit N, Bergman W & Peters G (2002) INK4a-deficient human diploid fibroblasts are resistant to RAS-induced senescence. *EMBO J* **21:** 2936–2945

Brown DC & Gatter KC (2002) Ki67 protein: the immaculate deception? *Histopathology* **40:** 2–11

Brown JP, Wei W & Sedivy JM (1997) Bypass of senescence after disruption of p21CIP1/ WAF1 gene in normal diploid human fibroblasts. *Science* **277:** 831–834

Bustin SA, Benes V, Garson JA, Hellemans J, Huggett J, Kubista M, Mueller R, Nolan T, Pfaffl MW, Shipley GL, Vandesompele J & Wittwer CT (2009) The MIQE guidelines: minimum information for publication of quantitative real-time PCR experiments. *Clin Chem* **55:** 611–622

C Heiser W (2004a) Gene delivery to mammalian cells. Vol. 2, Viral gene transfer techniques. Humana Press

C Heiser W (2004b) Gene delivery to mammalian cells. Vol. 1, Nonviral gene transfer techniques. Humana Press

Campisi J (2001a) Cellular senescence as a tumor-suppressor mechanism. *Trends Cell Biol* **11:** S27–S31

Campisi J (2001b) From cells to organisms: can we learn about aging from cells in culture? *Exp Gerontol* **36:** 607–618

Campisi J (2005) Senescent cells, tumor suppression, and organismal aging: good citizens, bad neighbors. *Cell* **120:** 513–522

Campisi J & d'Adda di Fagagna F (2007) Cellular senescence: when bad things happen to good cells. *Nat Rev Mol Cell Biol* **8:** 729–740

Carrel A (1912) ON THE PERMANENT LIFE OF TISSUES OUTSIDE OF THE ORGANISM. *J. Exp. Med.* **15:** 516–528

Cayuela ML, Flores JM & Blasco MA (2005) The telomerase RNA component Terc is required for the tumour-promoting effects of Tert overexpression. *EMBO Rep.* **6:** 268–274

Celis JE, Rasmussen HH, Vorum H, Madsen P, Honoré B, Wolf H & Orntoft TF (1996) Bladder squamous cell carcinomas express psoriasin and externalize it to the urine. *J Urol* **155:** 2105–2112

Chang S, Multani AS, Cabrera NG, Naylor ML, Laud P, Lombard D, Pathak S, Guarente L & DePinho RA (2004) Essential role of limiting telomeres in the pathogenesis of Werner syndrome. *Nat Genet* **36:** 877–882

Charruyer A, Barland CO, Yue L, Wessendorf HB, Lu Y, Lawrence HJ, Mancianti ML & Ghadially R (2009) Transit-Amplifying Cell Frequency and Cell Cycle Kinetics Are Altered in Aged Epidermis. *J Invest Dermatol* **129:** 2574–2583

Chen F, Kook H, Milewski R, Gitler AD, Lu MM, Li J, Nazarian R, Schnepp R, Jen K, Biben C, Runke G, Mackay JP, Novotny J, Schwartz RJ, Harvey RP, Mullins MC & Epstein JA (2002) Hop is an unusual homeobox gene that modulates cardiac development. *Cell* **110:** 713–723

Chen Y, Pacyna-Gengelbach M, Deutschmann N, Niesporek S & Petersen I (2007) Homeobox gene HOP has a potential tumor suppressive activity in human lung cancer. *Int J Cancer* **121:** 1021–1027

Chen Y, Petersen S, Pacyna-Gengelbach M, Pietas A & Petersen I (2003) Identification of a novel homeobox-containing gene, LAGY, which is downregulated in lung cancer. *Oncology* **64:** 450–458

Chen Z, Trotman LC, Shaffer D, Lin H-K, Dotan ZA, Niki M, Koutcher JA, Scher HI, Ludwig T, Gerald W, Cordon-Cardo C & Pandolfi PP (2005) Crucial role of p53-dependent cellular senescence in suppression of Pten-deficient tumorigenesis. *Nature* **436:** 725–730

Chin L, Artandi SE, Shen Q, Tam A, Lee SL, Gottlieb GJ, Greider CW & DePinho RA (1999) p53 deficiency rescues the adverse effects of telomere loss and cooperates with telomere dysfunction to accelerate carcinogenesis. *Cell* **97:** 527–538

Choudhury AR, Ju Z, Djojosubroto MW, Schienke A, Lechel A, Schaetzlein S, Jiang H, Stepczynska A, Wang C, Buer J, Lee H-W, Zglinicki Von T, Ganser A, Schirmacher P, Nakauchi H & Rudolph KL (2007) Cdkn1a deletion improves stem cell function and lifespan of mice with dysfunctional telomeres without accelerating cancer formation. *Nat Genet* **39:** 99–105

Comfort A (1979) The biology of senescence 3rd ed. Churchill Livingstone

Coppe J-P, Rodier F, Patil CK, Freund A, Desprez P-Y & Campisi J (2011) Tumor Suppressor and Aging Biomarker p16INK4a Induces Cellular Senescence without the Associated Inflammatory Secretory Phenotype. *J Biol Chem* **286:** 36396–36403

Coppé J-P, Desprez P-Y, Krtolica A & Campisi J (2010) The senescence-associated secretory phenotype: the dark side of tumor suppression. *Annu Rev Pathol* **5:** 99–118

Coppé J-P, Kauser K, Campisi J & Beauséjour CM (2006) Secretion of vascular endothelial growth factor by primary human fibroblasts at senescence. *J Biol Chem* **281:** 29568–29574

Coppé J-P, Patil CK, Rodier F, Sun Y, Muñoz DP, Goldstein J, Nelson PS, Desprez P-Y & Campisi J (2008) Senescence-associated secretory phenotypes reveal cell-nonautonomous functions of oncogenic RAS and the p53 tumor suppressor. *PLoS Biol* **6:** 2853–2868

Cordisco S, Maurelli R, Bondanza S, Stefanini M, Zambruno G, Guerra L & Dellambra E (2009) Bmi-1 Reduction Plays a Key Role in Physiological and Premature Aging of Primary Human Keratinocytes. *J Invest Dermatol***:** 1–15

Cristofalo VJ (2005) SA beta Gal staining: biomarker or delusion. *Exp Gerontol* **40:** 836–838

Cristofalo VJ & Sharf BB (1973) Cellular senescence and DNA synthesis. Thymidine incorporation as a measure of population age in human diploid cells. *Exp Cell Res* **76:** 419–427

Cristofalo VJ, Allen RG, Pignolo RJ, Martin BG & Beck JC (1998) Relationship between donor age and the replicative lifespan of human cells in culture: a reevaluation. *Proc Natl Acad Sci USA* **95:** 10614–10619

d'Adda di Fagagna F, Reaper PM, Clay-Farrace L, Fiegler H, Carr P, Zglinicki Von T, Saretzki G, Carter NP & Jackson SP (2003) A DNA damage checkpoint response in telomere-initiated senescence. *Nature* **426:** 194–198

Darbro BW, Schneider GB & Klingelhutz AJ (2005) Co-regulation of p16INK4A and migratory genes in culture conditions that lead to premature senescence in human keratinocytes. *J Invest Dermatol* **125:** 499–509

Davis HE, Morgan JR & Yarmush ML (2002) Polybrene increases retrovirus gene transfer efficiency by enhancing receptor-independent virus adsorption on target cell membranes. *Biophys Chem* **97:** 159–172

de Laat WL, Jaspers NG & Hoeijmakers JH (1999) Molecular mechanism of nucleotide excision repair. *Genes Dev* **13:** 768–785

de Lange T (2002) Protection of mammalian telomeres. *Oncogene* **21:** 532–540

de Lange T (2004) T-loops and the origin of telomeres. *Nat Rev Mol Cell Biol* **5:** 323–329

de Lange T (2005) Shelterin: the protein complex that shapes and safeguards human telomeres. *Genes Dev* **19:** 2100–2110

De Toni A, Zbinden M, Epstein JA, Ruiz i Altaba A, Prochiantz A & Caillé I (2008) Regulation of survival in adult hippocampal and glioblastoma stem cell lineages by the homeodomain-only protein HOP. *Neural development* **3:** 13

Devgan V, Nguyen B-C, Oh H & Dotto GP (2006) p21WAF1/Cip1 suppresses keratinocyte differentiation independently of the cell cycle through transcriptional up-regulation of the IGF-I gene. *J Biol Chem* **281:** 30463–30470

Di Cunto F, Topley G, Calautti E, Hsiao J, Ong L, Seth PK & Dotto GP (1998) Inhibitory function of p21Cip1/WAF1 in differentiation of primary mouse keratinocytes independent of cell cycle control. *Science* **280:** 1069–1072

Di Leonardo A, Linke SP, Clarkin K & Wahl GM (1994) DNA damage triggers a prolonged p53-dependent G1 arrest and long-term induction of Cip1 in normal human fibroblasts. *Genes Dev* **8:** 2540–2551

Dickson MA, Hahn WC, Ino Y, Ronfard V, Wu JY, Weinberg RA, Louis DN, Li FP & Rheinwald JG (2000) Human keratinocytes that express hTERT and also bypass a p16(INK4a)-enforced mechanism that limits life span become immortal yet retain normal growth and differentiation characteristics. *Mol Cell Biol* **20:** 1436–1447

Dimri GP, Itahana K, Acosta M & Campisi J (2000) Regulation of a senescence checkpoint response by the E2F1 transcription factor and p14(ARF) tumor suppressor. *Mol Cell Biol* **20:** 273–285

Dimri GP, Lee X, Basile G, Acosta M, Scott G, Roskelley C, Medrano EE, Linskens M, Rubelj I & Pereira-Smith O (1995) A biomarker that identifies senescent human cells in culture and in aging skin in vivo. *Proc Natl Acad Sci USA* **92:** 9363–9367

Dobbs TA, Tainer JA & Lees-Miller SP (2010) A structural model for regulation of NHEJ by DNA-PKcs autophosphorylation. *DNA Repair (Amst.)* **9:** 1307–1314

Dover R & Potten CS (1983) Cell cycle kinetics of cultured human epidermal keratinocytes. *J Invest Dermatol* **80:** 423–429

DuBridge RB, Tang P, Hsia HC, Leong PM, Miller JH & Calos MP (1987) Analysis of mutation in human cells by using an Epstein-Barr virus shuttle system. *Mol Cell Biol* **7:** 379–387

Dulić V, Drullinger LF, Lees E, Reed SI & Stein GH (1993) Altered regulation of G1 cyclins in senescent human diploid fibroblasts: accumulation of inactive cyclin E-Cdk2 and cyclin D1-Cdk2 complexes. *Proc Natl Acad Sci USA* **90:** 11034–11038

el-Deiry WS, Tokino T, Waldman T, Oliner JD, Velculescu VE, Burrell M, Hill DE, Healy E, Rees JL & Hamilton SR (1995) Topological control of p21WAF1/CIP1 expression in normal and neoplastic tissues. *Cancer Res* **55:** 2910–2919

Elbashir SM, Harborth J, Lendeckel W, Yalcin A, Weber K & Tuschl T (2001) Duplexes of 21-nucleotide RNAs mediate RNA interference in cultured mammalian cells. *Nature* **411:** 494–498

Feldser DM & Greider CW (2007) Short telomeres limit tumor progression in vivo by inducing senescence. *Cancer Cell* **11:** 461–469

Finkel T, Serrano M & Blasco MA (2007) The common biology of cancer and ageing. *Nature* **448:** 767–774

Fire A, Xu S, Montgomery MK, Kostas SA, Driver SE & Mello CC (1998) Potent and specific genetic interference by double-stranded RNA in Caenorhabditis elegans. *Nature* **391:** 806–811

Fisher GJ, Kang S, Varani J, Bata-Csorgo Z, Wan Y, Datta S & Voorhees JJ (2002) Mechanisms of photoaging and chronological skin aging. *Arch Dermatol* **138:** 1462–1470

Forsyth NR, Evans AP, Shay JW & Wright WE (2003) Developmental differences in the immortalization of lung fibroblasts by telomerase. *Aging Cell* **2:** 235–243

Freund A, Patil CK & Campisi J (2011) p38MAPK is a novel DNA damage response-independent regulator of the senescence-associated secretory phenotype. *EMBO J* **30:** 1536–1548

Frisch SM & Francis H (1994) Disruption of epithelial cell-matrix interactions induces apoptosis. *J Cell Biol*

Fumagalli M, Rossiello F, Clerici M, Barozzi S, Cittaro D, Kaplunov JM, Bucci G, Dobreva M, Matti V, Beauséjour CM, Herbig U, Longhese MP & d'Adda di Fagagna F (2012) Telomeric DNA damage is irreparable and causes persistent DNA-damage-response activation. *Nat Cell Biol* **14:** 355–365

Funayama R & Ishikawa F (2007) Cellular senescence and chromatin structure. *Chromosoma* **116:** 431–440

Garcia CK, Wright WE & Shay JW (2007) Human diseases of telomerase dysfunction: insights into tissue aging. *Nucleic Acids Res* **35:** 7406–7416

García-Cao I, García-Cao M, Martín-Caballero J, Criado LM, Klatt P, Flores JM, Weill J-C, Blasco MA & Serrano M (2002) 'Super p53' mice exhibit enhanced DNA damage response, are tumor resistant and age normally. *EMBO J* **21:** 6225–6235

García-Cao I, García-Cao M, Tomás-Loba A, Martín-Caballero J, Flores JM, Klatt P, Blasco MA & Serrano M (2006) Increased p53 activity does not accelerate telomere-driven ageing. *EMBO Rep.* **7:** 546–552

Garlick JA, Katz AB, Fenjves ES & Taichman LB (1991) Retrovirus-mediated transduction of cultured epidermal keratinocytes. *J Invest Dermatol* **97:** 824–829

Gavrilov LA & Gavrilova NS (2002) Evolutionary theories of aging and longevity. *ScientificWorldJournal* **2:** 339–356

Gemenetzidis E, Bose A, Riaz AM, Chaplin T, Young BD, Ali M, Sugden D, Thurlow JK, Cheong S-C, Teo S-H, Wan H, Waseem A, Parkinson EK, Fortune F & Teh M-T (2009) FOXM1 upregulation is an early event in human squamous cell carcinoma and it is enhanced by nicotine during malignant transformation. *PLoS ONE* **4:** e4849

Giangreco A, Qin M, Pintar JE & Watt FM (2008) Epidermal stem cells are retained in vivo throughout skin aging. *Aging Cell* **7:** 250–259

Gil J, Bernard D, Martínez D & Beach D (2004) Polycomb CBX7 has a unifying role in cellular lifespan. *Nat Cell Biol* **6:** 67–72

González-Suárez E, Flores JM & Blasco MA (2002) Cooperation between p53 mutation and high telomerase transgenic expression in spontaneous cancer development. *Mol Cell Biol* **22:** 7291–7301

González-Suárez E, Samper E, Ramírez A, Flores JM, Martín-Caballero J, Jorcano JL & Blasco MA (2001) Increased epidermal tumors and increased skin wound healing in transgenic mice overexpressing the catalytic subunit of telomerase, mTERT, in basal keratinocytes. *EMBO J* **20:** 2619–2630

Gordon KE, Ireland H, Roberts M, Steeghs K, McCaul JA, MacDonald DG & Parkinson EK (2003) High levels of telomere dysfunction bestow a selective disadvantage during the progression of human oral squamous cell carcinoma. *Cancer Res* **63:** 458–467

Gorgoulis VG, Vassiliou L-VF, Karakaidos P, Zacharatos P, Kotsinas A, Liloglou T, Venere M, Ditullio RA, Kastrinakis NG, Levy B, Kletsas D, Yoneta A, Herlyn M, Kittas C & Halazonetis TD (2005) Activation of the DNA damage checkpoint and genomic instability in human precancerous lesions. *Nature* **434:** 907–913

Graham FL, Smiley J, Russell WC & Nairn R (1977) Characteristics of a human cell line transformed by DNA from human adenovirus type 5. *J Gen Virol* **36:** 59–74

Green H (1978) Cyclic-amp in relation to proliferation of the epidermal cell: a new view. *Cell* **15:** 801–811

Green H (1980) The keratinocyte as differentiated cell type. *Harvey Lect* **74:** 101–139

Green H, Kehinde O & Thomas J (1979) Growth of cultured human epidermal cells into multiple epithelia suitable for grafting. *Proc Natl Acad Sci USA* **76:** 5665–5668

Greider CW & Blackburn EH (1985) Identification of a specific telomere terminal transferase activity in Tetrahymena extracts. *Cell* **43:** 405–413

Greider CW & Blackburn EH (1987) The telomere terminal transferase of Tetrahymena is a ribonucleoprotein enzyme with two kinds of primer specificity. *Cell* **51:** 887–898

Greider CW & Blackburn EH (1989) A telomeric sequence in the RNA of Tetrahymena telomerase required for telomere repeat synthesis. *Nature* **337:** 331–337

Griffith JD, Comeau L, Rosenfield S, Stansel RM, Bianchi A, Moss H & de Lange T (1999) Mammalian telomeres end in a large duplex loop. *Cell* **97:** 503–514

Grove GL & Cristofalo VJ (1977) Characterization of the cell cycle of cultured human diploid cells: effects of aging and hydrocortisone. *J Cell Physiol* **90:** 415–422

Haber JE (2000) Partners and pathwaysrepairing a double-strand break. *Trends Genet.* **16:** 259–264

Haga K, Ohno S-I, Yugawa T, Narisawa-Saito M, Fujita M, Sakamoto M, Galloway DA & Kiyono T (2007) Efficient immortalization of primary human cells by p16 INK4a-specific short hairpin RNA or Bmi-1, combined with introduction of hTERT. *Cancer Science* **98:** 147–154

Hanahan D & Weinberg R (2000) The hallmarks of cancer. *Cell* **100:** 57–70

Hara E, Smith R, Parry D, Tahara H, Stone S & Peters G (1996) Regulation of p16CDKN2 expression and its implications for cell immortalization and senescence. *Mol Cell Biol* **16:** 859–867

Harley CB, Futcher AB & Greider CW (1990) Telomeres shorten during ageing of human fibroblasts. *Nature* **345:** 458–460

Haussmann MF, Winkler DW, Huntington CE, Nisbet ICT & Vleck CM (2004) Telomerase expression is differentially regulated in birds of differing life span. *Ann N Y Acad Sci* **1019:** 186–190

Haussmann MF, Winkler DW, Huntington CE, Nisbet ICT & Vleck CM (2007) Telomerase activity is maintained throughout the lifespan of long-lived birds. *Exp Gerontol* **42:** 610–618

Hayflick L (1965) The limited in vitro lifetime of human diploid cell strains. *Exp Cell Res* **37:** 614–636

Hayflick L & Moorhead PS (1961) The serial cultivation of human diploid cell strains. *Exp Cell Res* **25:** 585–621

Hemann MT, Strong MA, Hao LY & Greider CW (2001) The shortest telomere, not average telomere length, is critical for cell viability and chromosome stability. *Cell* **107:** 67–77

Herbig U, Ferreira M, Condel L, Carey D & Sedivy JM (2006) Cellular senescence in aging primates. *Science* **311:** 1257

Herbig U, Jobling WA, Chen BPC, Chen DJ & Sedivy JM (2004) Telomere shortening triggers senescence of human cells through a pathway involving ATM, p53, and p21(CIP1), but not p16(INK4a). *Mol Cell* **14:** 501–513

Hewitt G, Jurk D, Marques FDM, Correia-Melo C, Hardy T, Gackowska A, Anderson R, Taschuk M, Mann J & Passos JF (2012) Telomeres are favoured targets of a persistent DNA damage response in ageing and stress-induced senescence. *Nat Commun* **3:** 708

Hoeijmakers JH (2001) Genome maintenance mechanisms for preventing cancer. *Nature* **411:** 366–374

Humke EW, Shriver SK, Starovasnik MA, Fairbrother WJ & Dixit VM (2000) ICEBERG: a novel inhibitor of interleukin-1beta generation. *Cell* **103:** 99–111

Hunter KD, Thurlow JK, Fleming J, Drake PJH, Vass JK, Kalna G, Higham DJ, Herzyk P, MacDonald DG, Parkinson EK & Harrison PR (2006) Divergent routes to oral cancer. *Cancer Res* **66:** 7405–7413

Inomata K, Aoto T, Binh NT, Okamoto N, Tanimura S, Wakayama T, Iseki S, Hara E, Masunaga T, Shimizu H & Nishimura EK (2009) Genotoxic stress abrogates renewal of melanocyte stem cells by triggering their differentiation. *Cell* **137:** 1088–1099

Itahana K, Dimri G & Campisi J (2001) Regulation of cellular senescence by p53. *Eur J Biochem* **268:** 2784–2791

Itahana K, Zou Y, Itahana Y, Martinez J-L, Beausejour C, Jacobs JJL, van Lohuizen M, Band V, Campisi J & Dimri GP (2003) Control of the replicative life span of human fibroblasts by p16 and the polycomb protein Bmi-1. *Mol Cell Biol* **23:** 389–401

Iwasa H, Han J & Ishikawa F (2003) Mitogen-activated protein kinase p38 defines the common senescence-signalling pathway. *Genes Cells* **8:** 131–144

Jacobs JJ, Kieboom K, Marino S, DePinho RA & van Lohuizen M (1999) The oncogene and Polycomb-group gene bmi-1 regulates cell proliferation and senescence through the ink4a locus. *Nature* **397:** 164–168

Jacobs JJL & de Lange T (2004) Significant role for p16INK4a in p53-independent telomere-directed senescence. *Curr Biol* **14:** 2302–2308

Jacobs JP, Jones CM & Baille JP (1970) Characteristics of a human diploid cell designated MRC-5. *Nature* **227:** 168–170

Janzen V, Forkert R, Fleming HE, Saito Y, Waring MT, Dombkowski DM, Cheng T, DePinho RA, Sharpless NE & Scadden DT (2006) Stem-cell ageing modified by the cyclin-dependent kinase inhibitor p16INK4a. *Nature* **443:** 421–426

Jaskelioff M, Muller FL, Paik J-H, Thomas E, Jiang S, Adams AC, Sahin E, Kost-Alimova M, Protopopov A, Cadiñanos J, Horner JW, Maratos-Flier E & DePinho RA (2011) Telomerase reactivation reverses tissue degeneration in aged telomerase-deficient mice. *Nature* **469:** 102–106

Jeyapalan JC, Ferreira M, Sedivy JM & Herbig U (2007) Accumulation of senescent cells in mitotic tissue of aging primates. *Mech Ageing Dev* **128:** 36–44

Jiang H, Schiffer E, Song Z, Wang J, Zürbig P, Thedieck K, Moes S, Bantel H, Saal N, Jantos J, Brecht M, Jenö P, Hall MN, Hager K, Manns MP, Hecker H, Ganser A, Döhner K, Bartke A, Meissner C, et al (2008) Proteins induced by telomere dysfunction and DNA damage represent biomarkers of human aging and disease. *Proceedings of the National Academy of Sciences* **105:** 11299–11304

Jiang XR, Jimenez G, Chang E, Frolkis M, Kusler B, Sage M, Beeche M, Bodnar AG, Wahl GM, Tlsty TD & Chiu CP (1999) Telomerase expression in human somatic cells does not induce changes associated with a transformed phenotype. *Nat Genet* **21:** 111–114

Ju Z, Jiang H, Jaworski M, Rathinam C, Gompf A, Klein C, Trumpp A & Rudolph KL (2007) Telomere dysfunction induces environmental alterations limiting hematopoietic stem cell function and engraftment. *Nat Med* **13:** 742–747

Kamb A, Shattuck-Eidens D, Eeles R, Liu Q, Gruis NA, Ding W, Hussey C, Tran T, Miki Y & Weaver-Feldhaus J (1994) Analysis of the p16 gene (CDKN2) as a candidate for the chromosome 9p melanoma susceptibility locus. *Nat Genet* **8:** 23–26

Kamijo T, Zindy F, Roussel MF, Quelle DE, Downing JR, Ashmun RA, Grosveld G & Sherr CJ (1997) Tumor suppression at the mouse INK4a locus mediated by the alternative reading frame product p19ARF. *Cell* **91:** 649–659

Kang MK, Kameta A, Shin K-H, Baluda MA, Kim H-R & Park N-H (2003) Senescence-associated genes in normal human oral keratinocytes. *Exp Cell Res* **287:** 272–281

Kang T-W, Yevsa T, Woller N, Hoenicke L, Wuestefeld T, Dauch D, Hohmeyer A, Gereke M, Rudalska R, Potapova A, Iken M, Vucur M, Weiss S, Heikenwalder M, Khan S, Gil J, Bruder D, Manns M, Schirmacher P, Tacke F, et al (2011) Senescence surveillance of pre-malignant hepatocytes limits liver cancer development. *Nature* **479:** 547–551

Karlseder J, Broccoli D, Dai Y, Hardy S & de Lange T (1999) p53- and ATM-dependent apoptosis induced by telomeres lacking TRF2. *Science* **283:** 1321–1325

Karlseder J, Smogorzewska A & de Lange T (2002) Senescence induced by altered telomere state, not telomere loss. *Science* **295:** 2446–2449

Kee HJ, Kim J-R, Nam K-I, Park HY, Shin S, Kim JC, Shimono Y, Takahashi M, Jeong MH, Kim N, Kim KK & Kook H (2007) Enhancer of polycomb1, a novel homeodomain only protein-binding partner, induces skeletal muscle differentiation. *J Biol Chem* **282:** 7700–7709

Kenyon C, Chang J, Gensch E, Rudner A & Tabtiang R (1993) A C. elegans mutant that lives twice as long as wild type. *Nature* **366:** 461–464

Kenyon CJ (2010) The genetics of ageing. *Nature* **464:** 504–512

Kill IR, Faragher RG, Lawrence K & Shall S (1994) The expression of proliferation-dependent antigens during the lifespan of normal and progeroid human fibroblasts in culture. *J Cell Sci* **107 (Pt 2):** 571–579

Kim DH & Rossi JJ (2007) Strategies for silencing human disease using RNA interference. *Nat Rev Genet* **8:** 173–184

Kim EB, Fang X, Fushan AA, Huang Z, Lobanov AV, Han L, Marino SM, Sun X, Turanov AA, Yang P, Yim SH, Zhao X, Kasaikina MV, Stoletzki N, Peng C, Polak P, Xiong Z, Kiezun A, Zhu Y, Chen Y, et al (2011) Genome sequencing reveals insights into physiology and longevity of the naked mole rat. *Nature* **479:** 223–227

Kim NW, Piatyszek MA, Prowse KR, Harley CB, West MD, Ho PL, Coviello GM, Wright WE, Weinrich SL & Shay JW (1994) Specific association of human telomerase activity with immortal cells and cancer. *Science* **266:** 2011–2015

Kipling D (1997) Telomere structure and telomerase expression during mouse development and tumorigenesis. *Eur J Cancer* **33:** 792–800

Kipling D & Cooke HJ (1990) Hypervariable ultra-long telomeres in mice. *Nature* **347:** 400–402

Kipling D, Davis T, Ostler E & Faragher R (2004) What can progeroid syndromes tell us about human aging? *Science* **305:** 1426–1431

Kirkwood TB (1977) Evolution of ageing. *Nature* **270:** 301–304

Kirkwood TB & Austad SN (2000) Why do we age? *Nature* **408:** 233–238

Kirwan M & Dokal I (2009) Dyskeratosis congenita, stem cells and telomeres. *Biochim Biophys Acta* **1792:** 371–379

Kook H & Epstein JA (2003) Hopping to the beat. Hop regulation of cardiac gene expression. *Trends Cardiovasc Med* **13:** 261–264

Kook H, Lepore JJ, Gitler AD, Lu MM, Wing-Man Yung W, Mackay J, Zhou R, Ferrari V, Gruber P & Epstein JA (2003) Cardiac hypertrophy and histone deacetylase-dependent transcriptional repression mediated by the atypical homeodomain protein Hop. *J Clin Invest* **112:** 863–871

Kook H, Yung WW, Simpson RJ, Kee HJ, Shin S, Lowry JA, Loughlin FE, Yin Z, Epstein JA & Mackay JP (2006) Analysis of the structure and function of the transcriptional coregulator HOP. *Biochemistry* **45:** 10584–10590

Krimpenfort P, Ijpenberg A, Song J-Y, van der Valk M, Nawijn M, Zevenhoven J & Berns A (2007) p15Ink4b is a critical tumour suppressor in the absence of p16Ink4a. *Nature* **448:** 943–946

Krishnamurthy J, Ramsey MR, Ligon KL, Torrice C, Koh A, Bonner-Weir S & Sharpless NE (2006) p16INK4a induces an age-dependent decline in islet regenerative potential. *Nature* **443:** 453–457

Krishnamurthy J, Torrice C, Ramsey MR, Kovalev GI, Al-Regaiey K, Su L & Sharpless NE (2004) Ink4a/Arf expression is a biomarker of aging. *J Clin Invest* **114:** 1299–1307

Krtolica A, Parrinello S, Lockett S, Desprez P & Campisi J (2001) Senescent fibroblasts promote epithelial cell growth and tumorigenesis: A link between cancer and aging. *Proc Natl Acad Sci USA* **98:** 12072–12077

Kruk PA, Rampino NJ & Bohr VA (1995) DNA damage and repair in telomeres: relation to aging. *Proc Natl Acad Sci USA* **92:** 258–262

Krunic D, Moshir S, Greulich-Bode KM, Figueroa R, Cerezo A, Stammer H, Stark H-J, Gray SG, Nielsen KV, Hartschuh W & Boukamp P (2009) Tissue context-activated telomerase in human epidermis correlates with little age-dependent telomere loss. *Biochim Biophys Acta* **1792:** 297–308

Laberge R-M, Zhou L, Sarantos MR, Rodier F, Freund A, de Keizer PLJ, Liu S, Demaria M, Cong Y-S, Kapahi P, Desprez P-Y, Hughes RE & Campisi J (2012) Glucocorticoids suppress selected components of the senescence-associated secretory phenotype. *Aging Cell* **11:** 569–578

Le ONL, Rodier F, Fontaine F, Coppé J-P, Campisi J, Degregori J, Laverdière C, Kokta V, Haddad E & Beauséjour CM (2010) Ionizing radiation-induced long-term expression of senescence markers in mice is independent of p53 and immune status. *Aging Cell* **9:** 398–409

Lee AC, Fenster BE, Ito H, Takeda K, Bae NS, Hirai T, Yu ZX, Ferrans VJ, Howard BH & Finkel T (1999) Ras proteins induce senescence by altering the intracellular levels of reactive oxygen species. *J Biol Chem* **274:** 7936–7940

Lee BY, Han JA, Im JS, Morrone A, Johung K, Goodwin EC, Kleijer WJ, DiMaio D & Hwang ES (2006) Senescence-associated beta-galactosidase is lysosomal beta-galactosidase. *Aging Cell* **5:** 187–195

Lee HW, Blasco MA, Gottlieb GJ, Horner JW, Greider CW & DePinho RA (1998) Essential role of mouse telomerase in highly proliferative organs. *Nature* **392:** 569–574

Lemaire F, Millon R, Muller D, Rabouel Y, Bracco L, Abecassis J & Wasylyk B (2004) Loss of HOP tumour suppressor expression in head and neck squamous cell carcinoma. *Br J Cancer* **91:** 258–261

Levy L, Broad S, Zhu AJ, Carroll JM, Khazaal I, Péault B & Watt FM (1998) Optimised retroviral infection of human epidermal keratinocytes: long-term expression of transduced integrin gene following grafting on to SCID mice. *Gene Ther* **5:** 913–922

Lewis KN, Andziak B, Yang T & Buffenstein R (2013) The naked mole-rat response to oxidative stress: just deal with it. *Antioxid. Redox Signal.* **19:** 1388–1399

Li G-Z, Eller MS, Firoozabadi R & Gilchrest BA (2003) Evidence that exposure of the telomere 3' overhang sequence induces senescence. *Proc Natl Acad Sci USA* **100:** 527–531

Li R, Waga S, Hannon GJ, Beach D & Stillman B (1994) Differential effects by the p21 CDK inhibitor on PCNA-dependent DNA replication and repair. *Nature* **371:** 534–537

Lindahl T & Wood RD (1999) Quality control by DNA repair. *Science* **286:** 1897–1905

Lindsey J, McGill NI, Lindsey LA, Green DK & Cooke HJ (1991) In vivo loss of telomeric repeats with age in humans. *Mutat Res* **256:** 45–48

Little JP, Safdar A, Bishop D, Tarnopolsky MA & Gibala MJ (2011) An acute bout of high-intensity interval training increases the nuclear abundance of PGC-1α and activates mitochondrial biogenesis in human skeletal muscle. *Am. J. Physiol. Regul. Integr. Comp. Physiol.* **300:** R1303–10

Liu Y, Sanoff HK, Cho H, Burd CE, Torrice C, Ibrahim JG, Thomas NE & Sharpless NE (2009) Expression ofp16INK4ain peripheral blood T-cells is a biomarker of human aging. *Aging Cell* **8:** 439–448

Loughran O, Malliri A, Owens D, Gallimore PH, Stanley MA, Ozanne B, Frame MC & Parkinson EK (1996) Association of CDKN2A/p16INK4A with human head and neck keratinocyte replicative senescence: relationship of dysfunction to immortality and neoplasia. *Oncogene* **13:** 561–568

Löbrich M, Ikpeme S & Kiefer J (1994) Measurement of DNA double-strand breaks in mammalian cells by pulsed-field gel electrophoresis: a new approach using rarely cutting restriction enzymes. *Radiat Res* **138:** 186–192

Luo D & Saltzman W (2000) Synthetic DNA delivery systems. *Nat Biotechnol* **18:** 33–37

Macleod KF, Sherry N, Hannon G, Beach D, Tokino T, Kinzler K, Vogelstein B & Jacks T (1995) p53-dependent and independent expression of p21 during cell growth, differentiation, and DNA damage. *Genes Dev* **9:** 935–944

Madsen P, Rasmussen HH, Leffers H, Honoré B, Dejgaard K, Olsen E, Kiil J, Walbum E, Andersen AH & Basse B (1991) Molecular cloning, occurrence, and expression of a novel partially secreted protein 'psoriasin' that is highly up-regulated in psoriatic skin. *J Invest Dermatol* **97:** 701–712

Malkin D, Li FP, Strong LC, Fraumeni JF, Nelson CE, Kim DH, Kassel J, Gryka MA, Bischoff FZ & Tainsky MA (1990) Germ line p53 mutations in a familial syndrome of breast cancer, sarcomas, and other neoplasms. *Science* **250:** 1233–1238

Mann R, Mulligan RC & Baltimore D (1983) Construction of a retrovirus packaging mutant and its use to produce helper-free defective retrovirus. *Cell* **33:** 153–159

Martin GM, Sprague CA & Epstein CJ (1970) Replicative life-span of cultivated human cells. Effects of donor's age, tissue, and genotype. *Lab. Invest.* **23:** 86–92

Martin K, Kirkwood TB & Potten CS (1998a) Age changes in stem cells of murine small intestinal crypts. *Exp Cell Res* **241:** 316–323

Martin K, Potten CS, Roberts SA & Kirkwood TB (1998b) Altered stem cell regeneration in irradiated intestinal crypts of senescent mice. *J Cell Sci* **111 (Pt 16):** 2297–2303

Martin-Ruiz C, Saretzki G, Petrie J, Ladhoff J, Jeyapalan J, Wei W, Sedivy J & Zglinicki Von T (2004) Stochastic variation in telomere shortening rate causes heterogeneity of human fibroblast replicative life span. *J Biol Chem* **279:** 17826–17833

Matheu A, Maraver A, Klatt P, Flores I, García-Cao I, Borrás C, Flores JM, Viña J, Blasco MA & Serrano M (2007) Delayed ageing through damage protection by the Arf/ p53 pathway. *Nature* **448:** 375–379

Matheu A, Pantoja C, Efeyan A, Criado LM, Martín-Caballero J, Flores JM, Klatt P & Serrano M (2004) Increased gene dosage of Ink4a/Arf results in cancer resistance and normal aging. *Genes Dev* **18:** 2736–2746

Mathor MB, Ferrari G, Dellambra E, Cilli M, Mavilio F, Cancedda R & De Luca M (1996) Clonal analysis of stably transduced human epidermal stem cells in culture. *Proc Natl Acad Sci USA* **93:** 10371–10376

Maurelli R, Zambruno G, Guerra L, Abbruzzese C, Dimri G, Gellini M, Bondanza S & Dellambra E (2006) Inactivation of p16INK4a (inhibitor of cyclin-dependent

kinase 4A) immortalizes primary human keratinocytes by maintaining cells in the stem cell compartment. *FASEB J* **20:** 1516–1518

McConnell BB, Starborg M, Brookes S & Peters G (1998) Inhibitors of cyclin-dependent kinases induce features of replicative senescence in early passage human diploid fibroblasts. *Curr Biol* **8:** 351–354

McGregor F, Muntoni A, Fleming J, Brown J, Felix DH, MacDonald DG, Parkinson EK & Harrison PR (2002) Molecular changes associated with oral dysplasia progression and acquisition of immortality: potential for its reversal by 5-azacytidine. *Cancer Res* **62:** 4757–4766

Medawar PB (1952) An Unsolved Problem of Biology H. K. Lewis, London

Medema RH (2004) Optimizing RNA interference for application in mammalian cells. *Biochem. J.* **380:** 593–603

Michaloglou C, Vredeveld LCW, Soengas MS, Denoyelle C, Kuilman T, van der Horst CMAM, Majoor DM, Shay JW, Mooi WJ & Peeper DS (2005) BRAFE600-associated senescence-like cell cycle arrest of human naevi. *Nature* **436:** 720–724

Miller AD (2002) PA 317 retrovirus packaging cells. *Mol Ther* **6:** 572–575

Miller AD & Chen F (1996) Retrovirus packaging cells based on 10A1 murine leukemia virus for production of vectors that use multiple receptors for cell entry. *J Virol* **70:** 5564–5571

Miller DG, Adam MA & Miller AD (1990) Gene transfer by retrovirus vectors occurs only in cells that are actively replicating at the time of infection. *Mol Cell Biol* **10:** 4239–4242

Minty F (2007) Telomere dysfunction in normal human epidermal keratinocytes.

Minty F, Thurlow JK, Harrison PR & Parkinson EK (2008) Telomere dysfunction in human keratinocytes elicits senescence and a novel transcription profile. *Exp Cell Res* **314:** 2434–2447

Missero C, Di Cunto F, Kiyokawa H, Koff A & Dotto GP (1996) The absence of p21Cip1/WAF1 alters keratinocyte growth and differentiation and promotes ras-tumor progression. *Genes Dev* **10:** 3065–3075

Moiseeva O, Bourdeau V, Roux A, Deschenes-Simard X & Ferbeyre G (2009) Mitochondrial Dysfunction Contributes to Oncogene-Induced Senescence. *Mol Cell Biol* **29:** 4495–4507

Moiseeva O, Mallette FA, Mukhopadhyay UK, Moores A & Ferbeyre G (2006) DNA damage signaling and p53-dependent senescence after prolonged beta-interferon stimulation. *Mol Biol Cell* **17:** 1583–1592

Mol CD, Parikh SS, Putnam CD, Lo TP & Tainer JA (1999) DNA repair mechanisms for the recognition and removal of damaged DNA bases. *Annu. Rev. Biophys. Biomol. Struct.* **28:** 101–128

Montgomery MK, Hulbert AJ & Buttemer WA (2012) Does the oxidative stress theory of aging explain longevity differences in birds? I. Mitochondrial ROS production. *Exp Gerontol* **47:** 203–210

Moubayed N, Weichenthal M, Harder J, Wandel E, Sticherling M & Gläser R (2007) Psoriasin (S100A7) is significantly up-regulated in human epithelial skin tumours. *J Cancer Res Clin Oncol* **133:** 253–261

Mulligan R (1993) The basic science of gene therapy. *Science* **260:** 926–932

Munro J, Barr NI, Ireland H, Morrison V & Parkinson EK (2004) Histone deacetylase inhibitors induce a senescence-like state in human cells by a p16-dependent mechanism that is independent of a mitotic clock. *Exp Cell Res* **295:** 525–538

Munro J, Steeghs K, Morrison V, Ireland H & Parkinson EK (2001) Human fibroblast replicative senescence can occur in the absence of extensive cell division and short telomeres. *Oncogene* **20:** 3541–3552

Munro J, Stott FJ, Vousden KH, Peters G & Parkinson EK (1999) Role of the alternative INK4A proteins in human keratinocyte senescence: evidence for the specific inactivation of p16INK4A upon immortalization. *Cancer Res* **59:** 2516–2521

Muntoni A, Fleming J, Gordon KE, Hunter K, McGregor F, Parkinson EK & Harrison PR (2003) Senescing oral dysplasias are not immortalized by ectopic expression of hTERT alone without other molecular changes, such as loss of INK4A and/or retinoic acid receptor-beta: but p53 mutations are not necessarily required. *Oncogene* **22:** 7804–7808

Nakamura K-I, Izumiyama-Shimomura N, Sawabe M, Arai T, Aoyagi Y, Fujiwara M, Tsuchiya E, Kobayashi Y, Kato M, Oshimura M, Sasajima K, Nakachi K & Takubo K (2002) Comparative analysis of telomere lengths and erosion with age in human epidermis and lingual epithelium. *J Invest Dermatol* **119:** 1014–1019

Nakamura TM, Morin GB, Chapman KB, Weinrich SL, Andrews WH, Lingner J, Harley CB & Cech TR (1997) Telomerase catalytic subunit homologs from fission yeast and human. *Science* **277:** 955–959

Napoli C, Lemieux C & Jorgensen R (1990) Introduction of a Chimeric Chalcone Synthase Gene into Petunia Results in Reversible Co-Suppression of Homologous Genes in trans. *Plant Cell* **2:** 279–289

Narita M, Nũnez S, Heard E, Narita M, Lin AW, Hearn SA, Spector DL, Hannon GJ & Lowe SW (2003) Rb-mediated heterochromatin formation and silencing of E2F target genes during cellular senescence. *Cell* **113:** 703–716

Natarajan E, Omobono JD, Guo Z, Hopkinson S, Lazar AJF, Brenn T, Jones JC & Rheinwald JG (2006) A keratinocyte hypermotility/growth-arrest response involving laminin 5 and p16INK4A activated in wound healing and senescence. *Am J Pathol* **168:** 1821–1837

Natarajan E, Saeb M, Crum CP, Woo SB, McKee PH & Rheinwald JG (2003) Co-expression of p16(INK4A) and laminin 5 gamma2 by microinvasive and superficial squamous cell carcinomas in vivo and by migrating wound and senescent keratinocytes in culture. *Am J Pathol* **163:** 477–491

Newbold RF (1997) Genetic control of telomerase and replicative senescence in human and rodent cells. *Ciba Found. Symp.* **211:** 177–89– discussion 189–97

Nichols WW, Murphy DG, Cristofalo VJ, Toji LH, Greene AE & Dwight SA (1977) Characterization of a new human diploid cell strain, IMR-90. *Science* **196:** 60–63

Norsgaard H, Clark BF & Rattan SI (1996) Distinction between differentiation and senescence and the absence of increased apoptosis in human keratinocytes undergoing cellular aging in vitro. *Exp Gerontol* **31:** 563–570

Obarzanek-Fojt M, Favre B, Kypriotou M, Ryser S, Huber M & Hohl D (2011) Homeodomain-only protein HOP is a novel modulator of late differentiation in keratinocytes. *Eur J Cell Biol* **90:** 279–290

Oikawa S, Tada-Oikawa S & Kawanishi S (2001) Site-specific DNA damage at the GGG sequence by UVA involves acceleration of telomere shortening. *Biochemistry* **40:** 4763–4768

Olovnikov AM (1971) [Principle of marginotomy in template synthesis of polynucleotides]. *Dokl. Akad. Nauk SSSR* **201:** 1496–1499

Olovnikov AM (1973) A theory of marginotomy. The incomplete copying of template margin in enzymic synthesis of polynucleotides and biological significance of the phenomenon. *J Theor Biol* **41:** 181–190

Ooki A, Yamashita K, Kikuchi S, Sakuramoto S, Katada N, Kokubo K, Kobayashi H, Kim MS, Sidransky D & Watanabe M (2010) Potential utility of HOP homeobox gene promoter methylation as a marker of tumor aggressiveness in gastric cancer. *Oncogene*

Ouellette MM, Aisner DL, Savre-Train I, Wright WE & Shay JW (1999) Telomerase activity does not always imply telomere maintenance. *Biochem Biophys Res Commun* **254:** 795–803

Owens DW, Brunton VG, Parkinson EK & Frame MC (2000) E-cadherin at the cell periphery is a determinant of keratinocyte differentiation in vitro. *Biochem Biophys Res Commun* **269:** 369–376

Panier S, Ichijima Y, Fradet-Turcotte A, Leung CCY, Kaustov L, Arrowsmith CH & Durocher D (2012) Tandem protein interaction modules organize the ubiquitin-dependent response to DNA double-strand breaks. *Mol Cell* **47:** 383–395

Parkinson EK & Minty F (2007) Anticancer therapy targeting telomeres and telomerase : current status. *BioDrugs : clinical immunotherapeutics, biopharmaceuticals and gene therapy* **21:** 375–385

Parkinson EK, Fitchett C & Cereser B (2008) Dissecting the non-canonical functions of telomerase. *Cytogenet. Genome Res.* **122:** 273–280

Passos JF, Nelson G, Wang C, Richter T, Simillion C, Proctor CJ, Miwa S, Olijslagers S, Hallinan J, Wipat A, Saretzki G, Rudolph KL, Kirkwood TBL & Zglinicki Von T (2010) Feedback between p21 and reactive oxygen production is necessary for cell senescence. *Mol Syst Biol* **6:** 347

Passos JF, Saretzki G & Zglinicki Von T (2007a) DNA damage in telomeres and mitochondria during cellular senescence: is there a connection? *Nucleic Acids Res* **35:** 7505–7513

Passos JF, Saretzki G, Ahmed S, Nelson G, Richter T, Peters H, Wappler I, Birket MJ, Harold G, Schaeuble K, Birch-Machin MA, Kirkwood TBL & Zglinicki Von T (2007b) Mitochondrial dysfunction accounts for the stochastic heterogeneity in telomere-dependent senescence. *PLoS Biol* **5:** e110

Pauws E, Sijmons GG, Yaka C & Ris-Stalpers C (2004) A novel homeobox gene overexpressed in thyroid carcinoma. *Thyroid* **14:** 500–505

Pear WS, Nolan GP, Scott ML & Baltimore D (1993) Production of high-titer helper-free retroviruses by transient transfection. *Proc Natl Acad Sci USA* **90:** 8392–8396

Peehl DM & Ham RG (1980a) Growth and differentiation of human keratinocytes without a feeder layer or conditioned medium. *In vitro* **16:** 516–525

Peehl DM & Ham RG (1980b) Clonal growth of human keratinocytes with small amounts of dialyzed serum. *In vitro* **16:** 526–540

Petersen S, Saretzki G & Zglinicki von T (1998) Preferential accumulation of single-stranded regions in telomeres of human fibroblasts. *Exp Cell Res* **239:** 152–160

Pérez VI, Buffenstein R, Masamsetti V, Leonard S, Salmon AB, Mele J, Andziak B, Yang T, Edrey Y, Friguet B, Ward W, Richardson A & Chaudhuri A (2009) Protein stability and resistance to oxidative stress are determinants of longevity in the longest-living rodent, the naked mole-rat. *Proceedings of the National Academy of Sciences* **106:** 3059–3064

Pitiyage GN, Slijepcevic P, Gabrani A, Chianea YG, Lim KP, Prime SS, Tilakaratne WM, Fortune F & Parkinson EK (2011) Senescent mesenchymal cells accumulate in human fibrosis by a telomere-independent mechanism and ameliorate fibrosis through matrix metalloproteinases. *J Pathol* **223:** 604–617

Ramirez RD, Morales CP, Herbert BS, Rohde JM, Passons C, Shay JW & Wright WE (2001) Putative telomere-independent mechanisms of replicative aging reflect inadequate growth conditions. *Genes Dev* **15:** 398–403

Reed AL, Califano J, Cairns P, Westra WH, Jones RM, Koch W, Ahrendt S, Eby Y, Sewell D, Nawroz H, Bartek J & Sidransky D (1996) High frequency of p16 (CDKN2/MTS-1/INK4A) inactivation in head and neck squamous cell carcinoma. *Cancer Res* **56:** 3630–3633

Ressler S, Bartkova J, Niederegger H, Bartek J, Scharffetter-Kochanek K, Jansen-Dürr P & Wlaschek M (2006) p16INK4A is a robust in vivo biomarker of cellular aging in human skin. *Aging Cell* **5:** 379–389

Rheinwald JG (1980) Serial cultivation of normal human epidermal keratinocytes. *Methods Cell Biol* **21A:** 229–254

Rheinwald JG & Green H (1975a) Serial cultivation of strains of human epidermal keratinocytes: the formation of keratinizing colonies from single cells. *Cell* **6:** 331–343

Rheinwald JG & Green H (1975b) Formation of a keratinizing epithelium in culture by a cloned cell line derived from a teratoma. *Cell* **6:** 317–330

Rheinwald JG & Green H (1977) Epidermal growth factor and multiplication of cultured Human Epidermal Keratinocytes. *Nature* **265:** 421–424

Rheinwald JG, Hahn WC, Ramsey MR, Wu JY, Guo Z, Tsao H, De Luca M, Catricalà C & O'Toole KM (2002) A two-stage, p16(INK4A)- and p53-dependent keratinocyte senescence mechanism that limits replicative potential independent of telomere status. *Mol Cell Biol* **22:** 5157–5172

Rice RH & Green H (1979) Presence in human epidermal cells of a soluble protein precursor of the cross-linked envelope: activation of the cross-linking by calcium ions. *Cell* **18:** 681–694

Robles SJ & Adami GR (1998) Agents that cause DNA double strand breaks lead to p16INK4a enrichment and the premature senescence of normal fibroblasts. *Oncogene* **16:** 1113–1123

Rodier F & Campisi J (2011) Four faces of cellular senescence. *J Cell Biol* **192:** 547–556

Rodier F, Coppé J-P, Patil CK, Hoeijmakers WAM, Muñoz DP, Raza SR, Freund A, Campeau E, Davalos AR & Campisi J (2009) Persistent DNA damage signalling triggers senescence-associated inflammatory cytokine secretion. *Nat Cell Biol* **11:** 973–979

Rodier F, Muñoz DP, Teachenor R, Chu V, Le O, Bhaumik D, Coppé J-P, Campeau E, Beauséjour CM, Kim S-H, Davalos AR & Campisi J (2011) DNA-SCARS: distinct nuclear structures that sustain damage-induced senescence growth arrest and inflammatory cytokine secretion. *J Cell Sci* **124:** 68–81

Rollins BJ, O'Connell TM, Bennett G, Burton LE, Stiles CD & Rheinwald JG (1989) Environment-dependent growth inhibition of human epidermal keratinocytes by recombinant human transforming growth factor-beta. *J Cell Physiol* **139:** 455–462

Rovillain E, Mansfield L, Caetano C, Alvarez-Fernandez M, Caballero OL, Medema RH, Hummerich H & Jat PS (2011) Activation of nuclear factor-kappa B signalling promotes cellular senescence. *Oncogene* **30:** 2356–2366

Rudolph KL, Chang S, Lee HW, Blasco M, Gottlieb GJ, Greider C & DePinho RA (1999) Longevity, stress response, and cancer in aging telomerase-deficient mice. *Cell* **96:** 701–712

Rudolph KL, Chang S, Millard M, Schreiber-Agus N & DePinho RA (2000) Inhibition of experimental liver cirrhosis in mice by telomerase gene delivery. *Science* **287:** 1253–1258

Sahin E & DePinho RA (2010) Linking functional decline of telomeres, mitochondria and stem cells during ageing. *Nature* **464:** 520–528

Sahin E & DePinho RA (2012) Axis of ageing: telomeres, p53 and mitochondria. *Nat Rev Mol Cell Biol*

Sahin E, Colla S, Liesa M, Moslehi J, Muller FL, Guo M, Cooper M, Kotton D, Fabian AJ, Walkey C, Maser RS, Tonon G, Foerster F, Xiong R, Wang YA, Shukla SA, Jaskelioff M, Martin ES, Heffernan TP, Protopopov A, et al (2011) Telomere dysfunction induces metabolic and mitochondrial compromise. *Nature* **470:** 359–365

Savitsky K, Bar-Shira A, Gilad S, Rotman G, Ziv Y, Vanagaite L, Tagle DA, Smith S, Uziel T, Sfez S, Ashkenazi M, Pecker I, Frydman M, Harnik R, Patanjali SR, Simmons A, Clines GA, Sartiel A, Gatti RA, Chessa L, et al (1995) A single ataxia telangiectasia gene with a product similar to PI-3 kinase. *Science* **268:** 1749–1753

Sedelnikova OA, Horikawa I, Zimonjic DB, Popescu NC, Bonner WM & Barrett JC (2004) Senescing human cells and ageing mice accumulate DNA lesions with unrepairable double-strand breaks. *Nat Cell Biol* **6:** 168–170

Serrano M, Lin AW, McCurrach ME, Beach D & Lowe SW (1997) Oncogenic ras provokes premature cell senescence associated with accumulation of p53 and p16INK4a. *Cell* **88:** 593–602

Severino J, Allen RG, Balin S, Balin A & Cristofalo VJ (2000) Is beta-galactosidase staining a marker of senescence in vitro and in vivo? *Exp Cell Res* **257:** 162–171

Sharpless NE & DePinho RA (2007) How stem cells age and why this makes us grow old. *Nat Rev Mol Cell Biol* **8:** 703–713

Sharpless NE, Bardeesy N, Lee KH, Carrasco D, Castrillon DH, Aguirre AJ, Wu EA, Horner JW & DePinho RA (2001) Loss of p16Ink4a with retention of p19Arf predisposes mice to tumorigenesis. *Nature* **413:** 86–91

Shelton DN, Chang E, Whittier PS, Choi D & Funk WD (1999) Microarray analysis of replicative senescence. *Curr Biol* **9:** 939–945

Sherr CJ (1998) Tumor surveillance via the ARF-p53 pathway. *Genes Dev* **12:** 2984–2991

Shieh SY, Ikeda M, Taya Y & Prives C (1997) DNA damage-induced phosphorylation of p53 alleviates inhibition by MDM2. *Cell* **91:** 325–334

Shiloh Y, Shema E, Moyal L & Oren M (2011) RNF20-RNF40: A ubiquitin-driven link between gene expression and the DNA damage response. *FEBS Lett* **585:** 2795–2802

Smith JR & Hayflick L (1974) Variation in the life-span of clones derived from human diploid cell strains. *J Cell Biol* **62:** 48–53

Smith JR & Whitney RG (1980) Intraclonal variation in proliferative potential of human diploid fibroblasts: stochastic mechanism for cellular aging. *Science* **207:** 82–84

Smogorzewska A & de Lange T (2002) Different telomere damage signaling pathways in human and mouse cells. *EMBO J* **21:** 4338–4348

Smogorzewska A, Karlseder J, Holtgreve-Grez H, Jauch A & de Lange T (2002) DNA ligase IV-dependent NHEJ of deprotected mammalian telomeres in G1 and G2. *Curr Biol* **12:** 1635–1644

Soder AI, Hoare SF, Muir S, Going JJ, Parkinson EK & Keith WN (1997) Amplification, increased dosage and in situ expression of the telomerase RNA gene in human cancer. *Oncogene* **14:** 1013–1021

Sohal RS & Orr WC (2012) The redox stress hypothesis of aging. *Free Radic. Biol. Med.* **52:** 539–555

Stein GH, Drullinger LF, Soulard A & Dulić V (1999) Differential roles for cyclin-dependent kinase inhibitors p21 and p16 in the mechanisms of senescence and differentiation in human fibroblasts. *Mol Cell Biol* **19:** 2109–2117

Stern MM & Bickenbach JR (2007) Epidermal stem cells are resistant to cellular aging. *Aging Cell* **6:** 439–452

Stott FJ, Bates S, James MC, McConnell BB, Starborg M, Brookes S, Palmero I, Ryan K, Hara E, Vousden KH & Peters G (1998) The alternative product from the human CDKN2A locus, p14(ARF), participates in a regulatory feedback loop with p53 and MDM2. *EMBO J* **17:** 5001–5014

Strehler BL (1962) Time, Cells, and Aging. Academic Press

Sugimoto M, Yamashita R & Ueda M (2006) Telomere length of the skin in association with chronological aging and photoaging. *Journal of Dermatological Science* **43:** 43–47

Sugrue MM, Shin DY, Lee SW & Aaronson SA (1997) Wild-type p53 triggers a rapid senescence program in human tumor cells lacking functional p53. *Proc Natl Acad Sci USA* **94:** 9648–9653

Suram A, Kaplunov J, Patel PL, Ruan H, Cerutti A, Boccardi V, Fumagalli M, Di Micco R, Mirani N, Lal Gurung R, Prakash Hande M, d'Adda di Fagagna F & Herbig U (2012) Oncogene-induced telomere dysfunction enforces cellular senescence in human cancer precursor lesions. *EMBO J*

Swift S, Lorens J, Achacoso P & Nolan GP (2001) Rapid production of retroviruses for efficient gene delivery to mammalian cells using 293T cell-based systems. *Current protocols in immunology / edited by John E Coligan [et al]* **Chapter 10:** Unit 10.17C

Takai H, Smogorzewska A & de Lange T (2003) DNA damage foci at dysfunctional telomeres. *Curr Biol* **13:** 1549–1556

Timmers S, Konings E, Bilet L, Houtkooper RH, van de Weijer T, Goossens GH, Hoeks J, van der Krieken S, Ryu D, Kersten S, Moonen-Kornips E, Hesselink MKC, Kunz I, Schrauwen-Hinderling VB, Blaak EE, Auwerx J & Schrauwen P (2011) Calorie restriction-like effects of 30 days of resveratrol supplementation on energy metabolism and metabolic profile in obese humans. *Cell Metabolism* **14:** 612–622

Todaro GJ & Green H (1963) Quantitative studies of the growth of mouse embryo cells in culture and their development into established lines. *J Cell Biol* **17:** 299–313

Tomás-Loba A, Flores I, Fernández-Marcos PJ, Cayuela ML, Maraver A, Tejera A, Borrás C, Matheu A, Klatt P, Flores JM, Viña J, Serrano M & Blasco MA (2008) Telomerase reverse transcriptase delays aging in cancer-resistant mice. *Cell* **135:** 609–622

Tyner SD, Venkatachalam S, Choi J, Jones S, Ghebranious N, Igelmann H, Lu X, Soron G, Cooper B, Brayton C, Hee Park S, Thompson T, Karsenty G, Bradley A & Donehower LA (2002) p53 mutant mice that display early ageing-associated phenotypes. *Nature* **415:** 45–53

Urasaki Y, Heath L & Xu CW (2012) Coupling of glucose deprivation with impaired histone H2B monoubiquitination in tumors. *PLoS ONE* **7:** e36775

van Gent D, Hoeijmakers J & Kanaar R (2001) Chromosomal stability and the DNA double-stranded break connection. *Nat Rev Genet* **2:** 196–206

van Steensel B, Smogorzewska A & de Lange T (1998) TRF2 protects human telomeres from end-to-end fusions. *Cell* **92:** 401–413

van Tuyn J & Adams PD (2012) Signalling the end of the line. *Nat Cell Biol* **14:** 339–341

Varmus H (1988) Retroviruses. *Science* **240:** 1427–1435

Vasiliev O, Rhodes SJ & Beebe DC (2007) Identification and expression of Hop, an atypical homeobox gene expressed late in lens fiber cell terminal differentiation. *Mol Vis* **13:** 114–124

Vaughan S & Jat PS (2011) Deciphering the role of nuclear factor-ϰB in cellular senescence. *Aging* **3:** 913–919

Velarde MC, Flynn JM, Day NU, Melov S & Campisi J (2012) Mitochondrial oxidative stress caused by Sod2 deficiency promotes cellular senescence and aging phenotypes in the skin. *Aging* **4:** 3–12

Venkatesan RN & Price C (1998) Telomerase expression in chickens: constitutive activity in somatic tissues and down-regulation in culture. *Proc Natl Acad Sci USA* **95:** 14763–14768

Ventura A, Kirsch DG, McLaughlin ME, Tuveson DA, Grimm J, Lintault L, Newman J, Reczek EE, Weissleder R & Jacks T (2007) Restoration of p53 function leads to tumour regression in vivo. *Nature* **445:** 661–665

Vulliamy T, Marrone A, Goldman F, Dearlove A, Bessler M, Mason PJ & Dokal I (2001) The RNA component of telomerase is mutated in autosomal dominant dyskeratosis congenita. *Nature* **413:** 432–435

Vulliamy T, Marrone A, Szydlo R, Walne A, Mason PJ & Dokal I (2004) Disease anticipation is associated with progressive telomere shortening in families with dyskeratosis congenita due to mutations in TERC. *Nat Genet* **36:** 447–449

Waaijer MEC, Parish WE, Strongitharm BH, van Heemst D, Slagboom PE, de Craen AJM, Sedivy JM, Westendorp RGJ, Gunn DA & Maier AB (2012) The number of p16INK4a positive cells in human skin reflects biological age. *Aging Cell* **11:** 722–725

Wang C, Jurk D, Maddick M, Nelson G, Martin-Ruiz C & Zglinicki Von T (2009) DNA damage response and cellular senescence in tissues of aging mice. *Aging Cell* **8:** 311–323

Wang J, Sun Q, Morita Y, Jiang H, Gross A, Lechel A, Hildner K, Guachalla LM, Gompf A, Hartmann D, Schambach A, Wuestefeld T, Dauch D, Schrezenmeier H, Hofmann W-K, Nakauchi H, Ju Z, Kestler HA, Zender L & Rudolph KL (2012) A differentiation

checkpoint limits hematopoietic stem cell self-renewal in response to DNA damage. *Cell* **148:** 1001–1014

Watson JD (1972) Origin of concatemeric T7 DNA. *Nature New Biol* **239:** 197–201

Watson PH, Leygue ER & Murphy LC (1998) Psoriasin (S100A7). *Int J Biochem Cell Biol* **30:** 567–571

Webley K, Bond JA, Jones CJ, Blaydes JP, Craig A, Hupp T & Wynford-Thomas D (2000) Posttranslational modifications of p53 in replicative senescence overlapping but distinct from those induced by DNA damage. *Mol Cell Biol* **20:** 2803–2808

Wenz T, Rossi SG, Rotundo RL, Spiegelman BM & Moraes CT (2009) Increased muscle PGC-1alpha expression protects from sarcopenia and metabolic disease during aging. *Proceedings of the National Academy of Sciences* **106:** 20405–20410

Wiemann SU, Satyanarayana A, Tsahuridu M, Tillmann HL, Zender L, Klempnauer J, Flemming P, Franco S, Blasco MA, Manns MP & Rudolph KL (2002) Hepatocyte telomere shortening and senescence are general markers of human liver cirrhosis. *FASEB J* **16:** 935–942

Wille JJ, Pittelkow MR, Shipley GD & Scott RE (1984) Integrated control of growth and differentiation of normal human prokeratinocytes cultured in serum-free medium: clonal analyses, growth kinetics, and cell cycle studies. *J Cell Physiol* **121:** 31–44

Williams BR (1997) Role of the double-stranded RNA-activated protein kinase (PKR) in cell regulation. *Biochem. Soc. Trans.* **25:** 509–513

Wong K-K, Maser RS, Bachoo RM, Menon J, Carrasco DR, Gu Y, Alt FW & DePinho RA (2003) Telomere dysfunction and Atm deficiency compromises organ homeostasis and accelerates ageing. *Nature* **421:** 643–648

Wootton M, Steeghs K, Watt D, Munro J, Gordon K, Ireland H, Morrison V, Behan W & Parkinson EK (2003) Telomerase alone extends the replicative life span of human skeletal muscle cells without compromising genomic stability. *Hum Gene Ther* **14:** 1473–1487

Wright WE, Piatyszek MA, Rainey WE, Byrd W & Shay JW (1996) Telomerase activity in human germline and embryonic tissues and cells. *Dev. Genet.* **18:** 173–179

Wyllie F, Jones C, Skinner J, Haughton M, Wallis C, Wynford-Thomas D, Faragher R & Kipling D (2000) Telomerase prevents the accelerated cell ageing of Werner syndrome fibroblasts. *Nat Genet* **24:** 16–17

Xue W, Zender L, Miething C, Dickins RA, Hernando E, Krizhanovsky V, Cordon-Cardo C & Lowe SW (2007) Senescence and tumour clearance is triggered by p53 restoration in murine liver carcinomas. *Nature* **445:** 656–660

Yamaguchi S, Asanoma K, Takao T, Kato K & Wake N (2009) Homeobox gene HOPX is epigenetically silenced in human uterine endometrial cancer and suppresses estrogen-stimulated proliferation of cancer cells by inhibiting serum response factor. *Int J Cancer* **124:** 2577–2588

Yamashita K, Kim MS, Park HL, Tokumaru Y, Osada M, Inoue H, Mori M & Sidransky D (2008) HOP/OB1/NECC1 promoter DNA is frequently hypermethylated and involved in tumorigenic ability in esophageal squamous cell carcinoma. *Mol Cancer Res* **6:** 31–41

Yang J-M, Sim SM, Kim H-Y & Park GT (2010) Expression of the homeobox gene, HOPX, is modulated by cell differentiation in human keratinocytes and is involved in the expression of differentiation markers. *Eur J Cell Biol* **89:** 537–546

Zhang H & Cohen SN (2004) Smurf2 up-regulation activates telomere-dependent senescence. *Genes Dev* **18:** 3028–3040

Zhang H, Hannon GJ & Beach D (1994) p21-containing cyclin kinases exist in both active and inactive states. *Genes Dev* **8:** 1750–1758

Zhang H, Zhao Q, Chen Y, Wang Y, Gao S, Mao Y, Li M, Peng A, He D & Xiao X (2008) Selective expression of S100A7 in lung squamous cell carcinomas and large cell carcinomas but not in adenocarcinomas and small cell carcinomas. *Thorax* **63:** 352–359

Zhang J, Pickering CR, Holst CR, Gauthier ML & Tlsty TD (2006) p16INK4a modulates p53 in primary human mammary epithelial cells. *Cancer Res* **66:** 10325–10331

Zhang R, Chen W & Adams PD (2007) Molecular dissection of formation of senescence-associated heterochromatin foci. *Mol Cell Biol* **27:** 2343–2358

Zhang R, Poustovoitov MV, Ye X, Santos HA, Chen W, Daganzo SM, Erzberger JP, Serebriiskii IG, Canutescu AA, Dunbrack RL, Pehrson JR, Berger JM, Kaufman PD & Adams PD (2005) Formation of MacroH2A-containing senescence-associated heterochromatin foci and senescence driven by ASF1a and HIRA. *Dev Cell* **8:** 19–30

Appendix - Copyright permissions

<div align="center">

**ELSEVIER LICENSE
TERMS AND CONDITIONS**

</div>

Jun 06, 2013

This is a License Agreement between Alice de Castro ("You") and Elsevier ("Elsevier") provided by Copyright Clearance Center ("CCC"). The license consists of your order details, the terms and conditions provided by Elsevier, and the payment terms and conditions.

All payments must be made in full to CCC. For payment instructions, please see information listed at the bottom of this form.

Supplier	Elsevier Limited The Boulevard,Langford Lane Kidlington,Oxford,OX5 1GB,UK
Registered Company Number	1982084
Customer name	Alice de Castro
Customer address	CDOS
	London, E1 2AT
License number	3163031051201
License date	Jun 06, 2013
Licensed content publisher	Elsevier
Licensed content publication	The International Journal of Biochemistry & Cell Biology
Licensed content title	The signals and pathways activating cellular senescence
Licensed content author	Ittai Ben-Porath,Robert A. Weinberg
Licensed content date	May 2005
Licensed content volume number	37
Licensed content issue number	5
Number of pages	16
Start Page	961
End Page	976
Type of Use	reuse in a thesis/dissertation
Intended publisher of new work	other
Portion	figures/tables/illustrations

Number of figures/tables/illustrations	3
Format	both print and electronic
Are you the author of this Elsevier article?	No
Will you be translating?	No
Order reference number	
Title of your thesis/dissertation	A mechanistic investigation into candidate markers of telomere-induced senescence in normal human epidermal keratinocytes
Expected completion date	Jul 2013
Estimated size (number of pages)	300
Elsevier VAT number	GB 494 6272 12
Permissions price	0.00 GBP
VAT/Local Sales Tax	0.0 USD / 0.0 GBP
Total	0.00 GBP
Terms and Conditions	

INTRODUCTION

1. The publisher for this copyrighted material is Elsevier. By clicking "accept" in connection with completing this licensing transaction, you agree that the following terms and conditions apply to this transaction (along with the Billing and Payment terms and conditions established by Copyright Clearance Center, Inc. ("CCC"), at the time that you opened your Rightslink account and that are available at any time at http://myaccount.copyright.com).

GENERAL TERMS

2. Elsevier hereby grants you permission to reproduce the aforementioned material subject to the terms and conditions indicated.

3. Acknowledgement: If any part of the material to be used (for example, figures) has appeared in our publication with credit or acknowledgement to another source, permission must also be sought from that source. If such permission is not obtained then that material may not be included in your publication/copies. Suitable acknowledgement to the source must be made, either as a footnote or in a reference list at the end of your publication, as follows:

"Reprinted from Publication title, Vol /edition number, Author(s), Title of article / title of chapter, Pages No., Copyright (Year), with permission from Elsevier [OR APPLICABLE SOCIETY COPYRIGHT OWNER]." Also Lancet special credit - "Reprinted from The Lancet, Vol. number, Author(s), Title of article, Pages No., Copyright (Year), with permission from Elsevier."

4. Reproduction of this material is confined to the purpose and/or media for which permission is hereby given.

5. Altering/Modifying Material: Not Permitted. However figures and illustrations may be altered/adapted minimally to serve your work. Any other abbreviations, additions, deletions and/or any other alterations shall be made only with prior written authorization of Elsevier Ltd. (Please contact Elsevier at permissions@elsevier.com)

6. If the permission fee for the requested use of our material is waived in this instance, please be advised that your future requests for Elsevier materials may attract a fee.

7. Reservation of Rights: Publisher reserves all rights not specifically granted in the combination of (i) the license details provided by you and accepted in the course of this licensing transaction, (ii) these terms and conditions and (iii) CCC's Billing and Payment terms and conditions.

8. License Contingent Upon Payment: While you may exercise the rights licensed immediately upon issuance of the license at the end of the licensing process for the transaction, provided that you have disclosed complete and accurate details of your proposed use, no license is finally effective unless and until full payment is received from you (either by publisher or by CCC) as provided in CCC's Billing and Payment terms and conditions. If full payment is not received on a timely basis, then any license preliminarily granted shall be deemed automatically revoked and shall be void as if never granted. Further, in the event that you breach any of these terms and conditions or any of CCC's Billing and Payment terms and conditions, the license is automatically revoked and shall be void as if never granted. Use of materials as described in a revoked license, as well as any use of the materials beyond the scope of an unrevoked license, may constitute copyright infringement and publisher reserves the right to take any and all action to protect its copyright in the materials.

9. Warranties: Publisher makes no representations or warranties with respect to the licensed material.

10. Indemnity: You hereby indemnify and agree to hold harmless publisher and CCC, and their respective officers, directors, employees and agents, from and against any and all claims arising out of your use of the licensed material other than as specifically authorized pursuant to this license.

11. No Transfer of License: This license is personal to you and may not be sublicensed, assigned, or transferred by you to any other person without publisher's written permission.

12. No Amendment Except in Writing: This license may not be amended except in a writing signed by both parties (or, in the case of publisher, by CCC on publisher's behalf).

13. Objection to Contrary Terms: Publisher hereby objects to any terms contained in any purchase order, acknowledgment, check endorsement or other writing prepared by you, which terms are inconsistent with these terms and conditions or CCC's Billing and Payment terms and conditions. These terms and conditions, together with CCC's Billing and Payment terms and conditions (which are incorporated herein), comprise the entire agreement between you and publisher (and CCC) concerning this licensing transaction. In the event of any conflict between your obligations established by these terms and conditions and those established by CCC's Billing and Payment terms and conditions, these terms and conditions

shall control.

14. Revocation: Elsevier or Copyright Clearance Center may deny the permissions described in this License at their sole discretion, for any reason or no reason, with a full refund payable to you. Notice of such denial will be made using the contact information provided by you. Failure to receive such notice will not alter or invalidate the denial. In no event will Elsevier or Copyright Clearance Center be responsible or liable for any costs, expenses or damage incurred by you as a result of a denial of your permission request, other than a refund of the amount(s) paid by you to Elsevier and/or Copyright Clearance Center for denied permissions.

LIMITED LICENSE

The following terms and conditions apply only to specific license types:

15. **Translation**: This permission is granted for non-exclusive world **English** rights only unless your license was granted for translation rights. If you licensed translation rights you may only translate this content into the languages you requested. A professional translator must perform all translations and reproduce the content word for word preserving the integrity of the article. If this license is to re-use 1 or 2 figures then permission is granted for non-exclusive world rights in all languages.

16. **Website**: The following terms and conditions apply to electronic reserve and author websites:
Electronic reserve: If licensed material is to be posted to website, the web site is to be password-protected and made available only to bona fide students registered on a relevant course if:
This license was made in connection with a course,
This permission is granted for 1 year only. You may obtain a license for future website posting,
All content posted to the web site must maintain the copyright information line on the bottom of each image,
A hyper-text must be included to the Homepage of the journal from which you are licensing at http://www.sciencedirect.com/science/journal/xxxxx or the Elsevier homepage for books at http://www.elsevier.com , and
Central Storage: This license does not include permission for a scanned version of the material to be stored in a central repository such as that provided by Heron/XanEdu.

17. **Author website** for journals with the following additional clauses:

All content posted to the web site must maintain the copyright information line on the bottom of each image, and the permission granted is limited to the personal version of your paper. You are not allowed to download and post the published electronic version of your article (whether PDF or HTML, proof or final version), nor may you scan the printed edition to create an electronic version. A hyper-text must be included to the Homepage of the journal from which you are licensing at http://www.sciencedirect.com/science/journal/xxxxx . As part of our normal production process, you will receive an e-mail notice when your article appears on Elsevier's online service ScienceDirect (www.sciencedirect.com). That e-mail will include the article's Digital Object Identifier (DOI). This number provides the electronic link to the published article and should be included in the posting of your personal version. We ask that you wait until you receive this e-mail and have the DOI to do any

posting.

Central Storage: This license does not include permission for a scanned version of the material to be stored in a central repository such as that provided by Heron/XanEdu.

18. **Author website** for books with the following additional clauses:
Authors are permitted to place a brief summary of their work online only.
A hyper-text must be included to the Elsevier homepage at http://www.elsevier.com . All content posted to the web site must maintain the copyright information line on the bottom of each image. You are not allowed to download and post the published electronic version of your chapter, nor may you scan the printed edition to create an electronic version.

Central Storage: This license does not include permission for a scanned version of the material to be stored in a central repository such as that provided by Heron/XanEdu.

19. **Website** (regular and for author): A hyper-text must be included to the Homepage of the journal from which you are licensing at http://www.sciencedirect.com/science/journal/xxxxx. or for books to the Elsevier homepage at http://www.elsevier.com

20. **Thesis/Dissertation**: If your license is for use in a thesis/dissertation your thesis may be submitted to your institution in either print or electronic form. Should your thesis be published commercially, please reapply for permission. These requirements include permission for the Library and Archives of Canada to supply single copies, on demand, of the complete thesis and include permission for UMI to supply single copies, on demand, of the complete thesis. Should your thesis be published commercially, please reapply for permission.

21. **Other Conditions**:

v1.6

Gratis licenses (referencing $0 in the Total field) are free. Please retain this printable license for your reference. No payment is required.

NATURE PUBLISHING GROUP LICENSE
TERMS AND CONDITIONS

Jun 06, 2013

This is a License Agreement between Alice de Castro ("You") and Nature Publishing Group ("Nature Publishing Group") provided by Copyright Clearance Center ("CCC"). The license consists of your order details, the terms and conditions provided by Nature Publishing Group, and the payment terms and conditions.

All payments must be made in full to CCC. For payment instructions, please see information listed at the bottom of this form.

License Number	3162570740234
License date	Jun 05, 2013
Licensed content publisher	Nature Publishing Group
Licensed content publication	Nature Reviews Molecular Cell Biology
Licensed content title	Cellular senescence: when bad things happen to good cells
Licensed content author	Judith Campisi, Fabrizio d'Adda di Fagagna
Licensed content date	Sep 1, 2007
Volume number	8
Issue number	9
Type of Use	reuse in a thesis/dissertation
Requestor type	academic/educational
Format	print and electronic
Portion	figures/tables/illustrations
Number of figures/tables/illustrations	2
High-res required	no
Figures	Figure 3	The DNA-damage response. Figure 4	Senescence controlled by the p53 and p16– prb pathways.
Author of this NPG article	no
Your reference number	None
Title of your thesis / dissertation	A mechanistic investigation into candidate markers of telomere-induced senescence in normal human epidermal keratinocytes
Expected completion date	Jul 2013
Estimated size (number of pages)	300
Total	**0.00 GBP**
Terms and Conditions	

Terms and Conditions for Permissions

Nature Publishing Group hereby grants you a non-exclusive license to reproduce this material for this purpose, and for no other use,subject to the conditions below:

1. NPG warrants that it has, to the best of its knowledge, the rights to license reuse of this material. However, you should ensure that the material you are requesting is original to Nature Publishing

Group and does not carry the copyright of another entity (as credited in the published version). If the credit line on any part of the material you have requested indicates that it was reprinted or adapted by NPG with permission from another source, then you should also seek permission from that source to reuse the material.

2. Permission granted free of charge for material in print is also usually granted for any electronic version of that work, provided that the material is incidental to the work as a whole and that the electronic version is essentially equivalent to, or substitutes for, the print version.Where print permission has been granted for a fee, separate permission must be obtained for any additional, electronic re-use (unless, as in the case of a full paper, this has already been accounted for during your initial request in the calculation of a print run).NB: In all cases, web-based use of full-text articles must be authorized separately through the 'Use on a Web Site' option when requesting permission.

3. Permission granted for a first edition does not apply to second and subsequent editions and for editions in other languages (except for signatories to the STM Permissions Guidelines, or where the first edition permission was granted for free).

4. Nature Publishing Group's permission must be acknowledged next to the figure, table or abstract in print. In electronic form, this acknowledgement must be visible at the same time as the figure/table/abstract, and must be hyperlinked to the journal's homepage.

5. The credit line should read:
   Reprinted by permission from Macmillan Publishers Ltd: [JOURNAL NAME] (reference citation), copyright (year of publication)
   For AOP papers, the credit line should read:
   Reprinted by permission from Macmillan Publishers Ltd: [JOURNAL NAME], advance online publication, day month year (doi: 10.1038/sj.[JOURNAL ACRONYM].XXXXX)

   Note: For republication from the _British Journal of Cancer,_ the following credit lines apply.
   Reprinted by permission from Macmillan Publishers Ltd on behalf of Cancer Research UK: [JOURNAL NAME] (reference citation), copyright (year of publication)For AOP papers, the credit line should read:
   Reprinted by permission from Macmillan Publishers Ltd on behalf of Cancer Research UK: [JOURNAL NAME], advance online publication, day month year (doi: 10.1038/sj.[JOURNAL ACRONYM].XXXXX)

6. Adaptations of single figures do not require NPG approval. However, the adaptation should be credited as follows:

   Adapted by permission from Macmillan Publishers Ltd: [JOURNAL NAME] (reference citation), copyright (year of publication)

   Note: For adaptation from the _British Journal of Cancer,_ the following credit line applies.
   Adapted by permission from Macmillan Publishers Ltd on behalf of Cancer Research UK: [JOURNAL NAME] (reference citation), copyright (year of publication)

7. Translations of 401 words up to a whole article require NPG approval. Please visit http://www.macmillanmedicalcommunications.com for more information.Translations of up to a 400 words do not require NPG approval. The translation should be credited as follows:

   Translated by permission from Macmillan Publishers Ltd: [JOURNAL NAME] (reference citation), copyright (year of publication).

   Note: For translation from the _British Journal of Cancer,_ the following credit line applies.

Translated by permission from Macmillan Publishers Ltd on behalf of Cancer Research UK: [JOURNAL NAME] (reference citation), copyright (year of publication)

We are certain that all parties will benefit from this agreement and wish you the best in the use of this material. Thank you.
Special Terms:
v1.1

If you would like to pay for this license now, please remit this license along with your payment made payable to "COPYRIGHT CLEARANCE CENTER" otherwise you will be invoiced within 48 hours of the license date. Payment should be in the form of a check or money order referencing your account number and this invoice number RLNK501036694.
Once you receive your invoice for this order, you may pay your invoice by credit card. Please follow instructions provided at that time.

Make Payment To:
Copyright Clearance Center
Dept 001
P.O. Box 843006
Boston, MA 02284-3006

For suggestions or comments regarding this order, contact RightsLink Customer Support: customercare@copyright.com or +1-877-622-5543 (toll free in the US) or +1-978-646-2777.

Gratis licenses (referencing $0 in the Total field) are free. Please retain this printable license for your reference. No payment is required.

NATURE PUBLISHING GROUP LICENSE
TERMS AND CONDITIONS

Jun 06, 2013

This is a License Agreement between Alice de Castro ("You") and Nature Publishing Group ("Nature Publishing Group") provided by Copyright Clearance Center ("CCC"). The license consists of your order details, the terms and conditions provided by Nature Publishing Group, and the payment terms and conditions.

All payments must be made in full to CCC. For payment instructions, please see information listed at the bottom of this form.

License Number	3162580005121
License date	Jun 05, 2013
Licensed content publisher	Nature Publishing Group
Licensed content publication	Nature Reviews Molecular Cell Biology
Licensed content title	T-loops and the origin of telomeres
Licensed content author	Titia de Lange
Licensed content date	Apr 1, 2004
Volume number	5
Issue number	4
Type of Use	reuse in a thesis/dissertation
Requestor type	academic/educational
Format	print and electronic
Portion	figures/tables/illustrations
Number of figures/tables/illustrations	3
High-res required	no
Figures	Figure 1	Solutions to the end-replication problem. Figure 2	Proposed structure of the human telomeric complex. Figure 3	T-loop formation resembles initiation of RDR.
Author of this NPG article	no
Your reference number	None
Title of your thesis / dissertation	A mechanistic investigation into candidate markers of telomere-induced senescence in normal human epidermal keratinocytes
Expected completion date	Jul 2013
Estimated size (number of pages)	300
Total	**0.00 GBP**
Terms and Conditions	

Terms and Conditions for Permissions

Nature Publishing Group hereby grants you a non-exclusive license to reproduce this material for this purpose, and for no other use,subject to the conditions below:

1. NPG warrants that it has, to the best of its knowledge, the rights to license reuse of this material.

However, you should ensure that the material you are requesting is original to Nature Publishing Group and does not carry the copyright of another entity (as credited in the published version). If the credit line on any part of the material you have requested indicates that it was reprinted or adapted by NPG with permission from another source, then you should also seek permission from that source to reuse the material.

2. Permission granted free of charge for material in print is also usually granted for any electronic version of that work, provided that the material is incidental to the work as a whole and that the electronic version is essentially equivalent to, or substitutes for, the print version.Where print permission has been granted for a fee, separate permission must be obtained for any additional, electronic re-use (unless, as in the case of a full paper, this has already been accounted for during your initial request in the calculation of a print run).NB: In all cases, web-based use of full-text articles must be authorized separately through the 'Use on a Web Site' option when requesting permission.

3. Permission granted for a first edition does not apply to second and subsequent editions and for editions in other languages (except for signatories to the STM Permissions Guidelines, or where the first edition permission was granted for free).

4. Nature Publishing Group's permission must be acknowledged next to the figure, table or abstract in print. In electronic form, this acknowledgement must be visible at the same time as the figure/table/abstract, and must be hyperlinked to the journal's homepage.

5. The credit line should read:
Reprinted by permission from Macmillan Publishers Ltd: [JOURNAL NAME] (reference citation), copyright (year of publication)
For AOP papers, the credit line should read:
Reprinted by permission from Macmillan Publishers Ltd: [JOURNAL NAME], advance online publication, day month year (doi: 10.1038/sj.[JOURNAL ACRONYM].XXXXX)

Note: For republication from the *British Journal of Cancer,* the following credit lines apply.
Reprinted by permission from Macmillan Publishers Ltd on behalf of Cancer Research UK: [JOURNAL NAME] (reference citation), copyright (year of publication)For AOP papers, the credit line should read:
Reprinted by permission from Macmillan Publishers Ltd on behalf of Cancer Research UK: [JOURNAL NAME], advance online publication, day month year (doi: 10.1038/sj.[JOURNAL ACRONYM].XXXXX)

6. Adaptations of single figures do not require NPG approval. However, the adaptation should be credited as follows:

Adapted by permission from Macmillan Publishers Ltd: [JOURNAL NAME] (reference citation), copyright (year of publication)

Note: For adaptation from the *British Journal of Cancer,* the following credit line applies.
Adapted by permission from Macmillan Publishers Ltd on behalf of Cancer Research UK: [JOURNAL NAME] (reference citation), copyright (year of publication)

7. Translations of 401 words up to a whole article require NPG approval. Please visit http://www.macmillanmedicalcommunications.com for more information.Translations of up to a 400 words do not require NPG approval. The translation should be credited as follows:

Translated by permission from Macmillan Publishers Ltd: [JOURNAL NAME] (reference citation), copyright (year of publication).

Note: For translation from the _British Journal of Cancer,_ the following credit line applies.
Translated by permission from Macmillan Publishers Ltd on behalf of Cancer Research UK:
[JOURNAL NAME] (reference citation), copyright (year of publication)

We are certain that all parties will benefit from this agreement and wish you the best in the use of this material. Thank you.
Special Terms:
v1.1

If you would like to pay for this license now, please remit this license along with your payment made payable to "COPYRIGHT CLEARANCE CENTER" otherwise you will be invoiced within 48 hours of the license date. Payment should be in the form of a check or money order referencing your account number and this invoice number RLNK501036711.
Once you receive your invoice for this order, you may pay your invoice by credit card. Please follow instructions provided at that time.

Make Payment To:
Copyright Clearance Center
Dept 001
P.O. Box 843006
Boston, MA 02284-3006

For suggestions or comments regarding this order, contact RightsLink Customer Support:
customercare@copyright.com or +1-877-622-5543 (toll free in the US) or +1-978-646-2777.

Gratis licenses (referencing $0 in the Total field) are free. Please retain this printable license for your reference. No payment is required.

From:	Mazzullo, Mala
Sent:	Monday, June 10, 2013 11:37 AM
To:	Garite, Bibi
Subject:	FW: CSHL Press Reprint Permission Request Form - G&D

On 6/10/13 6:22 AM, "reprint@cshl.edu" <reprint@cshl.edu> wrote:

>Default Intro
>Default Intro - line2
>
>
>Name: Alice de Castro
>CompanyInstitution: Queen Mary University of London Library Address:
>4 Newark Street Library Address (line 2):
>City: London
>State (US and Canada): London
>Country: United Kingdom
>Zip: SE8 4SL
>Title:
>Lab/Department:
>Phone: +442078827141
>Fax: +442073777064
>Email: a.m.de-castro@qmul.ac.uk
>Title of Publication: A mechanistic investigation into candidate
>markers of telomere-induced senescence in normal human epidermal
>keratinocytes
>Authors/Editors: I am the author as this is my PhD thesis
>
>Date of Publication: July 2013
>Publisher: Queen Mary University of London Title of CSHLP
>Journal/Book: Genes & Development Title of Article/Chapter:
>Shelterin: the protein complex that shapes and safeguards human
>telomeres CSHL Authors/Editors: Titia de Lange Page Numbers: 2101
>Figure Numbers: 1A and 1B Figure Page Numbers: 2101 Copyright Date:
>15 Sep 2005
>Language:
>Territory:
>Format: print and electronic
>Additional comments: I'm requesting permission to use 2 images in my
>PhD thesis
>
>ipaddress: 138.037.134.052
>view here: http://www.cshlpress.com/subs_admin.tpl
>
>Default Footer
>Default Footer - line2

![Springer logo]

July 4, 2013

<u>**Springer reference**</u>
C Heiser W (2004) Gene delivery to mammalian cells. Vol. 2, Viral gene transfer techniques.
Humana Press. Part VI - 31 - Figure 2. The retroviral life cycle. Page 466.

<u>**Your project**</u>
University:	Barts and The London School of Medicine and Dentistry
Title:	Dissertation/Thesis - Alice de Castro

With reference to your request to reuse material in which Springer Science+Business Media controls
the copyright, our permission is granted free of charge under the following conditions:

<u>**Springer material**</u>
- represents original material which does not carry references to other sources (if material in
  question refers with a credit to another source, authorization from that source is required as well);
- requires full credit (book title, year of publication, page, chapter title, name(s) of author(s),
  original copyright notice) is given to the publication in which the material was originally published
  by adding: "With kind permission of Springer Science+Business Media";
- may not be altered in any manner. Any other abbreviations, additions, deletions and/or any other
  alterations shall be made only with prior written authorization of the author and/or Springer
  Science+Business Media;

<u>**This permission**</u>
- is non-exclusive;
- is valid for one-time use only for the purpose of defending your thesis, and with a maximum of 100
  extra copies in paper.
- includes use in an electronic form, provided it is an author-created version of the thesis on his/her
  own website and his/her university's repository, including UMI (according to the definition on the
  Sherpa website: http://www.sherpa.ac.uk/romeo/);
- is subject to courtesy information to the corresponding author;
- is personal to you and may not be sublicensed, assigned, or transferred by you to any other person
  without Springer's written permission;
- is valid only when the conditions noted above are met.

Permission free of charge does not prejudice any rights we might have to charge for reproduction of our
copyrighted material in the future.

Best regards,

Rights and Permissions
Springer-Verlag GmbH
Tiergartenstr. 17
69121 Heidelberg
Germany
E-mail: permissions.heidelberg@springer.com

NATURE PUBLISHING GROUP LICENSE
TERMS AND CONDITIONS

Jun 06, 2013

This is a License Agreement between Alice de Castro ("You") and Nature Publishing Group ("Nature Publishing Group") provided by Copyright Clearance Center ("CCC"). The license consists of your order details, the terms and conditions provided by Nature Publishing Group, and the payment terms and conditions.

All payments must be made in full to CCC. For payment instructions, please see information listed at the bottom of this form.

License Number	3162580750972
License date	Jun 05, 2013
Licensed content publisher	Nature Publishing Group
Licensed content publication	Nature
Licensed content title	Genome maintenance mechanisms for preventing cancer
Licensed content author	Jan H. J. Hoeijmakers
Licensed content date	May 17, 2001
Volume number	411
Issue number	6835
Type of Use	reuse in a thesis/dissertation
Requestor type	academic/educational
Format	print and electronic
Portion	figures/tables/illustrations
Number of figures/tables/illustrations	4
Figures	Figure 1 DNA damage, repair mechanisms and consequences. Box 1 Model for mechanism of global genome nucleotide-excision repair and transcription-coupled repair Box 2 Mechanism for base-excision repair Box 3 Mechanism of homologous recombination and end joining
Author of this NPG article	no
Your reference number	None
Title of your thesis / dissertation	A mechanistic investigation into candidate markers of telomere-induced senescence in normal human epidermal keratinocytes
Expected completion date	Jul 2013
Estimated size (number of pages)	300
Total	**0.00 GBP**
Terms and Conditions	

Terms and Conditions for Permissions

Nature Publishing Group hereby grants you a non-exclusive license to reproduce this material for this purpose, and for no other use,subject to the conditions below:

1. NPG warrants that it has, to the best of its knowledge, the rights to license reuse of this material.

However, you should ensure that the material you are requesting is original to Nature Publishing Group and does not carry the copyright of another entity (as credited in the published version). If the credit line on any part of the material you have requested indicates that it was reprinted or adapted by NPG with permission from another source, then you should also seek permission from that source to reuse the material.

2. Permission granted free of charge for material in print is also usually granted for any electronic version of that work, provided that the material is incidental to the work as a whole and that the electronic version is essentially equivalent to, or substitutes for, the print version.Where print permission has been granted for a fee, separate permission must be obtained for any additional, electronic re-use (unless, as in the case of a full paper, this has already been accounted for during your initial request in the calculation of a print run).NB: In all cases, web-based use of full-text articles must be authorized separately through the 'Use on a Web Site' option when requesting permission.

3. Permission granted for a first edition does not apply to second and subsequent editions and for editions in other languages (except for signatories to the STM Permissions Guidelines, or where the first edition permission was granted for free).

4. Nature Publishing Group's permission must be acknowledged next to the figure, table or abstract in print. In electronic form, this acknowledgement must be visible at the same time as the figure/table/abstract, and must be hyperlinked to the journal's homepage.

5. The credit line should read:
   Reprinted by permission from Macmillan Publishers Ltd: [JOURNAL NAME] (reference citation), copyright (year of publication)
   For AOP papers, the credit line should read:
   Reprinted by permission from Macmillan Publishers Ltd: [JOURNAL NAME], advance online publication, day month year (doi: 10.1038/sj.[JOURNAL ACRONYM].XXXXX)

   Note: For republication from the *British Journal of Cancer,* the following credit lines apply.
   Reprinted by permission from Macmillan Publishers Ltd on behalf of Cancer Research UK: [JOURNAL NAME] (reference citation), copyright (year of publication)For AOP papers, the credit line should read:
   Reprinted by permission from Macmillan Publishers Ltd on behalf of Cancer Research UK: [JOURNAL NAME], advance online publication, day month year (doi: 10.1038/sj.[JOURNAL ACRONYM].XXXXX)

6. Adaptations of single figures do not require NPG approval. However, the adaptation should be credited as follows:

   Adapted by permission from Macmillan Publishers Ltd: [JOURNAL NAME] (reference citation), copyright (year of publication)

   Note: For adaptation from the *British Journal of Cancer,* the following credit line applies.
   Adapted by permission from Macmillan Publishers Ltd on behalf of Cancer Research UK: [JOURNAL NAME] (reference citation), copyright (year of publication)

7. Translations of 401 words up to a whole article require NPG approval. Please visit http://www.macmillanmedicalcommunications.com for more information.Translations of up to a 400 words do not require NPG approval. The translation should be credited as follows:

   Translated by permission from Macmillan Publishers Ltd: [JOURNAL NAME] (reference citation), copyright (year of publication).

<u>Note: For translation from the British Journal of Cancer, the following credit line applies.</u>
Translated by permission from Macmillan Publishers Ltd on behalf of Cancer Research UK:
[JOURNAL NAME] (reference citation), copyright (year of publication)

We are certain that all parties will benefit from this agreement and wish you the best in the use of this material. Thank you.
Special Terms:
v1.1

If you would like to pay for this license now, please remit this license along with your payment made payable to "COPYRIGHT CLEARANCE CENTER" otherwise you will be invoiced within 48 hours of the license date. Payment should be in the form of a check or money order referencing your account number and this invoice number RLNK501036722.
Once you receive your invoice for this order, you may pay your invoice by credit card. Please follow instructions provided at that time.

Make Payment To:
Copyright Clearance Center
Dept 001
P.O. Box 843006
Boston, MA 02284-3006

For suggestions or comments regarding this order, contact RightsLink Customer Support:
customercare@copyright.com or +1-877-622-5543 (toll free in the US) or +1-978-646-2777.

Gratis licenses (referencing $0 in the Total field) are free. Please retain this printable license for your reference. No payment is required.

NATURE PUBLISHING GROUP LICENSE
TERMS AND CONDITIONS

Jun 06, 2013

This is a License Agreement between Alice de Castro ("You") and Nature Publishing Group ("Nature Publishing Group") provided by Copyright Clearance Center ("CCC"). The license consists of your order details, the terms and conditions provided by Nature Publishing Group, and the payment terms and conditions.

All payments must be made in full to CCC. For payment instructions, please see information listed at the bottom of this form.

License Number	3162570079637
License date	Jun 05, 2013
Licensed content publisher	Nature Publishing Group
Licensed content publication	Nature
Licensed content title	The genetics of ageing
Licensed content author	Cynthia J. Kenyon
Licensed content date	Mar 24, 2010
Volume number	464
Issue number	7288
Type of Use	reuse in a thesis/dissertation
Requestor type	academic/educational
Format	print and electronic
Portion	figures/tables/illustrations
Number of figures/tables/illustrations	1
High-res required	no
Figures	Figure 3 | Pathways that influence lifespan extension in response to chronic dietary restriction.
Author of this NPG article	no
Your reference number	None
Title of your thesis / dissertation	A mechanistic investigation into candidate markers of telomere-induced senescence in normal human epidermal keratinocytes
Expected completion date	Jul 2013
Estimated size (number of pages)	300
Total	**0.00 GBP**
Terms and Conditions	

Terms and Conditions for Permissions

Nature Publishing Group hereby grants you a non-exclusive license to reproduce this material for this purpose, and for no other use,subject to the conditions below:

1. NPG warrants that it has, to the best of its knowledge, the rights to license reuse of this material. However, you should ensure that the material you are requesting is original to Nature Publishing

Group and does not carry the copyright of another entity (as credited in the published version). If the credit line on any part of the material you have requested indicates that it was reprinted or adapted by NPG with permission from another source, then you should also seek permission from that source to reuse the material.

2. Permission granted free of charge for material in print is also usually granted for any electronic version of that work, provided that the material is incidental to the work as a whole and that the electronic version is essentially equivalent to, or substitutes for, the print version.Where print permission has been granted for a fee, separate permission must be obtained for any additional, electronic re-use (unless, as in the case of a full paper, this has already been accounted for during your initial request in the calculation of a print run).NB: In all cases, web-based use of full-text articles must be authorized separately through the 'Use on a Web Site' option when requesting permission.

3. Permission granted for a first edition does not apply to second and subsequent editions and for editions in other languages (except for signatories to the STM Permissions Guidelines, or where the first edition permission was granted for free).

4. Nature Publishing Group's permission must be acknowledged next to the figure, table or abstract in print. In electronic form, this acknowledgement must be visible at the same time as the figure/table/abstract, and must be hyperlinked to the journal's homepage.

5. The credit line should read:
   Reprinted by permission from Macmillan Publishers Ltd: [JOURNAL NAME] (reference citation), copyright (year of publication)
   For AOP papers, the credit line should read:
   Reprinted by permission from Macmillan Publishers Ltd: [JOURNAL NAME], advance online publication, day month year (doi: 10.1038/sj.[JOURNAL ACRONYM].XXXXX)

   Note: For republication from the *British Journal of Cancer,* the following credit lines apply.
   Reprinted by permission from Macmillan Publishers Ltd on behalf of Cancer Research UK: [JOURNAL NAME] (reference citation), copyright (year of publication)For AOP papers, the credit line should read:
   Reprinted by permission from Macmillan Publishers Ltd on behalf of Cancer Research UK: [JOURNAL NAME], advance online publication, day month year (doi: 10.1038/sj.[JOURNAL ACRONYM].XXXXX)

6. Adaptations of single figures do not require NPG approval. However, the adaptation should be credited as follows:

   Adapted by permission from Macmillan Publishers Ltd: [JOURNAL NAME] (reference citation), copyright (year of publication)

   Note: For adaptation from the *British Journal of Cancer,* the following credit line applies.
   Adapted by permission from Macmillan Publishers Ltd on behalf of Cancer Research UK: [JOURNAL NAME] (reference citation), copyright (year of publication)

7. Translations of 401 words up to a whole article require NPG approval. Please visit http://www.macmillanmedicalcommunications.com for more information.Translations of up to a 400 words do not require NPG approval. The translation should be credited as follows:

   Translated by permission from Macmillan Publishers Ltd: [JOURNAL NAME] (reference citation), copyright (year of publication).

   Note: For translation from the *British Journal of Cancer,* the following credit line applies.

Translated by permission from Macmillan Publishers Ltd on behalf of Cancer Research UK: [JOURNAL NAME] (reference citation), copyright (year of publication)

We are certain that all parties will benefit from this agreement and wish you the best in the use of this material. Thank you.
Special Terms:
v1.1

If you would like to pay for this license now, please remit this license along with your payment made payable to "COPYRIGHT CLEARANCE CENTER" otherwise you will be invoiced within 48 hours of the license date. Payment should be in the form of a check or money order referencing your account number and this invoice number RLNK501036677.
Once you receive your invoice for this order, you may pay your invoice by credit card. Please follow instructions provided at that time.

Make Payment To:
Copyright Clearance Center
Dept 001
P.O. Box 843006
Boston, MA 02284-3006

For suggestions or comments regarding this order, contact RightsLink Customer Support: customercare@copyright.com or +1-877-622-5543 (toll free in the US) or +1-978-646-2777.

Gratis licenses (referencing $0 in the Total field) are free. Please retain this printable license for your reference. No payment is required.

NATURE PUBLISHING GROUP LICENSE
TERMS AND CONDITIONS

Jun 06, 2013

This is a License Agreement between Alice de Castro ("You") and Nature Publishing Group ("Nature Publishing Group") provided by Copyright Clearance Center ("CCC"). The license consists of your order details, the terms and conditions provided by Nature Publishing Group, and the payment terms and conditions.

All payments must be made in full to CCC. For payment instructions, please see information listed at the bottom of this form.

License Number	3162581022684
License date	Jun 05, 2013
Licensed content publisher	Nature Publishing Group
Licensed content publication	Nature Reviews Genetics
Licensed content title	Strategies for silencing human disease using RNA interference
Licensed content author	Daniel H. Kim, John J. Rossi
Licensed content date	Mar 1, 2007
Volume number	8
Issue number	3
Type of Use	reuse in a thesis/dissertation
Requestor type	academic/educational
Format	print and electronic
Portion	figures/tables/illustrations
Number of figures/tables/illustrations	2
High-res required	no
Figures	Figure 1	Mechanisms of RNA interference in mammalian cells. Figure 3	RNA interference effector molecules.
Author of this NPG article	no
Your reference number	None
Title of your thesis / dissertation	A mechanistic investigation into candidate markers of telomere-induced senescence in normal human epidermal keratinocytes
Expected completion date	Jul 2013
Estimated size (number of pages)	300
Total	**0.00 GBP**
Terms and Conditions	

Terms and Conditions for Permissions

Nature Publishing Group hereby grants you a non-exclusive license to reproduce this material for this purpose, and for no other use,subject to the conditions below:

1. NPG warrants that it has, to the best of its knowledge, the rights to license reuse of this material. However, you should ensure that the material you are requesting is original to Nature Publishing

Group and does not carry the copyright of another entity (as credited in the published version). If the credit line on any part of the material you have requested indicates that it was reprinted or adapted by NPG with permission from another source, then you should also seek permission from that source to reuse the material.

2. Permission granted free of charge for material in print is also usually granted for any electronic version of that work, provided that the material is incidental to the work as a whole and that the electronic version is essentially equivalent to, or substitutes for, the print version.Where print permission has been granted for a fee, separate permission must be obtained for any additional, electronic re-use (unless, as in the case of a full paper, this has already been accounted for during your initial request in the calculation of a print run).NB: In all cases, web-based use of full-text articles must be authorized separately through the 'Use on a Web Site' option when requesting permission.

3. Permission granted for a first edition does not apply to second and subsequent editions and for editions in other languages (except for signatories to the STM Permissions Guidelines, or where the first edition permission was granted for free).

4. Nature Publishing Group's permission must be acknowledged next to the figure, table or abstract in print. In electronic form, this acknowledgement must be visible at the same time as the figure/table/abstract, and must be hyperlinked to the journal's homepage.

5. The credit line should read:
Reprinted by permission from Macmillan Publishers Ltd: [JOURNAL NAME] (reference citation), copyright (year of publication)
For AOP papers, the credit line should read:
Reprinted by permission from Macmillan Publishers Ltd: [JOURNAL NAME], advance online publication, day month year (doi: 10.1038/sj.[JOURNAL ACRONYM].XXXXX)

   Note: For republication from the _British Journal of Cancer,_ the following credit lines apply.
Reprinted by permission from Macmillan Publishers Ltd on behalf of Cancer Research UK: [JOURNAL NAME] (reference citation), copyright (year of publication)For AOP papers, the credit line should read:
Reprinted by permission from Macmillan Publishers Ltd on behalf of Cancer Research UK: [JOURNAL NAME], advance online publication, day month year (doi: 10.1038/sj.[JOURNAL ACRONYM].XXXXX)

6. Adaptations of single figures do not require NPG approval. However, the adaptation should be credited as follows:

   Adapted by permission from Macmillan Publishers Ltd: [JOURNAL NAME] (reference citation), copyright (year of publication)

   Note: For adaptation from the _British Journal of Cancer,_ the following credit line applies.
Adapted by permission from Macmillan Publishers Ltd on behalf of Cancer Research UK: [JOURNAL NAME] (reference citation), copyright (year of publication)

7. Translations of 401 words up to a whole article require NPG approval. Please visit http://www.macmillanmedicalcommunications.com for more information.Translations of up to a 400 words do not require NPG approval. The translation should be credited as follows:

   Translated by permission from Macmillan Publishers Ltd: [JOURNAL NAME] (reference citation), copyright (year of publication).

   Note: For translation from the _British Journal of Cancer,_ the following credit line applies.

Translated by permission from Macmillan Publishers Ltd on behalf of Cancer Research UK: [JOURNAL NAME] (reference citation), copyright (year of publication)

We are certain that all parties will benefit from this agreement and wish you the best in the use of this material. Thank you.
Special Terms:
v1.1

If you would like to pay for this license now, please remit this license along with your payment made payable to "COPYRIGHT CLEARANCE CENTER" otherwise you will be invoiced within 48 hours of the license date. Payment should be in the form of a check or money order referencing your account number and this invoice number RLNK501036728.
Once you receive your invoice for this order, you may pay your invoice by credit card. Please follow instructions provided at that time.

Make Payment To:
Copyright Clearance Center
Dept 001
P.O. Box 843006
Boston, MA 02284-3006

For suggestions or comments regarding this order, contact RightsLink Customer Support:
customercare@copyright.com or +1-877-622-5543 (toll free in the US) or +1-978-646-2777.

Gratis licenses (referencing $0 in the Total field) are free. Please retain this printable license for your reference. No payment is required.

NATURE PUBLISHING GROUP LICENSE
TERMS AND CONDITIONS

Jun 06, 2013

This is a License Agreement between Alice de Castro ("You") and Nature Publishing Group ("Nature Publishing Group") provided by Copyright Clearance Center ("CCC"). The license consists of your order details, the terms and conditions provided by Nature Publishing Group, and the payment terms and conditions.

All payments must be made in full to CCC. For payment instructions, please see information listed at the bottom of this form.

License Number	3163111033953
License date	Jun 06, 2013
Licensed content publisher	Nature Publishing Group
Licensed content publication	Gene Therapy
Licensed content title	Optimised retroviral infection of human epidermal keratinocytes: long-term expression of transduced integrin gene following grafting on to SCID mice
Licensed content author	L Levy, S Broad, AJ Zhu, JM Carroll, I Khazaal, B Péault, FM Watt
Licensed content date	Jul 10, 1998
Volume number	5
Issue number	7
Type of Use	reuse in a thesis/dissertation
Requestor type	academic/educational
Format	print and electronic
Portion	figures/tables/illustrations
Number of figures/tables/illustrations	1
Figures	Figure 1b
Author of this NPG article	no
Your reference number	
Title of your thesis / dissertation	A mechanistic investigation into candidate markers of telomere-induced senescence in normal human epidermal keratinocytes
Expected completion date	Jul 2013
Estimated size (number	300

Estimated size (number   500
of pages)

Total   0.00 GBP

Terms and Conditions

Reprinted by permission from Macmillan Publishers Ltd on behalf of Cancer Research UK: [JOURNAL NAME], advance online publication, day month year (doi: 10.1038/sj.[JOURNAL ACRONYM].XXXXX)

6. Adaptations of single figures do not require NPG approval. However, the adaptation should be credited as follows:

   Adapted by permission from Macmillan Publishers Ltd: [JOURNAL NAME] (reference citation), copyright (year of publication)

   Note: For adaptation from the _British Journal of Cancer_, the following credit line applies.
   Adapted by permission from Macmillan Publishers Ltd on behalf of Cancer Research UK: [JOURNAL NAME] (reference citation), copyright (year of publication)

7. Translations of 401 words up to a whole article require NPG approval. Please visit http://www.macmillanmedicalcommunications.com for more information.Translations of up to a 400 words do not require NPG approval. The translation should be credited as follows:

   Translated by permission from Macmillan Publishers Ltd: [JOURNAL NAME] (reference citation), copyright (year of publication).

   Note: For translation from the _British Journal of Cancer_, the following credit line applies.
   Translated by permission from Macmillan Publishers Ltd on behalf of Cancer Research UK: [JOURNAL NAME] (reference citation), copyright (year of publication)

We are certain that all parties will benefit from this agreement and wish you the best in the use of this material. Thank you.

Special Terms:

v1.1

If you would like to pay for this license now, please remit this license along with your payment made payable to "COPYRIGHT CLEARANCE CENTER" otherwise you will be invoiced within 48 hours of the license date. Payment should be in the form of a check or money order referencing your account number and this invoice number RLNK501037575. Once you receive your invoice for this order, you may pay your invoice by credit card. Please follow instructions provided at that time.

Make Payment To: Copyright Clearance Center Dept 001 P.O. Box 843006 Boston, MA 02284-3006

For suggestions or comments regarding this order, contact RightsLink

Customer Support: customercare@copyright.com or +1-877-622-5543 (toll free in the US) or +1-978-646-2777.

Gratis licenses (referencing $0 in the Total field) are free. Please retain this printable license for your reference. No payment is required.

Dear Amber,

Thank you for writing. Let this email serve as our permission for you to reuse the figure in the manor described below.

Please note, our preferred citation styles:

© 2011 Rodier and Campisi. Originally published in J Cell Biol 192: 547–556.

With best wishes,
Suzanne O'Donnell
RUP Permissions Department

On 6/6/2013 7:20 AM, Alice de Castro wrote:

Dear Suzanne,

I am writing to you in order to obtain copyright permission to use 2 images from the figures in the publication below, in my PhD dissertation (for both print and electronic version).

Rodier F & Campisi J (2011) Four faces of cellular senescence. J Cell Biol 192: 547–556

Figure 1.
        Hallmarks of senescent cells.

Figure 2. Biological activities of cellular senescence.

I would appreciate your help in how to proceed. Many thanks!

Alice

Alice de Castro
PhD Student

Centre for Clinical and Diagnostic Oral Sciences
Blizard Institute
Barts and The London School of Medicine and Dentistry
4 Newark Street
London E1 2AT

Telephone +4420 7882 7141
Email a.m.de-castro@qmul.ac.uk

NATURE PUBLISHING GROUP LICENSE
TERMS AND CONDITIONS

Jun 06, 2013

This is a License Agreement between Alice de Castro ("You") and Nature Publishing Group ("Nature Publishing Group") provided by Copyright Clearance Center ("CCC"). The license consists of your order details, the terms and conditions provided by Nature Publishing Group, and the payment terms and conditions.

All payments must be made in full to CCC. For payment instructions, please see information listed at the bottom of this form.

License Number	3162580253274
License date	Jun 05, 2013
Licensed content publisher	Nature Publishing Group
Licensed content publication	Nature
Licensed content title	Linking functional decline of telomeres, mitochondria and stem cells during ageing
Licensed content author	Ergün Sahin, Ronald A. DePinho
Licensed content date	Mar 24, 2010
Volume number	464
Issue number	7288
Type of Use	reuse in a thesis/dissertation
Requestor type	academic/educational
Format	print and electronic
Portion	figures/tables/illustrations
Number of figures/tables/illustrations	1
High-res required	no
Figures	Figure 3 | A model of interaction between DNA damage, p53 activation and mitochondrial dysfunction.
Author of this NPG article	no
Your reference number	None
Title of your thesis / dissertation	A mechanistic investigation into candidate markers of telomere-induced senescence in normal human epidermal keratinocytes
Expected completion date	Jul 2013
Estimated size (number of pages)	300
Total	**0.00 GBP**
Terms and Conditions	

Terms and Conditions for Permissions

Nature Publishing Group hereby grants you a non-exclusive license to reproduce this material for this purpose, and for no other use,subject to the conditions below:

1. NPG warrants that it has, to the best of its knowledge, the rights to license reuse of this material.

However, you should ensure that the material you are requesting is original to Nature Publishing Group and does not carry the copyright of another entity (as credited in the published version). If the credit line on any part of the material you have requested indicates that it was reprinted or adapted by NPG with permission from another source, then you should also seek permission from that source to reuse the material.

2. Permission granted free of charge for material in print is also usually granted for any electronic version of that work, provided that the material is incidental to the work as a whole and that the electronic version is essentially equivalent to, or substitutes for, the print version.Where print permission has been granted for a fee, separate permission must be obtained for any additional, electronic re-use (unless, as in the case of a full paper, this has already been accounted for during your initial request in the calculation of a print run).NB: In all cases, web-based use of full-text articles must be authorized separately through the 'Use on a Web Site' option when requesting permission.

3. Permission granted for a first edition does not apply to second and subsequent editions and for editions in other languages (except for signatories to the STM Permissions Guidelines, or where the first edition permission was granted for free).

4. Nature Publishing Group's permission must be acknowledged next to the figure, table or abstract in print. In electronic form, this acknowledgement must be visible at the same time as the figure/table/abstract, and must be hyperlinked to the journal's homepage.

5. The credit line should read:
Reprinted by permission from Macmillan Publishers Ltd: [JOURNAL NAME] (reference citation), copyright (year of publication)
For AOP papers, the credit line should read:
Reprinted by permission from Macmillan Publishers Ltd: [JOURNAL NAME], advance online publication, day month year (doi: 10.1038/sj.[JOURNAL ACRONYM].XXXXX)

Note: For republication from the *British Journal of Cancer,* the following credit lines apply.
Reprinted by permission from Macmillan Publishers Ltd on behalf of Cancer Research UK: [JOURNAL NAME] (reference citation), copyright (year of publication)For AOP papers, the credit line should read:
Reprinted by permission from Macmillan Publishers Ltd on behalf of Cancer Research UK: [JOURNAL NAME], advance online publication, day month year (doi: 10.1038/sj.[JOURNAL ACRONYM].XXXXX)

6. Adaptations of single figures do not require NPG approval. However, the adaptation should be credited as follows:

Adapted by permission from Macmillan Publishers Ltd: [JOURNAL NAME] (reference citation), copyright (year of publication)

Note: For adaptation from the *British Journal of Cancer,* the following credit line applies.
Adapted by permission from Macmillan Publishers Ltd on behalf of Cancer Research UK: [JOURNAL NAME] (reference citation), copyright (year of publication)

7. Translations of 401 words up to a whole article require NPG approval. Please visit http://www.macmillanmedicalcommunications.com for more information.Translations of up to a 400 words do not require NPG approval. The translation should be credited as follows:

Translated by permission from Macmillan Publishers Ltd: [JOURNAL NAME] (reference citation), copyright (year of publication).

Note: For translation from the _British Journal of Cancer,_ the following credit line applies.
Translated by permission from Macmillan Publishers Ltd on behalf of Cancer Research UK: [JOURNAL NAME] (reference citation), copyright (year of publication)

We are certain that all parties will benefit from this agreement and wish you the best in the use of this material. Thank you.
Special Terms:
v1.1

If you would like to pay for this license now, please remit this license along with your payment made payable to "COPYRIGHT CLEARANCE CENTER" otherwise you will be invoiced within 48 hours of the license date. Payment should be in the form of a check or money order referencing your account number and this invoice number RLNK501036713.
Once you receive your invoice for this order, you may pay your invoice by credit card. Please follow instructions provided at that time.

Make Payment To:
Copyright Clearance Center
Dept 001
P.O. Box 843006
Boston, MA 02284-3006

For suggestions or comments regarding this order, contact RightsLink Customer Support:
customercare@copyright.com or +1-877-622-5543 (toll free in the US) or +1-978-646-2777.

Gratis licenses (referencing $0 in the Total field) are free. Please retain this printable license for your reference. No payment is required.

NATURE PUBLISHING GROUP LICENSE
TERMS AND CONDITIONS

Jun 06, 2013

This is a License Agreement between Alice de Castro ("You") and Nature Publishing Group ("Nature Publishing Group") provided by Copyright Clearance Center ("CCC"). The license consists of your order details, the terms and conditions provided by Nature Publishing Group, and the payment terms and conditions.

All payments must be made in full to CCC. For payment instructions, please see information listed at the bottom of this form.

License Number	3162571159416
License date	Jun 05, 2013
Licensed content publisher	Nature Publishing Group
Licensed content publication	Nature Reviews Molecular Cell Biology
Licensed content title	<!-- Stem cells -->How stem cells age and why this makes us grow old
Licensed content author	Norman E. Sharpless, Ronald A. DePinho
Licensed content date	Sep 1, 2007
Volume number	8
Issue number	9
Type of Use	reuse in a thesis/dissertation
Requestor type	academic/educational
Format	print and electronic
Portion	figures/tables/illustrations
Number of figures/tables/illustrations	1
High-res required	no
Figures	Figure 1	How stem cells age.
Author of this NPG article	no
Your reference number	None
Title of your thesis / dissertation	A mechanistic investigation into candidate markers of telomere-induced senescence in normal human epidermal keratinocytes
Expected completion date	Jul 2013
Estimated size (number of pages)	300
Total	**0.00 GBP**
Terms and Conditions	

Terms and Conditions for Permissions

Nature Publishing Group hereby grants you a non-exclusive license to reproduce this material for this purpose, and for no other use,subject to the conditions below:

1. NPG warrants that it has, to the best of its knowledge, the rights to license reuse of this material. However, you should ensure that the material you are requesting is original to Nature Publishing Group and does not carry the copyright of another entity (as credited in the published version). If the

credit line on any part of the material you have requested indicates that it was reprinted or adapted by NPG with permission from another source, then you should also seek permission from that source to reuse the material.

2. Permission granted free of charge for material in print is also usually granted for any electronic version of that work, provided that the material is incidental to the work as a whole and that the electronic version is essentially equivalent to, or substitutes for, the print version.Where print permission has been granted for a fee, separate permission must be obtained for any additional, electronic re-use (unless, as in the case of a full paper, this has already been accounted for during your initial request in the calculation of a print run).NB: In all cases, web-based use of full-text articles must be authorized separately through the 'Use on a Web Site' option when requesting permission.

3. Permission granted for a first edition does not apply to second and subsequent editions and for editions in other languages (except for signatories to the STM Permissions Guidelines, or where the first edition permission was granted for free).

4. Nature Publishing Group's permission must be acknowledged next to the figure, table or abstract in print. In electronic form, this acknowledgement must be visible at the same time as the figure/table/abstract, and must be hyperlinked to the journal's homepage.

5. The credit line should read:
Reprinted by permission from Macmillan Publishers Ltd: [JOURNAL NAME] (reference citation), copyright (year of publication)
For AOP papers, the credit line should read:
Reprinted by permission from Macmillan Publishers Ltd: [JOURNAL NAME], advance online publication, day month year (doi: 10.1038/sj.[JOURNAL ACRONYM].XXXXX)

Note: For republication from the _British Journal of Cancer,_ the following credit lines apply.
Reprinted by permission from Macmillan Publishers Ltd on behalf of Cancer Research UK: [JOURNAL NAME] (reference citation), copyright (year of publication)For AOP papers, the credit line should read:
Reprinted by permission from Macmillan Publishers Ltd on behalf of Cancer Research UK: [JOURNAL NAME], advance online publication, day month year (doi: 10.1038/sj.[JOURNAL ACRONYM].XXXXX)

6. Adaptations of single figures do not require NPG approval. However, the adaptation should be credited as follows:

Adapted by permission from Macmillan Publishers Ltd: [JOURNAL NAME] (reference citation), copyright (year of publication)

Note: For adaptation from the _British Journal of Cancer,_ the following credit line applies.
Adapted by permission from Macmillan Publishers Ltd on behalf of Cancer Research UK: [JOURNAL NAME] (reference citation), copyright (year of publication)

7. Translations of 401 words up to a whole article require NPG approval. Please visit http://www.macmillanmedicalcommunications.com for more information.Translations of up to a 400 words do not require NPG approval. The translation should be credited as follows:

Translated by permission from Macmillan Publishers Ltd: [JOURNAL NAME] (reference citation), copyright (year of publication).

Note: For translation from the _British Journal of Cancer,_ the following credit line applies.
Translated by permission from Macmillan Publishers Ltd on behalf of Cancer Research UK:

[JOURNAL NAME] (reference citation), copyright (year of publication)

We are certain that all parties will benefit from this agreement and wish you the best in the use of this material. Thank you.
Special Terms:
v1.1

If you would like to pay for this license now, please remit this license along with your payment made payable to "COPYRIGHT CLEARANCE CENTER" otherwise you will be invoiced within 48 hours of the license date. Payment should be in the form of a check or money order referencing your account number and this invoice number RLNK501036705.
Once you receive your invoice for this order, you may pay your invoice by credit card. Please follow instructions provided at that time.

Make Payment To:
Copyright Clearance Center
Dept 001
P.O. Box 843006
Boston, MA 02284-3006

For suggestions or comments regarding this order, contact RightsLink Customer Support:
customercare@copyright.com or +1-877-622-5543 (toll free in the US) or +1-978-646-2777.

Gratis licenses (referencing $0 in the Total field) are free. Please retain this printable license for your reference. No payment is required.

ELSEVIER LICENSE
TERMS AND CONDITIONS

Jun 06, 2013

This is a License Agreement between Alice de Castro ("You") and Elsevier ("Elsevier") provided by Copyright Clearance Center ("CCC"). The license consists of your order details, the terms and conditions provided by Elsevier, and the payment terms and conditions.

All payments must be made in full to CCC. For payment instructions, please see information listed at the bottom of this form.

Supplier	Elsevier Limited The Boulevard,Langford Lane Kidlington,Oxford,OX5 1GB,UK
Registered Company Number	1982084
Customer name	Alice de Castro
Customer address	CDOS
	London, E1 2AT
License number	3163040021827
License date	Jun 06, 2013
Licensed content publisher	Elsevier
Licensed content publication	Cell
Licensed content title	TRF2 Protects Human Telomeres from End-to-End Fusions
Licensed content author	Bas van Steensel,Agata Smogorzewska,Titia de Lange
Licensed content date	6 February 1998
Licensed content volume number	92
Licensed content issue number	3
Number of pages	13
Start Page	401
End Page	413
Type of Use	reuse in a thesis/dissertation
Intended publisher of new work	other
Portion	figures/tables/illustrations

Portion	figures/tables/illustrations
Number of figures/tables/illustrations	1
Format	both print and electronic
Are you the author of this Elsevier article?	No
Will you be translating?	No
Order reference number	
Title of your thesis/dissertation	A mechanistic investigation into candidate markers of telomere-induced senescence in normal human epidermal keratinocytes
Expected completion date	Jul 2013
Estimated size (number of pages)	300
Elsevier VAT number	GB 494 6272 12
Permissions price	0.00 GBP
VAT/Local Sales Tax	0.0 USD / 0.0 GBP
Total	0.00 GBP

Terms and Conditions

INTRODUCTION

1. The publisher for this copyrighted material is Elsevier. By clicking "accept" in connection with completing this licensing transaction, you agree that the following terms and conditions apply to this transaction (along with the Billing and Payment terms and conditions established by Copyright Clearance Center, Inc. ("CCC"), at the time that you opened your Rightslink account and that are available at any time at http://myaccount.copyright.com).

GENERAL TERMS

2. Elsevier hereby grants you permission to reproduce the aforementioned material subject to the terms and conditions indicated.

3. Acknowledgement: If any part of the material to be used (for example, figures) has appeared in our publication with credit or acknowledgement to another source, permission must also be sought from that source. If such permission is not obtained then that material may not be included in your publication/copies. Suitable acknowledgement to the source must be made, either as a footnote or in a reference list at the end of your publication, as follows:

"Reprinted from Publication title, Vol /edition number, Author(s), Title of article / title of chapter, Pages No., Copyright (Year), with permission from Elsevier [OR APPLICABLE SOCIETY COPYRIGHT OWNER]." Also Lancet special credit - "Reprinted from The Lancet, Vol. number, Author(s), Title of article, Pages No., Copyright (Year), with permission from Elsevier."

4. Reproduction of this material is confined to the purpose and/or media for which permission is hereby given.

5. Altering/Modifying Material: Not Permitted. However figures and illustrations may be altered/adapted minimally to serve your work. Any other abbreviations, additions, deletions and/or any other alterations shall be made only with prior written authorization of Elsevier Ltd. (Please contact Elsevier at permissions@elsevier.com)

6. If the permission fee for the requested use of our material is waived in this instance, please be advised that your future requests for Elsevier materials may attract a fee.

7. Reservation of Rights: Publisher reserves all rights not specifically granted in the combination of (i) the license details provided by you and accepted in the course of this licensing transaction, (ii) these terms and conditions and (iii) CCC's Billing and Payment terms and conditions.

8. License Contingent Upon Payment: While you may exercise the rights licensed immediately upon issuance of the license at the end of the licensing process for the transaction, provided that you have disclosed complete and accurate details of your proposed use, no license is finally effective unless and until full payment is received from you (either by publisher or by CCC) as provided in CCC's Billing and Payment terms and conditions. If full payment is not received on a timely basis, then any license preliminarily granted shall be deemed automatically revoked and shall be void as if never granted. Further, in the event that you breach any of these terms and conditions or any of CCC's Billing and Payment terms and conditions, the license is automatically revoked and shall be void as if never granted. Use of materials as described in a revoked license, as well as any use of the materials beyond the scope of an unrevoked license, may constitute copyright infringement and publisher reserves the right to take any and all action to protect its copyright in the materials.

9. Warranties: Publisher makes no representations or warranties with respect to the licensed material.

10. Indemnity: You hereby indemnify and agree to hold harmless publisher and CCC, and their respective officers, directors, employees and agents, from and against any and all claims arising out of your use of the licensed material other than as specifically authorized pursuant to this license.

11. No Transfer of License: This license is personal to you and may not be sublicensed, assigned, or transferred by you to any other person without publisher's written permission.

12. No Amendment Except in Writing: This license may not be amended except in a writing signed by both parties (or, in the case of publisher, by CCC on publisher's behalf).

13. Objection to Contrary Terms: Publisher hereby objects to any terms contained in any purchase order, acknowledgment, check endorsement or other writing prepared by you, which terms are inconsistent with these terms and conditions or CCC's Billing and Payment terms and conditions. These terms and conditions, together with CCC's Billing and Payment terms and conditions (which are incorporated herein), comprise the entire agreement between you and publisher (and CCC) concerning this licensing transaction. In the event of any conflict between your obligations established by these terms and conditions and those established by CCC's Billing and Payment terms and conditions, these terms and conditions

shall control.

14. Revocation: Elsevier or Copyright Clearance Center may deny the permissions described in this License at their sole discretion, for any reason or no reason, with a full refund payable to you. Notice of such denial will be made using the contact information provided by you. Failure to receive such notice will not alter or invalidate the denial. In no event will Elsevier or Copyright Clearance Center be responsible or liable for any costs, expenses or damage incurred by you as a result of a denial of your permission request, other than a refund of the amount(s) paid by you to Elsevier and/or Copyright Clearance Center for denied permissions.

LIMITED LICENSE

The following terms and conditions apply only to specific license types:

15. **Translation**: This permission is granted for non-exclusive world **English** rights only unless your license was granted for translation rights. If you licensed translation rights you may only translate this content into the languages you requested. A professional translator must perform all translations and reproduce the content word for word preserving the integrity of the article. If this license is to re-use 1 or 2 figures then permission is granted for non-exclusive world rights in all languages.

16. **Website**: The following terms and conditions apply to electronic reserve and author websites:
Electronic reserve: If licensed material is to be posted to website, the web site is to be password-protected and made available only to bona fide students registered on a relevant course if:
This license was made in connection with a course,
This permission is granted for 1 year only. You may obtain a license for future website posting,
All content posted to the web site must maintain the copyright information line on the bottom of each image,
A hyper-text must be included to the Homepage of the journal from which you are licensing at http://www.sciencedirect.com/science/journal/xxxxx or the Elsevier homepage for books at http://www.elsevier.com , and
Central Storage: This license does not include permission for a scanned version of the material to be stored in a central repository such as that provided by Heron/XanEdu.

17. **Author website** for journals with the following additional clauses:

All content posted to the web site must maintain the copyright information line on the bottom of each image, and the permission granted is limited to the personal version of your paper. You are not allowed to download and post the published electronic version of your article (whether PDF or HTML, proof or final version), nor may you scan the printed edition to create an electronic version. A hyper-text must be included to the Homepage of the journal from which you are licensing at http://www.sciencedirect.com/science/journal/xxxxx . As part of our normal production process, you will receive an e-mail notice when your article appears on Elsevier's online service ScienceDirect (www.sciencedirect.com). That e-mail will include the article's Digital Object Identifier (DOI). This number provides the electronic link to the published article and should be included in the posting of your personal version. We ask that you wait until you receive this e-mail and have the DOI to do any

posting.

Central Storage: This license does not include permission for a scanned version of the material to be stored in a central repository such as that provided by Heron/XanEdu.

18. **Author website** for books with the following additional clauses:
Authors are permitted to place a brief summary of their work online only.
A hyper-text must be included to the Elsevier homepage at http://www.elsevier.com . All content posted to the web site must maintain the copyright information line on the bottom of each image. You are not allowed to download and post the published electronic version of your chapter, nor may you scan the printed edition to create an electronic version.

Central Storage: This license does not include permission for a scanned version of the material to be stored in a central repository such as that provided by Heron/XanEdu.

19. **Website** (regular and for author): A hyper-text must be included to the Homepage of the journal from which you are licensing at
http://www.sciencedirect.com/science/journal/xxxxx. or for books to the Elsevier homepage at http://www.elsevier.com

20. **Thesis/Dissertation**: If your license is for use in a thesis/dissertation your thesis may be submitted to your institution in either print or electronic form. Should your thesis be published commercially, please reapply for permission. These requirements include permission for the Library and Archives of Canada to supply single copies, on demand, of the complete thesis and include permission for UMI to supply single copies, on demand, of the complete thesis. Should your thesis be published commercially, please reapply for permission.

21. **Other Conditions**:

v1.6

Gratis licenses (referencing $0 in the Total field) are free. Please retain this printable license for your reference. No payment is required.

NATURE PUBLISHING GROUP LICENSE
TERMS AND CONDITIONS

Jun 06, 2013

This is a License Agreement between Alice de Castro ("You") and Nature Publishing Group ("Nature Publishing Group") provided by Copyright Clearance Center ("CCC"). The license consists of your order details, the terms and conditions provided by Nature Publishing Group, and the payment terms and conditions.

All payments must be made in full to CCC. For payment instructions, please see information listed at the bottom of this form.

License Number	3162580425370
License date	Jun 05, 2013
Licensed content publisher	Nature Publishing Group
Licensed content publication	Nature Cell Biology
Licensed content title	Signalling the end of the line
Licensed content author	John van Tuyn, Peter D. Adams
Licensed content date	Apr 2, 2012
Volume number	14
Issue number	4
Type of Use	reuse in a thesis/dissertation
Requestor type	academic/educational
Format	print and electronic
Portion	figures/tables/illustrations
Number of figures/tables/illustrations	1
High-res required	no
Figures	Figure 1 The DNA-damage response differs at telomeric and non-telomeric DNA.
Author of this NPG article	no
Your reference number	None
Title of your thesis / dissertation	A mechanistic investigation into candidate markers of telomere-induced senescence in normal human epidermal keratinocytes
Expected completion date	Jul 2013
Estimated size (number of pages)	300
Total	**0.00 GBP**
Terms and Conditions	

Terms and Conditions for Permissions

Nature Publishing Group hereby grants you a non-exclusive license to reproduce this material for this purpose, and for no other use,subject to the conditions below:

1. NPG warrants that it has, to the best of its knowledge, the rights to license reuse of this material. However, you should ensure that the material you are requesting is original to Nature Publishing

Group and does not carry the copyright of another entity (as credited in the published version). If the credit line on any part of the material you have requested indicates that it was reprinted or adapted by NPG with permission from another source, then you should also seek permission from that source to reuse the material.

2. Permission granted free of charge for material in print is also usually granted for any electronic version of that work, provided that the material is incidental to the work as a whole and that the electronic version is essentially equivalent to, or substitutes for, the print version.Where print permission has been granted for a fee, separate permission must be obtained for any additional, electronic re-use (unless, as in the case of a full paper, this has already been accounted for during your initial request in the calculation of a print run).NB: In all cases, web-based use of full-text articles must be authorized separately through the 'Use on a Web Site' option when requesting permission.

3. Permission granted for a first edition does not apply to second and subsequent editions and for editions in other languages (except for signatories to the STM Permissions Guidelines, or where the first edition permission was granted for free).

4. Nature Publishing Group's permission must be acknowledged next to the figure, table or abstract in print. In electronic form, this acknowledgement must be visible at the same time as the figure/table/abstract, and must be hyperlinked to the journal's homepage.

5. The credit line should read:
   Reprinted by permission from Macmillan Publishers Ltd: [JOURNAL NAME] (reference citation), copyright (year of publication)
   For AOP papers, the credit line should read:
   Reprinted by permission from Macmillan Publishers Ltd: [JOURNAL NAME], advance online publication, day month year (doi: 10.1038/sj.[JOURNAL ACRONYM].XXXXX)

   Note: For republication from the _British Journal of Cancer,_ the following credit lines apply.
   Reprinted by permission from Macmillan Publishers Ltd on behalf of Cancer Research UK: [JOURNAL NAME] (reference citation), copyright (year of publication)For AOP papers, the credit line should read:
   Reprinted by permission from Macmillan Publishers Ltd on behalf of Cancer Research UK: [JOURNAL NAME], advance online publication, day month year (doi: 10.1038/sj.[JOURNAL ACRONYM].XXXXX)

6. Adaptations of single figures do not require NPG approval. However, the adaptation should be credited as follows:

   Adapted by permission from Macmillan Publishers Ltd: [JOURNAL NAME] (reference citation), copyright (year of publication)

   Note: For adaptation from the _British Journal of Cancer,_ the following credit line applies.
   Adapted by permission from Macmillan Publishers Ltd on behalf of Cancer Research UK: [JOURNAL NAME] (reference citation), copyright (year of publication)

7. Translations of 401 words up to a whole article require NPG approval. Please visit http://www.macmillanmedicalcommunications.com for more information.Translations of up to a 400 words do not require NPG approval. The translation should be credited as follows:

   Translated by permission from Macmillan Publishers Ltd: [JOURNAL NAME] (reference citation), copyright (year of publication).

   Note: For translation from the _British Journal of Cancer,_ the following credit line applies.

Translated by permission from Macmillan Publishers Ltd on behalf of Cancer Research UK: [JOURNAL NAME] (reference citation), copyright (year of publication)

We are certain that all parties will benefit from this agreement and wish you the best in the use of this material. Thank you.
Special Terms:
v1.1

If you would like to pay for this license now, please remit this license along with your payment made payable to "COPYRIGHT CLEARANCE CENTER" otherwise you will be invoiced within 48 hours of the license date. Payment should be in the form of a check or money order referencing your account number and this invoice number RLNK501036716.
Once you receive your invoice for this order, you may pay your invoice by credit card. Please follow instructions provided at that time.

Make Payment To:
Copyright Clearance Center
Dept 001
P.O. Box 843006
Boston, MA 02284-3006

For suggestions or comments regarding this order, contact RightsLink Customer Support: customercare@copyright.com or +1-877-622-5543 (toll free in the US) or +1-978-646-2777.

Gratis licenses (referencing $0 in the Total field) are free. Please retain this printable license for your reference. No payment is required.

JOHN WILEY AND SONS LICENSE
TERMS AND CONDITIONS

Jun 06, 2013

This is a License Agreement between Alice de Castro ("You") and John Wiley and Sons ("John Wiley and Sons") provided by Copyright Clearance Center ("CCC"). The license consists of your order details, the terms and conditions provided by John Wiley and Sons, and the payment terms and conditions.

All payments must be made in full to CCC. For payment instructions, please see information listed at the bottom of this form.

License Number	3163101331509
License date	Jun 06, 2013
Licensed content publisher	John Wiley and Sons
Licensed content publication	Aging Cell
Licensed content title	The number of p16INK4a positive cells in human skin reflects biological age
Licensed copyright line	© 2012 The Authors. Aging Cell © 2012 Blackwell Publishing Ltd/Anatomical Society of Great Britain and Ireland
Licensed content author	Mariëtte E.C. Waaijer,William E. Parish,Barbara H. Strongitharm,Diana van Heemst,Pieternella E. Slagboom,Anton J.M. de Craen,John M. Sedivy,Rudi G.J. Westendorp,David A. Gunn,Andrea B. Maier
Licensed content date	Jun 11, 2012
Start page	722
End page	725
Type of use	Dissertation/Thesis
Requestor type	University/Academic
Format	Print and electronic
Portion	Figure/table
Number of figures/tables	1
Original Wiley figure/table number(s)	Figure 1
Will you be translating?	No
Total	0.00 USD

Terms and Conditions

TERMS AND CONDITIONS

This copyrighted material is owned by or exclusively licensed to John Wiley & Sons, Inc. or one of its group companies (each a "Wiley Company") or a society for whom a Wiley Company has exclusive publishing rights in relation to a particular journal (collectively "WILEY"). By clicking "accept" in connection with completing this licensing transaction, you agree that the following terms and conditions apply to this transaction (along with the billing and payment terms and conditions established by the Copyright Clearance Center Inc., ("CCC's Billing and Payment terms and conditions"), at the time that you opened your RightsLink account (these are available at any time at http://myaccount.copyright.com).

Terms and Conditions

1. The materials you have requested permission to reproduce (the "Materials") are protected by copyright.

2. You are hereby granted a personal, non-exclusive, non-sublicensable, non-transferable, worldwide, limited license to reproduce the Materials for the purpose specified in the licensing process. This license is for a one-time use only with a maximum distribution equal to the number that you identified in the licensing process. Any form of republication granted by this license must be completed within two years of the date of the grant of this license (although copies prepared before may be distributed thereafter). The Materials shall not be used in any other manner or for any other purpose. Permission is granted subject to an appropriate acknowledgement given to the author, title of the material/book/journal and the publisher. You shall also duplicate the copyright notice that appears in the Wiley publication in your use of the Material. Permission is also granted on the understanding that nowhere in the text is a previously published source acknowledged for all or part of this Material. Any third party material is expressly excluded from this permission.

3. With respect to the Materials, all rights are reserved. Except as expressly granted by the terms of the license, no part of the Materials may be copied, modified, adapted (except for minor reformatting required by the new Publication), translated, reproduced, transferred or distributed, in any form or by any means, and no derivative works may be made based on the Materials without the prior permission of the respective copyright owner. You may not alter, remove or suppress in any manner any copyright, trademark or other notices displayed by the Materials. You may not license, rent, sell, loan, lease, pledge, offer as security, transfer or assign the Materials, or any of the rights granted to you hereunder to any other person.

4. The Materials and all of the intellectual property rights therein shall at all times remain the exclusive property of John Wiley & Sons Inc or one of its related companies (WILEY) or their respective licensors, and your interest therein is only that of having possession of and the right to reproduce the Materials pursuant to Section 2 herein during the continuance of this Agreement. You agree that you own no right, title or interest in or to the Materials or any of the intellectual property rights therein. You shall have no rights hereunder other than the license as provided for above in Section 2. No right, license or interest to any trademark, trade name, service mark or other branding ("Marks") of WILEY or its licensors is granted hereunder, and you agree that you shall not assert any such right, license or interest with respect thereto.

5. NEITHER WILEY NOR ITS LICENSORS MAKES ANY WARRANTY OR REPRESENTATION OF ANY KIND TO YOU OR ANY THIRD PARTY, EXPRESS, IMPLIED OR STATUTORY, WITH RESPECT TO THE MATERIALS OR THE ACCURACY OF ANY INFORMATION CONTAINED IN THE MATERIALS, INCLUDING, WITHOUT LIMITATION, ANY IMPLIED WARRANTY OF MERCHANTABILITY, ACCURACY, SATISFACTORY QUALITY, FITNESS FOR A PARTICULAR PURPOSE, USABILITY, INTEGRATION OR NON-INFRINGEMENT AND ALL SUCH WARRANTIES ARE HEREBY EXCLUDED BY WILEY AND ITS LICENSORS AND WAIVED BY YOU.

6. WILEY shall have the right to terminate this Agreement immediately upon breach of this Agreement by you.

7. You shall indemnify, defend and hold harmless WILEY, its Licensors and their respective directors, officers, agents and employees, from and against any actual or threatened claims, demands, causes of action or proceedings arising from any breach of this Agreement by you.

8. IN NO EVENT SHALL WILEY OR ITS LICENSORS BE LIABLE TO YOU OR ANY OTHER PARTY OR ANY OTHER PERSON OR ENTITY FOR ANY SPECIAL, CONSEQUENTIAL, INCIDENTAL, INDIRECT, EXEMPLARY OR PUNITIVE DAMAGES, HOWEVER CAUSED, ARISING OUT OF OR IN CONNECTION WITH THE DOWNLOADING, PROVISIONING, VIEWING OR USE OF THE MATERIALS REGARDLESS OF THE FORM OF ACTION, WHETHER FOR BREACH OF CONTRACT, BREACH OF WARRANTY, TORT, NEGLIGENCE, INFRINGEMENT OR OTHERWISE (INCLUDING, WITHOUT LIMITATION, DAMAGES BASED ON LOSS OF PROFITS, DATA, FILES, USE, BUSINESS OPPORTUNITY OR CLAIMS OF THIRD PARTIES), AND WHETHER OR NOT THE PARTY HAS BEEN ADVISED OF THE POSSIBILITY OF SUCH DAMAGES. THIS LIMITATION SHALL APPLY NOTWITHSTANDING ANY FAILURE OF ESSENTIAL PURPOSE OF ANY LIMITED REMEDY PROVIDED HEREIN.

9. Should any provision of this Agreement be held by a court of competent jurisdiction to be illegal, invalid, or unenforceable, that provision shall be deemed amended to achieve as nearly as possible the same economic effect as the original provision, and the legality, validity and enforceability of the remaining provisions of this Agreement shall not be affected or impaired thereby.

10. The failure of either party to enforce any term or condition of this Agreement shall not constitute a waiver of either party's right to enforce each and every term and condition of this Agreement. No breach under this agreement shall be deemed waived or excused by either party unless such waiver or consent is in writing signed by the party granting such waiver or consent. The waiver by or consent of a party to a breach of any provision of this Agreement shall not operate or be construed as a waiver of or consent to any other or subsequent breach by such other party.

11. This Agreement may not be assigned (including by operation of law or otherwise) by you without WILEY's prior written consent.

12. Any fee required for this permission shall be non-refundable after thirty (30) days from receipt

13. These terms and conditions together with CCC's Billing and Payment terms and conditions (which are incorporated herein) form the entire agreement between you and WILEY concerning this licensing transaction and (in the absence of fraud) supersedes all prior agreements and representations of the parties, oral or written. This Agreement may not be amended except in writing signed by both parties. This Agreement shall be binding upon and inure to the benefit of the parties' successors, legal representatives, and authorized assigns.

14. In the event of any conflict between your obligations established by these terms and conditions and those established by CCC's Billing and Payment terms and conditions, these terms and conditions shall prevail.

15. WILEY expressly reserves all rights not specifically granted in the combination of (i) the license details provided by you and accepted in the course of this licensing transaction, (ii) these terms and conditions and (iii) CCC's Billing and Payment terms and conditions.

16. This Agreement will be void if the Type of Use, Format, Circulation, or Requestor Type was misrepresented during the licensing process.

17. This Agreement shall be governed by and construed in accordance with the laws of the State of New York, USA, without regards to such state's conflict of law rules. Any legal action, suit or proceeding arising out of or relating to these Terms and Conditions or the breach thereof shall be instituted in a court of competent jurisdiction in New York County in the State of New York in the United States of America and each party hereby consents and submits to the personal jurisdiction of such court, waives any objection to venue in such court and consents to service of process by registered or certified mail, return receipt requested, at the last known address of such party.

Wiley Open Access Terms and Conditions

Wiley publishes Open Access articles in both its Wiley Open Access Journals program [http://www.wileyopenaccess.com/view/index.html] and as Online Open articles in its subscription journals. The majority of Wiley Open Access Journals have adopted the Creative Commons Attribution License (CC BY) which permits the unrestricted use, distribution, reproduction, adaptation and commercial exploitation of the article in any medium. No permission is required to use the article in this way provided that the article is properly cited and other license terms are observed. A small number of Wiley Open Access journals have retained the Creative Commons Attribution Non Commercial License (CC BY-NC), which permits use, distribution and reproduction in any medium, provided the original work is properly cited and is not used for commercial purposes.

Online Open articles - Authors selecting Online Open are, unless particular exceptions apply, offered a choice of Creative Commons licenses. They may therefore select from the CC BY, the CC BY-NC and the Attribution-NoDerivatives (CC BY-NC-ND). The CC BY-NC-ND is more restrictive than the CC BY-NC as it does not permit adaptations or modifications without rights holder consent.

Wiley Open Access articles are protected by copyright and are posted to repositories and websites in accordance with the terms of the applicable Creative Commons license referenced on the article. At the time of deposit, Wiley Open Access articles include all changes made during peer review, copyediting, and publishing. Repositories and websites

that host the article are responsible for incorporating any publisher-supplied amendments or retractions issued subsequently.
Wiley Open Access articles are also available without charge on Wiley's publishing platform, **Wiley Online Library** or any successor sites.

Conditions applicable to all Wiley Open Access articles:

- The authors' moral rights must not be compromised. These rights include the right of "paternity" (also known as "attribution" - the right for the author to be identified as such) and "integrity" (the right for the author not to have the work altered in such a way that the author's reputation or integrity may be damaged).

- Where content in the article is identified as belonging to a third party, it is the obligation of the user to ensure that any reuse complies with the copyright policies of the owner of that content.

- If article content is copied, downloaded or otherwise reused for research and other purposes as permitted, a link to the appropriate bibliographic citation (authors, journal, article title, volume, issue, page numbers, DOI and the link to the definitive published version on Wiley Online Library) should be maintained. Copyright notices and disclaimers must not be deleted.
  - Creative Commons licenses are copyright licenses and do not confer any other rights, including but not limited to trademark or patent rights.

- Any translations, for which a prior translation agreement with Wiley has not been agreed, must prominently display the statement: "This is an unofficial translation of an article that appeared in a Wiley publication. The publisher has not endorsed this translation."

Conditions applicable to non-commercial licenses (CC BY-NC and CC BY-NC-ND)

For non-commercial and non-promotional purposes individual non-commercial users may access, download, copy, display and redistribute to colleagues Wiley Open Access articles. In addition, articles adopting the CC BY-NC may be adapted, translated, and text- and data-mined subject to the conditions above.

Use by commercial "for-profit" organizations

Use of non-commercial Wiley Open Access articles for commercial, promotional, or marketing purposes requires further explicit permission from Wiley and will be subject to a fee. Commercial purposes include:

- Copying or downloading of articles, or linking to such articles for further redistribution, sale or licensing;

- Copying, downloading or posting by a site or service that incorporates advertising with such content;

- The inclusion or incorporation of article content in other works or services (other than normal quotations with an appropriate citation) that is then available for sale or licensing, for a fee (for example, a compilation produced for marketing purposes, inclusion in a sales pack)

- Use of article content (other than normal quotations with appropriate citation) by for-profit organizations for promotional purposes

- Linking to article content in e-mails redistributed for promotional, marketing or educational purposes;

- Use for the purposes of monetary reward by means of sale, resale, license, loan, transfer or other form of commercial exploitation such as marketing products

- Print reprints of Wiley Open Access articles can be purchased from: corporatesales@wiley.com

The modification or adaptation for any purpose of an article referencing the CC BY-NC-ND License requires consent which can be requested from RightsLink@wiley.com .

Other Terms and Conditions:

BY CLICKING ON THE "I AGREE..." BOX, YOU ACKNOWLEDGE THAT YOU HAVE READ AND FULLY UNDERSTAND EACH OF THE SECTIONS OF AND PROVISIONS SET FORTH IN THIS AGREEMENT AND THAT YOU ARE IN AGREEMENT WITH AND ARE WILLING TO ACCEPT ALL OF YOUR OBLIGATIONS AS SET FORTH IN THIS AGREEMENT.

v1.8

For suggestions or comments regarding this order, contact RightsLink Customer Support: customercare@copyright.com or +1-877-622-5543 (toll free in the US) or +1-978-646-2777.

Gratis licenses (referencing $0 in the Total field) are free. Please retain this printable license for your reference. No payment is required.

![Copyright Clearance Center RightsLink]

AMERICAN SOCIETY FOR MICROBIOLOGY

Title: Posttranslational Modifications of p53 in Replicative Senescence Overlapping but Distinct from Those Induced by DNA Damage

Author: Katherine Webley, Jane A. Bond, Christopher J. Jones et al.

Publication: Molecular and Cellular Biology

Publisher: American Society for Microbiology

Date: Apr 15, 2000

Copyright © 2000, American Society for Microbiology

Permissions Request

ASM authorizes an advanced degree candidate to republish the requested material in his/her doctoral thesis or dissertation. If your thesis, or dissertation, is to be published commercially, then you must reapply for permission.

BACK | CLOSE WINDOW